Synthesis of Functional Buckybowls and Related Nanostructures via Regioselective Cyclodehydrofluorination

---

Synthese von funktionellen Buckybowls und verwandten Nanostrukturen über die regioselektive Zyklodehydrofluorierung

der Naturwissenschaftlichen Fakultät
der Friedrich-Alexander-Universität Erlangen-Nürnberg

zur

Erlangung des Doktorgrades Dr. rer. nat.

vorgelegt von

Olena Papaianina
aus Donetsk, Ukraine

Als Dissertation genehmigt von der Naturwissenschaftlichen Fakultät der Friedrich-Alexander-Universität Erlangen-Nürnberg (FAU).

Tag der mündlichen Prüfung:	15.10.2019
Vorsitzender des Promotionsorgans:	Prof. Dr. Georg Kreimer
Gutachter:	PD Dr. habil. Konstantin Amsharov
	Prof. Dr. Andreas Hirsch

Mein besonderer Dank gilt meinem Doktorvater Dr. habil. Konstantin Amsharov für die Bereitstellung des interessanten und herausfordernden Themas, seine Förderungen, fachliche Unterstützung und das Interesse am Fortschritt dieser Arbeit.

Die vorliegende Arbeit entstand in der Zeit von Januar 2015 bis März 2018 am Lehrstuhl für Organische Chemie II des Departments Chemie und Pharmazie der Friedrich Alexander-Universität Erlangen-Nürnberg (FAU).

In loving memory of my grandparents

“Even a mistake may turn out to be the one thing necessary to a worthwhile achievement.”

Henry Ford

List of Abbreviations, Acronyms and Symbols

acac	acetylacetonate
AcOH	acetic acid
ACN, MeCN	acetonitrile
APPI	atmospheric pressure photo ionization
Ar	aryl
B3LYP	Becke, three-parameter, LeeYang-Parr exchangecorrelation functional
BS	bowl-shaped
Bu	butyl group
CDHF	cyclodehydrofluorination
cod	cyclooctadiene
conc.	concentrated
CV	cyclic voltammetry
CVD	chemical vapor deposition
d	day(s)
δ	chemical shift
dba	dibenzylideneacetone
DBATT	2.3,8.9-dibenzanthanthrene
DBPO	dibenzoyl peroxide
DBU	1,8-diazabicyclo[5.4.0]undec-7-ene
DCM	dichloromethane
DCTB	*trans*-2-[3-(4-*tert*-butylphenyl)-2-methyl-2-propenylidene]malononitrile
DDQ	2,3-dichloro-5,6-dicyanoparabenzoquinone
DEPT	Distorsionless Enhancement by Polarisation Transfer
DFT	density functional theory
DHB	2,5-dihydroxybenzoic acid
DMAc	dimethylacetamide
DMF	*N,N*-dimethylformamide
DMSO	dimethyl sulfoxide
dppf	1,1'-bis(diphenylphosphino)ferrocene
EI	electron impact
eq.	equivalent(s)
Et	ethyl
Et_2O	diethyl ether
EtOAc	ethyl acetate
EtOH	ethanol
ESI	electrospray ionization
FLC	flash liquid chromatography

FL	fluorescence (spectroscopy)
FT-	fourier transform
FVP	flash vacuum pyrolysis
h	hour(s)
HBC	hexabenzocoronene
HETCOR	HETeronuclear CORrelation
HMBC	Heteronuclear Multiple Bond Correlation
HOMO	highest occupied molecular orbital
HPLC	high-performance liquid chromatography
HSQC	Heteronuclear Single Quantum Coherence
HRMS	high-resolution mass spectrometry
hv	light, photonic energy
Hz	Hertz
IN	intermediate
IPr	1,3-Bis(2,6-diisopropylphenyl)-1,3-dihydro-2H-imidazol-2-ylidene
i-Pr	2-propanol
IR	infrared (spectroscopy)
IUPAC	International Union of Pure and Applied Chemistry
J	coupling constant (NMR)
λ	wavelength
LDA	lithium diisopropylamide
LDI	Laser Desorption Ionization (Mass Spectrometry)
LUMO	lowest unoccupied molecular orbital
m-	meta
M	molar
MALDI	matrix-assisted laser desorption/ionization
MAO	methylaluminoxane
Me	methyl
Mes	2,4,6-trimethylbenzene
MS	mass spectrometry
MeOH	methanol
MW	microwave (assisted experiments)
m/z	mass to charge ratio
min	minute(s)
NBS	*N*-Bromosuccinimide
NMR	Nuclear magnetic resonance
NOESY	Nuclear Overhauser effect spectroscopy
o-	ortho
OAc, AcO	acetoxy group
o-DCB	1,2-dichlorobenzene

OTf	triflate group
on	overnight
ORTEP	Oak Ridge Thermal Ellipsoids Plot
p-	para
PAH(s), PAK	polycyclic aromatic hydrocarbon(s)
PBB	pentabromobenzyl bonded silica
PBr	pentabromobenzyl bonded silica
PCC	pyridinium chlorochromate
$P(Cy)_3$	tricyclohexylphosphine
$Pd(PPh_3)_4$	tetrakis(triphenylphosphine)palladium(0)
Ph	phenyl
Pin	pinacol ester
P(*o*-tol)$_3$	tri(*o*-tolyl)phosphine
PPh_3	triphenylphosphine
ppm	parts per million
PPO	propylene oxide
PYE	pyrenylethyl
quant.	quantitative
RBF	round bottom flask
ROESY	Rotating frame nuclear Overhauser effect spectroscopy
t_R	retention time
rt	room temperature
SIPr	1,3-bis(2,6-diisopropylphenyl)-4,5-dihydroimidazolium
STM	scanning tunneling microscopy
t-	tert, tertiary
t-BuOK	potassium tert-butoxide
TBAB	tetrabutylammonium bromide
TEM	Transmission electron microscopy
TfOH	trifluoromethanesulfonic acid, triflic acid
THF	tetrahydrofuran
TLC	thin-layer chromatography
Tol	Toluene
TS	Transition state
UV/Vis	Ultraviolet-visible (spectroscopy)
X-ray	X-ray (crystallography), X-ray diffraction spectroscopy
XRD	X-ray powder diffraction
ZPE	Zero-point energy

Table of Contents

1 Advances in PAHs Chemistry

Buckybowls present the class of curved polycyclic aromatic compounds (PAH) that contain pentagons among six-membered rings responsible for their bowl shape geometry. These compounds can be considered as “fullerene fragments” or parts of the end-cap of carbon nanotubes. Other term that could be applied for buckybowls is ***geodesic polyarenes*** as they are units of geodesic structure of C_{60}.[1] Corannulene and sumanene are smallest representative members of this family. Corannulene comprises central five-membered ring surrounded by five fused hexagons and possesses C_{5v} symmetry[2], whereas sumanene is composed of central hexagon surrounded by three pentagons and three hexagons in an alternating fashion and possesses C_{3v} symmetry.[3],[4].

The first 17-step synthesis of corranulene **1.1** was reported by Barth and Lawton in 1966 providing target molecule **1.1** in overall 0.4% yield starting from acenaphthene **1.2**.[5],[6] In 1991 the group of Prof. L. Scott applied Flash Vacuum Pyrolysis (FVP) approach for the synthesis of corannulene **1.1** starting with 7,10-diethynylfluoranthene **1.4**.[7] Later they modified procedure to three steps synthesis starting from diketoacenaphthene allowing preparative production in multi milligram scale.[8] Independently, J. Siegel group presented a wet chemical approach to corannulene **1.1** from tetramethylfluoranthrene where a low valent titanium was used for ring closure yielding target product after oxidation by DDQ.[9],[10] Sygula and Rabideau found that corannulene can be synthesized by direct hydrolysis of 1,6,7,10-tetrakis(dibromomethyl)fluoranthene **1.6**.[11],[12],[13] Remarkable, following this route, Siegel *et al*. suggested an optimized kilogram-scale synthesis of corannulene **1.1** in 2012.[14] Apart from mentioned approaches the low valent vanadium coupling [15],[16] and nickel induced[12],[17] synthesis of corannulene derivatives were successfully conducted. All known approaches towards corannulene are summarized in Figure 1.

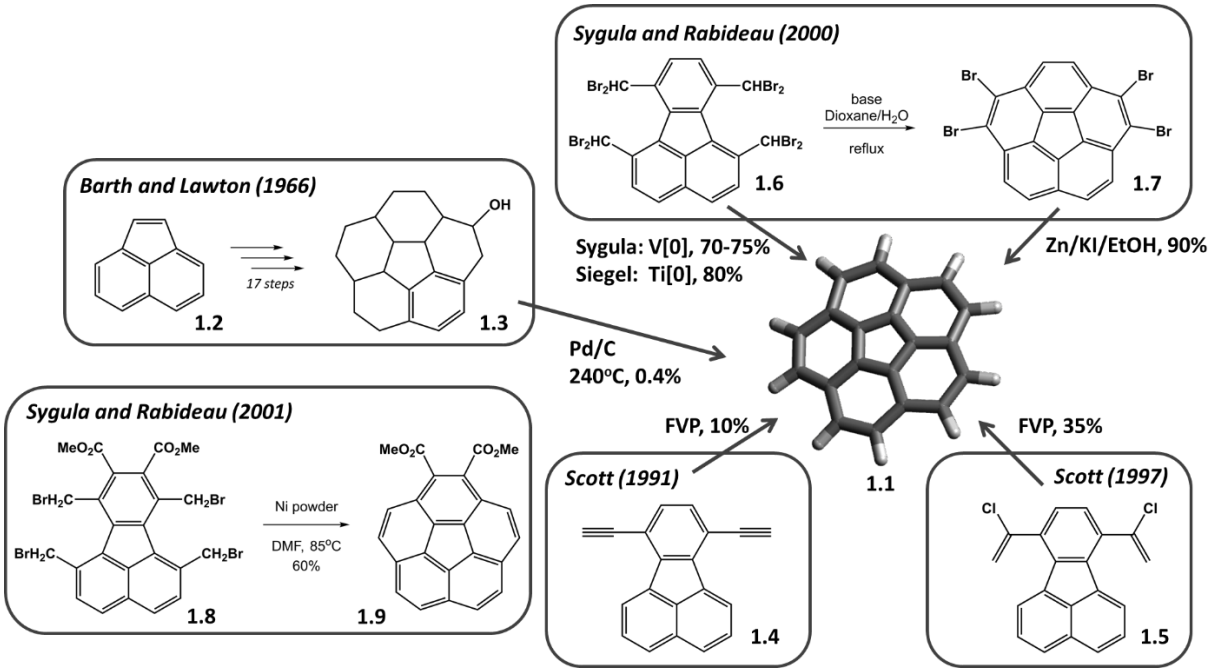

Figure 1. Synthetic routs towards corannulene **1.1**.[5],[7],[8],[10],[11],[12]

Attempts to obtain sumanene **1.13** starting from trinaphthotriphenylene[18], trindane[19] or trindene[20] derivatives were useless.[21] The first synthesis of sumanene was reported by Hirao *et al.* applying a four-step non-pyrolytic route, in which trimer of norbornadiene **1.11** underwent Ru-catalyzed tandem ring-opening/ring-closing metathesis reaction followed by dehydrogenation with DDQ leading to the target compound **1.13** in 70 % yield (Scheme 1).[3],[21]

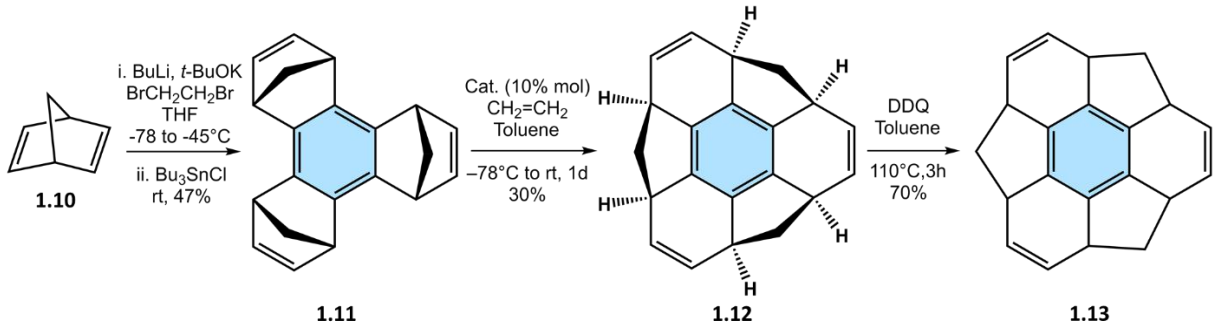

Scheme 1. Synthetic route to sumanene **1.13**. Catalyst $[P(C_6H_{11})_3]_2RuCl_2$=CHPh.[3]

A. Sygula and P.W. Rabideau explained the interest to buckybowls by following reasons:

- buckybowls possess accessible convex and concave surfaces; and it is possible to study exo vs. endo preferences of reactivity;
- buckybowls of different sizes and curvatures allow to investigate dependence of the reactivity on curvature;

- buckybowls are considered to be starting materials for further derivatization and synthesis of fullerenes, nanotubes and other carbon-based structures;
- buckybowls could be used as molecular receptors (host/guest chemistry).[22]

1.1. Nomenclature of Polycyclic Aromatic Hydrocarbons

The large library of polycyclic aromatic compounds was synthesized and characterized in pioneering works of Erich Clar,[23],[24] - the father of PAHs chemistry. Modern nomenclature of PAHs was approved by IUPAC,[25] but the terminology of regions on the polyarenes periphery (***bay***, ***cove***, and ***fjord***) is not included in the reported document (Figure 2).

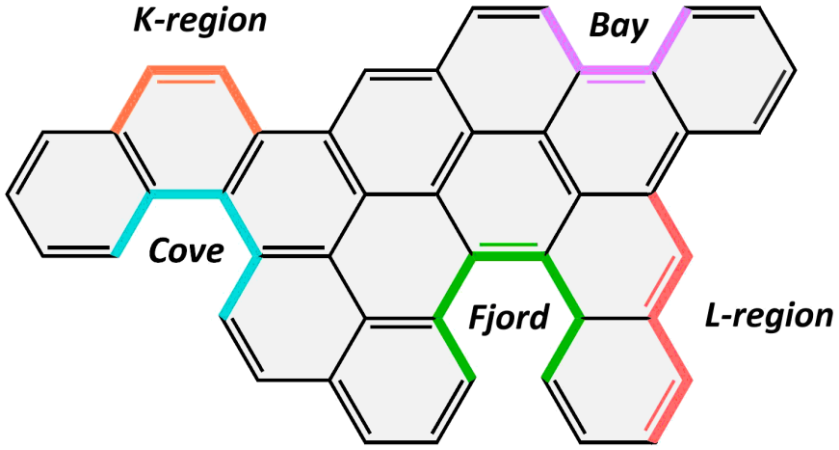

Figure 2. Topological regions in polycyclic aromatic compounds.

Bay regions are regions between two angularly fused aromatic rings that do not cause any remarkable perturbation of the pi-system whereas cove and fjord regions lead to the substantial molecular strain due to atom crowding. Fusion of additional benzene fragment close to the fjord region resulted in a molecule possesing helixe-like configuration.[25] Fjord-region closure leads to flat structures consisting of six-membered rings, whereas cove-region closure leads to the five-ring formation and resulting in bowl-shaped geometry of the molecule.[26] The K- and L-regions (Figure 2) can be described as peripheral armchair and zig-zag configuration corresponding to the phene- and acene-like motif respectively.[25],[27]

1.2 Synthetic Approaches towards Extended PAHs

1.2.1 Photocyclization

Photo-induced cyclization of stilbenes was extensively studied by Mallory *et al.*[28] The most prominent example is the conversion of 1,2-diphenylethene (stilbene) **1.14** into phenathrene **1.15** under UV-irradiation (Scheme 2).[28]

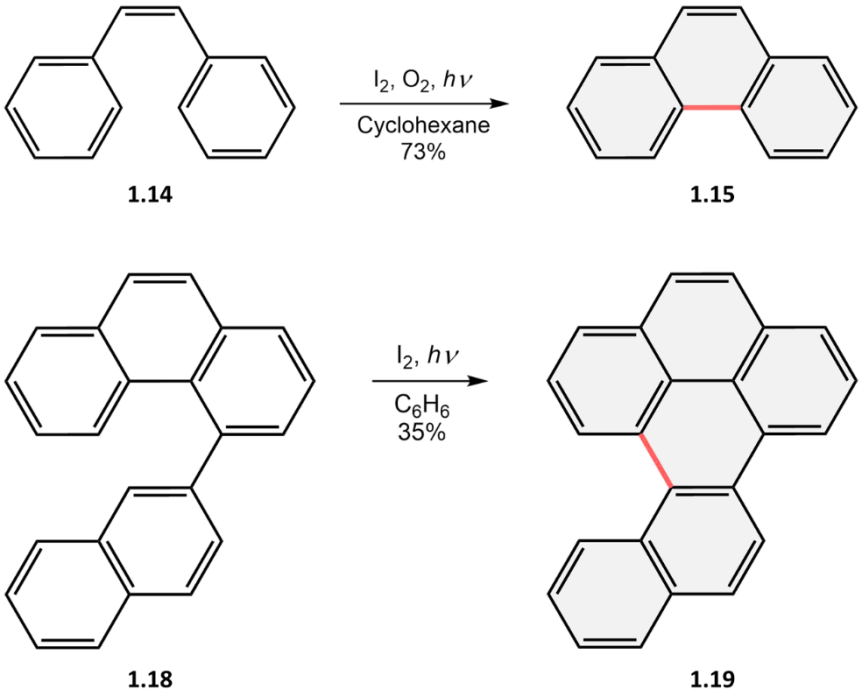

Scheme 2. Photochemical cyclization of a) 1,2-diphenylethene **1.15** and b) 4-(naphthalen-2-yl)phenanthrene **1.17**.[28],[29]

This reaction provides the facile access to large number of extended PAHs such as triphenylene **1.16** from *o*-terphenyl **1.17** (88 %)[30] or dibenzo[*ij,no*]tetraphene **1.18** (Scheme 2) from 4-(naphthalen-2-yl) phenanthrene **1.19** (35 %)[29]. In 1991 Katz *et al.* presented the improved conditions for the photocyclization, which allowed to reduce the influence of the hydrogen iodide on reaction yiedls and thus to avoid side reactions.[31] Propylene oxide was used as a scavenger for hydrogen iodide.[32] For instance, under Katz's conditions the respective stilbene was converted to 87 % of 9-bromodinaphtho[*2,1-c:1',2'-g*]phenanthrene after 1.2 h and under Mallory's conditions to 66 %[31].

Twieg *et al.* reported that fluorinated stilbenes underwent ring closure *via* HF-elimination (photocyclodehydrofluorination) under Mallory conditions (Scheme 3).[33]

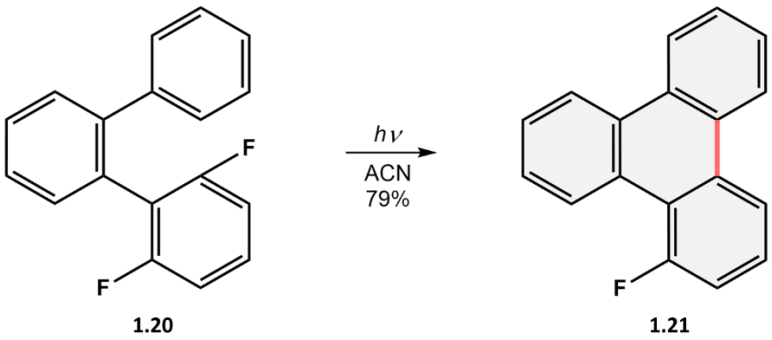

Scheme 3. Photocyclodehydrofluorination of 1-fluorotriphenylene-2,6-difluoro-1,1':2',1''-terphenyl **1.20**.[33]

Photochemical method was also applied for the synthesis of extended PAHs , for instance, contorted hexabenzocoronene **1.23** was obtained by photocyclization in yield close to 100 % (Scheme 4)[34] and contorted octabenzocircumbiphenyl – in 83 % yield[35].

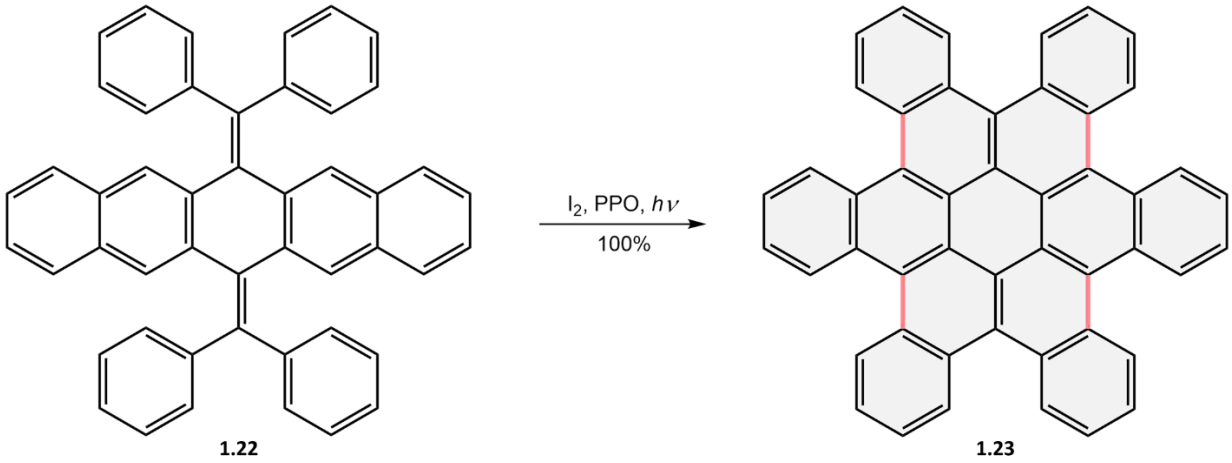

Scheme 4. Synthetic pathway to contorted hexabenzocoronene **1.23**.[34]

However, the photocyclization approach was found to be not applicable for pentagon formation and in general not effective for the synthesis of non-alternant PAHs bearing pentagons in the structure.

Attempt to synthesize non-alternant PAHs by oxidative photocyclization was carried out in the group of Prof. Agranat. [36] After first step of photocyclization (Scheme 5a, Scheme 5b) products **1.25** and **1.27** were formed in 50 % yield (both reactions), although, the next step was unsuccessful in both cases.

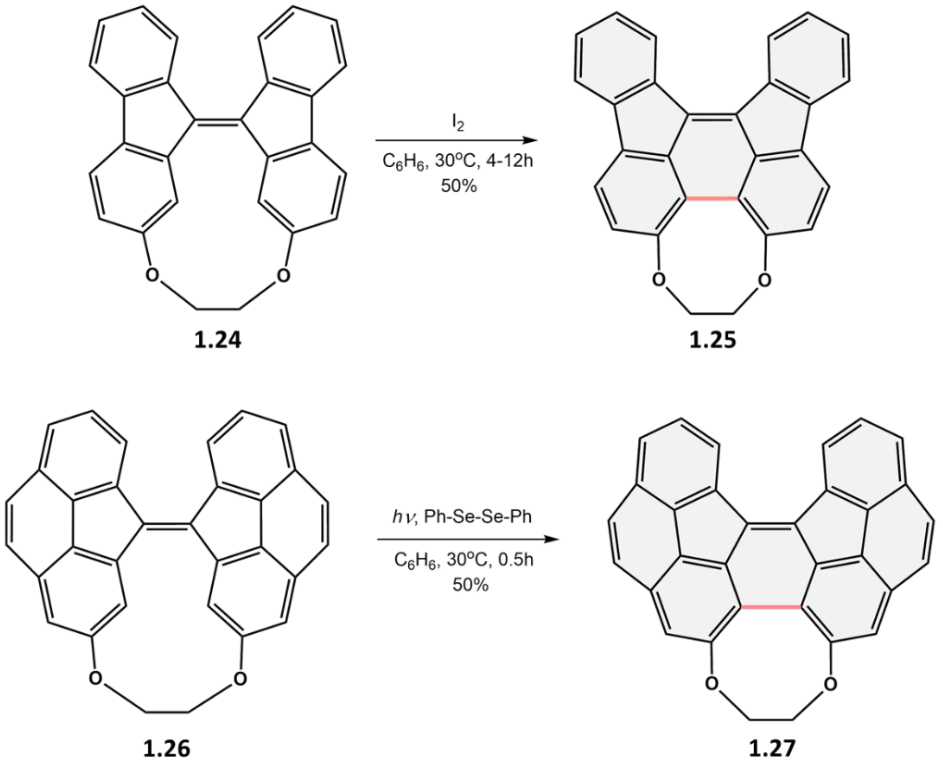

Scheme 5. Oxidative photocyclization of ylidene derivatives **1.25** and **1.27**.[36]

1.2.2 Oxidative Cyclodehydrogenation – "Scholl Reaction"

The Scholl reaction [37] is widely used for the synthesis of large PAHs. Typically, Scholl cyclodehydrogenation is carried in presence of such reagents as $AlCl_3$, $MoCl_5$, $FeCl_3$ or DDQ + Brønsted (or Lewis) acid.[38] A demonstrative example of Scholl reaction is the synthesis of hexabenzocoronene **1.29** (Scheme 6) and its derivatives from respective hexaphenyl benzene derivatives[38]. Moreover, Scholl reaction appears to be a powerful tool for the synthesis of very large PAHs – the so called nanographenes, which could be considered as a model of graphene. The approach often provides the desired planar nanographenes with good to excellent yield. Thus, for example a "Giant 222 Carbon" PAHs was prepared utilizing $Cu(CF_3SO_3)_2/AlCl_3$ in CS_2 in 62 % yield.[39]

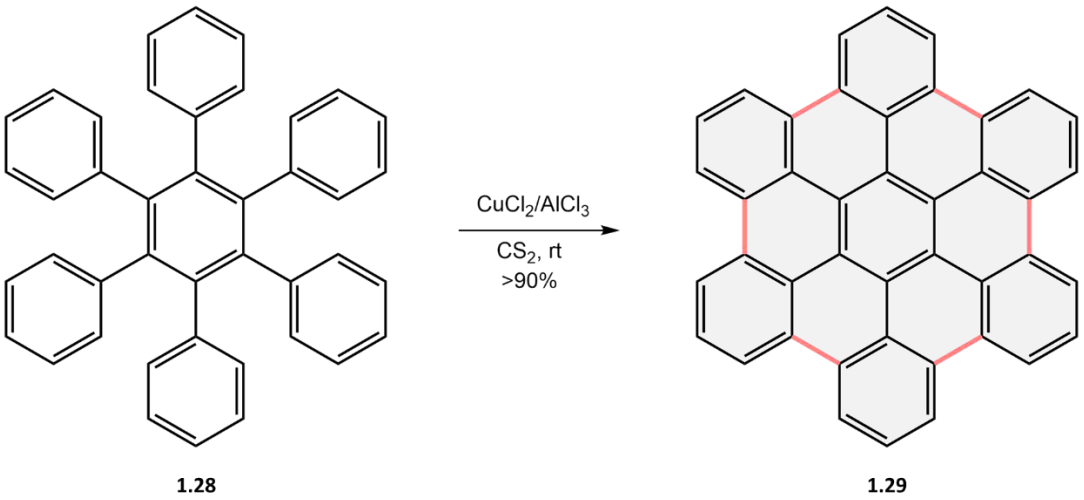

Scheme 6. Cyclodehydrogenation of hexaphenylbenzene **1.28** towards hexabenzocoronene **1.29**.[38]

The formation of non-hexagonal ring under Scholl reaction is rare. However, recent studies demonstrated the general possibility of five-membered ring formation under Scholl conditions. Thus, Kawamura *et al*. presented the synthesis of rubicene **1.31** with 80% yield from 9,10-diphenylanthracene **1.30** in the presence of DDQ/TfOH in dry DCM (Scheme 7).[40]

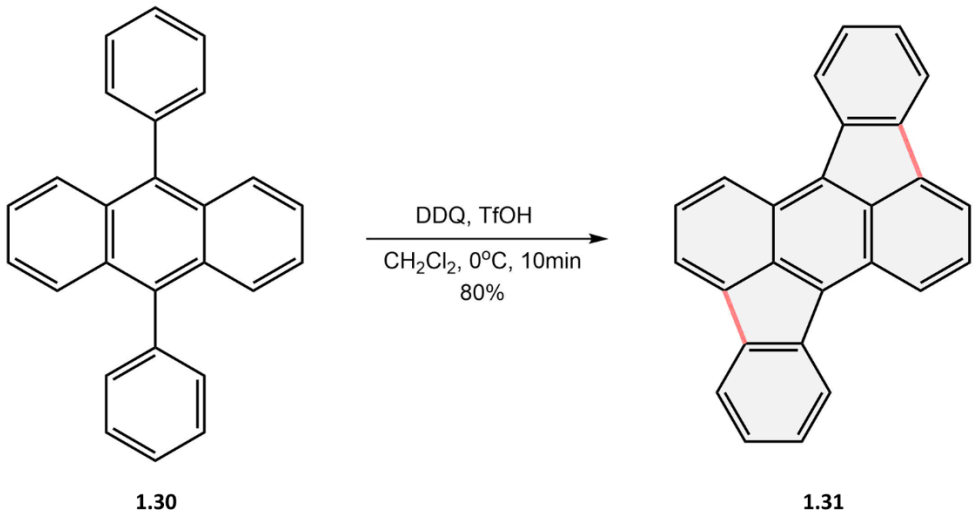

Scheme 7. Synthesis of rubicene **1.31** under Scholl conditions.[40]

Müllen *et al.* succeeded in the synthesis of an extended rubicene derivative **1.32** from tetraphene **1.33** under specially optimized reaction conditions, preventing side reactions.[41] Note that the formation of strained PAH by Scholl approach in general is difficult and frequently accompanied by the rearrangement of the carbon skeleton as a result of the cationic (cation-radical) nature of the intermediates.[38,42]

1.2.3 Flash Vacuum Pyrolysis

In contrast to Scholl or Mallory cyclodehydrogenations a Flash Vacuum Pyrolysis approach consisting in the heating of molecule in the gas phase for a very high temperatures (up to 1300 ºC) for a very short time (10^{-3} to 10^{-4} s) allows to synthesize a wide-range of non-planar PAHs including highly strained fullerenes C_{60}[43], C_{78}[44] and C_{84}[45]. In 1991 Scott's group presented the successful synthesis of corannulene **1.1** from diethynylfluoranthen **1.4** by FVP (Figure 3).[7] Later the same group developed a facile three-step synthesis of corannulene from 7,10-bis(1-chlorovinyl)fluoranthene **1.5** providing the desired corannulene **1.1** in gram amounts (Figure 3).[8]

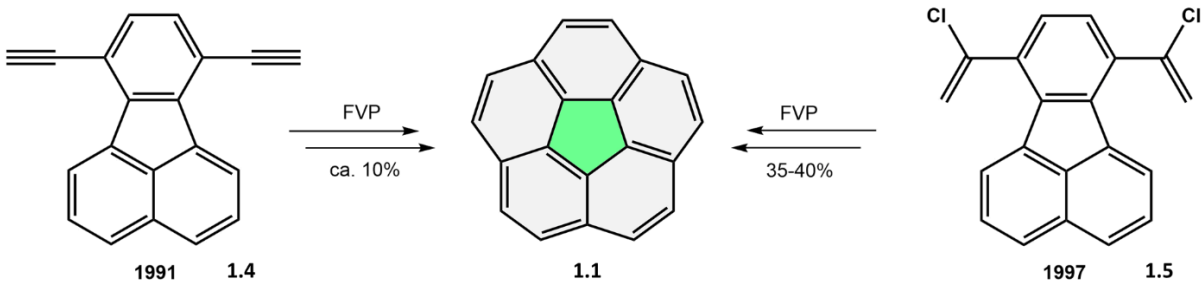

Figure 3. Synthetic approaches to corannulene **1.1** by FVP.[7],[8]

Shortly after it was discovered that the introduction of the halogen atoms such as chlorine or bromine into the regions where the formation on new C-C bond is desired remarkably increases the reaction's efficiency. This optimization allows to prepare wide range of various bowl-shaped PAHs by FVP.[46],[47]

Several representative syntheses are depicted on the Figure 4. Thus, benzo[*ghi*]fluoranthene $C_{26}H_{12}$ **1.32** was synthesized by two-fold cyclization of **1.33** in 12%.[48]

Tetrabenzopyracylene $C_{26}H_{12}$ **1.34** was produced from brominated bifluorenylidenes **1.35** with 25-35 % yield. [49], [50] Triindenotriphenylene $C_{30}H_{12}$ **1.37** was obtained via triple ring closure of brominated tribenzo[*c,i,o*]triphenylene **1.36** (2-3%).[51] Later Sygula et al. reported the synthesis of **1.37** with 5-10% yield by the pyrolysis of chlorinated trisfulvene **1.38**.[52]

The Scott's group succeeded in the synthesis of larger bowl - circumtrindene $C_{36}H_{12}$ **1.40** - by FVP route (Figure 4). Three-fold cyclodehydrochlorination of precursor **1.39** yielded 25-27 % of product **1.40** .[53],[54]

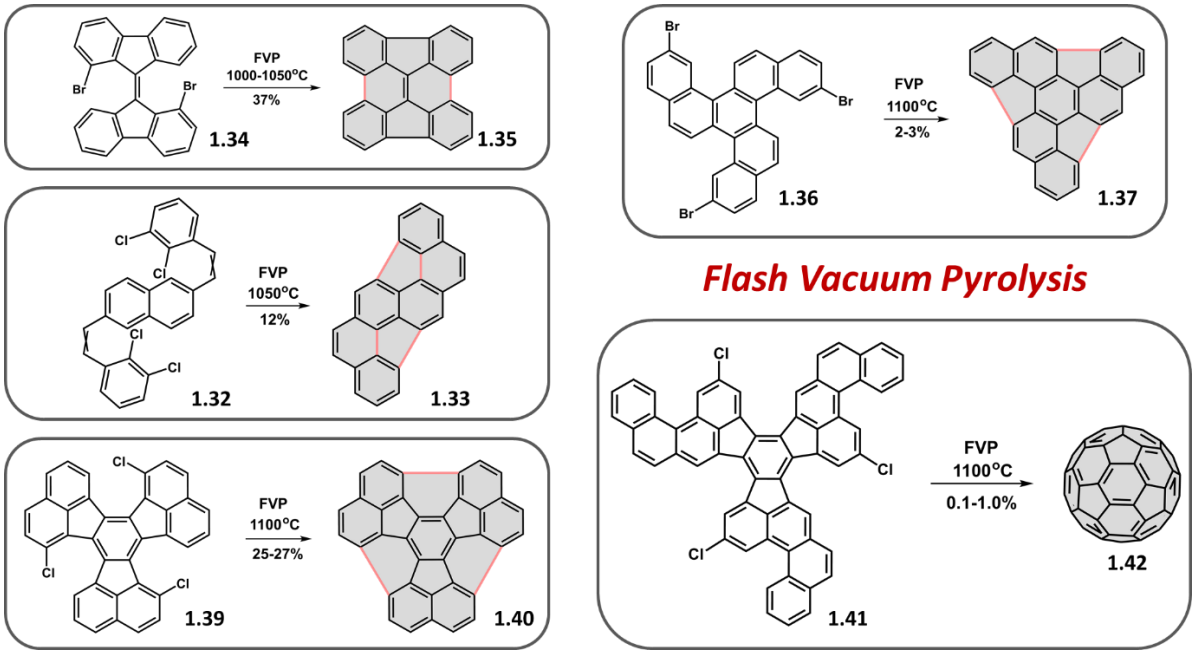

Figure 4. Selected buckybowls obtained by FVP approach.[48],[49],[50], [51], [53], [54],[55],

As a logical consequence of the success of FVP in the synthesis of bowl-shaped PAHs the several attempts were undertaken to synthesize buckminsterfullerene C_{60}. The extended chlorinated decacyclene **1.41** [55] (Figure 4) and the hexamer of naphthalene **1.43** [43] were suggested as possible precursors. In both cases only small amounts of C_{60} **1.42** were observed.

These results demonstrate the limitation of FVP for the synthesis of large systems, which is mainly connected with difficulties to bring large precursor molecules into the gas phase without decomposition at the typical for FVP (1-10 mbar) pressure.

1.2.4 Palladium-Catalyzed Arylation

Direct intramolecular Pd-catalyzed arylation appears to be an alternative way for the synthesis of buckybowls. Commonly, halogenated and triflated precursors undergo transformations in presence of Pd(II) complexes at the mild temperatures (100-170°C) in DMF or DMAc medium.[56]

Synthesis of benzo[*ghi*]fluoranthene from aryl triflates **1.43** or bromides **1.45** was reported by Wang and Shevlin (Scheme 8).[57] $Pd(PPh_3)_2Cl_2$ and $Pd(PCy_3)_2Cl_2$ appeared to be excellent catalysts which afforded targeted product **1.44** in high yields (80-90 %).

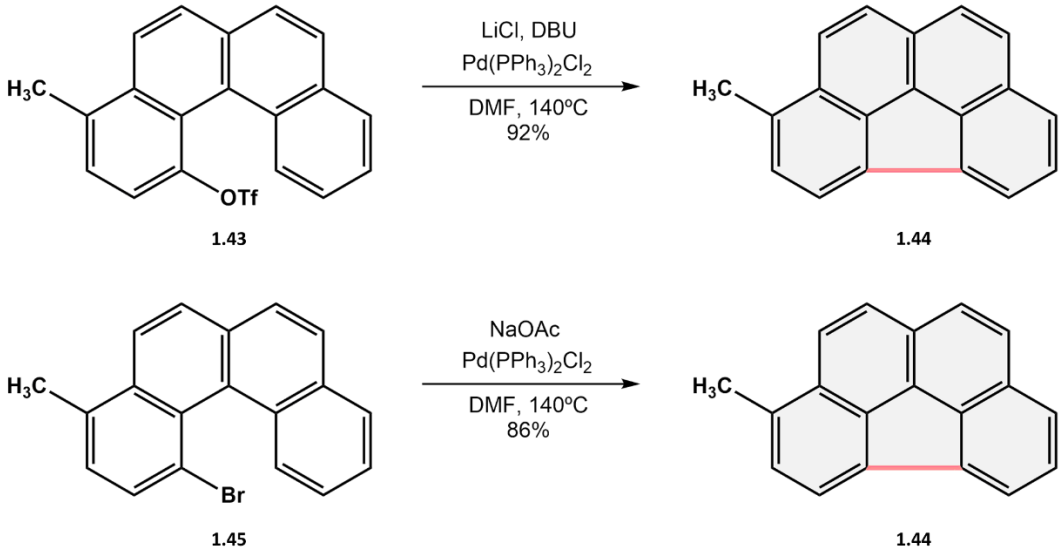

Scheme 8. Palladium-mediated intramolecular coupling of methylbenzo[*c*]phenanthrene **1.43** and **1.45** derivatives.[57]

This approach was also applied for the double palladium-mediated cove region closure yielding bowl-shaped indacenopicenes **1.47** with up to 90 % yield (Scheme 9).[58]

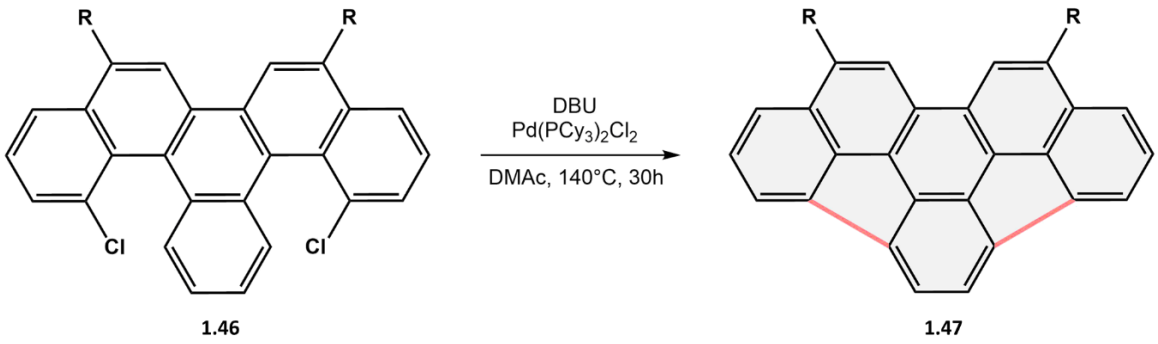

Scheme 9. Palladium-mediated intramolecular coupling of dichlorobenzo[*s*]picene derivatives (R=CH_3, 91 %, R=OCH_3, 70 %).[58]

Scott et al. described synthesis of di-, tri and tetraindenopyrenes from respective brominated pyrene derivatives. For instance, the reaction of 1,6-bis(2-bromophenyl) pyrene **1.48** in presence of $Pd(PPh_3)_2Cl_2$-DBU system gave the desired product **1.49** in 44 % yield (Scheme 10).[59]

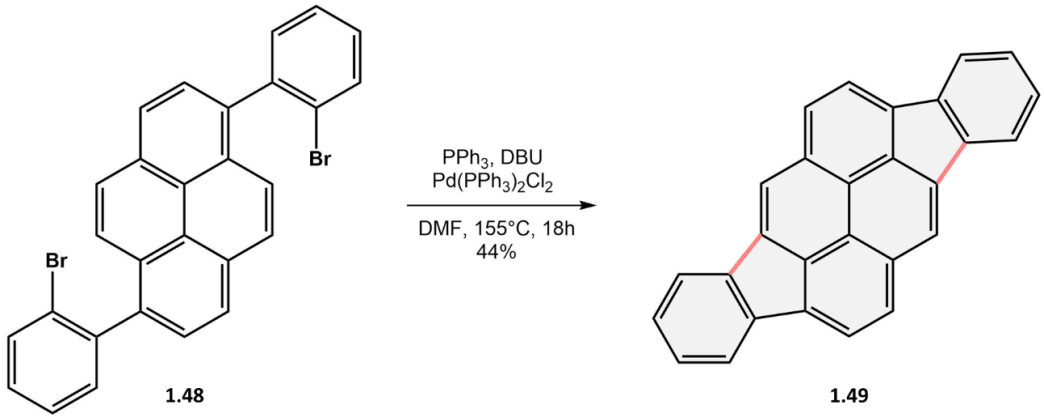

Scheme 10. Palladium-mediated synthesis of diindeno[*1,2,3-cd:1',2',3'-jk*]pyrene **1.49**.[59]

Attempt to extend the approach to tetraindenopyrene **1.51** by one-pot procedure provided dissapointed low yield (1 %), and the improvement of the reaction conditions did not increase the conversion (Scheme 11).[59]

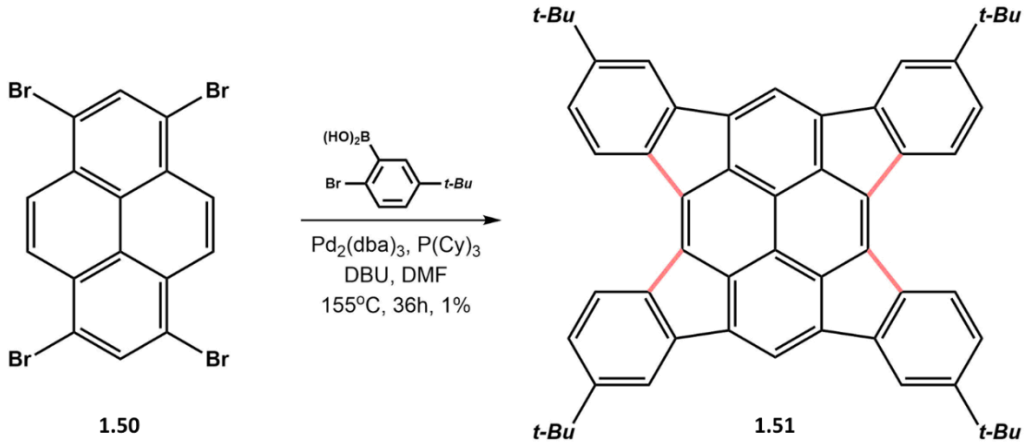

Scheme 11. Palladium-mediated synthesis of 2,7,11,16-tetra-tert-butyltetraindeno[*1,2,3-cd:1',2',3'-fg:1'',2'',3''-jk:1''',2''',3'''-mn*]pyrene **1.51** in DMF ($Pd_2(dba)_3$, $P(Cy)_3$, 2-bromo-5-tert-butylbenzeneboronic acid, DBU, 155 °C, 36 h, 1 %).[59]

Nevertheless, the Scott's group achieved significant results in the synthesis of extended corannulene derivatives utilizing microwave heating (Scheme 12). Thus, pentaindenocorannulene **1.53** ($C_{50}H_{20}$) and tetraindeno-corannulene **1.55** ($C_{44}H_{18}$) were obtained in 35 % and 15 % yield respectively.[60],[56]

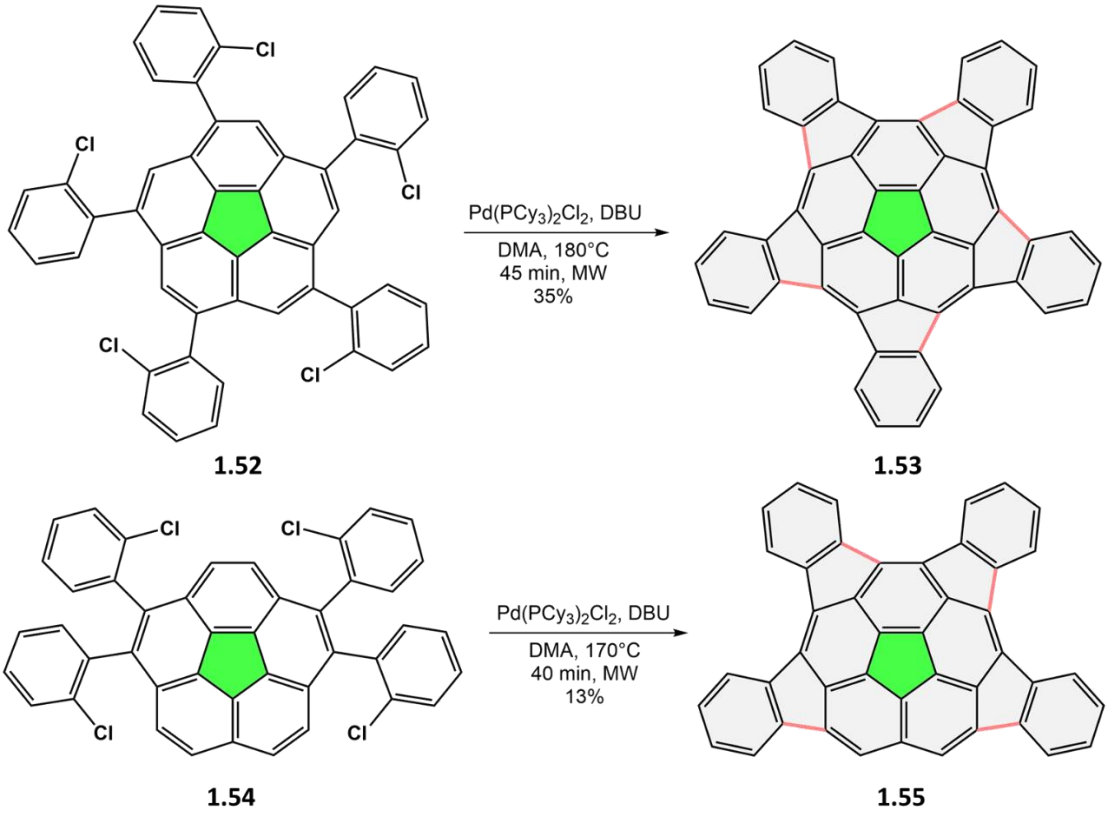

Scheme 12. Synthesis of pentaindenocorannulene **1.53** and tetraindenocorannulene **1.55** by microwave assisted Pd-catalyzed arylation reaction.[60]

1.2.5 Surface-Assisted Cyclodehydrogenation

Surface-catalyzed cyclodehydrogenation processes attracted attention of researches in the last years since this method allows the effective transformation of non-functionalyzed precursors into various nanostructures including fullerenes[61], nanotubes[62] and nanoribbons[63]. The first example of the synthesis of bowl-shaped PAH by cyclodehydrogenation was reported by Flynn and Nuckolls demonstrating the formation of a hemispheres from hexabenzocoronene on the ruthenium surface.[64]
The formation of hemisphere **1.57** was conducted by thermal activation of **1.23** on Ru(0001) surface and visualized by means of Scanning Tunneling Microscopy (STM).[64],[65] Annealing of precursor **1.23** was carried out at 750 K (Scheme 13).[64]

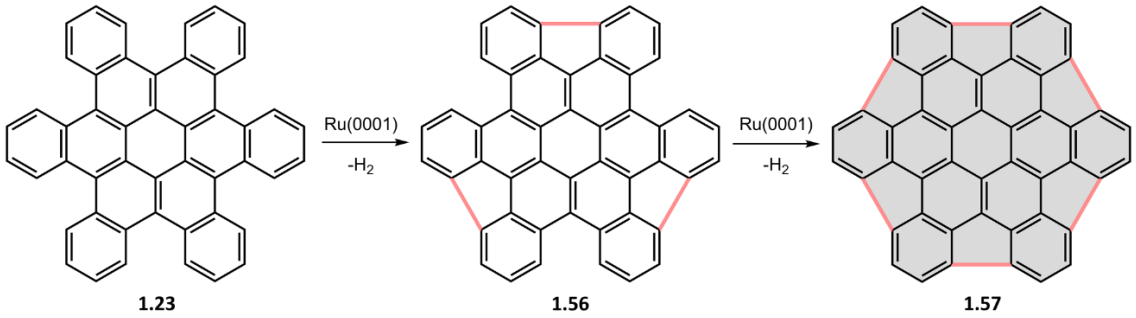

Scheme 13. Proposed stages of HBC **1.57** dehydrogenation on Ru(0001) surface.[64]

Later, syntheses of fullerenes C_{60} **1.42** [66], C_{84} **1.60** [66] and heterofullerene $C_{57}N_3$ **1.62** [61] from respectively preprogrammed precursors $C_{60}H_{30}$ **1.58**, $C_{84}H_{42}$ **1.59** and $C_{57}N_3H_{30}$ **1.61** (Figure 5) were successfully conducted on Pt(111) surfaces.

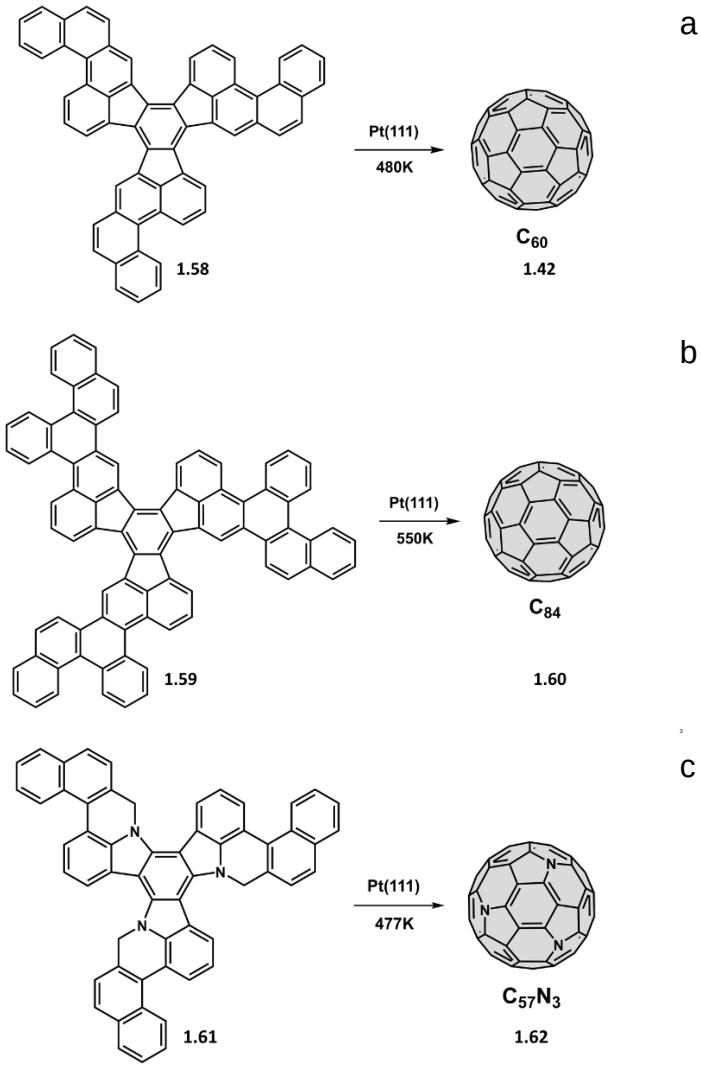

Figure 5. Precursors **1.58** (a)[66], **1.59** (b)[66] and **1.61** (c)[61] for surface-assisted cyclodehydrogenation.

Annealing was carried out at the temperature in range of 477-550 K. However, this approach is limited for picomole amount synthesis and can not be extended to the preparative scale.

1.3 C-F Bond Activation in Aromatic Compounds

Carbon-fluorine bond is the strongest single bond to carbon, thus its activation is in general a challenging task for organic chemistry.[67],[68] As a result of high stability the C-F bond cleavage typically requires harsh reaction conditions, which do not tolerate functional groups and lead to the low selectivity of the reaction.[67],[69],[70],[71],[72] Therefore, the improvement and exploration of mild conditions for transformation of aromatic C-F bond are continuously investigated by numerous scientific groups.[69],[72],[73]

1.3.1 Ni- or Pd-Catalyzed Reactions

Kumada *et al.* [74] published the study of cross-coupling reaction of organic halides with Grignard reagents in the presence of Ni catalyst and demonstrated the efficiency on several examples.[75],[76],

For instance, $Ni(acac)_2$/SIPr-HBF_4 and/or $Ni(cod)_2$/IPr systems were found to be effective in C-F bond activation providing the selective aryl-aryl coupling already at the room temperatures (Scheme 14).[75]

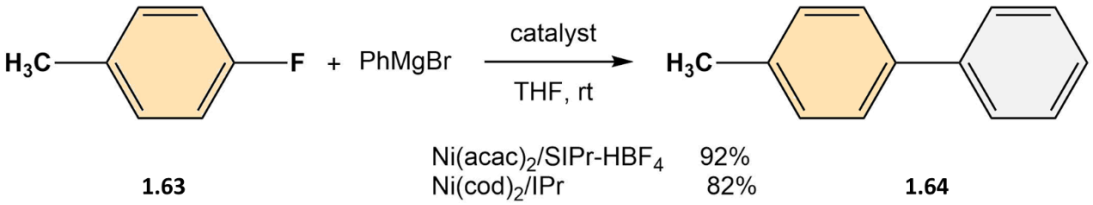

Scheme 14. C-F bond activation and selective C-C bond formation in presence of Ni catalyst.[75]

In 2005 Tamao *et al*. reported the successful C-F bond activation of mono-, di- and trifluoroarenes in presence of $NiCl_2$(dppf) catalyst in THF at the room temperature (Scheme 15).[76]

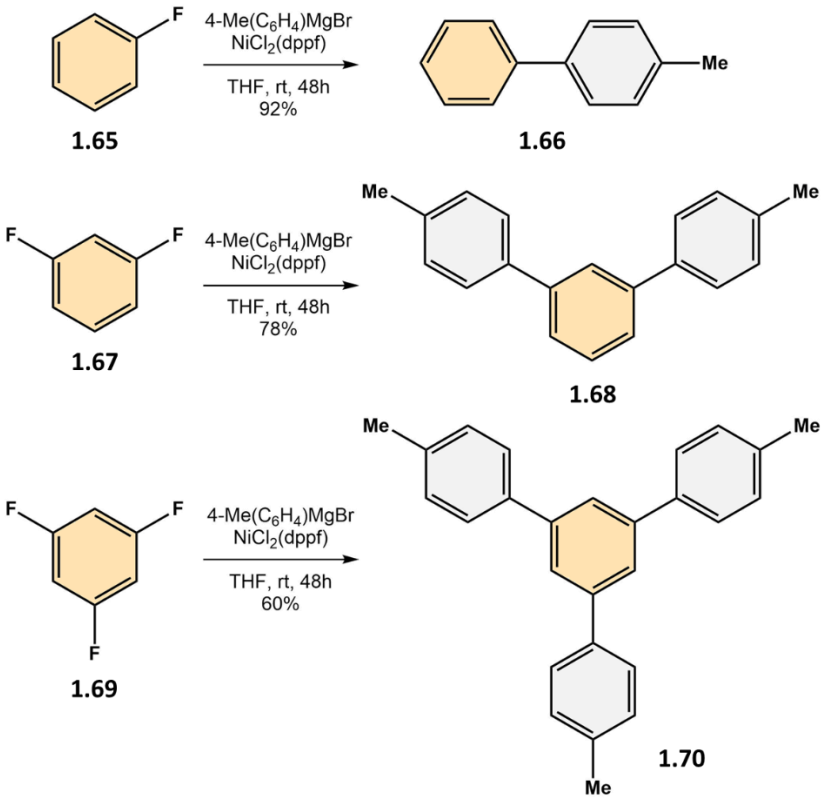

Scheme 15. C-F bond activation and C-C bond formation in presence of $NiCl_2$(dppp) catalyst.[76]

It was also demonstrated that perfluoropyridyl and pyrimidyl Ni complexes with PEt_3 ligands selectively activated the C-F bond tolerating the C-Cl bond.[77],[78] To improve catalytic activity Nakamura *et al.* applied hydroxy phosphine ligand that promoted reaction and yielded 93 % of the product.[79]

Similar transformations were also demonstrated using Pd-catalyst. For instance, $PdCl_2$(dppf) provided partial coupling of di- and trifluorobenzenes with Gringnard reagent.[76] Thus, cross-coupling of 1,2-difluorobenzene with Gringnard reagent gave product **1.72** in 91 % yield (Scheme 16). The same catalytic system was applied to 1,3- (**1.73**) and 1,4-difluorobenzenes (**1.74**), but the products of cross-coupling were obtained in significantly lower yields (15 and 6 % respectively). Reaction of 1,2,3-trifluorobenzene **1.75** with aryl Grignard reagent afforded mostly mono-coupled product **1.76** in 69 % yield.[76]

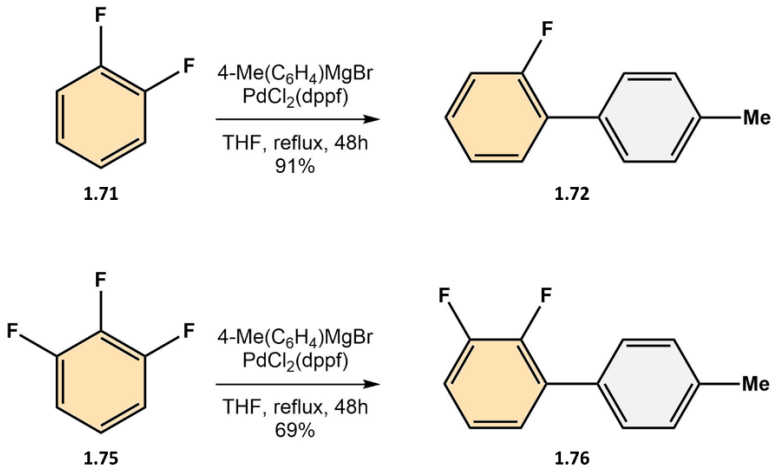

Scheme 16. C-F bond activation and C-C bond formation in presence of $PdCl_2$(dppf) catalyst.[76]

It was found that introduction of hydroxy, hydroxymethyl and amino groups in *ortho*-position to fluorine atom in aromatic compounds improves cross-coupling reactions (Scheme 17).[80]

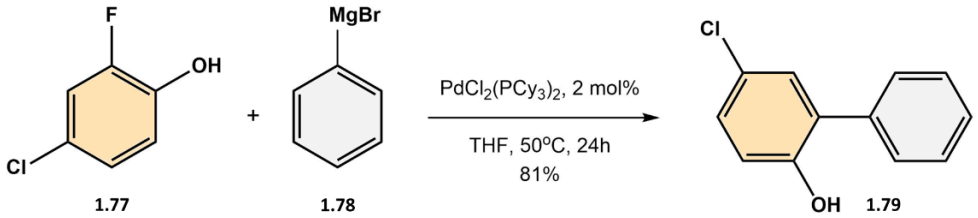

Scheme 17. C-F bond activation and C-C bond formation in presence of $PdCl_2(PCy_3)_2$ catalyst.[80]

Ortho-nitro and carboxyl substituents in fluoroaromatics also promote C-F bond activation in Suzuki-Miyaura and Stille cross-coupling (Scheme 18).[81],[82],[83],[84]

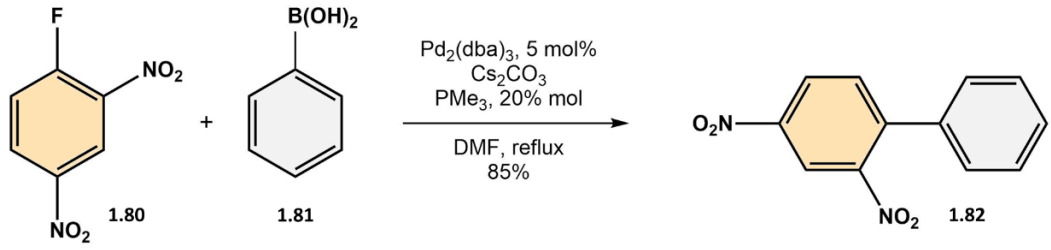

Scheme 18. C-F bond activation and C-C bond formation in presence of $Pd_2(dba)_3$ catalyst.[81]

1.3.2 C-F Bond Activation in Difluoroalkenes

Ichikawa and co-workers developed a new approach of C-F bond activation in 1,1-difluoroallenes derivatives allowing synthesis of various PAHs. Previously, they reported that treatment of 2-benzyl-1,1-difluorohex-1-ene with Magic acid

($FSO_3H{\cdot}SbF_5$) or TfOH in the $(CF_3)_2CHOH$ medium promoted Friedel-Crafts cyclization and gave 2-butyl-1-indanone with up to 72 % yield.[85] In this case the Magic acid was found to be selective protonating agent leading to the effective generation of the difluorocarbocation which attacks the neighboring aromatic system resulting in desired C-C bond formation.

The methodology was found to be powerful enough to prepare helicenes. Moreover, domino-like Friedel-Crafts-type cyclization allows formation of fused ring systems in a facile way with high yields (Scheme 19).[86]

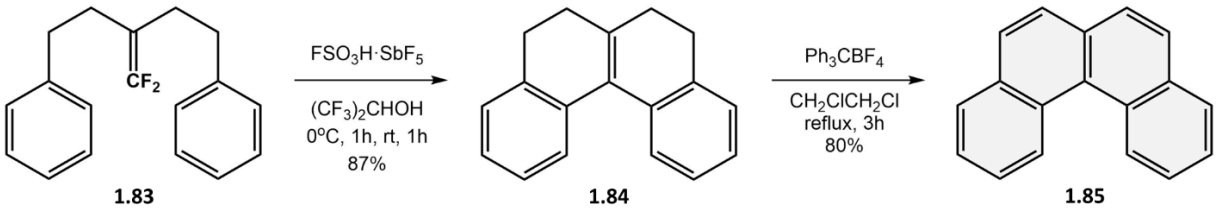

Scheme 19. Domino cyclizations of difluoroalkene derivative **1.83** by Magic acid.[86]

The similar conditions were applied for the synthesis of dibenzo[*g,p*]chrysenes bearing double helical structures. A wide range of Brønsted and Lewis acids was tested as promoters of Friedel-Crafts-type cyclization.[87] Reaction of 1,1-bis(biphenyl-2-yl)-2,2-difluoroethene with TsOH, TfOH and Magic acid was carried out in $(CF_3)_2CHOH$. The formation of product **1.87** was not observed utilizing TsOH, while TfOH and Magic acid gave product **1.88** in 59 and 95 % yield respectively. Among the Lewis acids $BF_3{\cdot}OEt_2$, Me_3SiOTf, ZrF_4, $TiCl_4$ and TiF_4 in $(CF_3)_2CHOH$ only TiF_4 promoted cyclization in 93% yield (Scheme 20). Remarkably, the reaction of 1,1-bis(biphenyl-2-yl)-2,2-difluoroethene **1.86** with TiF_4 in DCM gave the monocyclizated product in 85% yield.[87]

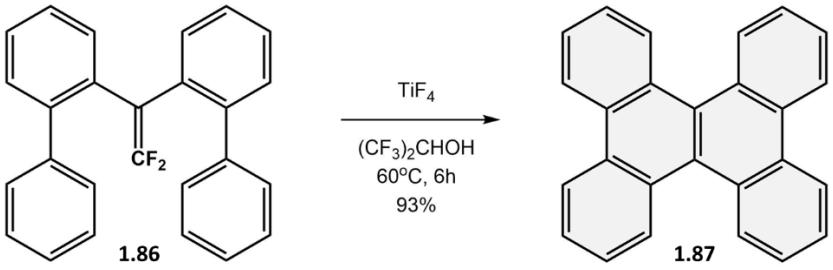

Scheme 20. Synthesis of dibenzo[*g,p*]chrysene **1.87** in presence of TiF_4.[87]

Magic acid and TiF_4 were used for synthesis of substituted dibenzo[*g,p*]chrysenes. According to obtained data, TiF_4 was more effective for alkyl- and aryl-substituted precursors whereas magic acid for halogen-substituted substrates.[87] It should be

emphasized that all experiments were carried out in $(CF_3)_2CHOH$, which provides stabilization of CF_2 cation.[86],[88],[89],[90]

Ichikawa et al. also found that catalytic amount of *indium(III) bromide* promoted formation of allylic CF_2 cations in 1,1-difluoroallenes. The subsequent Friedel-Crafts cyclization afforded the fluorinated PAHs in appropriate yields (for example, 90 % yield of 9-fluorophenanthrene).[91]

1.3.3 C-F bond Activation by Silylium Carboranes

Siegel and co-workers presented different approach of C-F bond activation by *silyl cations (silylium carboranes)* and subsequent intramolecular Friedel-Crafts cyclization in cove region.[92],[93] To optimize Friedel-Crafts reaction conditions 1-(2-fluorophenyl)naphthalene **1.88** was chosen as model compound, which was treated by different silyl cations in presence of Brønsted bases (P(*o*-tol)$_3$, 2,6-di-*t*Bu-pyridine or $Me_2Si(Mes)_2$) in chlorobenzene medium for 8 to 17 h at 110 ºC (Scheme 21).[92] The best yield (93 %) was obtained in system *i*-Pr_3Si-$CB_{11}H_6Cl_6$/Me_2SiMes_2. These reaction conditions were employed for synthesis of PAHs containing the five- and six-membered rings and the yields were in range 49-99 %. Small molecules, such as 2-fluoro-*o*-terphenyl and its derivatives showed full conversion to products, whereas the transformation of large PAHs (1,2-benzofluoranthene, rubicene, indenocorannulene) was more difficult to perform.[92]

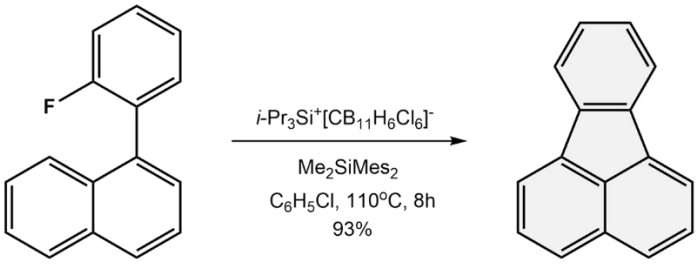

Scheme 21. C-F bond activation by silyl cations and intramolecular Friedel-Crafts cyclization.[92]

Siegel et al. applied silane-fueled Friedel-Crafts cyclization for synthesis of the buckybowls-graphene hybrid “nanobud” **1.92**[94] that conjugates planar graphene nanosheet with curved surface of corannulene. Synthesis of target molecule started from diester dichlorocorannulene **1.90** and included six stages. Microwave-assisted C-F bond activation by silylium carborane gave a product **1.92** in 40 % yield (Scheme 22).[95]

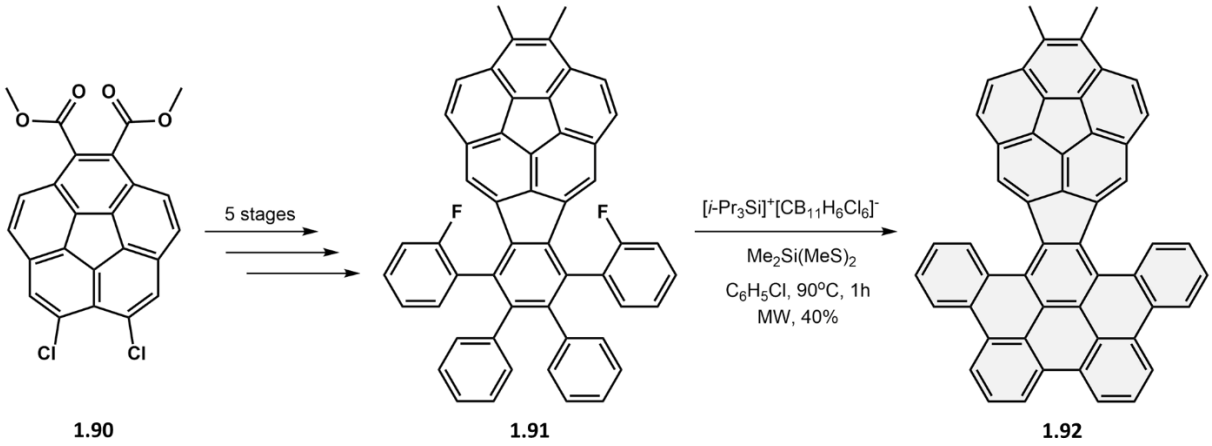

Scheme 22. Synthesis of buckybowl-graphene "nanobud" **1.92**.[95]

1.3.4 Aluminium Oxide Mediated C-F Bond Activation

Amsharov and co-workers suggested Al_2O_3-mediated HF elimination, which leads to intramolecular aryl−aryl coupling in fjord and cove regions of PAHs in quantitative yields.[96],[97] Condensation of PAHs was carried out on activated *γ*-Al_2O_3; and a wide range of fluoroarenes underwent cyclization at 100-250 ºC. It was found that effective condensation depends on pretreatment activation of *γ*-alumina.[98] Activation promotes formation of highly reactive Al-O sites or "defects" on alumina[98],[99],[100]

Activity of other oxides towards C-F bond activation was investigated on 1-fluorobenzo[*c*]phenanthrene **1.93** and 1,4-bis(biphenyl-2-yl)-2,5-difluorobenzene **1.95**. 1-fluorobenzo[*c*]phenanthrene **1.93** which were chosen as model compounds for mono-fold cyclization (300°C, 10 min)[97], and 1,4-bis(biphenyl-2-yl)-2,5-difluorobenzene **1.95** – for two-fold (400°C, 10 min)[101] cyclization (Scheme 23). In case of SiO_2, Ga_2O_3, In_2O_3, Nb_2O_5, and HfO_2, trace amounts of the product **1.94** were detected. For BeO, B_2O_3, MgO, Sc_2O_3, TiO_2, ZnO, GeO_2, ZrO_2 and SnO no product formation was observed.[97] In case of double-fold cyclization oxides such as Eu_2O_3, Sc_2O_3, Gd_2O_3, Dy_2O_3, and V_2O_5 were found to be inactive, whereas low activity was found for MgO, HfO_2, and Yb_2O_3. The most active oxides appeared to be TiO_2, In_2O_3, and ZrO_2; and a moderate degree of activation were presented by SiO_2, Ga_2O_3, and Nb_2O_5.[101]

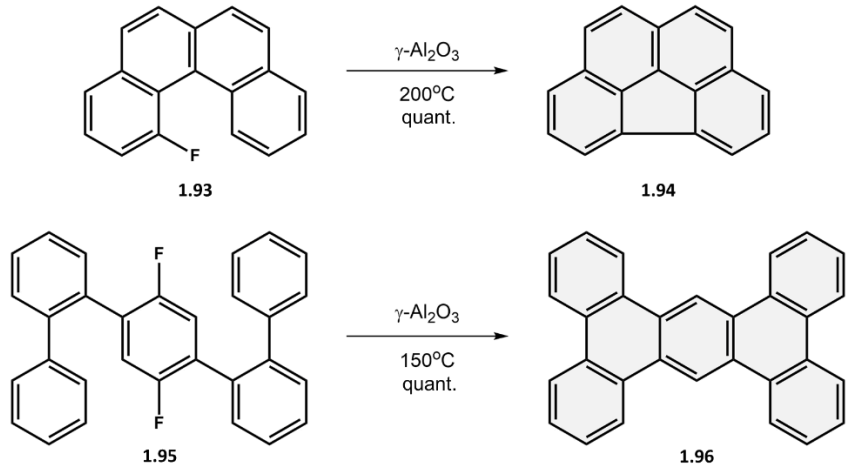

Scheme 23. Examples of mono[97] and double[101] aryl-aryl coupling *via* Al_2O_3-mediated cyclo-dehydrofluorination.

Aryl-aryl coupling via HF elimination on aluminium oxide was carried out for large bowl-shaped system and even in this case yields were near to quantitative. Remarkably, no evidence of side reactions was observed during condensation and no further purification of products was required.[102] Moreover, reaction is tolerant to halogen functionalities, thus, chlorinated and brominated phenanthrenes (2-chlorobenzo[*c*]phenanthrene and 2-bromobenzo[*c*]phenanthrene) remain completely intact during condensation.[100]

1.3.5 C-F Bond Activation in Trifluoromethylated Arenes

While sp^2 C-F bond activation was studied broadly, in sp^3 C-F bond activation was achieved less success. However, there are known few examples of the conversion of sp^3 C-F bonds into C-C bond. For instance, Nbº species, which can be generated by reduction of $NbCl_5$ with lithium aluminium hydride, are the convenient catalysts for intramolecular C-C coupling reaction of *o*-aryl and *o*-alkenyl α,α,α-trifluorotoluene derivatives (Figure 6).[103],[104],[105] Organoaluminium reagents, such as trimethylaluminium, triethylaluminium or methylaluminoxane $(MeAlO)_n$ were found to be efficient catalysts for the C-F bond activation (Figure 6).[106],[107] Triflic acid among the Brønsted acids was able to activate benzylic C-F bond, for instance, thrifluoromethylated arenes were converted in appropriate benzophenones (**1.101**) in range from moderate to good yields (Figure 6).[108],[109]

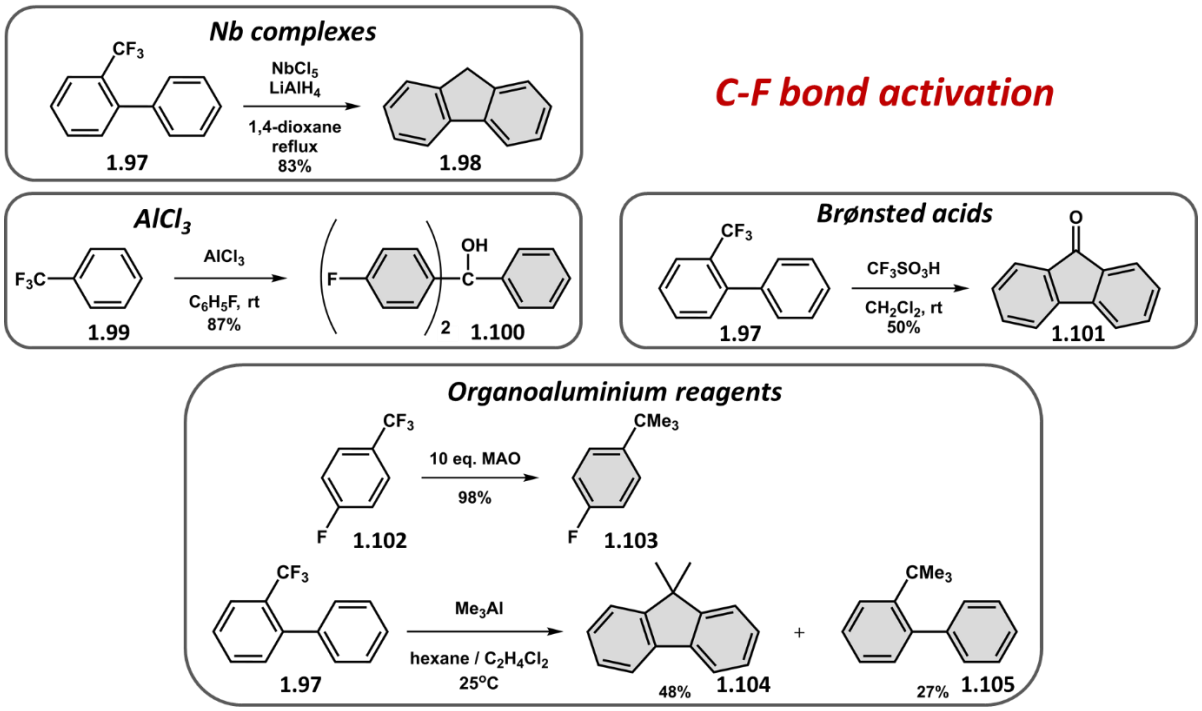

Figure 6. An overview of synthetic approaches towards C-F bond activation of the CF_3 group .[103],[106],[107],[108],[110]

$AlCl_3$ mediated C-F bond activation was applied on 4-trifluoromethylbenzoyl chloride **1.99** in halogenated benzene medium. After defluorination, diarylation and convertion into diarylhydroxymethyl group the product **1.100** was obtained in a good yield (Figure 6).[110] Other methods of C-F bond activation are represented by electroreductive coupling (carbon dioxide, acetone, and *N,N*-dimethylformamide)[111], lanthanoid induced activation[112] and defluorinative silylation using Mg-Cu bimetal systems.[113]

1.4 Structure of *γ*-Aluminium Oxide

Catalytical properties of aluminium oxide (γ-Al_2O_3) is widely used in automobile and petroleum industry.[114],[115],[116] Therefore, formation, structure and properties of aluminium oxide were investigated by a number of scientists and, however, still have been under consideration. It was found that formation of γ-Al_2O_3 occurs in range 350-1000 °C from crystalline[117] or amorphous[118] precursors and remains stable at the temperatures 700-800 °C[119] and at higher than 1200 °C (in case of amorphous precursor). Characterization of structure was carried out by NMR[120], IR-spectroscopy[121], XRD[122], TEM[123] etc. However, the structure and chemical stability of alumina are still under consideration. It is known that lattice of *γ*-alumina is dependent on starting material. For instance, cubic lattice was obtained from amorphous alumina[124],[125],[126],[127], both cubic[128],[129],[130] and tetragonal[131],[132] distortion – from boehmite [AlO(OH)]- or gibbsite [$Al(OH)_3$] precursors, and tetragonal lattice – from boehmite at 450-750 °C[122].

Knözinger and Ratnasamy presented model of γ-Al_2O_3 surface, which is mostly accepted nowadays.[133] They suggested ideal oxide surface, which is connected with five types of hydroxyl groups bearing different “net electric charges”. These charges are dependent on number of Al neighbours and on Al coordination. Respectively, these OH-groups should possess different properties.[133]

DFT calculations predicted that temperature treatment of alumina led to changes in the concentration of hydroxyl groups and of coordinated unsaturated aluminium sites. Thus, at 450 K concentration of hydroxyls was estimated at 12.0 OH nm^{-2},and at 880 K – 4.9 OH nm^{-2}.[134] Experimentally, it was found that at the same temperature ranges concentration hydroxyl groups drops from 8.2 to 2.1 OH nm^{-2} (NMR measure-ments).[135]

Wischert *et al.* defined the density of active sites on alumina surface. For this purpose, they conducted the alumina-mediated C-H bond activation in methane and determined the amount of the formed Al-CH_3 moieties. Additionally, DFT calculations were carried out in order to determine the nature of active sites.[136] It was found that below 400 ºC no active sites were generated, whereas at 700 ºC the concentration of active sites reached the maximum (0.03 per nm^2). Surprisingly, at temperatures above 800ºC their density decreased. Reactive site can be described as Lewis acid-base pair (Al and O),

in which both oxygen basicity and Al acidity play the key role in the reactivity of sites.[136]

By means of DFT calculations (at 500 ºC) it was found that the strongest Lewis acidic sites correspond to three- (**Al_{III}**) four-coordinated (**Al_{IV}**) sites. In addition, reactivity of the Al_{III} sites was investigated by C-H bond activation of methane. Two reactive pairs involved in activation were detected: two-fold coordinated **O** atoms that bonded to **Al_{III}** and three-fold coordinated **O** atoms that facing **Al_{III}**. The highly reactive pair appeared to be **Al_{III},O_3** that enables low-energy pathways for activation and splitting of the C-H bond in methane.[136]

It is worth to mention that the amount of hydroxyl groups on alumina surface depends on the activation mode. Thus, Nguefack *et al*. carried out thermal analysis of the hydrated boehmite at 723-1373 K and found out that the formation of *γ*-Al_2O_3 (1-0.5 OH nm^{-2}) occurred at 873 K. At higher temperatures the hydrated boehmite underwent transformation to *δ*- (at 1053 K) and *θ*-alumina (at 1233 K).[137]

Recently, Amsharov and co-workers presented a DFT study of C-F bond activation in cove and fjord regions by *γ*-Al_2O_3. The mono-protonated adamantine-like Al_4O_6 cluster was chosen as a fragment of activated *γ*-Al_2O_3 surface .[99],[138] They conclude that the fjord-region undergoes synchronous Friedel-Crafts arylation reaction. It was also found that for cove-region closure the hydrogen-bridge effect plays a crucial role.[99]

2 Aims

The C-F bond is one of the most thermally, photochemically and chemically stable bond, which cleavage and subsequent functionalization are of the great importance for the modification of organic fluorocompounds. The aim of this study was the development of a simple and facile approach for the activation C-F bond in aromatic compunds. The most attractive from a synthetic point of view appears to be the intermolecular aryl-aryl coupling leading to the formation of bowl-shaped polycyclic aromatic hydrocarbons. Thus, the study should include following steps:

1. The synthetic pathway to aromatic ketones through the C-F bond activation in trifluoromethylated arenes should be presented. This reaction could be interesting due to functional group tolerance to many organic reactions.
2. The conditions for the intramolecular aryl−aryl coupling via C-F bond activation in presence of γ-aluminium oxide should be developed.
3. Preparation of the halogenated bowl-shaped polycyclic aromatic hydrocarbons, namely indacenopicenes and diindenochrysenes, which could be considered as precursors of fullerenes, nanotubes and other complex architectures.
4. Synthesis of complex architectures – extended highly-curved buckybowls based on diindenochrysene derivatives and molecular receptors (buckycatchers) containing indacenopicene subunits. Study of the buckycather binding affinity towards C_{60} and C_{70} fullerenes.
5. Synthesis of halogenated cyclic trimers and tetramers from the functionalized acenaphthenones and their subsequent cyclization by aluminium oxide mediated C-F bond activation or by thermal annealing on metal surfaces should be carried out.
6. Synthesis of bowl-shaped acene-type structure by the developed protocol of acid-promoted intramolecular reductive cyclization of arylaldehydes leading to PAHs with zig-zag periphery.

The structure confirmation and photophysical properties of all novel structures will be carried out by NMR-, UV/Vis- and fluorescence spectroscopy, mass spectrometry and X-ray diffraction analysis.

3 Results and Discussion

3.1 C-F Bond Activation in Trifluoromethylated Arenes

In this chapter we presented the activation of C-F bond by aluminium oxide under mild conditions in C_{Aryl}–CF_3 group.[100] The 2-trifluoromethylbiphenyl **1** was chosen as a model compound (substrate) for the study of intramolecular condensation. Compound **1** was synthesized by Suzuki cross-coupling (Scheme 24) of 2-bromobenzotrifluoride **2** with phenyl boronic acid **3** in the presence of K_2CO_3 and catalytic amount of $Pd(PPh_3)_4$ in Tol:MeOH mixture (2:1).

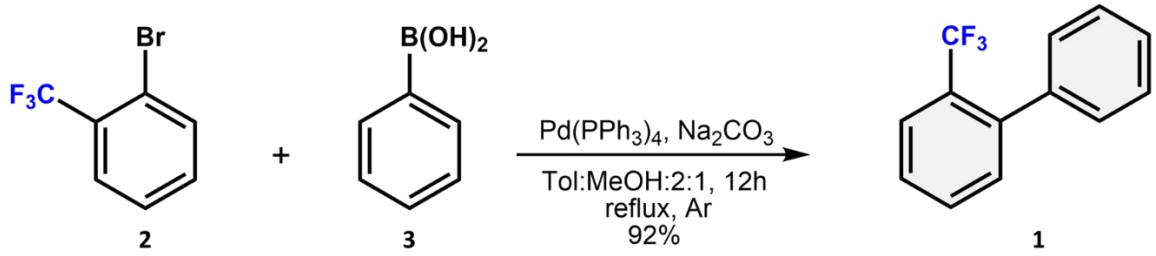

Scheme 24. Synthesis of 2-trifluoromethylbiphenyl **1**.[100]

In the next step, aluminium oxide was activated at the high temperatures (450-550 ºC) under vacuum according to [97]. It is known that the formation of reactive sites (frustrated Lewis acid–base pairs) takes place at these temperatures in alumina.[90] Then, we deposited 2-trifluoromethylbiphenyl **1** on alumina and observed the changes in colour from white to pink (Figure 7a, Scheme 25). Reaction proceeded 30 min at room temperature. The resulting 9-fluorenone **4** was extracted using MeOH, while 2-biphenyl carboxylic acid **5** (as aluminium salt) was extracted by addition of acetic acid into MeOH.

Figure 7. 2-trifluoromethylbiphenyl **1** deposited on activated aluminium oxide: a) at the room temperature; b) at 200 ºC for 10 min. Adapted with permission from O. Papaianina and K. Yu. Amsharov, Chem. Commun., **2016**, 52, 1505. DOI: 10.1039/C5CC08747 Copyright 2016 The Royal Society of Chemistry.

Analysis of the product mixture showed that at rt only 20 % of **1** was converted to **4** (5-7 %) and acid **5** (10-15 %). It is worth to mention that no significant improvement in yields was observed even after one week (9 % of **4** and 19 % of acid **5**). Thus, we can conclude that at the room temperature only 20 % “reactive cites” in aluminium oxide can activate the C-F bond.[100] The molecular mobility of reagent, which adsorbed on less reactive sites of the alumina, was significantly reduced due to the chelate effect, namely, aluminium-fluorine interaction. Such interaction can be realized in the so-called aluminium oxide “nanopore”. The presumable cationic mechanism of the C–F bond activation in trifluoromethylated arenes is described in [100].

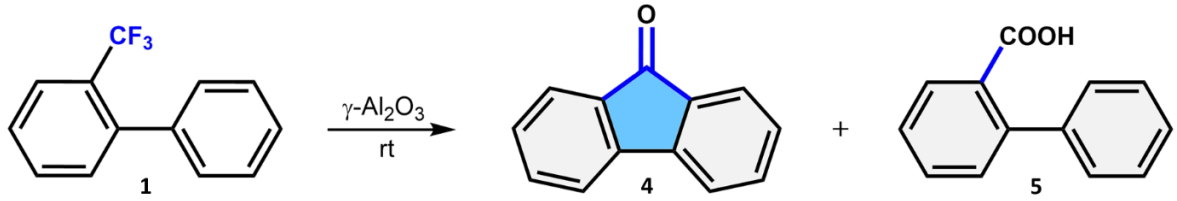

Scheme 25. Condensation of 2-trifluoromethylbiphenyl **1** on alumina.[100]

In order to confirm our assumption, we carried out the C-F bond activation on aluminium oxide in the presence of benzene at 50 ºC (Scheme 26). HPLC analysis showed that 9-phenyl-*9H*-fluoren-9-ol (**6**) and 9,9-diphenyl-*9H*-fluorene (**7**) were found in the reaction mixture in addition to the main product 9-fluorenone **4** (Figure 8). Also, we revealed that the diffusion of benzene into nanopore is very difficult and concentration of benzene inside pore is very low.

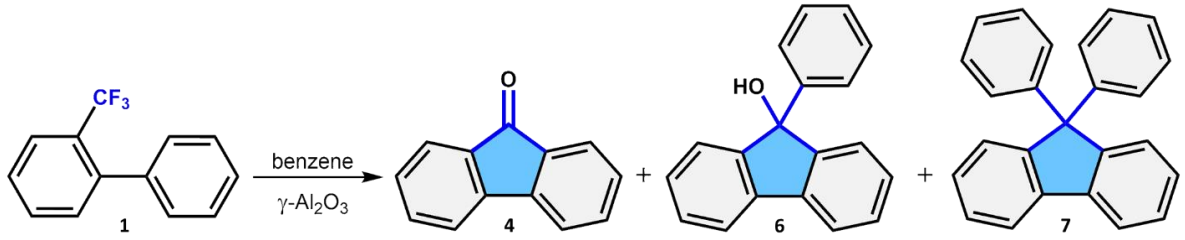

Scheme 26. Condensation of 2-trifluoromethylbiphenyl **1** on alumina in the presence of benzene.[100]

Moreover, no products of arylation were detected at the same reaction conditions by changing the solvent to mesitylene. Hence, we can consider nanopore as a nanoreactor, which is “loaded” with a single molecule and prevents intermolecular reactions.

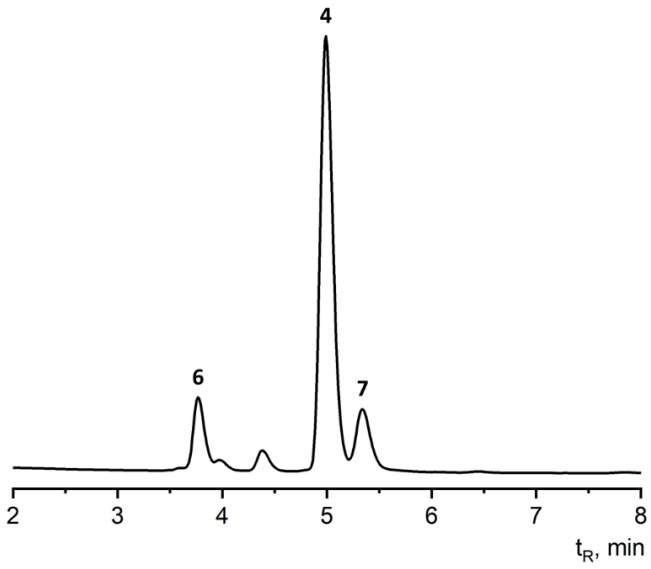

Figure 8. HPLC profile of MeOH extract as obtained after condensation of 2-trifluoromethylbiphenyl **1** in the presence of benzene on activated alumina at 50 ºC for 30 min. HPLC conditions: 5PYE column, MeOH:cyclohexane:80:20 as an eluent, 1 mL min^{-1}, 30 ºC, detection 300 nm. Adapted with permission from O. Papaianina and K. Yu. Amsharov, Chem. Commun., **2016**, 52, 1505. DOI: 10.1039/C5CC08747 Copyright 2016 The Royal Society of Chemistry.

At the higher temperatures the conversion level of 2-trifluoromethylbiphenyl **1** was increased to 38 % for **4** and 29 % for acid **5** (100 ºC, 30 min) and up to 80 % for **4** at 150 ºC. The temperature increase to 200-250 ºC did not alter the product yield. According to NMR and HPLC data neither product of intermolecular condensation nor side products were observed during reaction. Thus, the conditions for conversion of 2-trifluoromethylbiphenyl **1** in 9-fluorenone **4** were determined to be optimal at 150 ºC for 30 min.[100]

It is important to emphasise that 9-fluorenone **4** can be obtained in pure form by MeOH extraction, whereas 2-biphenyl carboxylic acid **5** can be only extracted by acetic acid. We conducted an additional experiment and deposited acid **5** on activated aluminium oxide. At 150 ºC the acid **5** underwent intramolecular cyclization into 9-fluorenone **4**.[100]

It is known that Brønsted acids (trifluoroacetic acid, *p*-toluenesulfonic acid and triflic acid) are used for the C-F bond activation. For instance, 2-(trifluoromethyl)biphenyl was converted into 9-fluorenone **4** in 50 % yield by triflic acid in anhydrous dichlormethane at the room temperature.[108] We carried out this experiment also in the dry benzene and dichloromethane. As can be seen from the Figure 9 the

fluorenone **4** was mainly generated in benzene, while the reaction in DCM led to the formation of many side products.

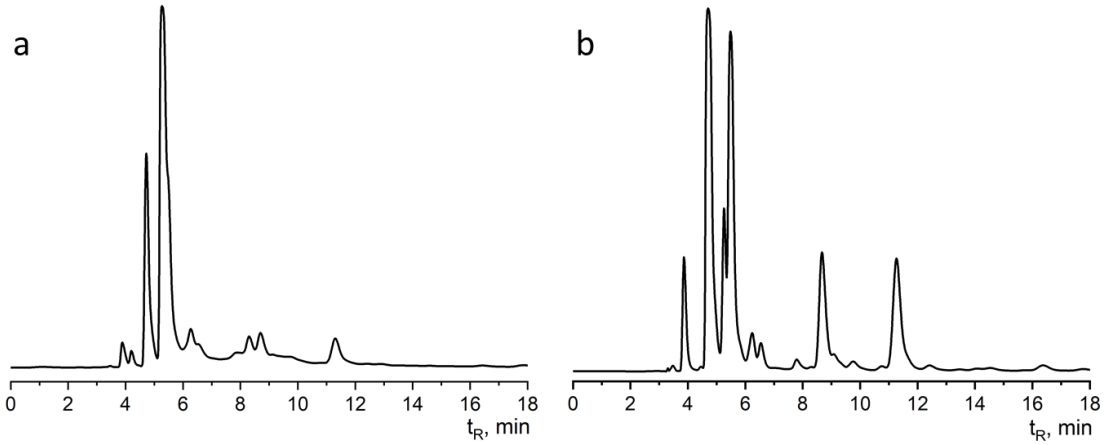

Figure 9. HPLC-profile after reaction of 2-(trifluoromethyl)-1,1'-biphenyl **1** with triflic acid in dry benzene (a) and dichloromethane (b). HPLC conditions: 5PYE column, eluent Tol:MeOH:1:9, 30 °C, 1 mL min^{-1}, detection at 300 nm.

Similar results were achieved for methylated homologue of 2-trifluoromethylbiphenyl **8** under above-mentioned reaction conditions. However, our approach allowed us to obtain 2-methyl-*9H*-fluoren-9-one **9** in 72 % yield. In accordance with HPLC analysis no side products were observed (Figure 10). The remaining 25% of 4'-methyl-2-(trifluoromethyl)-1,1'-biphenyl was converted to the corresponding acid **10** (4-methyl-2'-biphenylcarboxylic acid).

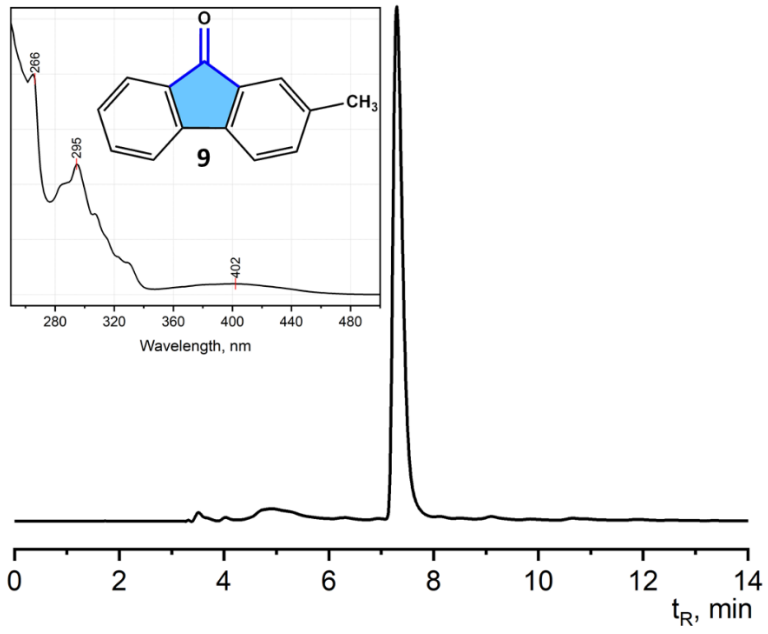

Figure 10. HPLC profile of MeOH extract as obtained after condensation of 4'-methyl-2-(trifluoromethyl)-1,1'-biphenyl **8** on activated alumina at 150 ºC for 30 minutes. HPLC conditions: 5PYE column, MeOH as eluent, 1 mL min^{-1}, 30 ºC, detection 300 nm. (inset) UV-Vis spectrum of 2-methyl-

9H-fluoren-9-one **9** (MeOH).[100] Adapted with permission from O. Papaianina and K. Yu. Amsharov, Chem. Commun., **2016**, 52, 1505. DOI: 10.1039/C5CC08747 Copyright 2016 The Royal Society of Chemistry.

Additionally, we treated **1** with $AlCl_3$ in *o*-DCB under reflux for 4 h (Figure 11a) and in dichloromethane at the room temperature (Figure 11b). HPLC analysis of obtained reaction mixture revealed that in both cases 9-fluorenone and mixture of side products were formed.

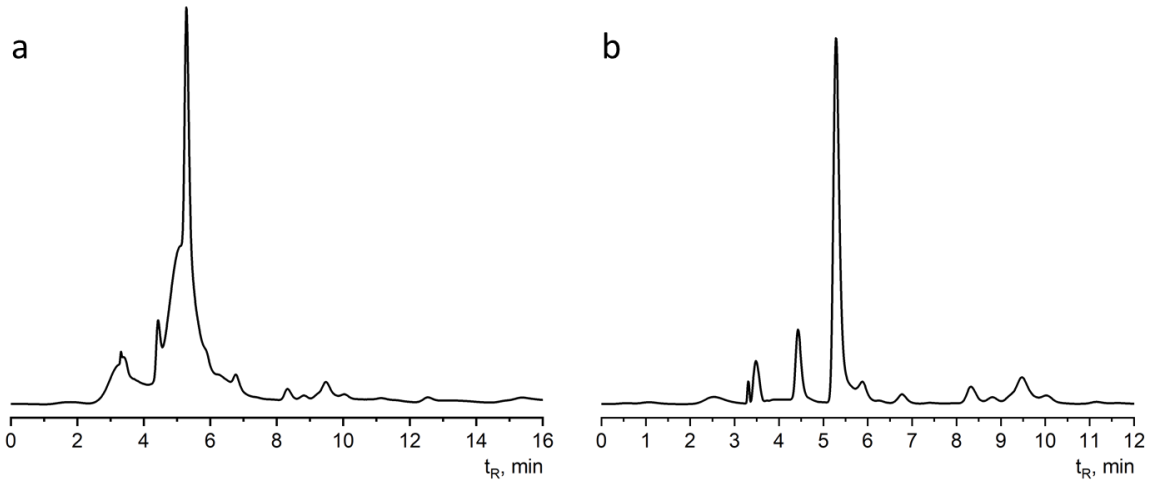

Figure 11. HPLC-profile after reaction of 2-(trifluoromethyl)-1,1'-biphenyl **1** with $AlCl_3$: a) in *o*-DCB, reflux, 4 h; b) in DCM, rt, 4 h. HPLC conditions: 5PYE column, Tol:MeOH:10:90, 1 mL min^{-1}, 30 ºC, detection at 300 nm.

In the next investigations, 1-[2-(trifluoromethyl)phenyl]naphthalene **10** was used as the model compound. It was synthesized from 1-naphthylboronic acid **11** and 2-bromo-benzotrifluoride **13** by Suzuki cross-coupling as white solid (92 %). We performed an experiment according to [108] using triflic acid. Neither *7H*-benzo[*c*]fluoren-7-one **14** nor *7H*-benz[*de*]anthracen-7-one **15** was detected in the rection mixture (Figure 12).

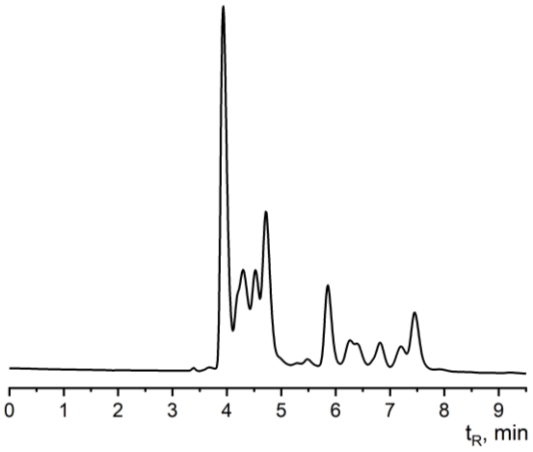

Figure 12. HPLC-profile after reaction of 1-[2-(trifluoromethyl)phenyl]naphthalene **10** with triflic acid in dry dichloromethane. HPLC conditions: 5PYE column, Tol:MeOH:20:80, 1 mL min^{-1}, 30 ºC, detection

at 300 nm.[100] Adapted with permission from O. Papaianina and K. Yu. Amsharov, *Chem. Commun*., **2016**, *52*, 1505. DOI: 10.1039/C5CC08747 Copyright 2016 The Royal Society of Chemistry.

In contrast, aluminium oxide mediated C-F bond activation (Scheme 27) allowed to obtain *7H*-benzo[*c*]fluoren-7-one **14** in 18 % yield, *7H*-benz[*de*]anthracen-7-one **15** in 40 % yield and the 2-(1-naphthalenyl)benzoic acid **16** in 40 % yield (Figure 13a). Influence of temperature on molar ratio **14/15** was investigated at 50, 100, 150, 200 and 250 °C. It was found that molar ratio did not change at the different temperatures. This fact could be explained by low mobility of naphthalene species inside nanopore and the molecule cannot easily change configuration for more favourable nucleophilic attack.[100]

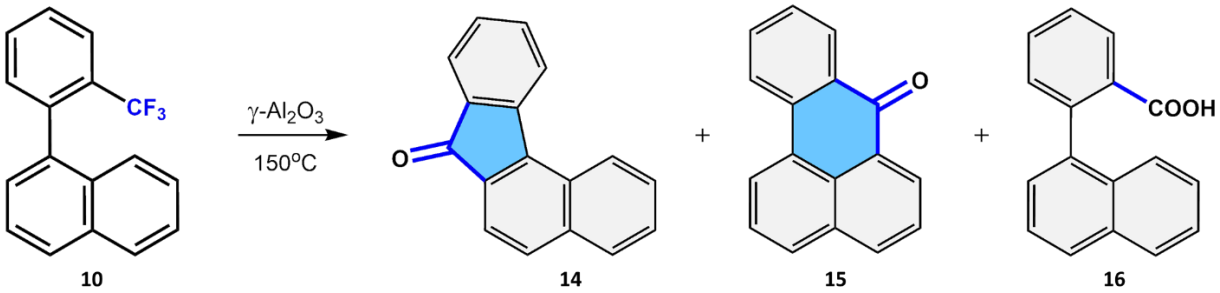

Scheme 27. Condensation of 1-[2-(trifluoromethyl)phenyl]naphthalene **10** on activated alumina.[100]

Also, we deposited 2-(1-naphthalenyl)benzoic acid on activated aluminium oxide, and the HPLC analysis revealed that acid **16** underwent intramolecular cyclization at 250 ºC to *7H*-benzo[*c*]fluoren-7-one **14** and *7H*-benz[*de*]anthracen-7-one **15** in 61 and 32 % yield respectively (Figure 13b).

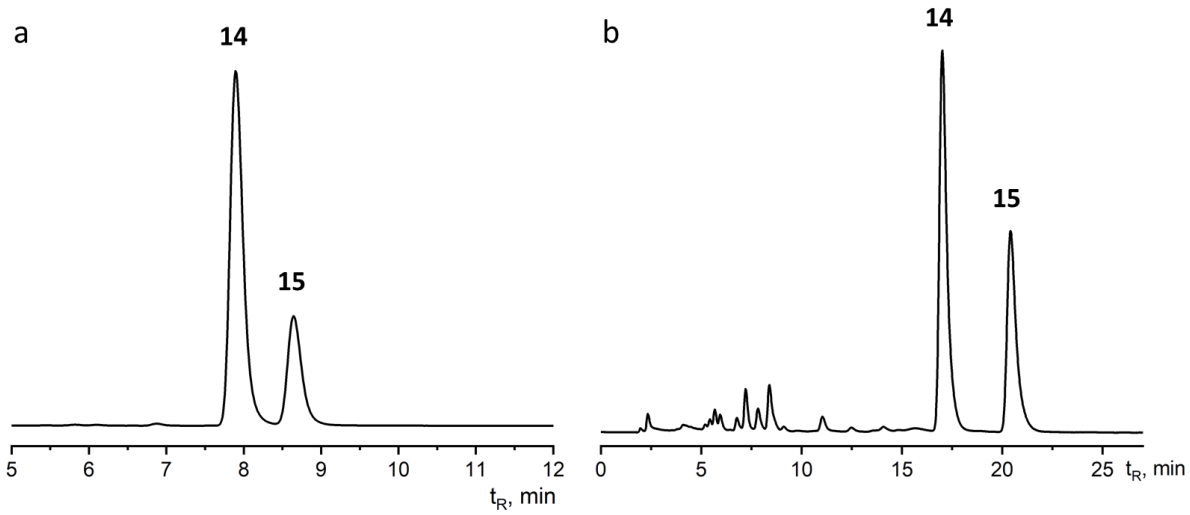

Figure 13. HPLC profiles of MeOH extract as obtained after condensation of: a) 1-[2-(trifluoromethyl) phenyl]naphthalene **10** on *γ*-Al_2O_3 at 150 ºC for 30 min. HPLC conditions: BP column, Tol:MeOH:20:80

as eluent, 1 mL min^{-1}, 30 ºC, detection 300 nm. Adapted with permission from O. Papaianina and K. Yu. Amsharov, Chem. Commun., **2016**, 52, 1505. DOI: 10.1039/C5CC08747 Copyright 2016 The Royal Society of Chemistry; b) 2-(1-naphthalenyl)benzoic acid **16** on *γ*-Al_2O_3 at 250ºC. HPLC conditions: 5PYE column, MeOH as eluent, 1 mL min^{-1}, 30 ºC, detection 300 nm.

In order to investigate the assumption that the molecular mobility is limited inside the pore we studied condensation of 2-(trifluoromethyl)terphenyl **17** on *γ*-alumina (Scheme 28). Friedel-Crafts acylation of **17** can lead to two ketones 4-phenyl-*9H*-fluoren-9-one **18** and tribenzoheptanone **19**, although formation of seven-ring ketone **19** seems to be unlikely.[139]

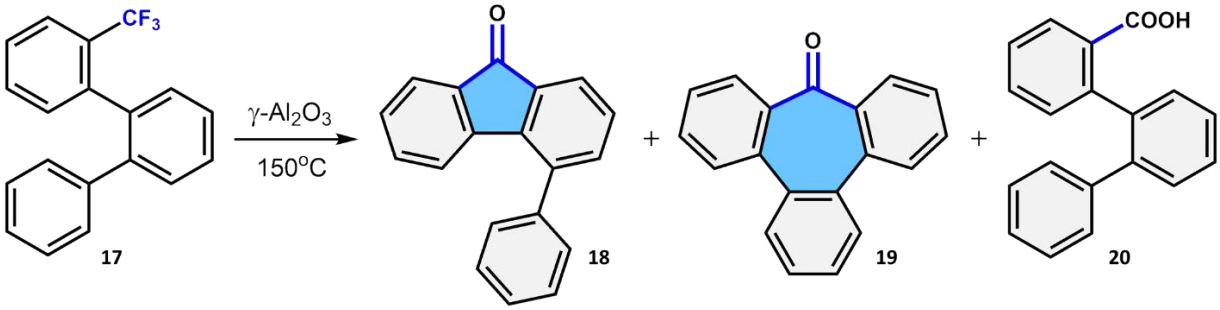

Scheme 28. Condensation of 2-(trifluoromethyl)terphenyl **17** on activated alumina.[100]

To our surprise, the C-F bond activation of **17** on aluminium oxide gave tribenzo-heptanone in 50 % yield, and 4-phenyl-*9H*-fluoren-9-one – only 8 % yield (Figure 14). These results confirmed that alumina “nanoreactor” prevents the side reactions and defines the regiochemistry of condensation.

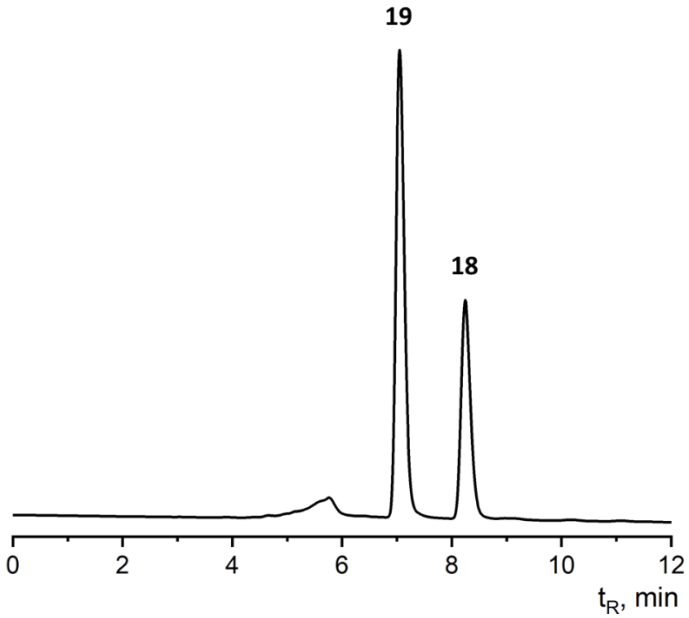

Figure 14. HPLC profile of the reaction mixture as obtained after condensation of 2-(trifluoromethyl)-terphenyl **17** on activated alumina (200 °C, 30 min, MeOH extract). HPLC conditions: 5PYE column,

eluent MeOH, 30 °C, 1 mL min^{-1}, detection at 300 nm. Adapted with permission from O. Papaianina and K. Yu. Amsharov, Chem. Commun., **2016**, 52, 1505. DOI: 10.1039/C5CC08747 Copyright 2016 The Royal Society of Chemistry.

Our experiments revealed that “badly” activated aluminium oxide promoted the hydrolysis of the trifluoromethyl group (at 100ºC after 5 h 89 % of the CF_3 group was converted into carboxyl group, after 8 h – 94 %). These findings prompted us to examine influence of the non-activated aluminium oxide on hydrolysis of CF_3 group. We found that at 150°C CF_3 group can be successfully converted to COOH group. In contrast, the investigation of Sautet *et al.* [136] demonstrated formation of Lewis acid-base pairs only at temperatures higher than 400 °C. Further tests showed that at 200 °C CF_3 groups underwent effective hydrolysis for few minutes.[100]

These reaction conditions were employed for synthesis of 1,1'-biphenyl-2-carboxylic acid, 4-methyl-2'-biphenylcarboxylic acid, 2-(1-naphthalenyl)benzoic acid and o-terphenyl-2-carboxylic acid from respective biphenyls (2-trifluoromethyl-1,1'-biphenyl, 4'-methyl-2-(trifluoromethyl)-1,1'-biphenyl, 1-[2-(trifluoromethyl) phenyl]-naphthalene and 2-(trifluoromethyl)-terphenyl). All yields were in near to quantitative. Our results can be used in synthetical chemistry as a simple way for conversion CF_3 group to carboxylic acids. Previous studies suggested the treatment trifluoromethylated group with concentrated sulfuric acid or super acids for its hydrolysis.[140] However, under these reaction conditions the extended PAHs, for instance, trifluoromethylated benzophenanthrene was converted into polymers and various side products (Figure 15).

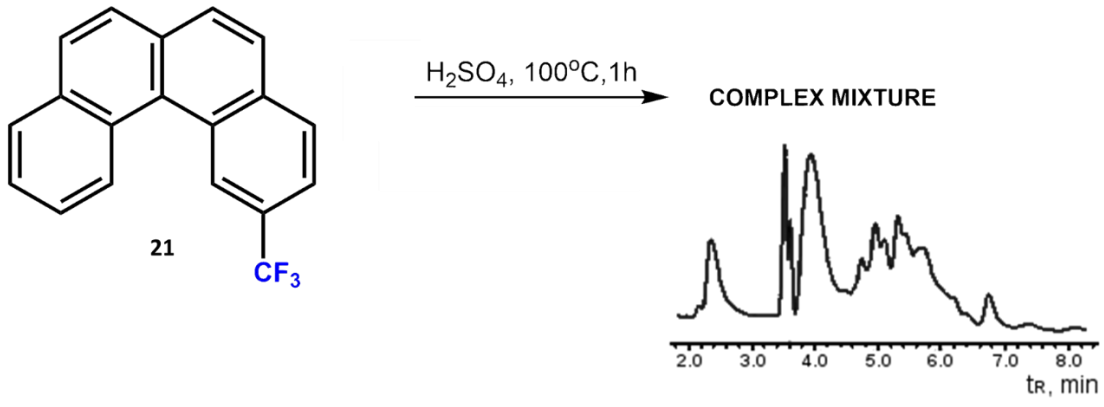

Figure 15. Hydrolysis of trifluoromethylated benzophenanthrene **21**. HPLC profile of the reaction products after reaction of **21** with sulphuric acid. HPLC conditions: 5PYE column, eluent MeOH:Tol:4:1, 30 °C, 1 mL min^{-1}, detection 300 nm. Reproduced with permission from O. Papaianina and K. Yu. Amsharov, *Chem. Commun.*, **2016**, *52*, 1505. DOI: 10.1039/C5CC08747 Copyright 2016 The Royal Society of Chemistry.

The HPLC-chromatograms after reaction at different temperatures (100, 150 and 200 °C) are presented in the Figure 16. The full conversion of CF_3 group was observed after 1 hour at 200 °C. The conversion of trifluoromethylated benzophenanthrene **21** yielded 92 % of benzo[*c*]-phenanthrene-2-carboxylic acid **22** at the lower temperatures (150 °C, 2 h).

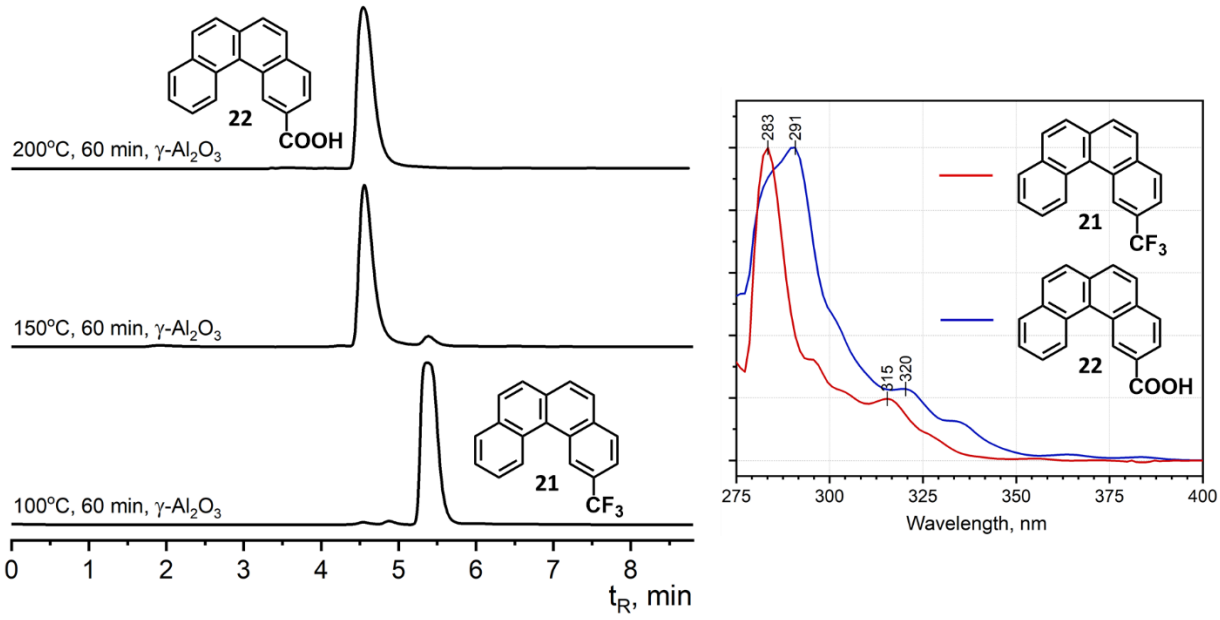

Figure 16. HPLC profile of MeOH/acetic acid extract as obtained after reaction of trifluoromethylated benzophenanthrene **21** with non-activated alumina during 60 min. HPLC conditions: 5PYE column, Tol:MeOH:2:8 (0.2% of acetic acid in MeOH) as eluent, 1 mL min^{-1}, 30 ºC, detection 300 nm. (inset) UV- Vis spectra of trifluoromethylated benzophenanthrene **21** and benzo[c]-phenanthrene-2-carboxylic acid **22** (Tol:MeOH:2:8). Adapted with permission from O. Papaianina and K. Yu. Amsharov, *Chem. Commun.*, **2016**, *52*, 1505. DOI: 10.1039/C5CC08747 Copyright 2016 The Royal Society of Chemistry.

Encouraged by above-mentioned results we tested the hydrolysis ability of the non-activated aluminium oxide towards the bistrifluoromethylated arenes. As a model compound was chosen 1,6-bis(2-(trifluoromethyl)phenyl)pyrene **23** (Scheme 29). It was synthesized by Suzuki-Miyaura cross-coupling of 1,6-dibromobenzene **24** with 2-(trifluoromethyl)phenyl)boronic acid **25** in presence of palladium catalyst (yield: 95.6 %).

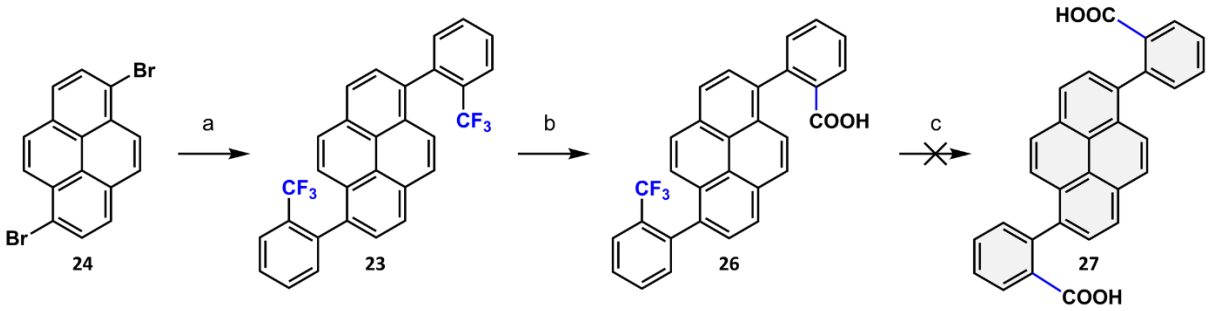

Scheme 29. Synthetic route to 2,2'-(pyrene-1,6-diyl)dibenzoic acid **27**: a) $CF_3C_6H_4B(OH)_2$ **25**, K_2CO_3, $Pd(PPh_3)_4$, Tol:MeOH:2:1, reflux, 15 h, N_2, 95.6 %; b), c) γ-Al_2O_3, 150-300 ºC, 1-24 h.

The C-F bond activation and hydrolysis of **23** on non-activated alumina was carried out at 150 ºC for 1 h. According to TLC (Tol:Acetone:4:1) the starting reagent **23** and product of monohydrolysis **26** were presented in the reaction mixture. The increase of

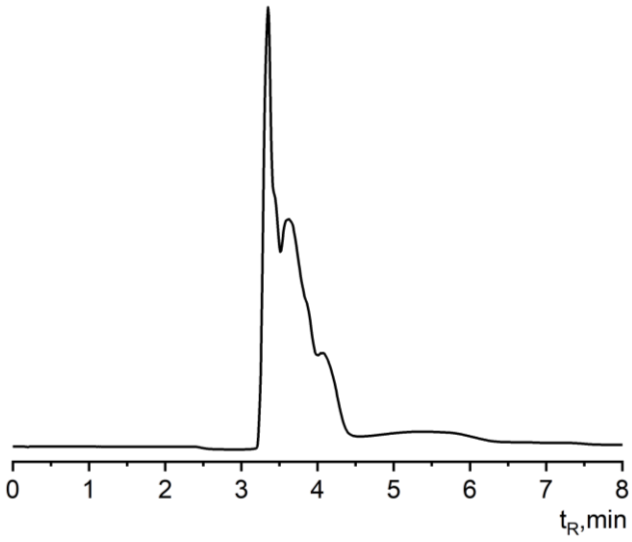

Figure 17. HPLC profile of MeOH/AcOH extract as obtained after reaction of 1,6-bis(2-(trifluoromethyl)phenyl)pyrene **23** with non-activated alumina during 16 h. HPLC conditions: BP column, MeOH:Tol:8.5:1.5 (0.1% of acetic acid in MeOH), 1 mL min^{-1}, 30 ºC, detection 350 nm.

both reaction time (24 h) and temperature (200-250 ºC) did not improve the conversion of **23** to product **27**. Even at 300 ºC the trifluoromethylated groups were not hydrolised (Figure 17), therefore, we can conclude that their formation did not occure simultaneously. After the first hydrolysis of CF_3 group the reaction failed to proceed further due to the limitations caused by the presence of carboxylic group. It was found previously that the heretoatoms deactivate the active sites in aluminium oxide and, thus inhibite the reaction.

3.2 C-F Bond Activation of Rationally Halogenated PAHs

The interest to the bowl-shaped polycyclic aromatic hydrocarbons (BS-PAHs) or “fullerene fragments” increased due to their unique properties originating from the curved π-system.[141],[142] Harsh reaction conditions for the synthesis of buckybowls are determined by their strained structure which frequently do not tolerate functional groups. Although, functionalized buckybowls consider to be the starting materials for the synthesis of fullerenes, nanotubes and other carbon-based structures. Halogenated, namely brominated, bowls are the most appropriate derivatives for the further modification.[143],[144]

Intramolecular aryl–aryl coupling is widely used for the synthesis of buckybowls, for instance, flash vacuum pyrolysis[47], surface-assisted cyclodehydrogenation[64],[145] and palladium-catalyzed direct arylation[56]. However, halogenated BS-PAHs cannot be synthesized by these methods.[10] Post-halogenation is considered to be an alternative approach. It was proven in case of corannulene, while the functionalization of larger or non-symmetrical molecules appeared to be unsuccessful.

Previous works of Ichikawa[87,91], Siegel[92] and Amsharov[96,97] were focused on the strategy of the C-F bond activation for the synthesis of PAH systems. The results of the Amsharov’s group revealed that aluminium oxide mediated cyclodehydrofluorination tolerates other halogens and could be applied for the synthesis of halogenated buckybowls.[102] In this study the activation of C−F bond in the presence of C-Br and C-Cl bonds under mild conditions was demonstrated. This approach allows the selective and fully controllable synthesis of halogenated BS-PAHs.

The aluminium oxide mediated C-F bond activation was performed in solid-state.[97,102] The condensation of fluoroarenes resulted in products in pure form with near to quantitative yield. In our research the intramolecular aryl-aryl coupling was studied in liquid media. It was found that the solvent plays a significant role. On the one hand, the solvent helps to distribute the reagent homogeneously over aluminium oxide, on the other hand, it influences the efficiency of the condensation.

In order to study the solvent’s a series of experiments were performed using different media (1,2-dichlorobenzene, chlorobenzene, fluorobenzene, bromobenzene, mesitylene, DMSO, DMF and DMAc). As a model reaction the conversion of 1-fluoro-4-bromobenzo[*c*]phenanthrene **28** into 3-bromobenzo[*ghi*]fluoranthene **29** was

chosen. The cyclodehydrofluorination was carried out for 30 min at 120 °C (Scheme 30). Under solid-state conditions (120 ºC, 30 min) the conversion of **28** into **29** amounted to 0.5 %.[98]

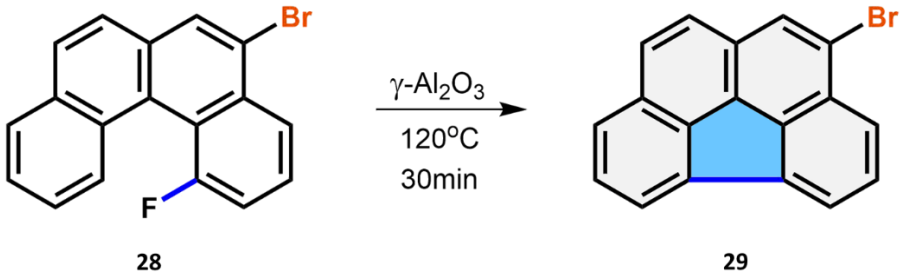

28 **29**

Scheme 30. Model reaction of 1-fluoro-4-bromobenzo[*c*]phenanthrene **28** into 3-bromobenzo[*ghi*]-fluoranthene **29** for optimization of cyclodehydrofluorination.[98]

The Table 1 below illustrates the reaction yields in different media. Polar aprotic solvents (DMSO, DMF, DMAc) are not depicted in the table, due to deactivation of active centres at the alumina interface and complete inhibition of the reaction.

Table 1. Solvent's effect on the conversion of 1-fluoro-4-bromobenzo[*c*]phenanthrene **28** to 3-bromobenzo[*ghi*]fluoranthene **29**. All reactions were carried out at 120 °C. Yields were measured after 10 and 30 minutes of reaction.

Solvent	***Yield$_{10min}$, %***	***Yield$_{30min}$, %***
Benzene	0.3	0.4
Bromobenzene	1.1	4.9
Chlorobenzene	3.5	13.5
1,2-Dichlorobenzene	11.7	60.8
Fluorobenezene	0.4	0.8
Mesitylene	0.1	0.3

From the data in the Table 1, we can see that such solvents as fluorobenzene (0.8 %), benzene (0.5 %) and mesytilene (0.3 %) practically did not affect the conversion. In contrast, chlorobenzene (13.5 %) and bromobenzene (4.9 %) showed an adequate reaction acceleration. The most remarkable effect was observed in *o*-dichlorobenzene. The reaction rate was 200 times faster compared to the solid-state strategy (60 % yield after 30 min).

Raising the temperature and/or the time of reaction led to the full conversion **28** into **29** in *o*-DCB. Thus, after 30 min of reaction at 150 °C the pure product was obtained

in nearly quantitative yield. HPLC analysis revealed the absence of side products formation. The cyclodehydrofluorination in *o*-DCB was conducted by microwave-assisted heating, although, the same efficiency of the condensation was achieved by conventional heating in the sealed glass ampoules.[98]

The new approach was also examined on known precursors of extended buckybowls: *as*-indaceno[*3,2,1,8,7,6-pqrstuv*]picene (**31**) and fluoreno[*2',1',9',8':5,6,7,8*]acephenanthryleno[*4,3-bc*]-*as*-indaceno[*3,2,1,8,7,6-pqrstuv*]picene (**33**). The reaction time was significantly reduced in comparison with solid-state approach. It allowed to obtain the products in near to quantitative yields (according to HPLC measurements, Figure 18).

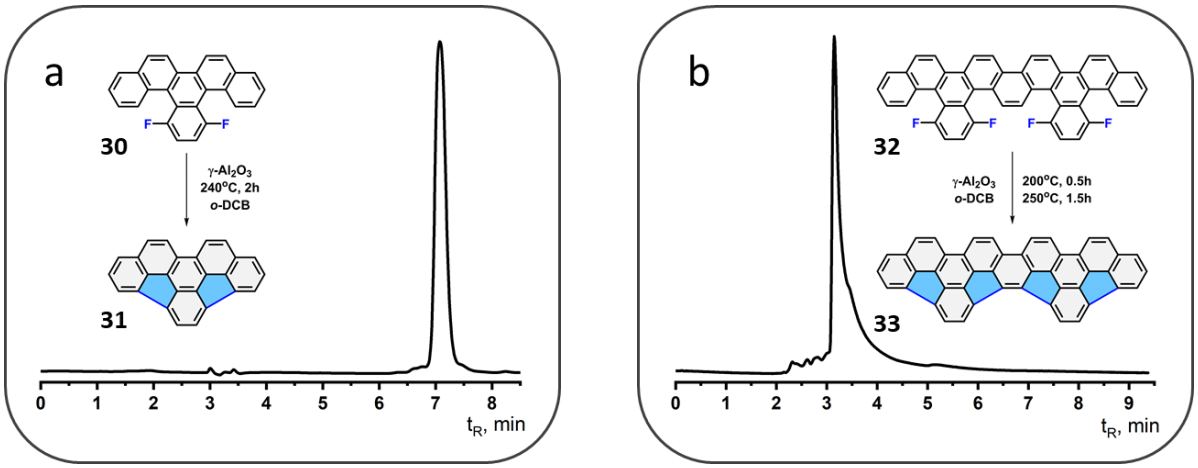

Figure 18. HPLC profile of product: a) **31** as obtained (240 ºC, 2 h, *o*-DCB) detected at 320 nm (PBr column, Tol:MeOH:1:1 as eluent, 1.0 mL min^{-1}, 40 ºC); b) **33** as obtained (200-250ºC, 2 h, *o*-DCB) detected at 340 nm (5PYE column, Tol as eluent, 1.5 mL min^{-1}, 60 ºC).

In addition, these reaction conditions were applied to the precursors of halogenated bowl-shaped PAHs. For this purpose, the indacenopicene or diindenochrysene derivatives were chosen. The synthesis of brominated indacenopicenes starts with the free radical bromination of 1,4-difluoro-6-methyl-benzo[*c*]phenanthrene **34** (synthesis is described in [102]) using NBS in the presence of DBPO in CCl_4 (Scheme 31). The solution of 1,4-difluoro-6-bromomethylbenzo[*c*]phenanthrene **35** and triphenylphosphine in toluene was refluxed for 16 h to form the phosphonium salt **36**, which was filtered and used for the next step. The Wittig reaction was carried out in anhydrous ethanol utilizing potassium *tert*-butoxide as base and corresponding aldehydes (benzaldehyde, 2-bromobenzaldehyde, 4-bromobenzaldehyde).[102] The obtained *cis/trans* isomer mixture of arylethenes **37** was used without additional

separation since isomers interconvert in each other under photocyclization conditions. The halogenated benzo[*s*]picenes (**31**, **39a** and **39b**) were synthesized by the modified Mallory photocyclization protocol in cyclohexane from corresponding arylethenes (**30**, **38a** and **38b**).[31]

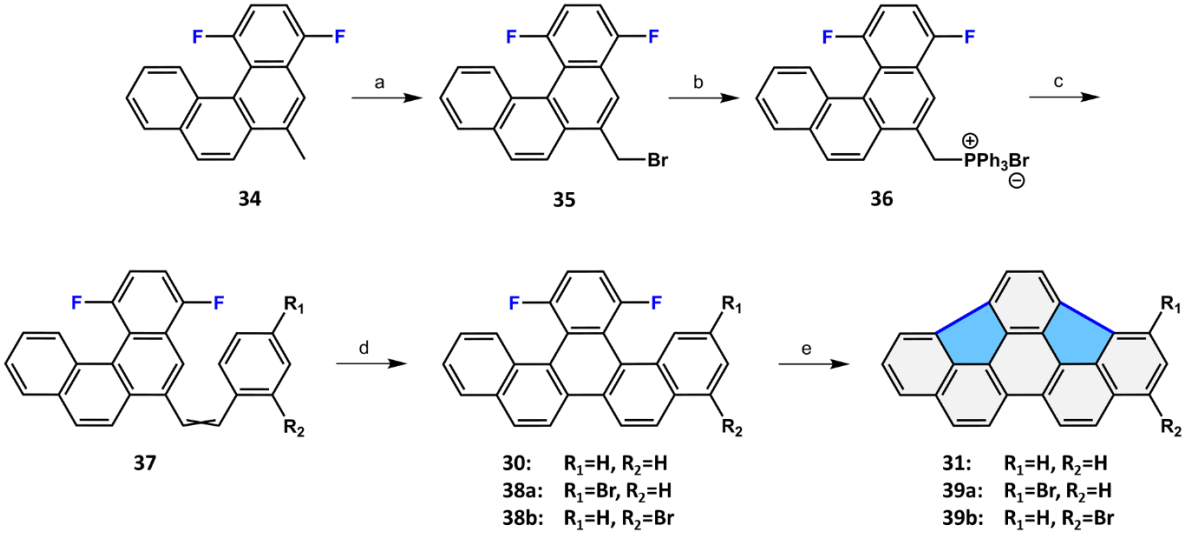

Scheme 31. Synthesis of brominated indacenopicenes: a) NBS, DBPO, CCl_4, reflux, 4 h, 85 %; b) PPh_3, toluene, reflux, 16 h, 98 %; c) ArCHO (**R_1**, **R_2=H**: 81%; **R_1=Br**, **R_2=H**: 76%; **R_1=H**, **R_2=Br**: 79%), *t*-BuOK, EtOH, reflux, 10 h; d) *hv*, I_2, propylene oxide, cyclohexane (**30**: 84 %; **38a**: 50 %; **38b**: 55 %); e) *γ*-Al_2O_3, *o*-DCB, MW (**31**: 150 °C, 30 min, 99 %; **39a**: 150 °C, 1.5 h, 96 %; **39b**: 240 °C, 1.5 h, 80 %).[98]

We decided to synthesize the symmetrical double-brominated bowls. For this purpose, we defined the selectivity of halogenation by stability estimation of the dibenzo[*s*]picene's *σ*-complexes. The AM1 level of theory was applied for current calculations. The results of the calculations are presented in Table 2. From this data, we can see that the most probable position for electrophilic substitution is depicted in Inset 5.

Table 2. Possible transition states and activation energies brominated 13,16-difluorobenzo[*s*]picene **30**.

	***σ*-complex**	***Relative energy, kcal mol^{-1}***
1	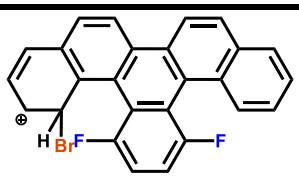	4.5

2	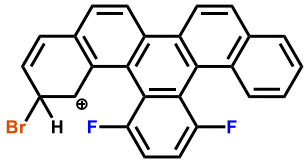	6.2
3	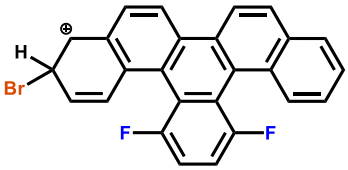	4.6
4	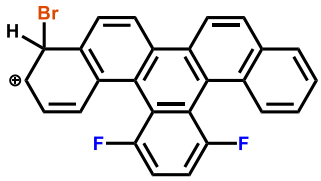	4.4
5	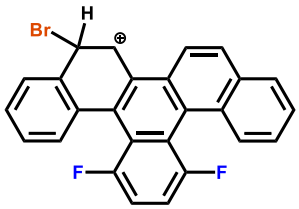	0.0
6	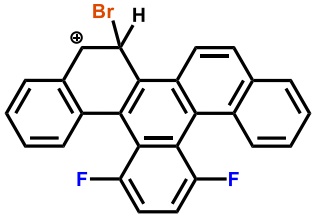	5.7
7	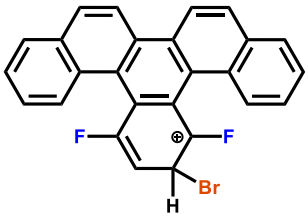	8.2

In order to reduce the number of reacton steps we chose another strategy for synthesis of 13,16-difluorobenzo[*s*]picene **30** (Scheme 32), which was performed in cooperation with S. Shkolnikov.[146] The synthesis of **30** started with the metalation of 2-bromo-1,4-difluorobenzene **40** and subsequent bromination which gave 3,4-dibromo-1,4-difluorbenzene **40** in 68 % yield. The 3,4-dibromo-1,4-difluorbenzene **40** was converted into the 1,1'-(3,6-difluoro-1,2-phenyl)dinaphthalene **43** by Pd-catalyzed Suzuki cross-coupling (42 % yield). Next, the photocyclization **43** was conducted in the cyclohexane/benzene mixture for 24 h. After 24 h the only traces of desired product **30** were detected. The reaction was repeated twice with the same result. According to X-ray diffraction analysis of **43** the naphthalene rings are not in-plane

and twisted to each other. In this case the fluorine and hydrogen repel mutually and, thus, the molecule probably does not adopt the optimal geometry for the photocyclization. Consequently, the previous approach (Scheme 31) was favoured for synthesis of 13,16-difluorobenzo[*s*]picene **30** precursor.

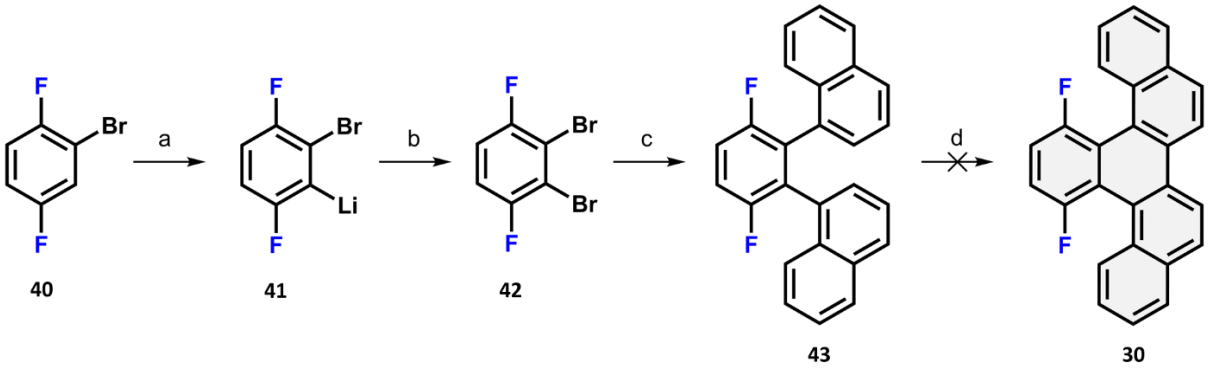

Scheme 32. Synthesis of 13,16-difluorobenzo[*s*]picene **30**. a) LDA, THF, -78 °C, 1h; b) Br_2, THF, -78 °C to rt (68 %); c) 1-naphthaleneboronic acid, K_2CO_3, Cs_2CO_3, $Pd(PPh_3)_4$, Tol:MeOH:2:1, reflux, 16 h, 42 %; d) *hv*, I_2, propylene oxide, cyclohexane, benzene, 24 h (traces).[146]

For synthesis of 5,8-dibromo-13,16-difluorobenzo[*s*]picene **30** we selected two standard approaches: bromination with NBS in DMF[147] and bromination with Br_2 in chloroform[148]. The both reactions were carried out at the room temperatures for 2.5 h. Reaction was monitored by the thin-layer chromatography (DCM:Hexane:1:2). After 2.5 h the formation of the products was observed only in the $Br_2/CHCl_3$ system (Scheme 33).

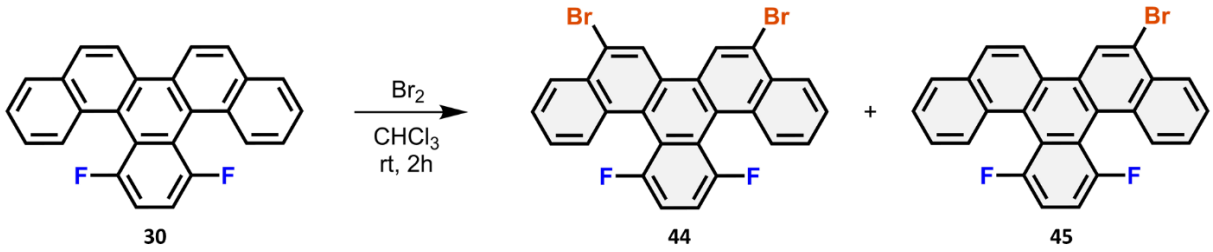

Scheme 33. Synthesis of 5,8-dibromo-13,16-difluorobenzo[*s*]picene **44** and 5-bromo-13,16-difluoro benzo[*s*]picene **45**.

The products were analyzed and purified by semi-preparative HPLC (Tol:MeOH:3:7 as eluent). The two major products were identified as 5-bromo-13,16-difluorobenzo[*s*]picene **44** and 5,8-dibromo-13,16-difluorobenzo[*s*]picene **45** with retention times t_R = 6.0 min and t_R = 6.9 min correspondingly (Figure 19).

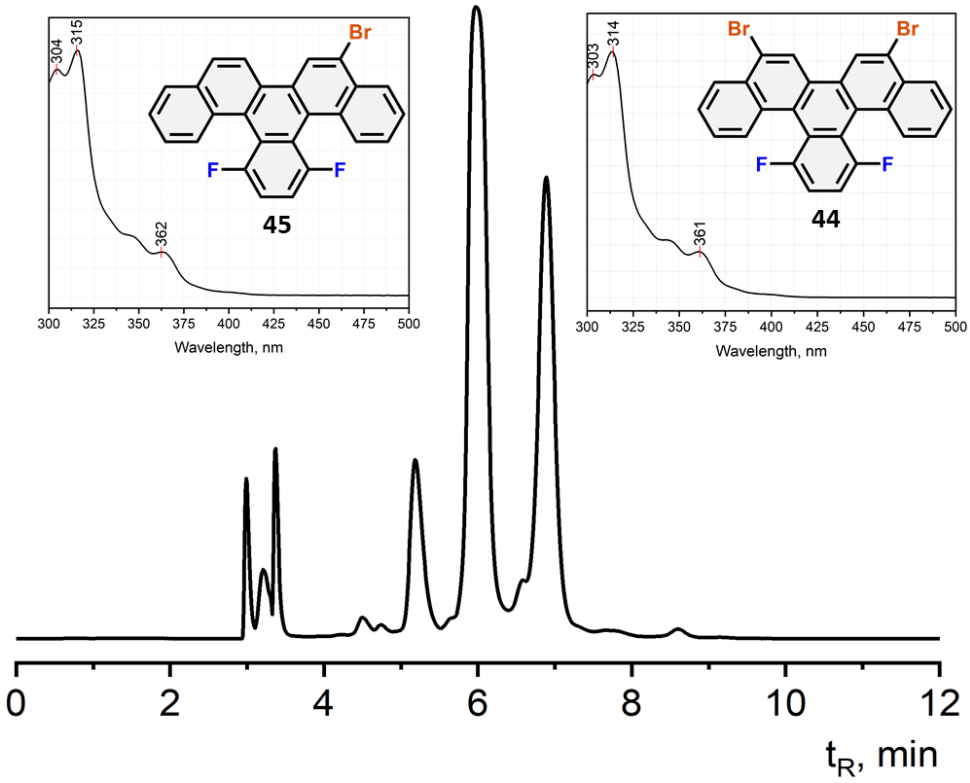

Figure 19. HPLC profile of reaction mixture after bromination detected at 320 nm (PBr column, 1.0 mL min^{-1}, Tol:MeOH:4:6, 35 °C). Inset: UV-Vis spectra of 5-bromo-13,16-difluorobenzo[*s*]picene **44** and 5,8-dibromo-13,16-difluorobenzo[*s*]picene **45** in Tol:MeOH:4:6.

In the next step, we applied aluminium oxide mediated C-F bond activation that proceeded slower in the brominated indacenopicenes than in the 1-fluoro-4-bromobenzo[*c*]phenanthrene. In solid state the full conversion of non-brominated 13,16-difluorobenzo[*s*]picene **30** into *as*-indaceno[*3,2,1,8,7,6-pqrstuv*]picene **31** required 60 h at 150 °C. Introduction of bromine functionality in **30** causes some difficulties in HF-elimination. Synthesis of **39b** by solid-state approach demonstrated the low conversion even after 100 h at 150 °C. The temperature increase up to 200-250 °C did not lead to the significant improvement in the yield. According to the HPLC analysis, the high-temperature reactions were accompanied by the partial debromination and the formation of unidentified products. In the presence of *o*-DCB the reaction rate rose, e.g., after 1.5 h at 150 °C 4-bromo-13,16-difluorobenzo[*s*]picene **38b** was converted in 1-bromo-as-indaceno[*3,2,1,8,7,6-pqrstuv*]picene in near quantitative yield (Figure 20a). The temperature growth to 250 °C did not enhance the selectivity of the process. It should be mentioned that in the comparison with solid-state approach neither the significant debromination nor side products were observed. The cyclodehydrofluorination of 5-bromo-13,16-

difluorobenzo[*s*]picene **45** was carried out at 230 ºC for 1.5 h; the pure product **46** was obtained in near-quantitative yield (Figure 20b).

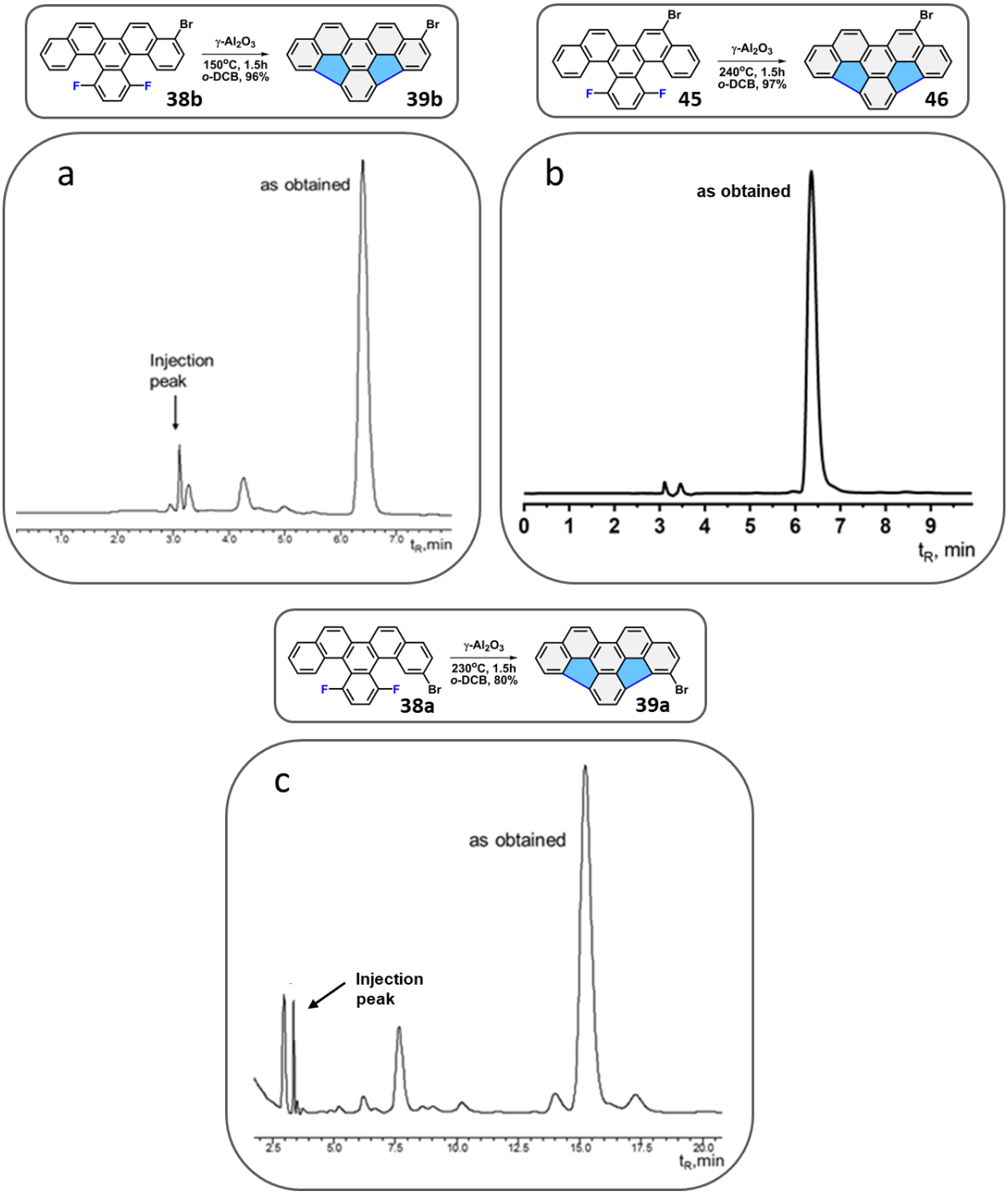

Figure 20. HPLC profile (5PYE column, 1.0 mL min^{-1}, 35 ºC) of: a) 1-bromo-as-indaceno[*3,2,1,8,7,6-pqrstuv*]picene **39b** as obtained after reaction detected at 320 nm (Tol:MeOH:1:1); b) 9-bromo-*as*-indaceno[*3,2,1,8,7,6-pqrstuv*]picene **46** as obtained after reaction, detected at 380 nm (Tol:MeOH:1:1); c) 3-bromo-as-indaceno[*3,2,1,8,7,6-pqrstuv*]picene **39a** as obtained after reaction, detected at 320 nm (Tol:MeOH:1:4).[98] Reproduced with permission from O. Papaianina, V. A. Akhmetov, et al., *Angew. Chem. Int. Ed.* **2017**, *56*, 4834. Copyright 2017 Wiley-VCH Verlag GmbH & Co. KGaA, Weinheim.

The condensation of 2-bromo-13,16-difluorobenzo[*s*]picene **38a** at 150 °C resulted mainly in the monocyclized product. It can be explained by closeness of bromine functionality to the cove region and steric hindrance around the C-F bond. Higher conversion level of **38a** into 3-bromo-as-indaceno[*3,2,1,8,7,6-pqrstuv*]picene **39a** was gained after 1.5 h at 240°C; however, the presence of the monocyclized product was detected by HPLC analysis (Figure 20c).

The solution of brominated indacenopicenes after cyclodehydrofluorination was concentrated. After addition of MeOH the pure product precipitated, was dried under reduced vacuum and characterized by NMR-spectroscopy and MS-spectrometry (Figure 21a, b, c).

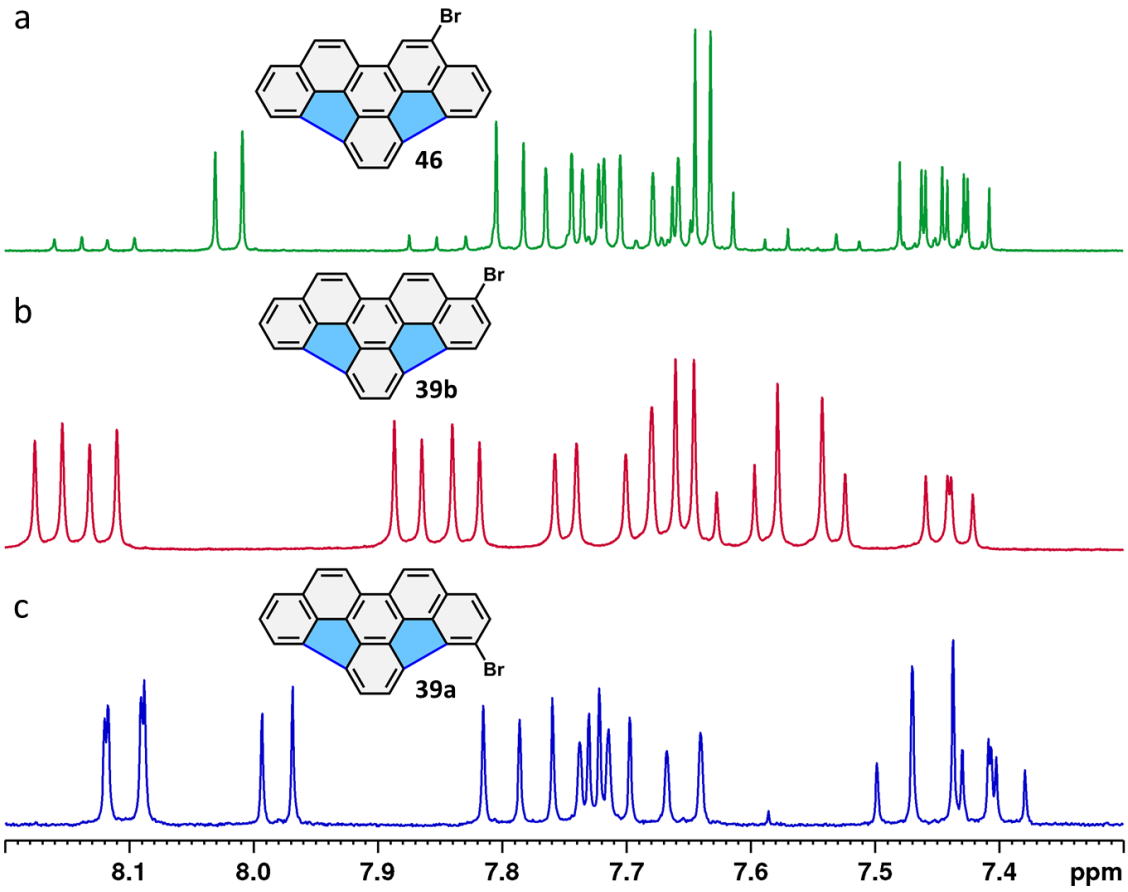

Figure 21. ^{1}H NMR spectra of: a) 9-bromo-as-indaceno[3,2,1,8,7,6-pqrstuv]picene **46** (400 MHz, CD_2Cl_2, 293 K); b) 1-bromo-as-indaceno[3,2,1,8,7,6-pqrstuv]picene **39b** (400 MHz, CD_2Cl_2, 293 K); c) 3-bromo-as-indaceno[3,2,1,8,7,6-pqrstuv]picene **39a** (300 MHz, $CDCl_3$, 293 K).[98] Adapted with permission from O. Papaianina, V. A. Akhmetov, et al., *Angew. Chem. Int. Ed.* **2017**, *56*, 4834. Copyright 2017 Wiley-VCH Verlag GmbH & Co. KGaA, Weinheim.

Cyclization of the 5,8-dibromo-13,16-difluorobenzo[*s*]picene **44** was performed in *o*-DCB at 220 °C for 30 min and yielded the pure dibrominated bowl. ^{1}H NMR spectrum

of 9,12-dibromo-as-indaceno[*3,2,1,8,7,6-pqrstuv*]picene **47** (Figure 22) was measured in $C_2D_2Cl_4$ due to low solubility in common solvents for NMR spectroscopy ($CDCl_3$ and CD_2Cl_2). X-ray analysis confirmed the desired positions of bromine functionalities in **47** (Figure 22). The single crystals were obtained by slow evaporation from the toluene solution.

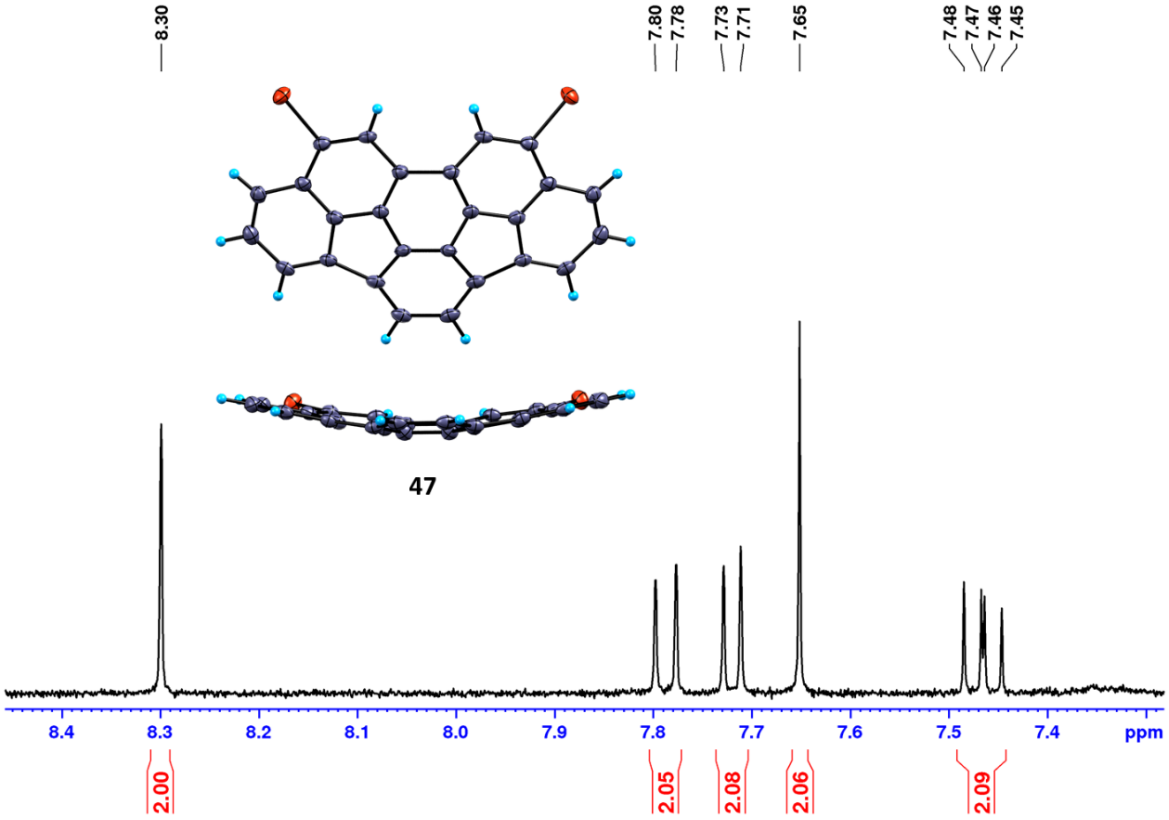

Figure 22. ^{1}H NMR (400 MHz, $C_2D_2Cl_4$, 353 K) spectrum of 9,12-dibromo-as-indaceno[3,2,1,8,7,6-pqrstuv]picene **47** and its molecular structure as determined by X-ray diffraction analysis. Thermal ellipsoids are set at the 50%probability level.[98] Adapted with permission from O. Papaianina, V. A. Akhmetov, et al., *Angew. Chem. Int. Ed.* **2017**, *56*, 4834. Copyright 2017 Wiley-VCH Verlag GmbH & Co. KGaA, Weinheim.

It must be emphasized that all halogenated buckybowls were obtained as sole product (except 3-bromo-as-indaceno[*3,2,1,8,7,6-pqrstuv*]picene) without purification in 95-98 % yield by the precipitation with methanol from concentrated reaction mixture. All indacenopicenes are air-stable deep-orange crystalline solids with moderate to low solubility in such solvents as toluene, dichloromethane and chlorobenzene.

Synthetic route to diindenochrysenes bearing Cl, Br, and F functionalities started with naphthalene-2,6-dicarbaldehyde **48** (synthesis described in [149]). Arylethenes **49a-c** were synthesized by double Wittig cross-coupling according to general procedure

utilizing the naphthalene-2,6-dicarbaldehyde **48** and respective triphenylphosphonium bromide (2-bromo-5-fluorobenzyl, 2-chloro-5-fluorobenzyl and 2,5-difluorobenzyl). Dibenzo[*c,l*]chrysenes **50a-c** were prepared by double photocyclization of the corresponding arylethenes in toluene in accordance with modified protocol (Scheme 34).[102]

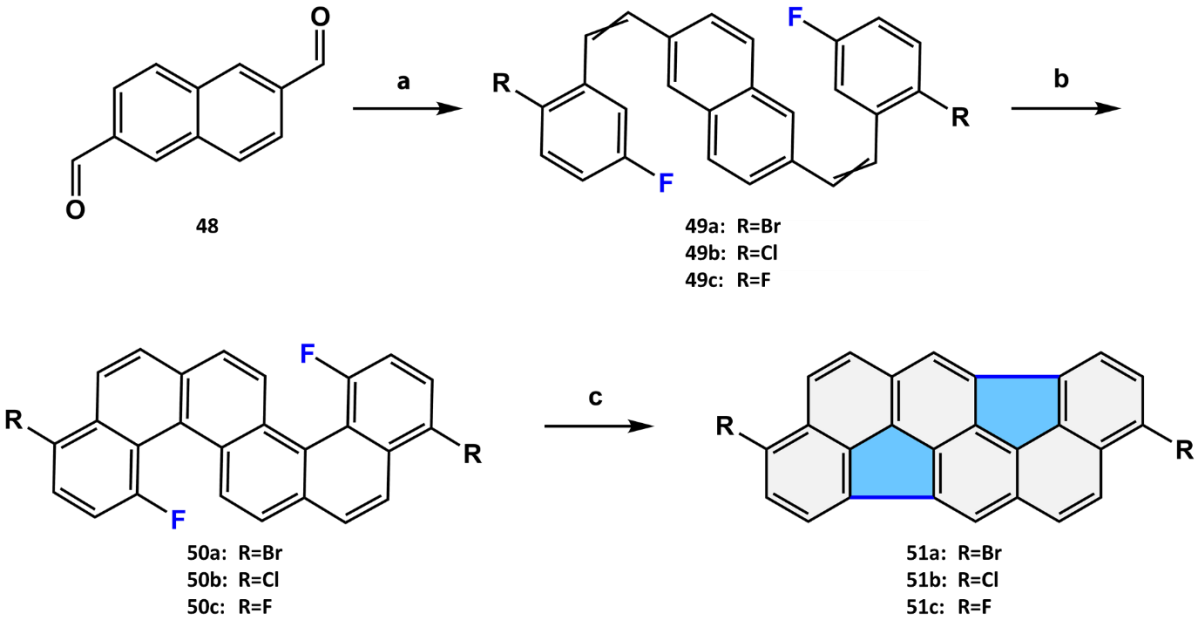

Scheme 34. Synthetic route to the halogenated diindenochrysenes. a) $ArCH_2PPh_3Br$ (**R=Br**: 36%, **R=Cl**: 44%, **R=F**: 61%), *t*-BuOK, EtOH, reflux, 10 h; b) *hv*, I_2, propylene oxide, cyclohexane(**50a**: 50 %; **50b**: 42 %; **50c**: 47 %); c) *γ*-Al_2O_3, *o*-DCB, MW (**51a**: 240 ºC, 1 h, 95 %; **51b**: 220 ºC, 0.5 h, 98 %; **51c**: 230 ºC, 1 h, 63 %).[98]

In comparison with indacenopicenes, the intramolecular aryl-aryl coupling of diindenochrysenes required higher temperatures due to the enhanced strain of structure. The high-yielding HF-elimination was achieved by heating at 200-240 °C after several hours. The dibrominated **51a** and dichlorinated bowls **51b** were obtained in close to quantitative yields (direct precipitation with MeOH from toluene extract) by cyclization in *o*-DCB at 240 °C for 1 h. The HPLC chromatography confirmed the purity of **51a** and **51b** after precipitation[98], and NMR spectroscopy verified the structure of **51a** and **51b** (Figure 23a, b).

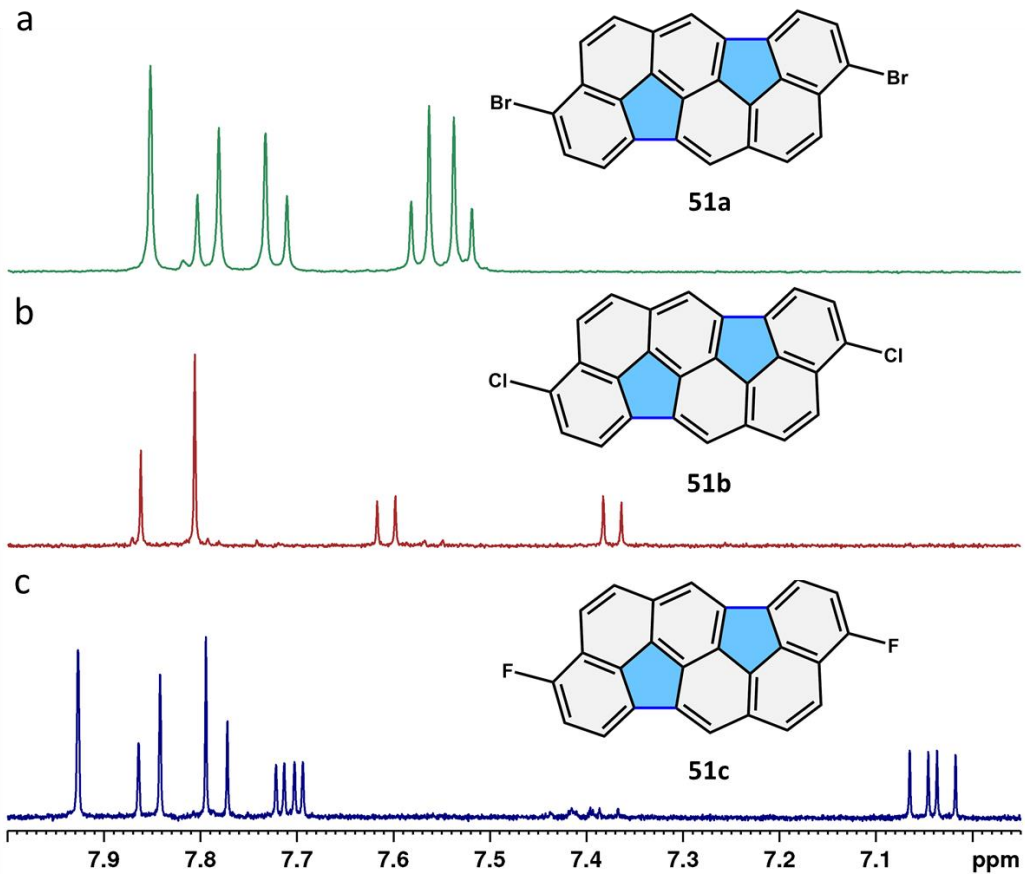

Figure 23. ^{1}H NMR (400 MHz) spectra of: a) 3,9-dibromodiindeno[4,3,2,1-cdef:4',3',2',1'-lmno]chrysene **51a** ($C_2D_2Cl_4$, 353 K); b) 3,9-dichlorodiindeno[4,3,2,1-cdef:4',3',2',1'-lmno]chrysene **51b** ($C_2D_2Cl_4$, 353 K); c) 3,9-difluorodiindeno[4,3,2,1-cdef:4',3',2',1'-lmno]chrysene **51c** ($CDCl_2$, 293 K).[98] Adapted with permission from O. Papaianina, V. A. Akhmetov, et al., *Angew. Chem. Int. Ed.* **2017**, *56*, 4834. Copyright 2017 Wiley-VCH Verlag GmbH & Co. KGaA, Weinheim.

During cyclization of fluorinated dibenzo[*c,l*]chrysene **50c** several products were observed. MS analysis showed that main product corresponds to 3,9-difluorodiindeno[*4,3,2,1-cdef:4',3',2',1'-lmno*]chrysene **51c**. The presence of side product reveals that at high temperatures (above 200 °C) the C-F bond activation occurs both in the cove region and on the periphery of 1,4,9,12-tetrafluoro-dibenzo[*c,l*]chrysene. In other words, the activation on periphery resulted in the coupling products (e.g., dimers).

The temperature descent to 180 °C allowed to avoid dimerization, meanwhile the condensation of **50c** stopped after the first ring closure and monocyclized product was observed as main product after reaction. During optimization of the reaction conditions, we determined that the highest yield was achieved by heating at 220 °C for 2 h (Figure 23c, Figure 24).

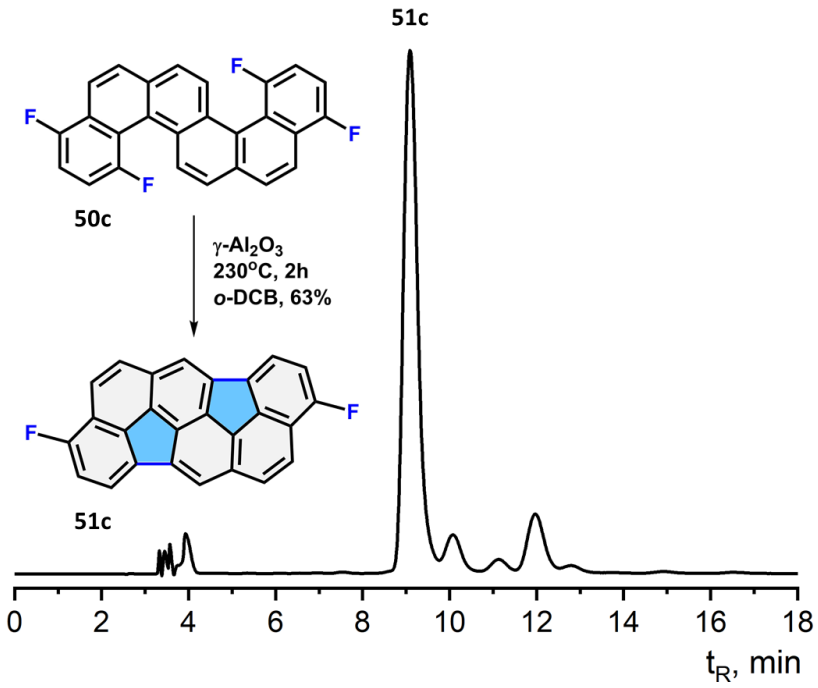

Figure 24. HPLC profile of 3,9-difluorodiindeno[*4,3,2,1-cdef:4',3',2',1'-lmno*]chrysene **51c** as obtained after reaction (220 ºC, 2 h, *o*-DCB), detected at 380 nm (5PYE column, 1.0 mL min^{-1}, Tol:MeOH:3:7 as eluent, 40 ºC).

The crystal growth of diindenochrisenes encountered difficulties, namely the formation of long and thin needles of the chlorinated and fluorinated bowls **51b** and **51c**, which was inappropriate for the X-ray crystallographic analysis. The crystals of the dibrominated bowl **51a** were grown as the thin needles and showed a weak diffraction. In order to obtain suitable crystals, the phenyl groups were incorporated into diindenochrysene skeletone by double Suzuki cross-coupling leading to **52** in 95 % yield. The product **52** was characterized by ^{1}H NMR spectroscopy (Figure 25). The single-crystal structure of **52** is displayed in the Figure 25 revealing the bowl-shaped character of the diindenochrysene core.

The molecular structures and electronic properties of halogenated diindenochrysene and indacenopicene were calculated at the DFT level of the theory. According to the calculations, the halogenation does not influence the C-C bond lengths and the bond orders with respect to the pristine bowls. Diindenochrysene is more curved than indacenopicene, the bowl depths appeared to be 1.78 and 1.62 Å respectively. That means that the diflurodibenzochrysenes possess the larger steric strain in comparison with the difluorobenzopicenes. The detailed description of DFT calculation can be found in [98].

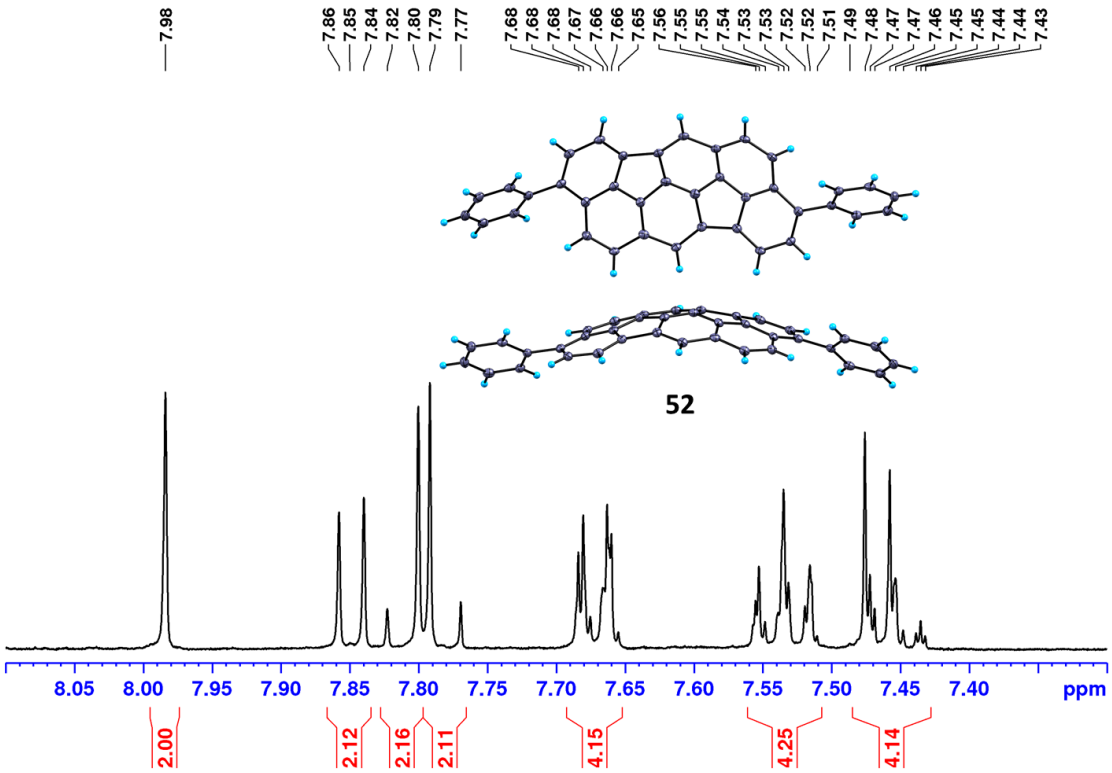

Figure 25. ^{1}H NMR (400 MHz, CD_2Cl_2, 293 K) spectrum of 3,9-diphenyldiindeno[*4,3,2,1-cdef:4',3',2',1'-lmno*]chrysene **52** and its molecular structure as determined by X-ray diffraction analysis. Thermal ellipsoids are set at the 50% probability level.[98] Adapted with permission from O. Papaianina, V. A. Akhmetov, et al., *Angew. Chem. Int. Ed.* **2017**, *56*, 4834. Copyright 2017 Wiley-VCH Verlag GmbH & Co. KGaA, Weinheim.

In collaboration with group of Prof. Petrukhina the limits of reduction and coordination abilities of the non-brominated *as*-indaceno[*3,2,1,8,7,6-pqrstuv*]picene **30** were investigated. Its reduction properties were studied by CV measurements. All measurements were carried out in *o*-DCB with Bu_4NBF_4 as a supporting electrolyte at the room temperatures. A cell was fitted with a working (platinum disc), a counter (platinum coil) and a reference ($Ag/AgNO_3$) electrode.[150]

The reduction potentials of two reversible one-electron reduction processes were found to be −1.92 and −2.29 V vs $Fc^{+/0}$;[150] the cathodic and anodic currents were equivalent. These results illustrate chemical and electrochemical reversibility of both reduction steps and the stability of the corresponding mono- and dianionic states during the experiment. According to the electrochemical measurements the HOMO−LUMO gap at 2.8 eV (HOMO and LUMO energy level estimations −5.8 and −3.0 eV) was estimated. The value of the optical HOMO-LUMO gap was found to be 2.4 eV (on the basis of the absorption band onset observed for **30** at 510 nm).[150]

Along with the electrochemical study, the reduction of **30**, leading to the formation of the dianion, was conducted by alkali metals.

Excess of Li, Rb and Cs was added to *as*-indaceno[*3,2,1,8,7,6-pqrstuv*]picene in THF medium. The formation of $C_{26}H_{12}^{-}$ anion was accompanied by the change of colour from yellow-orange to green with the following coloration to deep purple resulted in formation of the $C_{26}H_{12}^{2-}$. The lithium-excess promoted the formation of $C_{26}H_{12}^{2-}$ dianion only.[150]

The use of rubidium and caesium counter-cations enabled the isolation of the corresponding dianion in the solid state. The X-ray analysis of $[Rb^{+}_{4}$(18-crown-6)$_3(C_{26}H_{12}^{2-})_2]$ and $[Cs^{+}_{2}$(18-crown-6)$_2$(THF)$(C_{26}H_{12}^{2-})]$ crystals demonstrated that product **53** possesses tetrameric structure of **30** with $[Rb_2$(18-crown-6)$]^{2+}$ dication, which fills the cavities of two indacenopicene bowls.[150] The complexation product of **30** with caesium has an chain-extended structure. The binding pattern of $C_{26}H_{12}^{2-}$ with caesium is similar to rubidium complex. The distance between the indacenopicenes after replacing of Rb^{+} ions with Cs^{+} ions has been enlarged.[150]

3.3 Indacenopicene-based Buckycather

The complexation ability of the molecular receptors (tweezers, sensors) via non-covalent *π–π* interactions with fullerenes due to their importance in the field of supramolecular and material chemistry appears to be of great interest.[151],[152],[153] The planar (porphyrins)[154] and bowl-shaped (subphthalocyanines[155], porphyrins[156], corannulenes[12]) molecules have been already used as host. However, the planar structure of porphyrins does not allow a proper complexation with spherical fullerenes. The decline of binding constant values and electronic interaction in complexes are observed. In contrast, the binding ability of bowl-shaped structures towards fullerenes is significantly higher.

Sygula *et al.* [151,157] studied the association of fullerene with a wide-range of corannulene-based "buckycatchers".[158] Deng-Chen Yang *et al.* proposed the molecular tweezer with two corannulene subunits linked by [*5*]helicene derivative. Such tweezer showed a strong complexation ability with C_{70} (K_a=64200±2600 M^{-1}) compared to the fullerene C_{60} (K_a=2790±180 M^{-1}).[159]

In this chapter, we developed another type of the molecular receptor using two bromo-indacenopicene, and tolyl as a tether. The synthesis of molecular receptor is depicted in the Scheme 35. Starting with 4-bromo-13,16-difluorobenzo[*s*]picene **38b**, the indaceno[*3,2,1,8,7,6-pqrstuv*]picen-1-yl)-4,4,5,5-tetramethyl-1,3,2-dioxaborolane **54** was prepared by the modified Miyaura borylation in 60-70 % yield [160]. The purification of **54** was conducted by flash chromatography (DCM:Hexane:1:2). Apart from the main product **54** we isolated a bright orange precipitate corresponding to dimer form of indacenopicene **55** (1,1'-bias-indaceno[*3,2,1,8,7,6-pqrstuv*]picene). The obtained side product was insoluble in the standard for PAHs solvents (benzene, toluene and dichloromethane). Surprisingly, it was found that dimer **55** can be dissolved in 1,1,2,2-tetrachloroethane. Hence, we were able to measure ^{1}H NMR-spectrum and to verify the structure of **55** (Figure 26).

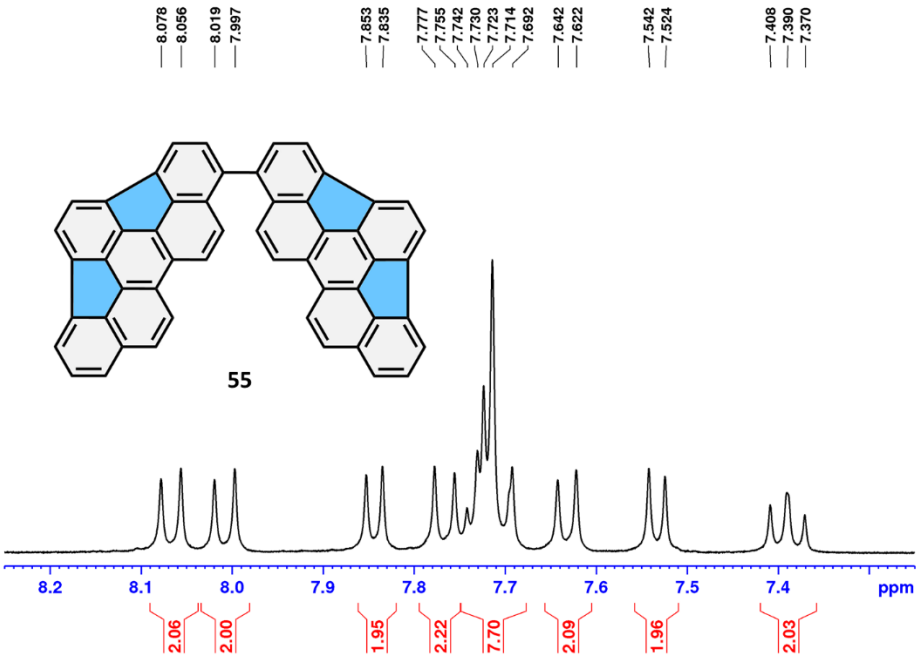

Figure 26. ^{1}H NMR spectrum of **55** 1,1'-bias-indaceno[*3,2,1,8,7,6-pqrstuv*]picene (400 MHz, $C_2D_2Cl_4$, 293 K).

The attempt to synthesize **56** was undertaken utilizing Suzuki cross-coupling of the bromoindacenopicene **38b** with 1,3-dibromo-5-methylbenzene **57** in the presence of K_2CO_3 and $Pd(PPh_3)_4$ in Tol:MeOH mixture (Scheme 35). The reaction, monitored by HPLC chromatography, failed to conduct. Hence, after 16 h no product was detected. The replacement of the catalyst by $Pd(dppf)Cl_2$ did not affect the formation of **56**.

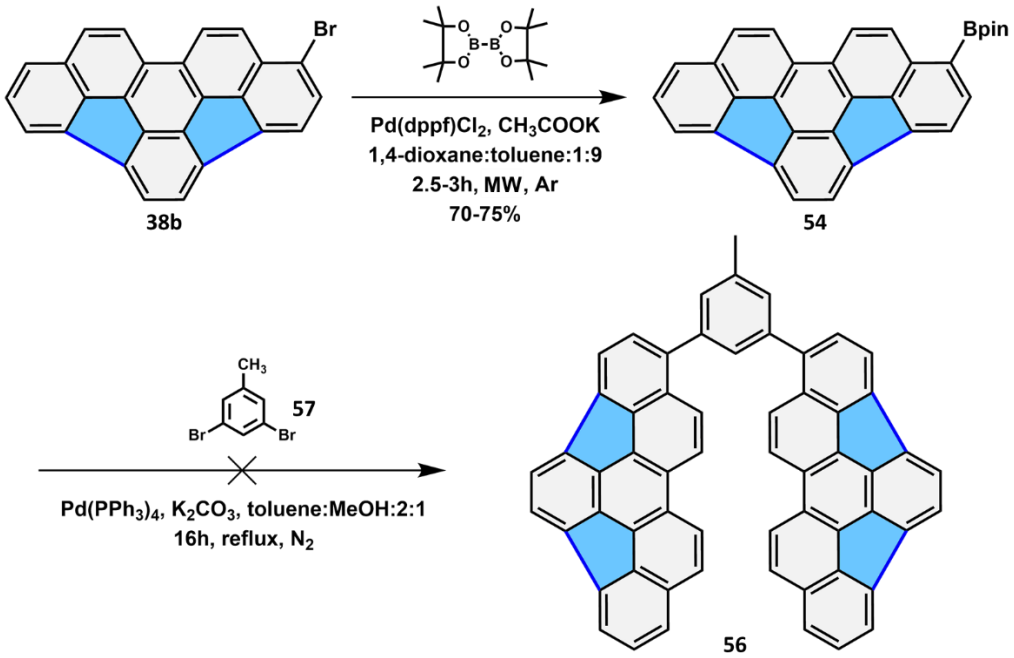

Scheme 35. Synthetic route to indacenopicene-based “buckycatcher” **56**.

Therefore, the buckycatcher was prepared by another synthetic approach (Scheme 36). Miyaura borylation of 1,3-dibromo-5-methylbenzene **57** was carried out in 1,4-dioxane in the presence of CH_3COOK and Pd catalyst (yield: 48%). Following Suzuki cross-coupling of 1-bromo-*as*-indaceno[*3,2,1,8,7,6-pqrstuv*]picene with 2,2'-(5-methyl-1,3-phenylene)bis(4,4,5,5-tetramethyl-1,3,2-dioxaborolane) **58** yielded 53 % of the 4,4'-(5-methyl-1,3-phenylene)bis(benzo[*s*]picene) **56**.

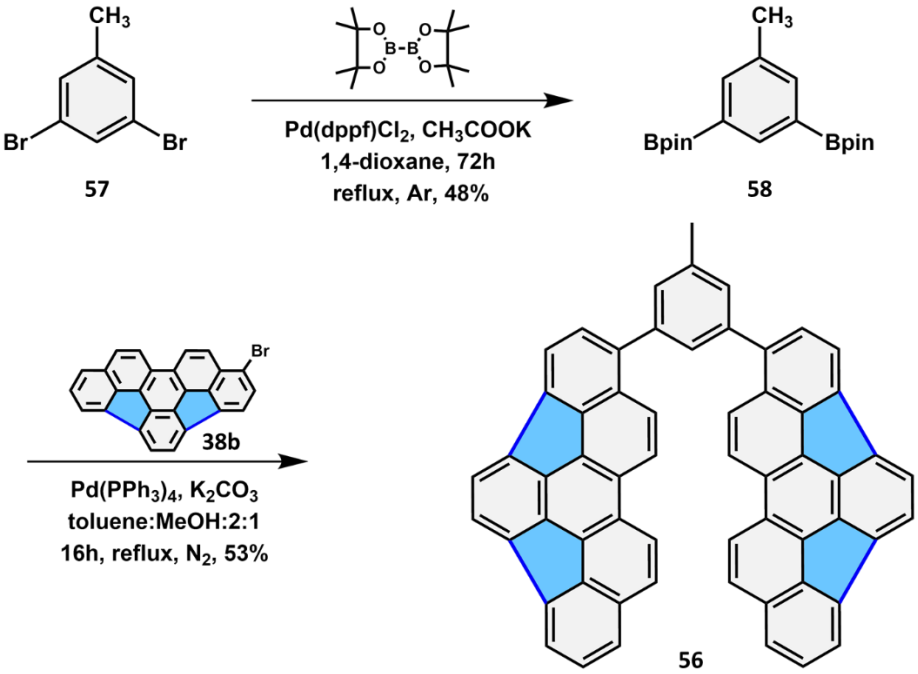

Scheme 36. Synthetic route to 4,4'-(5-methyl-1,3-phenylene)bis(benzo[*s*]picene) **56**.

Structural elucidation of **56** was conducted by employing the NMR-spectroscopy in cooperation with Dr. Harald Maid. Implementing one- and two-dimensional NMR measurements (^1H, ^{13}C, DEPT, COSY, NOESY, ROESY, HETCOR, HMBC) the proton signals of buckycatcher were assigned to corresponding nuclei. The ^1H NMR assignements are presented in the Figure 27. Additionally, new compound was characterized by the HRMS.

In the previous studies, the complexation of fullerene with buckycatchers has been measured by NMR, UV and fluorescence spectroscopy.[159,161] Consequently, we investigated the photophysical properties of indacenopicene-based catcher.

The UV-spectrum of **56** is depicted in the Figure 28 and illustrates the intence absorbtion in the region from 300 to 510 nm. The maximum absorption band is observed at 388 nm. The fluorescence emission is detected in range between 450 and has two maximum peaks at 526 and 557 nm.

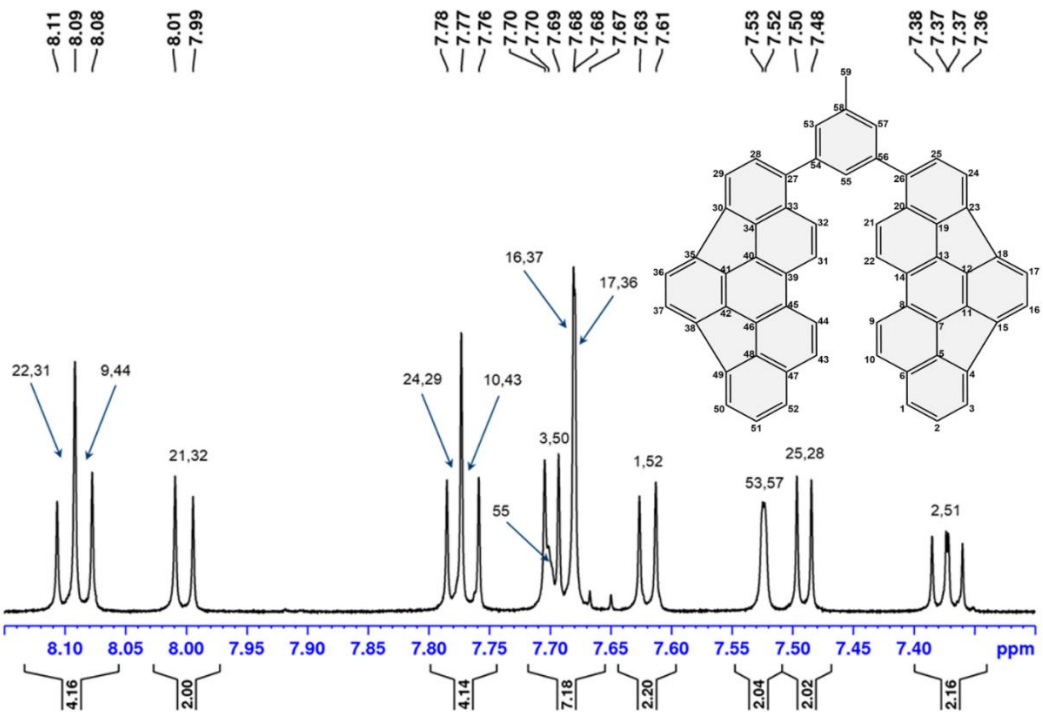

Figure 27. ^{1}H NMR (600 MHz, $C_2D_2Cl_4$, 293 K) spectrum of 4,4'-(5-methyl-1,3-phenylene)bis(benzo[*s*]picene) **56**.

To analyze the interaction between buckycatcher **56** and C_{60} and C_{70} we carried out the titration experiments in toluene monitored by fluorescence spectroscopy. For this

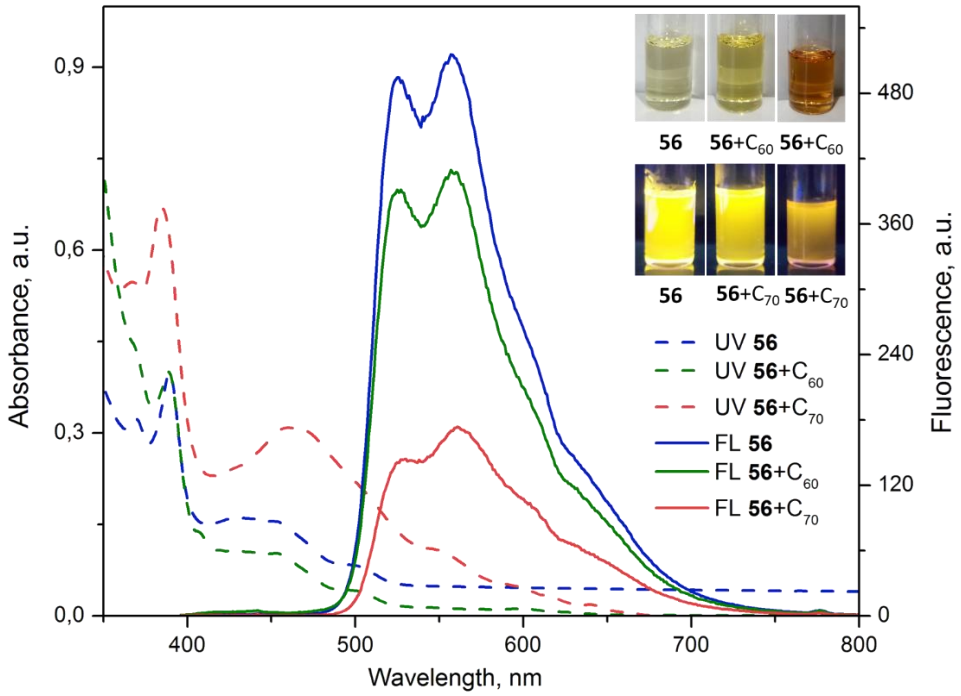

Figure 28. Absorption (UV) and fluorescence (FL) spectra of 4,4'-(5-methyl-1,3-phenylene)bis(benzo[*s*]picene) (0.32×10^{-4}M) with 1:1 eq. of C_{60} and 1:1 eq. of C_{70}. Insets: Photographs of **56** after addition of 1.0 eq. of C_{60} and C_{70} under day light and under irradiation by UV lamp at 365 nm.

purpose, three solutions were prepared:

a) stock solution A of the host molecule **56** (buckycatcher), 0.32×10^{-4} M in toluene;

b) solution B of the guest C_{60} in the solution A, 0.332×10^{-3} M;

c) solution C of the guest C_{70} in the solution A, 0.266×10^{-3} M.

The concentration of the host **56** was kept constant during the titration with the solution B or C (solution B or C was added into 1.0 mL of the solution A). The experimental details are summarized in the Table 3. For each guest solution (B and C) were collected 3 titrations with 19 data points.

From the spectroscopic data the quenching of fluorescence while adding of the guest solution to the solution of buckycatcher can be observed (Figure 29 a,b). Such quenching behaviour, namely reduction of intensity, can be explained by decrease of free host's concentration (fluorochrome) owing to the interaction between fullerene and catcher **56**. Although, the degree of fluorescence quenching by C_{70} is larger than by C_{60} at the equal concentrations.

Table 3. Summarized data of 4,4'-(5-methyl-1,3-phenylene)bis(benzo[*s*]picene) titration by C_{60} and C_{70} solution in toluene. V_A – volume of the stock solution (buckycatcher), μL; V_B – volume of the C_{60} solution, μL; V_C- volume of the C_{70} solution, μL; C_A – concentration of the stock solution 0.32×10^{-4} M; C_{60} – concentration of the fullerene C_{60}, $M\times10^{-4}$; C_{70} – concentration of the fullerene C_{70}, $M\times10^{-4}$.

V_B, μL	V_{A+B}, μL	C_{60}, $M\times10^{-4}$	C_{60}/C_A	V_C, μL	V_{A+C}, μL	C_{70}, $M\times10^{-4}$	C_{70}/C_A
0	1000	0.000	***0.00***	0	1000	0.000	***0.00***
10	1010	0.033	***0.10***	10	1010	0.026	***0.08***
20	1020	0.065	***0.20***	20	1020	0.052	***0.16***
40	1040	0.013	***0.40***	30	1030	0.077	***0.24***
50	1050	0.016	***0.49***	40	1040	0.010	***0.32***
60	1060	0.188	***0.59***	50	1050	0.127	***0.40***
80	1080	0.246	***0.77***	60	1060	0.151	***0.47***
100	1100	0.302	***0.94***	70	1070	0.174	***0.54***
110	1110	0.329	***1.03***	80	1080	0.197	***0.62***
120	1120	0.356	***1.11***	90	1090	0.220	***0.69***
140	1140	0.408	***1.27***	100	1100	0.242	***0.76***
160	1160	0.458	***1.43***	120	1120	0.285	***0.89***
180	1180	0.506	***1.58***	130	1130	0.306	***0.96***

240	1240	0.643	***2.01***	160	1160	0.367	***1.15***
280	1280	0.726	***2.27***	190	1190	0.425	***1.33***
320	1320	0.805	***2.52***	220	1220	0.480	***1.50***
360	1360	0.879	***2.75***	250	1250	0.532	***1.66***
400	1400	0.949	***2.96***	310	1310	0.629	***1.97***
410	1410	0.965	***3.02***	380	1380	0.732	***2.29***

For instance, in case of the fluorescence quenching for 1:1 host-to-guest equilibria by C_{60} led to 21 % decrease of intensity, while by C_{70} – to 81 % (Figure 29). This fact indirectly can be proved by naked-eye colour change (Figure 28) from light-yellow to bright-yellow (C_{60}) and brown (C_{70}). The most significant drop in fluorescence intensity was observed for 1:2 host-to-guest equilibria:90 % for C_{70} and 40 % for C_{60}. This fact indicates a stronger *π–π* interactions between buckycatcher **56** and C_{70}.

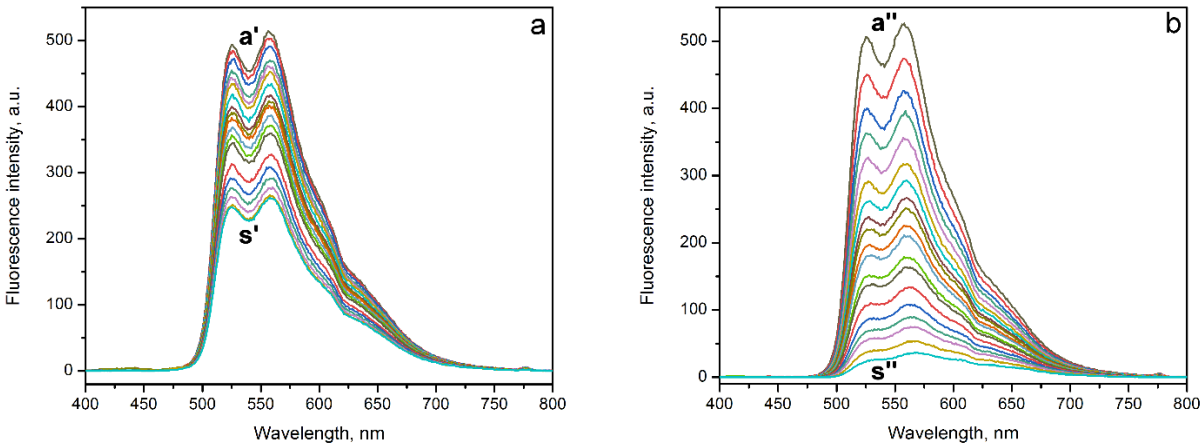

Figure 29. Emission spectra (λ_{ex} = 388 nm) of 4,4'-(5-methyl-1,3-phenylene)bis(benzo[*s*]picene) **56** (0.32×10^{-4}M) upon the addition of solution B (0.332×10^{-3}M, **a**) and solution C in toluene (0.266×10^{-3}M, **b**). Curves a'-s': 0-3.0 eq., curves a''-s'': 0-2.3 eq.

Figure 30 presents the Stern-Volmer plots at concentrations in range from 0 to 0.096 and 0.097 mM L^{-1} for C_{60} and C_{70} respectively. Dependence of parameter $\mathbf{F_0/F}$ from concentration of guest molecule C_{60} is resulted in linear plot which fitted to the linear Stern-Volmer equation, whereas dependence $\mathbf{F_0/F}$ from C_{70} is nonlinear and appears to be the upward-sloping curve. It is known that quenching appears to be by static and dynamic mechanism. Thus, static quenching resulted in formation of fluorophore-fluorescence quencher complex, while dynamic or collision quenching leads to reduce of fluorescence emission without complex formation. Commonly, both static and dynamic interaction mechanism of quenching are included. From the data in the Figure

30a it can be seen that by applying C_{60} as fluorescence quencher mostly static mechanism occurs.

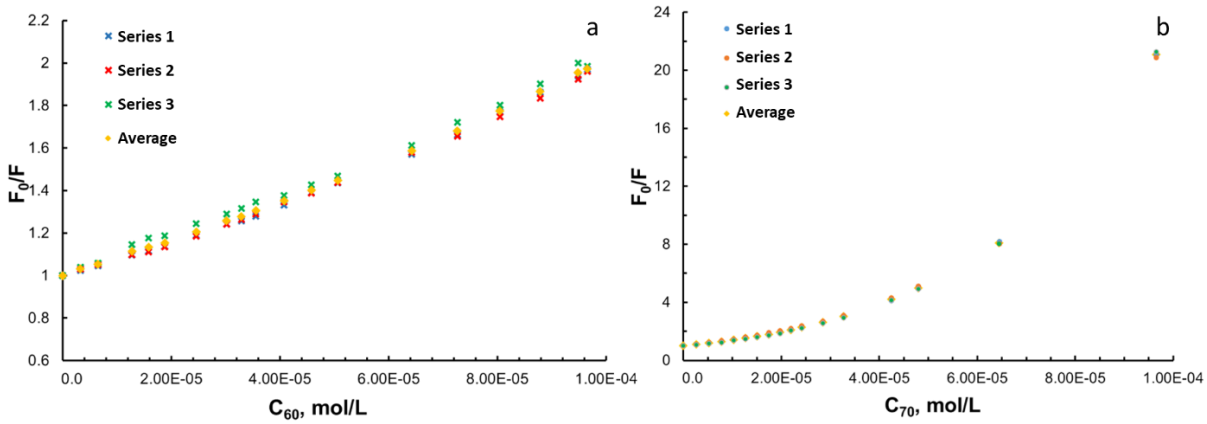

Figure 30. Plot of relative fluorescence intensity change of receptor 4,4'-(5-methyl-1,3-phenylene) bis(benzo[*s*]picene) **56** ($0.32x10^{-4}$M) against: a) varied concentrations of C_{60} from 0.0 to 0.096 mM, λ_{ex}=388 nm; b) varied concentrations of C_{70} from 0.0 to 0.097 mM, λ_{ex}=388 nm.

It is apparent from the nonlinear graph (Figure 30b) that another interaction mechanism is also presented, however, the static mechanism is dominant. The preliminary values of the binding constant can be estimated using Stern-Volmer equation. We determined the **K_{SV}** constant for 1:1 host-to-guest equilibria of **56** with C_{60} and C_{70} in toluene. As depicted in the Figure 31a in the 1:1 complex (catcher:C_{60}) binding constant corresponds to 8.65×10^3 M^{-1}. In case of fullerene C_{70} the affinity towards fullerene is higher and was calculated to be 6.04×10^4 M^{-1}. Hence, the the **K_{C70}/K_{C60}** value was found to be 7/1.

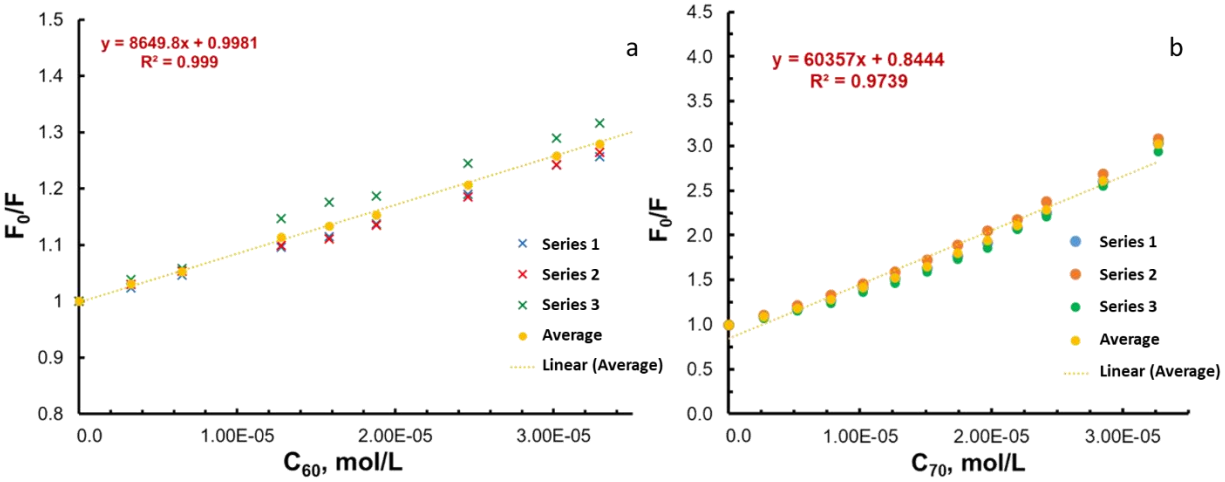

Figure 31. Plot of relative fluorescence intensity change of receptor 4,4'-(5-methyl-1,3-phenylene)bis (benzo[*s*]picene) **56** ($0.32x10^{-4}$M) with increasing of a) C_{60} concentration R = 0.999, $3\sigma = 1.49\times10^3 M^{-1}$, $\mathbf{K_{60}} = 8.65\times10^3 M^{-1}$; b) C_{70} concentration R = 0.974, $3\sigma = 6.51\times10^3$ M^{-1}, $\mathbf{K_{70}} = 6.04\times10^4$ M^{-1}.

Comparison of the two results with published on other buckycatchers reveals the stronger binding affinity of fullerene C_{70}.[151]

Additionally, we employed the ^{1}H NMR measurements for the complexation study. Preliminary investigations were carried out by adding to the solution of buckycatcher **56** were added solution of C_{60} or C_{70}. All experiments were done in $C_2D_2Cl_4$.

The NMR data indicated that the complex formation took place (Figure 32). Following the addition of fullerene C_{60} to the buckycatcher solution, the shielding of protons was observed. The majority of proton signals are shielded upfield, for instance, protons **H_{21}/H_{32}** (δ = 0.15 ppm), **H_{17}/H_{36}** (δ = 0.08 ppm) and **H_{25}/H_{28}** (δ = 0.12 ppm), whereas only protons corresponding to methyl group and **H_{53}/H_{57}** are shifted downfield by 0.05 ppm (Figure 32).

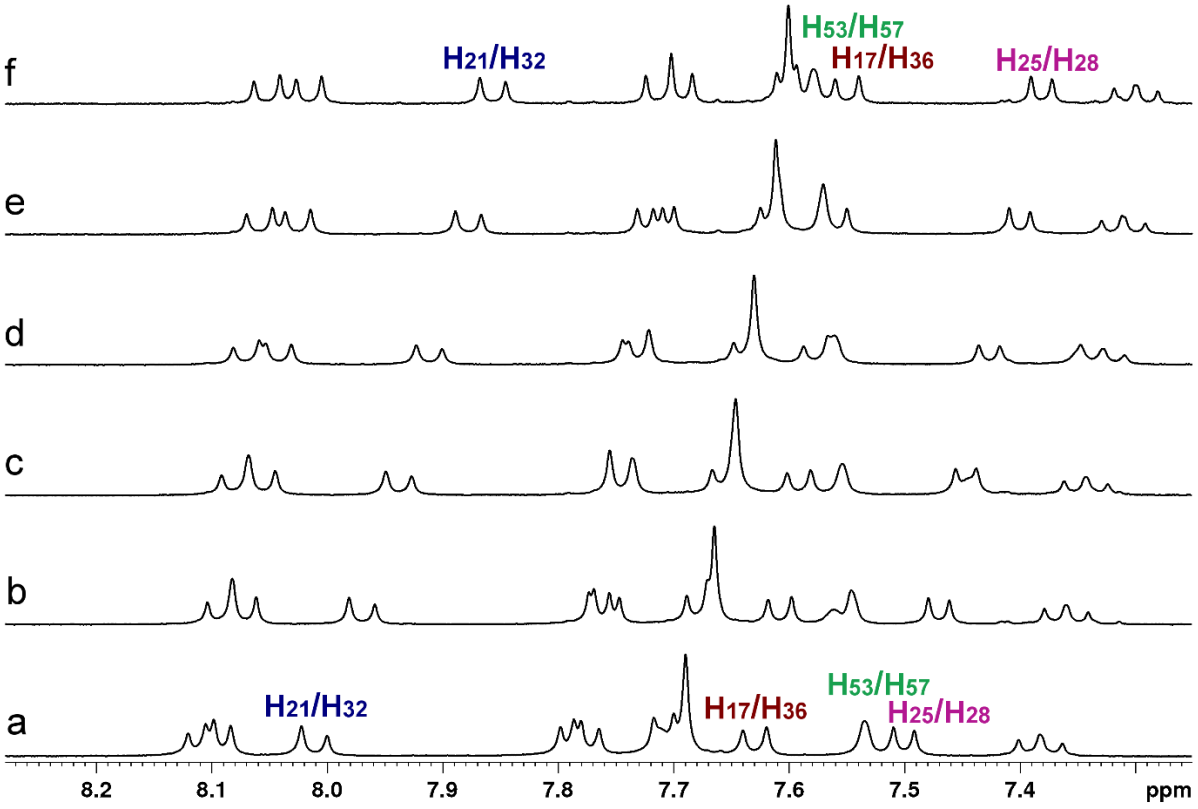

Figure 32. Partial ^{1}H NMR spectra (400 MHz, $C_2D_2Cl_4$, 298 K) of (a) free receptor 4,4'-(5-methyl-1,3-phenylene)bis(benzo[*s*]picene) **56**; (b-f) receptor **56** after addition of C_{60}.

At the same conditions, addition of C_{70} to the solution of buckycatcher also lead to changes in NMR spectra (Figure 33). Most of the proton peaks were shifted in upfield. Larger shifts were observed for protons **H_{21}/H_{32}** (0.22 ppm after addition of 300 µL solution) and **H_{25}/H_{28}** (0.20 ppm after addition of 300 µL solution). Protons of methyl group and **H_{53}/H_{57}** were shifted downfield by 0.05 ppm and 0.04 ppm respectively.

Thus, preliminary NMR measurements also confirmed complexation of C_{60} and C_{70} with buckycatcher **56**.

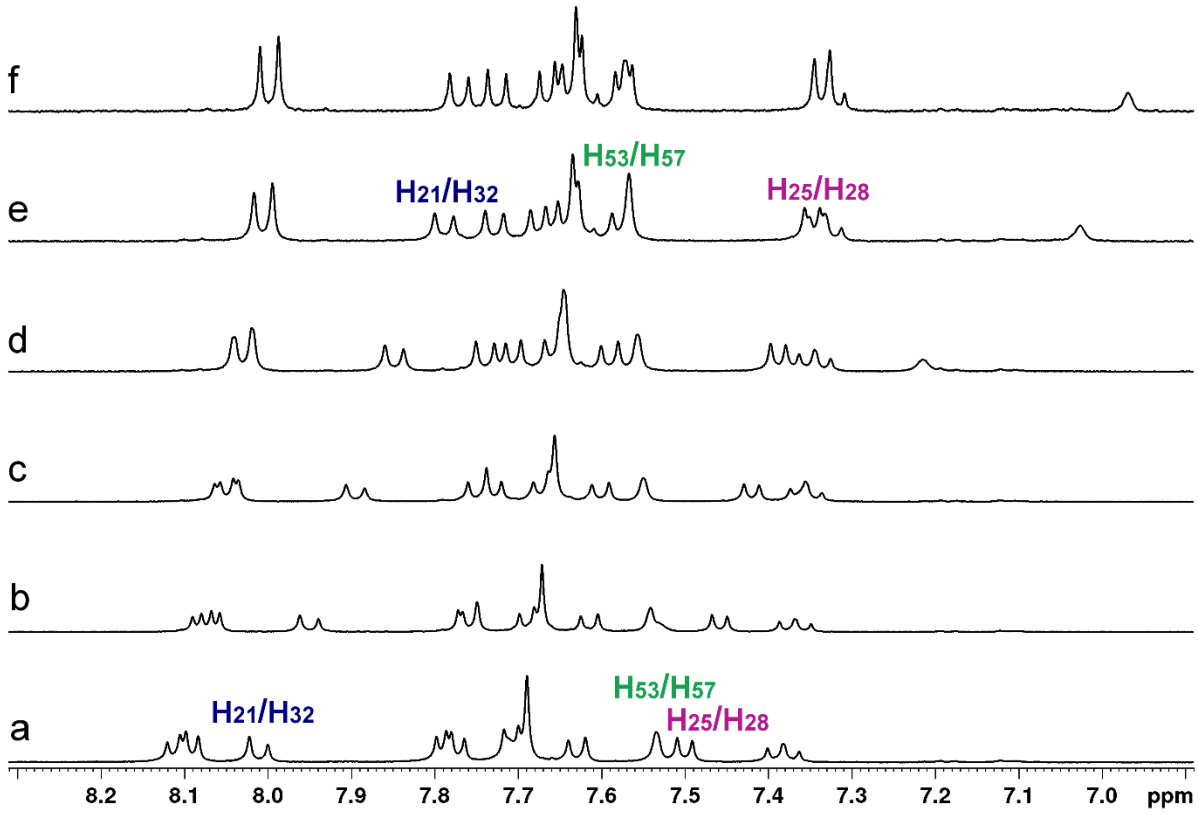

Figure 33. Partial ^{1}H NMR spectra (400 MHz, $C_2D_2Cl_4$, 298 K) of (a) free receptor 4,4'-(5-methyl-1,3-phenylene)bis(benzo[*s*]picene) **56**; (b-f) receptor **56** after addition of C_{70}.

In conclusion, we found that indacenopicene catcher **56** forms in toluene 1:1 complexes with C_{60} and C_{70} with association constants of 8.65×10^{-3} and $6.04\times10^{4}M^{-1}$ respectively.

3.4 Introduction of Indene Fragments into Chrysene and Pyrene Derivatives

The several reports about the class of indenopyrenes have been presented in literature by now. Scott and co-workers [59] presented a synthetical way including Suzuki cross-coupling and intramolecular Pd-catalyzed C-H arylation from dibromopyrenes with yields up to 50%, however for tri- and tetrabromopyrenes reaction yields were very low (less than 5%). F. Eisenhut *et al.* reported synthesis of diindenopyrene on surface of Au(111) [162] that allows to obtain the “preprogrammed” nonalternant polyaromatic hydrocarbons.

In this research we presented the aluminium oxide mediated synthesis of di- and tetraindenopyrenes. Similar approach wa applied for introduction additional indene fragments in diindenochrysenes.

The strategy for synthesis of diindeno[*1,2,3-cd:1',2',3'-jk*]pyrene **60** is shown on the Scheme 37. Firstly, the bromination of pyrene was carried out in $CHCl_3$ with subsequent recrystallisation from xylene (11.8 g, 33 %).[148] Suzuki coupling cross-coupling of 1,6-dibromopyrene **24** with 2-fluorophenylboronic acid **58** gave the 1,6-bis-(2-fluorophenyl)pyrene **59** in 63 % yield (Scheme 37).

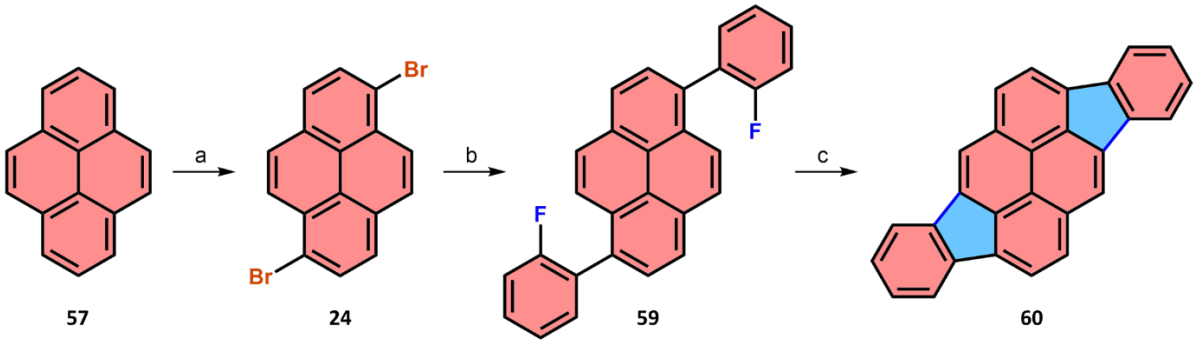

Scheme 37. Synthetic route to diindeno[*1,2,3-cd:1',2',3'-jk*]pyrene **60**: a) Br_2, $CHCl_3$, rt, 36 %; b) F-PhB(OH)$_2$ **58**, K_2CO_3, $Pd(PPh_3)_4$, Tol:MeOH:2:1, reflux, N_2, 16 h, 63 %; c) *γ*-Al_2O_3, *o*-DCB, MW, 240 ºC, 1.5 h.

Cyclodehydrofluorination of 1,6-bis(2-fluorophenyl)pyrene **59** was conducted at 240ºC for 1.5 hour in o-DCB medium. After the reaction the yellow crystals of diindeno[*1,2,3-cd:1',2',3'-jk*]pyrene **60** precipitated in *o*-DCB. The obtained crystals of **60** were suitable for X-ray crystallographic analysis, which confirmed structure of product (Figure 34).

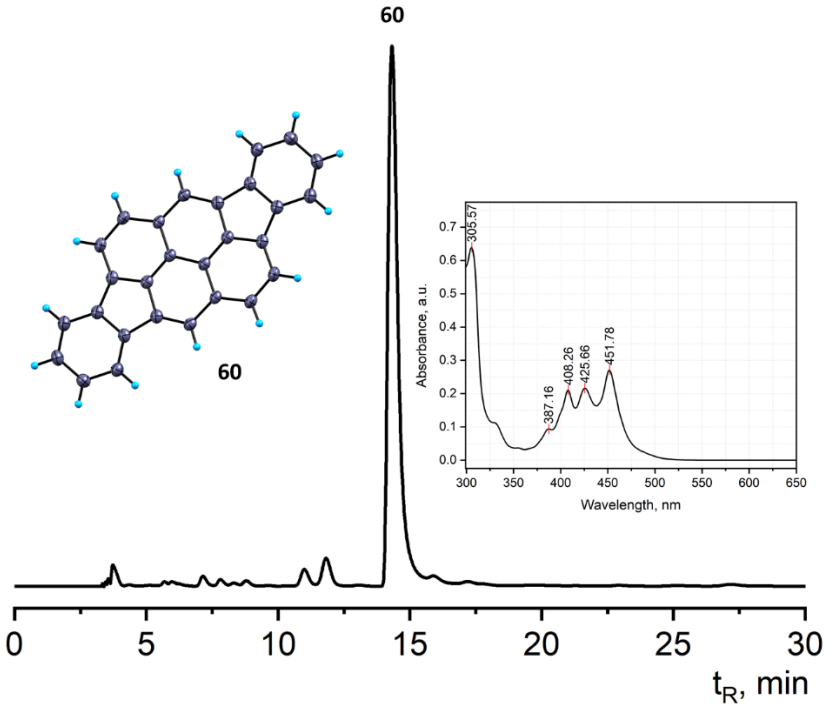

Figure 34. HPLC profile of reaction mixture as obtained (240 ºC, 1.5 h, *o*-DCB) detected at 300 nm (5 PYE column, Tol:MeOH:2:8, 1.0 mL min^{-1}, 40º C). Inset: The molecular structure of the diindeno[*1,2,3-cd:1',2',3'-jk*]pyrene **60** as determined by X-ray diffraction analysis. Thermal ellipsoids are set at the 50 % probability level.

Additionally, *o*-DCB solution was analyzed by HPLC chromatography and it was found that main peak (t_R = 14.5 min) corresponds to the **60** (Figure 34).

Tetraindeno[*1,2,3-cd:1',2',3'-fg:1'',2'',3''-jk:1''',2''',3'''-mn*]pyrene **63** was prepared according to the same procedure. (Scheme 38). The Suzuki cross-coupling between 1,3,6,8-tetrabromopyrene **61** and 2-fluorophenylboronic acid **58** in presence of Pd catalyst afforded the 1,3,6,8-tetrakis(2-fluorophenyl)pyrene **62** in 75 % yield.

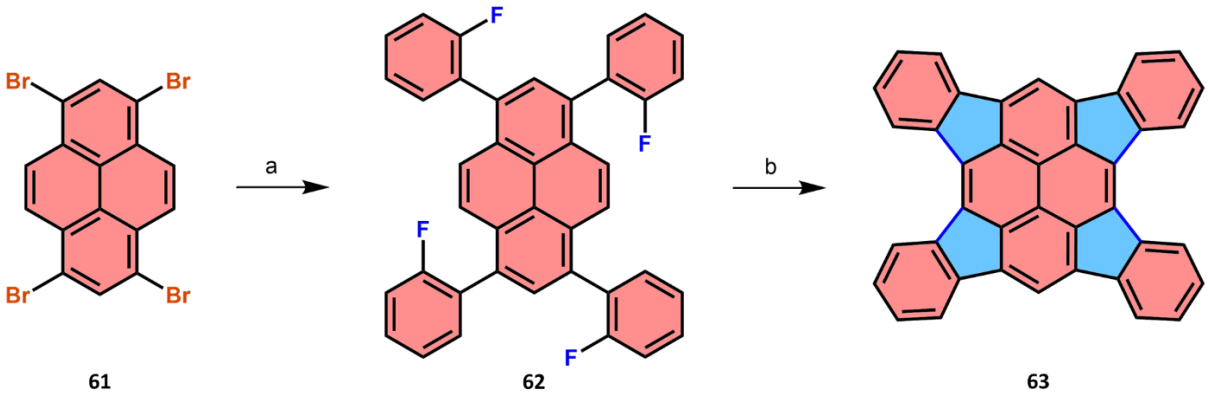

Scheme 38. Synthetic route to tetraindeno[*1,2,3-cd:1',2',3'-fg:1'',2'',3''-jk:1''',2''',3'''-mn*]pyrene **63**: a) F-PhB$(OH)_2$ **58**, K_2CO_3, $Pd(PPh_3)_4$, Tol:MeOH:2:1, reflux, N_2, 16h, 75%; b) γ-Al_2O_3, *o*-DCB, MW, 240 ºC, 1.5 h.

In the next step, the cyclodehydrofluorination of 1,3,6,8-tetrakis(2-fluorophenyl)pyrene **58** was carried out at 240 ºC for 1.5 h in *o*-DCB medium. In this case, we observed a mixture of products on HPLC chromatogram that can be assigned to different stages of multi-fold cyclization (Figure 35). The peak at t_R = 4.5 min was identified as a product of three-fold cyclization (based on comparison of the obtained UV-spectrum with the data presented in [59]). In all subsequent experiments we did not succeed in synthesizing of pure product **63**. Indeed, we assume that substantial part of synthesized product **63** was adsorbed on the alumina surface (red-coloured). Soxhlet extraction of product **63** with toluene/*o*-DCB mixture from aluminium oxide did not allowed to extract the product. This result can be explained by the extremely low solubility of tetraindenopyrene. Later it was found that the product can be partially extracted by the long-time extraction with *o*-DCB.

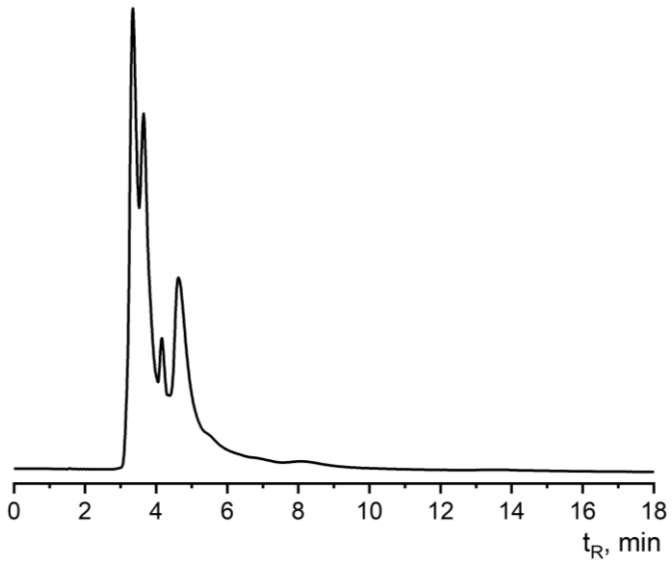

Figure 35. HPLC profile of reaction mixture as obtained (250 ºC, 1.5 h, *o*-DCB) detected at 360 nm (5 PYE column, toluene as eluent, 1.0 mL min^{-1}, 60 ºC).

Introduction of additional indene fragments in diindenochrysene molecule appears to be difficult due to an enhanced strain in comparison with indenopyrenes. In order to investigate this process, the synthetic route presented in Scheme 39 was chosen. As starting material, the 3,9-dibromodiindenochrysene **51a** was selected. Suzuki cross-coupling of **51a** with 2-fluorophenylboronic **58** or 2-fluoro-5-methylphenylboronic acid **64** was carried out in Tol:MeOH mixture in the presence of Pd catalyst. The 3,9-bis(2-fluorophenyl)diindenochrysene **65a** and the 3,9-bis(2-fluoro-5-methylphenyl)diindeno-chrysene **65b** were obtained in 95 and 92 % yield correspondingly.

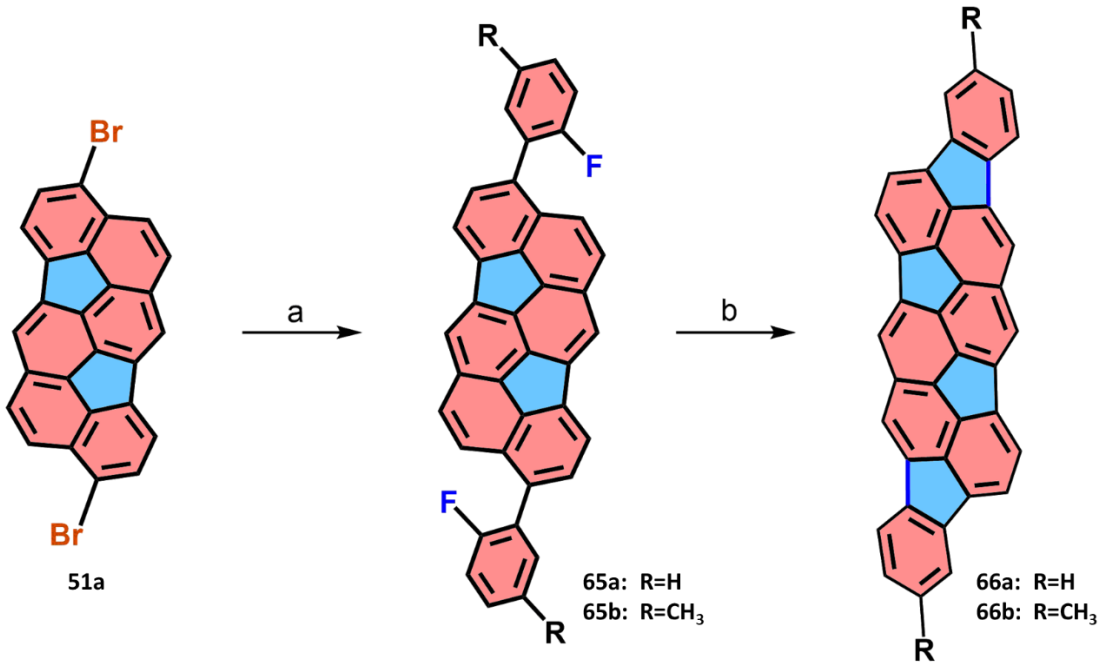

Scheme 39. Synthetic route to **66a** and **66b**: a) R-PhFB(OH)$_2$ **58** or **64**, K_2CO_3, $Pd(PPh_3)_4$, Tol:MeOH:2:1, reflux, N_2, 16 h (**65a**: 95 %; **65b**: 92 %); b) γ-Al_2O_3, *o*-DCB, MW, 240 ºC, 16 h (**66a**: 35 %).

Initially, we used **66a** for alumina-promoted HF elimination. The reaction proceeded after 3 h (*o*-DCB, 240 ºC). Figure 36 illustrates the HPLC chromatogram, which contains three major peaks corresponding to the starting material **65a** (t_R = 6.75 min), the product of one-fold CDHF **67a** (t_R = 9.92 min) and the product of two-fold CDHF **66a** (t_R = 14.51 min).

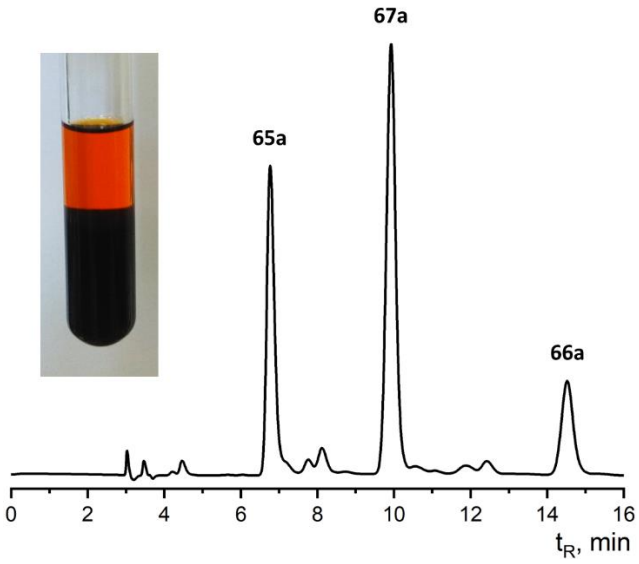

Figure 36. HPLC profile as obtained after reaction (240ºC, 3 h, *o*-DCB), detected at 360 nm (PBr column, Tol:MeOH:1:1 as eluent, 1.0 mL min^{-1}, 35ºC). Inset: the reaction mixture as obtained in the microvawe vial.

The increase of the reaction time to 16 h remarkably improved the yield of product (Figure 37). The semi-preparative chromatography was employed for the separation of reaction products (HPLC: PBB column, Tol:MeOH:7:3 as eluent, 5.0 mL min^{-1}, 35 ºC). Both products **66a** and **67a** were identified and characterized by NMR-spectroscopy (Figure 38) and mass spectrometry.

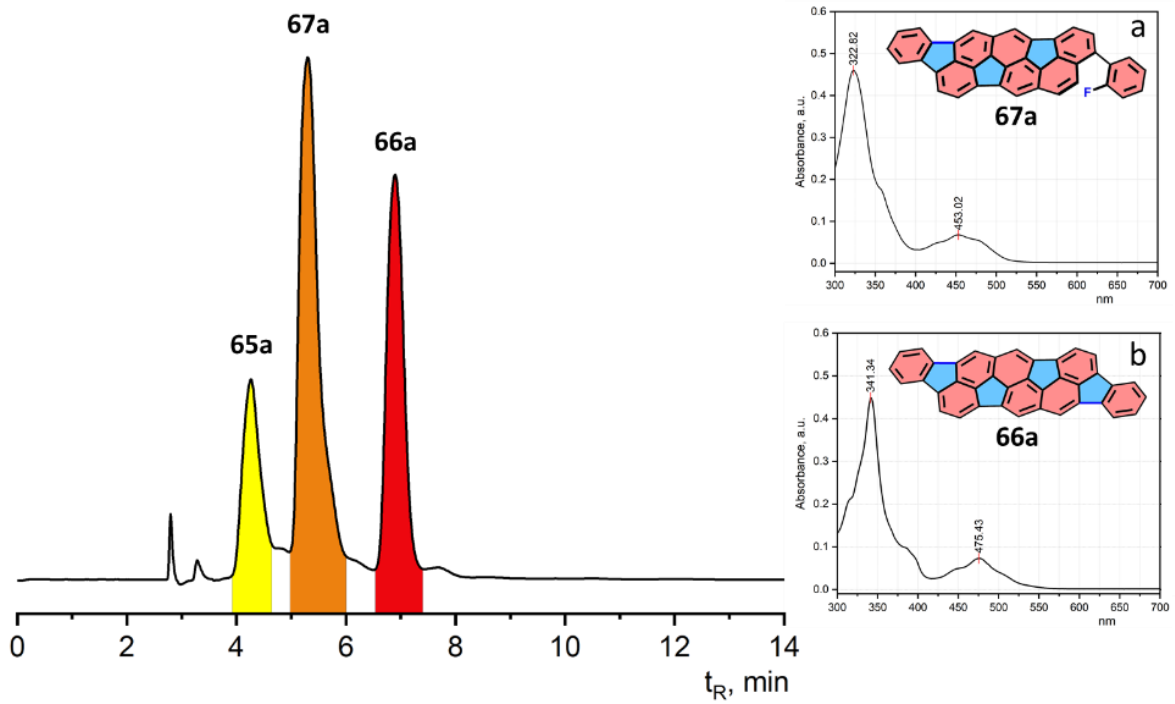

Figure 37. HPLC profiles as obtained after reaction at 230 ºC for 16 h in *o*-DCB detected at 360 nm (PBr column, Tol:MeOH:7:3 as eluent, 1.0 mL min^{-1}, 35ºC). UV-Vis spectra: product of two-fold CDHF **66a** (Inset **a**) and product of one-fold CDHF **67a** (Inset **b**) in Tol:MeOH:7:3.

Previously, we have observed that introduction of methyl group in *para*-position to fluorine (in 1-(2-fluorophenyl)-naphthalene) can influence the C-F bond activation and

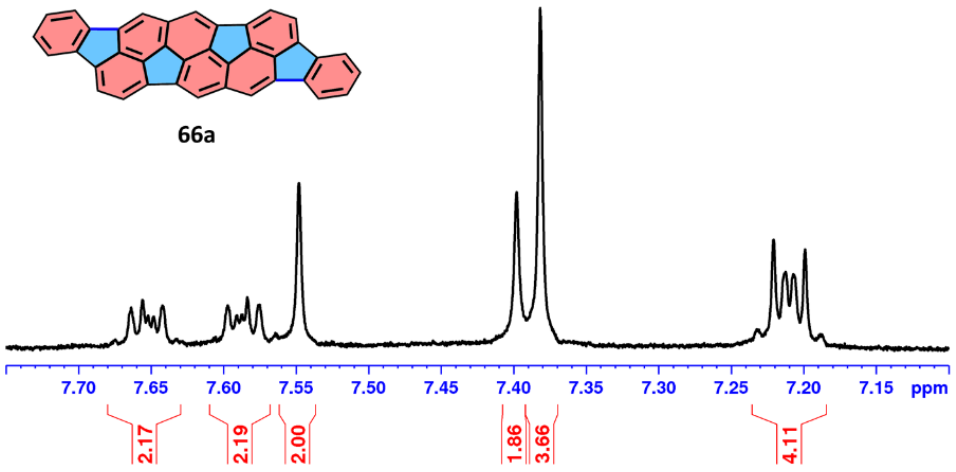

Figure 38. ^1H NMR spectra (400 MHz, 298 K, CD_2Cl_2) of **66a**.

increase the yield of CDHF. For this purpose, we used methylated homologue of diindenochrysene derivative. However, considerable improvements in product yield was not achieved. The product of two-fold CDHF **66b** was purified by semi-preparative chromatography and characterized by means of NMR and MS.

The photophysical properties of bowls benzo[6,7]-*as*-indaceno[*8,1,2,3-bcdef*]benzo [*6,7*]-*as*-indaceno[*8,1,2,3-klmno*]chrysene **66a** and 3,11-dimethylbenzo[*6,7*]-*as*-indaceno[*8,1,2,3-bcdef*]benzo[*6,7*]-*as*-indaceno[*8,1,2,3-klmno*]chrysene **66b** in DCM at room temperature were investigated and elucidated by UV/Vis and fluorescence spectroscopy (Figure 39). Both compounds demonstrate almost identical absorption and emission profiles with the significant absorption maximum at 341 and 475 nm, emission peaks at 575 and 603 nm and a shoulder starting at approximately 630 nm. Additionally, we conducted the preliminary experiments to investigate the complexation between benzo[*6,7*]-*as*-indaceno[*8,1,2,3-bcdef*]benzo[6,7]-*as*-indaceno [*8,1,2,3-klmno*]chrysene **66a** and fullerene C_{60}. However, no evidence of complexation was found.

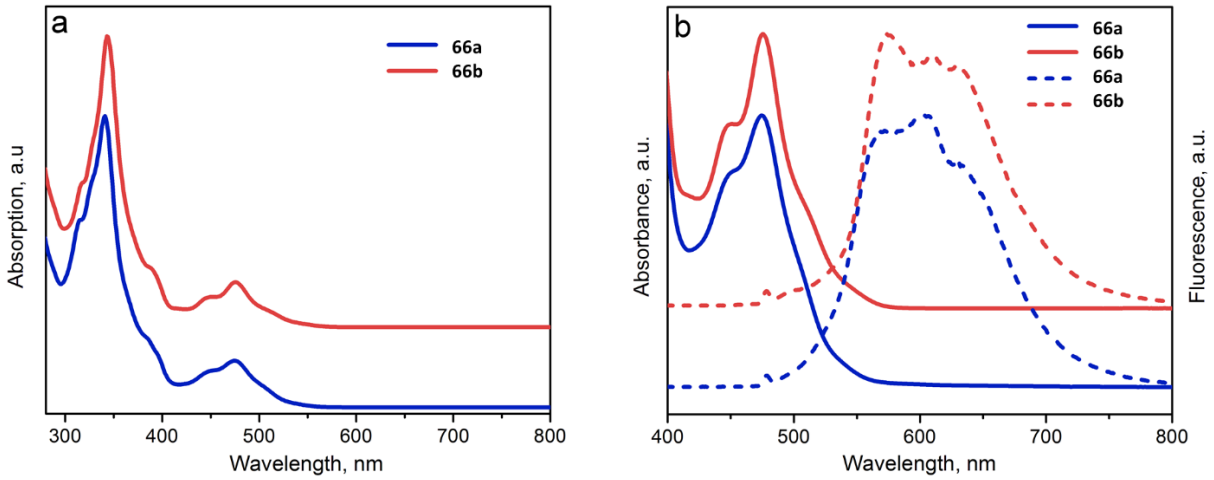

Figure 39. a) UV spectra of benzo[*6,7*]-*as*-indaceno[*8,1,2,3-bcdef*]benzo[*6,7*]-*as*-indaceno[*8,1,2,3-klmno*]chrysene **66a** and 3,11-dimethylbenzo[*6,7*]-*as*-indaceno[*8,1,2,3-bcdef*]benzo[*6,7*]-*as*-indaceno [*8,1,2,3-klmno*]chrysene **66b** in DCM; b) UV (solid) and fluorescence (dot) spectra of **66a** and **66b** in DCM.

Molecular structure of the **66a** was determined by X-ray diffraction analysis of a single crystal (Figure 40). In the crystal the bowl-shaped form with the maximum bowl depth of 5.2 Å remained, which is significantly higher than that of the 3,9-diphenyldiindeno [*4,3,2,1-cdef:4',3',2',1'-lmno*]chrysene **52** (1.78 Å).

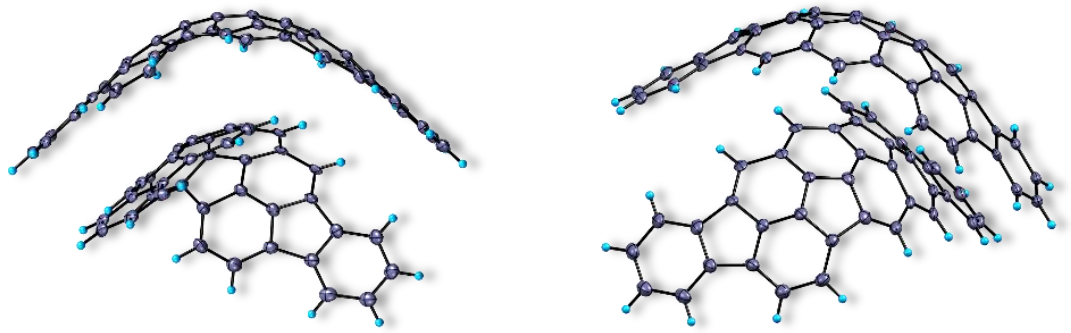

Figure 40. The molecular structure of the benzo[*6,7*]-*as*-indaceno[*8,1,2,3-bcdef*]benzo[*6,7*]-*as*-indaceno[*8,1,2,3-klmno*]chrysene **66a** as determined by X-ray diffraction analysis. Thermal ellipsoids are set at the 50 % probability level.

We proposed a two-step method for synthes of the highly curved buckybowls introducing the indene fragments by the selective C-F bond activation. Such structures can be formed by easily obtained 3,9-dibromodiindenochrysene under mild conditions. This simple approach allows to synthesize molecules with extremely large bowl depth.

3.5 Catalyst-Free Cyclodehydrofluorination of PAHs

3.5.1 Synthesis of Model Compounds for Cyclodehydrofluorination

For analysis of cyclodehydrofluorination process four different model compounds were chosen, which were synthesized for investigation of multi-fold HF-elimination (from single till quadruple) and depicted in the Figure 41.

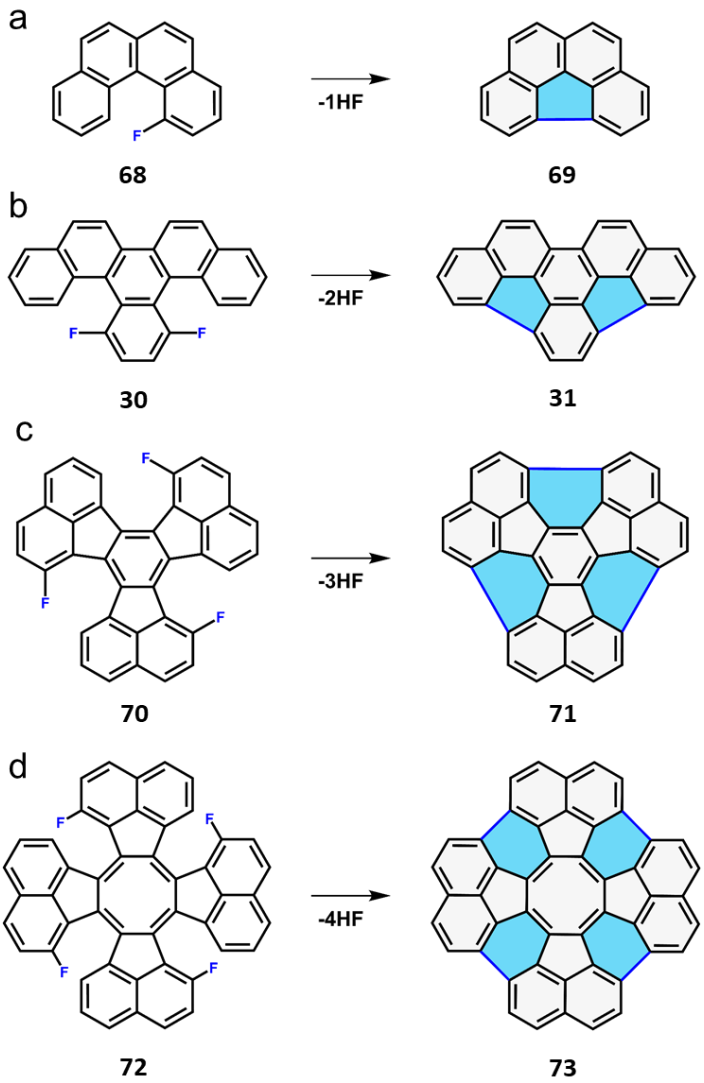

Figure 41. Model reactions for HF elimination study: a) 1-fluorobenzo[*c*]phenanthrene **68** to benzo[*ghi*] fluoranthene **69**; b) 13,16-difluorobenzo[*s*]picene **30** to *as*-indaceno[*3,2,1,8,7,6-pqrstuv*]picene **31**; c) 1,7,13-trifluorodecacyclene **70** to circumtrindene **71**; d) 1,7,13,19-tetrafluorotridecacyclene **72** to bowl $C_{48}H_{16}$ **73**.

The precursors 1-fluorobenzo[*c*]phenanthrene[163] **68** and 13,16-difluorobenzo[*s*]-picene[102] **30** were synthesized according to the known procedures. Precursors

1,7,13-trifluorodecacyclene **70** and 1,7,13,19-tetrafluorotridecacyclene **72** were synthesized in eight steps (Scheme 40). As starting material for both molecules, the commercially available 7-fluoro-1-tetralone **74** was used. It was converted to the corresponding tetrahydronaphthalene **75** by Wittig reaction. The isomerisation of 7-fluoro-1-methylene-1,2,3,4-tetrahydronaphthalene in presence of TsOH into 6-fluoro-4-methyl-1,2-dihydronaphthalene **76** and further dehydrogenation by DDQ gave 91 % of the 7-fluoro-1-methylnaphthalene **77**. After benzylic bromination of **77** into 1-(bromomethyl)-7-fluoronaphthalene **78** the bromine functionality was substituted by the cyanide ion in presence of TBAB to produce nitrile **79** in 96 % yield. Hydrolysis of 2-(7-fluoronaphthalen-1-yl)acetonitrile **79** in presence of the acetic and sulfuric acids to the carboxylic acid **80** (2-(7-fluoronaphthalen-1-yl)acetic acid), followed by transformation in acid chloride with thionyl chloride and further Friedel-Crafts cyclization yielded 87% of 8-fluoroacenaphthylen-1(*2H*)-one **81**.

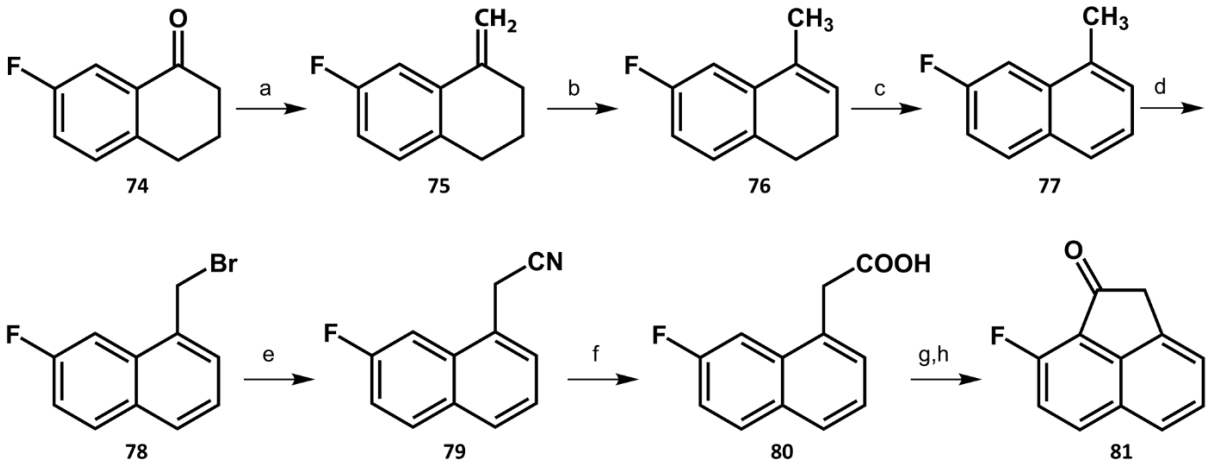

Scheme 40. Reaction pathway to fluorinated decacyclene **70** and tridecacyclene **72**: a) CH_3PPh_3Br, Et_2O, rt, 15 h, 97 %; b) TsOH, DCM, rt, 15 h, 99 %; c) DDQ, DCM, rt, 2 h, 91 %; d) NBS, DBPO, CCl_4, 1 h reflux, 88 % e) KCN, TBAB, DCM, H_2O, rt, 15 h, 96 %; f) H_2SO_4, AcOH, reflux, 3 h, 55 %; h), j) $SOCl_2$, 1 h, reflux, then $AlCl_3$, DCM, rt, 3 h, 87 %.

Synthesis of the fluorinated decacyclene **70** and tridecacyclene **72** obtained according to [164] is depicted in the Scheme 41. The aldol polymerization of 8-fluoroacenaphthylen-1(*2H*)-one **81** was carried out using titanium tetrachloride in hot *o*-DCB. After the work-up two fractions were obtained: one fraction mainly consisted of 1,7,13-trifluorodecacyclene **70** and the other – of 1,7,13,19-tetrafluorotrideca-cyclene **72**. For the work-up of the first fraction we applied the extraction technique reported by Scott *et al*. [165]

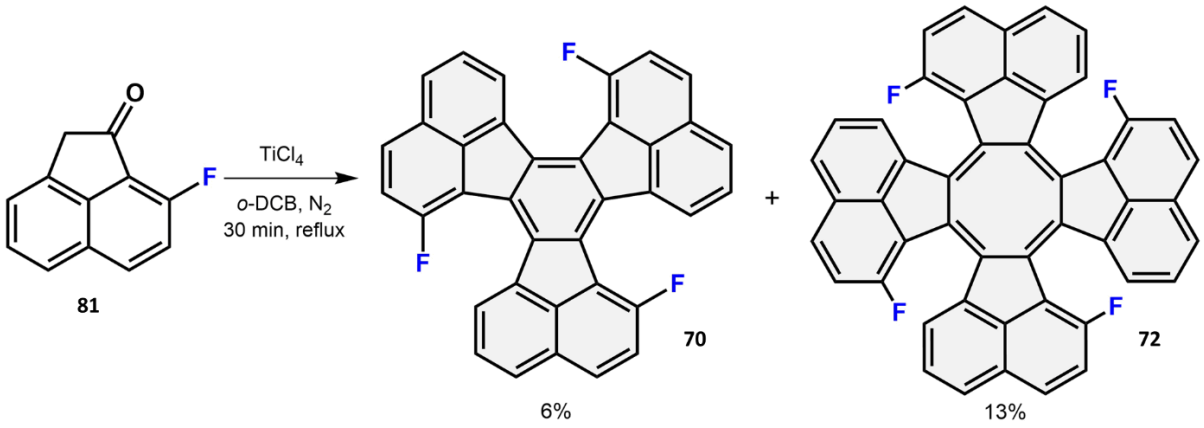

Scheme 41. Reaction pathway to fluorinated decacyclene **70** and tridecacyclene **72**.

The first fraction was dissolved in 3 mL of toluene and adsorbed onto alumina; further it was placed into a Soxhlet extractor. At the beginning the dark coloured impurities were extracted with dichloromethane and removed. The full extraction of trimer **70** occurred after 16 hours, and the yellow crystals were observed in the solution of dichloromethane. In the Figure 42 the HPLC chromatogram of obtained product after extraction is displayed; peak at t_R = 7.9 min corresponds to the desired 1,7,13-trifluoro-decacyclene. In spite of the low solubility of fluorinated decacyclene we succeeded in measurement of the ^{1}H NMR spectrum (Figure 43).

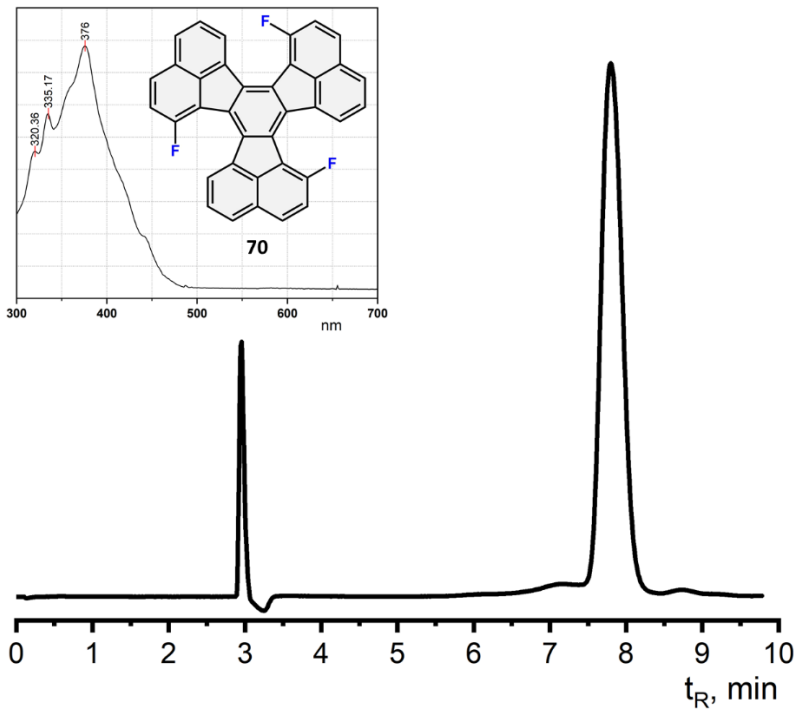

Figure 42. HPLC profile of fluorinated decacyclene **70** after extraction with dichloromethane, detected at 350 nm (PBr column, Tol:MeOH:1:1 as eluent, 1.0 mL min^{-1}, 40 ºC). UV-Vis spectrum of 1,7,13-trifluorodecacyclene **70** in Tol:MeOH 1:1.

The second fraction was dissolved in a small amount of acetone, and then MeOH was added. The formed precipitate was centrifuged, decanted and the solid product was dried in vacuo. The HPLC chromatogram of 1,7,13,19-tetrafluorotridecacyclene **72** after purification is depicted in the Figure 44 (t_R = 4.7 min). The obtained product was characterized by NMR spectroscopy and mass spectrometry. In the Figure 45 is presented ^{1}H NMR spectrum of 1,7,13,19-tetrafluorotridecacyclene.

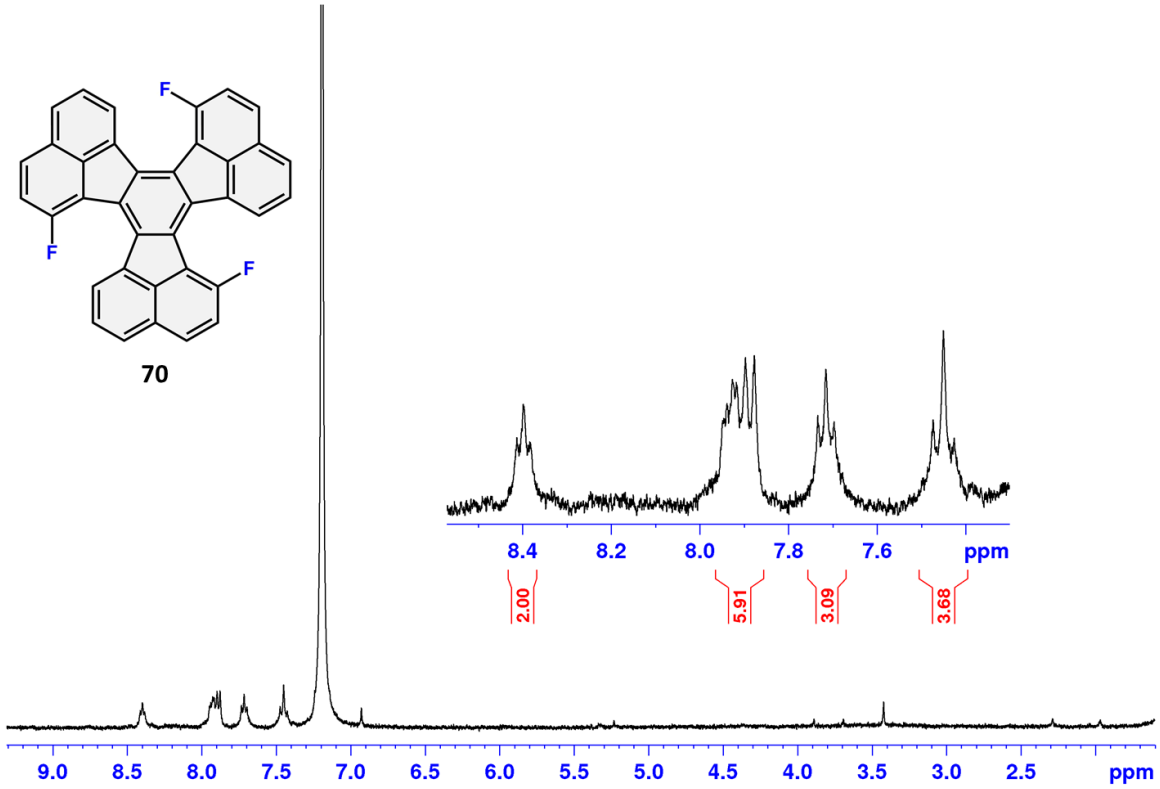

Figure 43. ^{1}H NMR spectrum (400 MHz, $C_2D_2Cl_4$, 298 K) of 1,7,13-trifluorodecacyclene **70**.

All model molecules possess either a cove or fjord region where a selective ring closure via HF elimination could occur. In case of a cove region closure a new pentagonal ring is formed, while in case of a fjord region – a hexagonal one.

The 1-fluorobenzo[*c*]phenanthrene **68** was used as a reference compound for synthesis of the smallest PAHs possessing a cove region. Previously, it was shown that precursor undergoes intramolecular condensation via HF-elimination under FVP conditions.[163] Although, benzo[*ghi*]fluoranthene **69** has a planar geometry, introduction of pentagon in its structure leads to strain in molecular geometry.

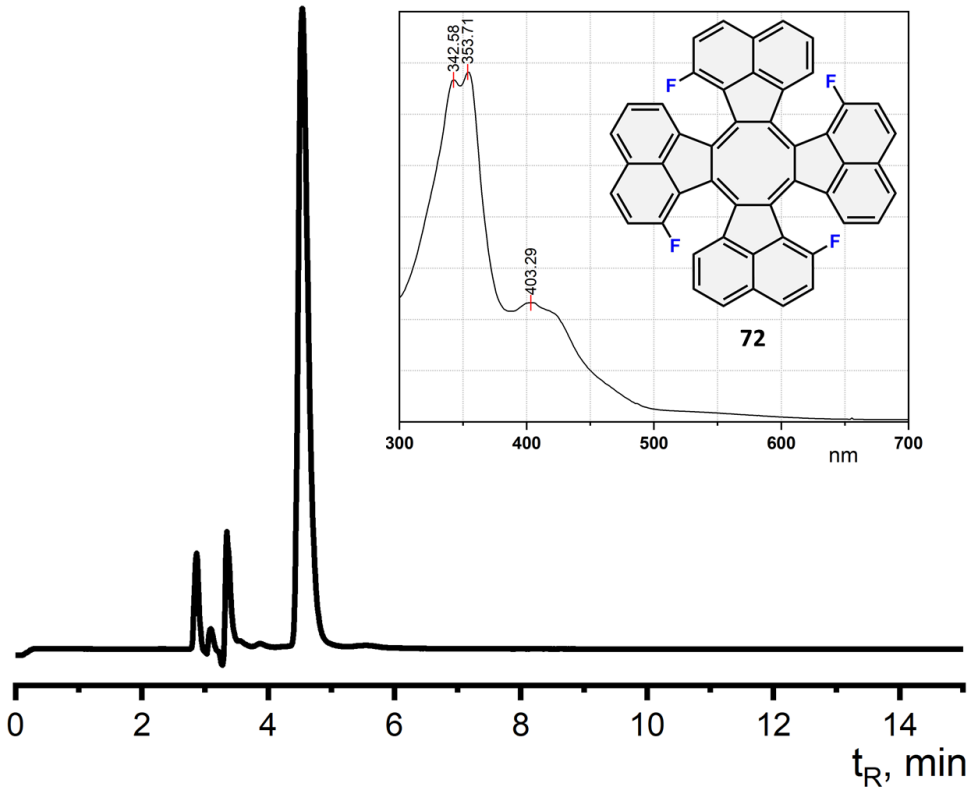

Figure 44. HPLC profile of fluorinated tridecacyclene **72** after purification, detected at 350 nm (PBr column, Tol:MeOH:1:1 as eluent, 1.0 mL min^{-1}, 40 ºC). UV-Vis spectrum of 1,7,13,19-tetrafluorotrideca-cyclene **72** in Tol:MeOH 1:1.

The 13,16-difluorobenzo[*s*]picene **30** was chosen for double-CHDF via cove region closure resulting in formation of the known bowl-shaped *as*-indaceno[*3,2,1,8,7,6-pqrstuv*]picene **32**.[102] The fluorinated decacyclene **70** and tridecacyclene **72** were applied for the triple- and quadruple- fjord region closure. It is worth to mention that the triple CDHF in 1,7,13-trifluorodecacyclene **70** should lead to the formation of fullerene's fragment synthesized by FVP approach from chlorinated analogue of 1,7,13-trifluorodecacyclene **70**.[54,166] The 1,7,13,19-tetrafluorotridecacyclene **72** is a precursor for non-classical bowl $C_{48}H_{16}$ **72** containing an eight-membered ring in the structure. According to our literature search the buckybowls, possessing formally antiaromatic eight-membered ring in their structure were not described.

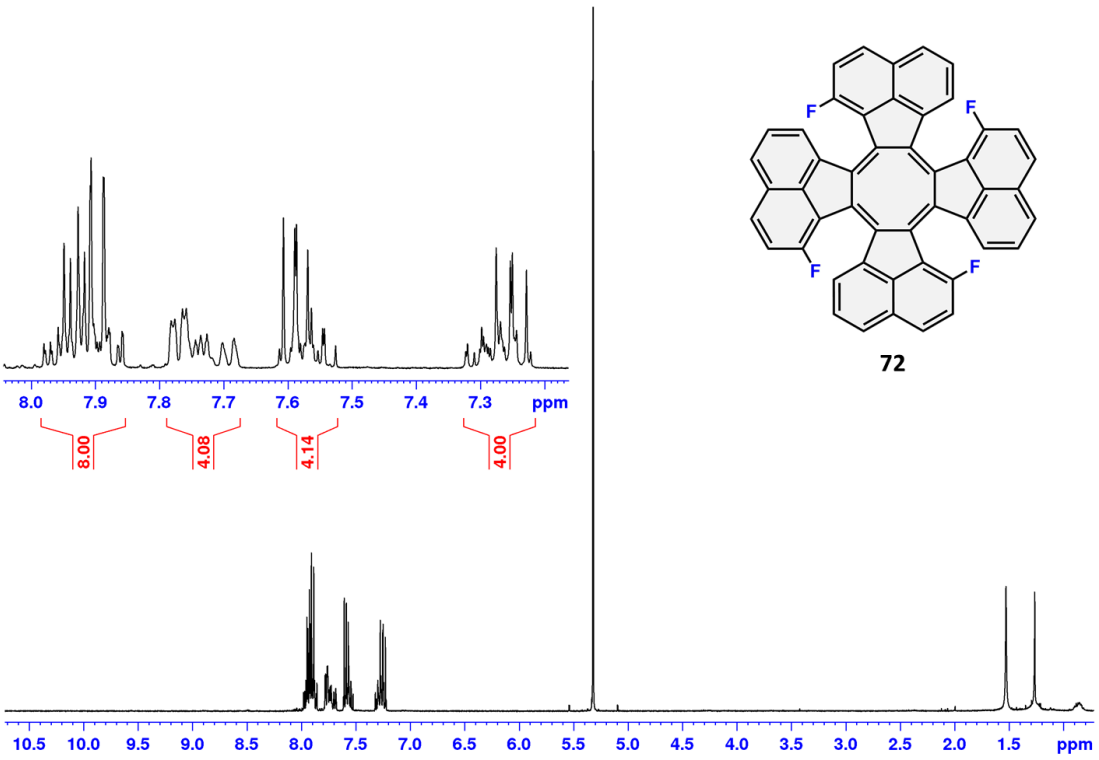

Figure 45. ^{1}H NMR spectrum (400 MHz, $CDCl_3$, 298 K) of 1,7,13,19-tetrafluorotridecacyclene **72**.

The study of CDHF process was carried out theoretically (computation of transition states for each CHDF step at PBE0/cc-pVDZ level of theory) and experimentally (on-surface cyclization).

3.5.2 Computation Study

In collaboration with Dr. A.Yu. Rogachev the computational study was carried out. The activation barrier of the CDHF reaction of the 1-fluorobenzo[*c*]phenanthrene **68** is 79.0 kcal mol^{-1}, whereas the activation barrier of H_2 elimination in the non-fluorinated analogue of the **68** was found to be significantly higher (110.6 kcal mol^{-1}).[163] Additionally, the influence of substituents and their position on the CDHF efficiency as well as on *1,2*-elimination was studied (Scheme 42).

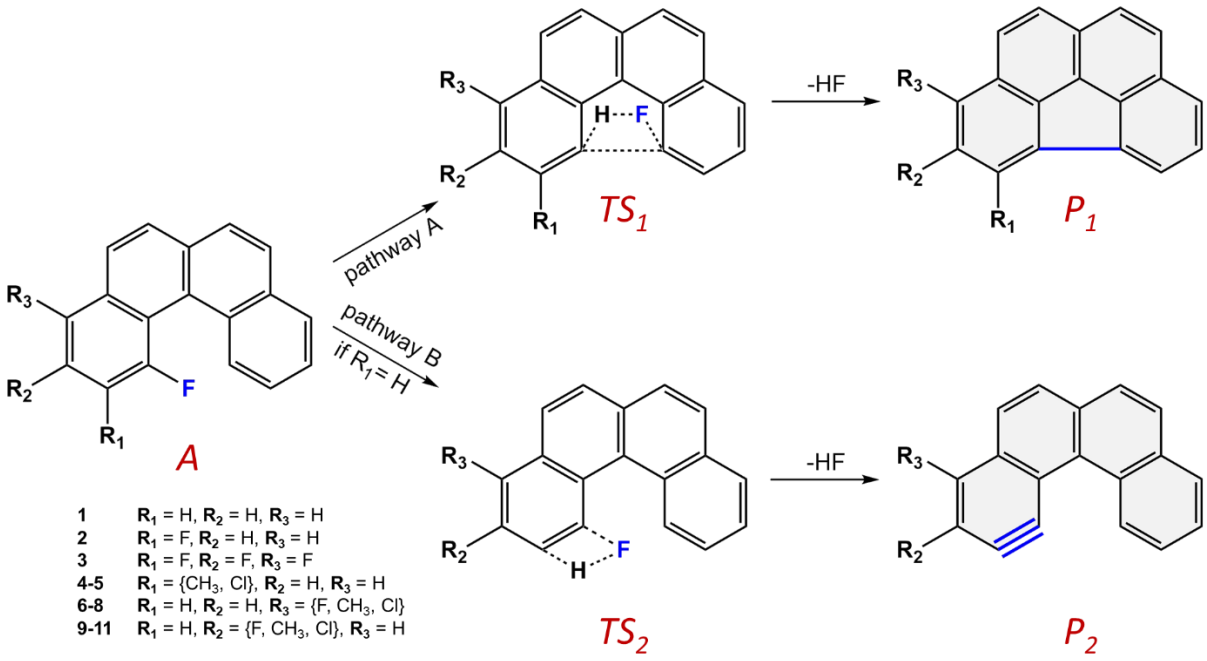

Scheme 42. Cyclodehydrofluorination of fluorinated 1-benzo[*c*]phenanthrene's analogues (pathway A – condensation; pathway B – *1,2*-elimination reaction).

According to the obtained data (Table 4), the introduction of F and Cl functionalities in *ortho*-position to the fluorinated carbon in a cove region reduces the activation barrier from 82.7 kcal mol^{-1} to 77.8 kcal mol^{-1} (chlorine substituent) and to 77.5 kcal mol^{-1} (fluorine substituent). Substituents in *meta*- and *para*-position do not have significant influence on reaction barrier as well as the methyl groups in same position. In the tetrafluorinated analogue of **68** the CDHF barrier was smaller (73.7 kcal mol^{-1}) in comparison with the compound **68**. In the *1,2*-elimination the halogen functionality in *para*-position to the fluorinated carbon in a cove region has the greatest impact on a reaction barrier.

Table 4. The effect of the substituents on the cyclodehydrofluorination and *1,2*-elimination in fluorinated benzo[*c*]phenanthrene. (All energies are in kcal mol^{-1}).

Com-pound	***E_{rel} (TS_1)***	***E_{rel} + ZPE (TS_1)***	***E_{rel} (P_1)***	***E_{rel} + ZPE (P_1)***	***E_{rel} (TS_2)***	***E_{rel} + ZPE (TS_2)***	***E_{rel} (P_2)***	***E_{rel} + ZPE (P_2)***
A1	82.7	79.0	4.8	2.3	93.2	88.1	81.0	76.2
A2	77.5	74.0	-0.7	-3.1	-	-	-	-
A3	77.1	73.7	-2.0	-4.5	-	-	-	-
A4	81.4	77.9	4.6	2.0	-	-	-	-

A5	77.8	74.2	1.1	-1.4	-	-	-	-
A6	83.3	79.7	3.8	1.3	92.9	88.0	81.4	76.6
A7	82.3	78.5	3.3	0.7	93.2	88.1	80.9	76.1
A8	80.9	77.3	2.8	0.3	93.3	88.4	81.3	76.5
A9	81.5	77.9	4.6	2.1	90.6	85.9	79.4	74.8
A10	83.6	79.9	5.8	3.2	92.2	87.1	79.8	75.1
A11	81.7	78.1	4.8	2.3	91.7	86.9	80.5	75.8

In the larger systems (13,16-difluorobenzo[*s*]picene **30**, 1,7,13-trifluorodecacyclene **70** and 1,7,13,19-tetrafluorotridecacyclene **72**) the significant differences in the values of activation barriers of the CDHF were detected. In the 13,16-difluorobenzo[*s*]picene (Scheme 43) the first HF elimination barrier was found to be 4.7 kcal mol^{-1} smaller (74.7 kcal mol^{-1}) in comparison to the 1-fluorobenzo[*c*]phenanthrene **68**, while the second HF elimination is less favourable (87.5 kcal mol^{-1}).

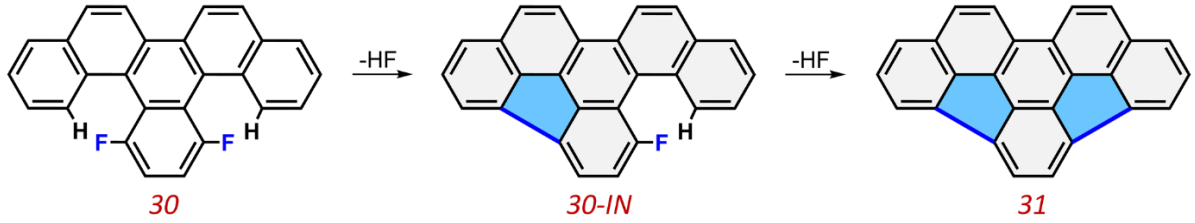

Scheme 43. Pathway for cyclodehydrofluorination of 13,16-difluorobenzo[*s*]picene **30**.

In the CDHF of the 1,7,13-trifluorodecacyclene **71** (Scheme 44) the reaction barrier for the first cyclization reduced to 68.4 kcal mol^{-1} and the increase in energy for the second step (72.5 kcal mol^{-1}) was observed. The activation barrier of 61.7 kcal mol^{-1} was found for the last step of CDHF. It is worth to mention that pathway to the most strained system (**71**) does not include high energy barriers.

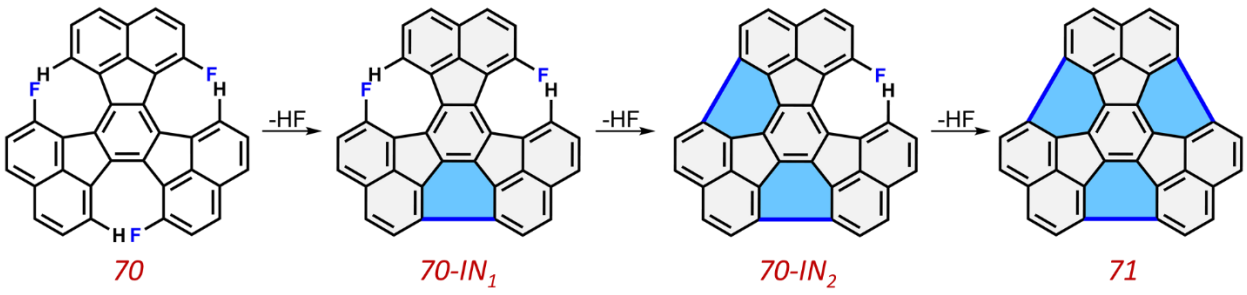

Scheme 44. Pathway for cyclodehydrofluorination of 1,7,13-trifluorodecacyclene **70**.

The CDHF of 1,7,13,19-tetrafluorotridecacyclene **72** is more complicated and can include different alternative pathways (Scheme 45). In contrast to the described systems **30**, **68** and **70** the first cyclization in 1,7,13,19-tetrafluorotridecacyclene **72** is highly unfavourable (88.0 kcal mol^{-1}), while the next three cyclization steps presume lower activation barriers (45-55 kcal mol^{-1}).

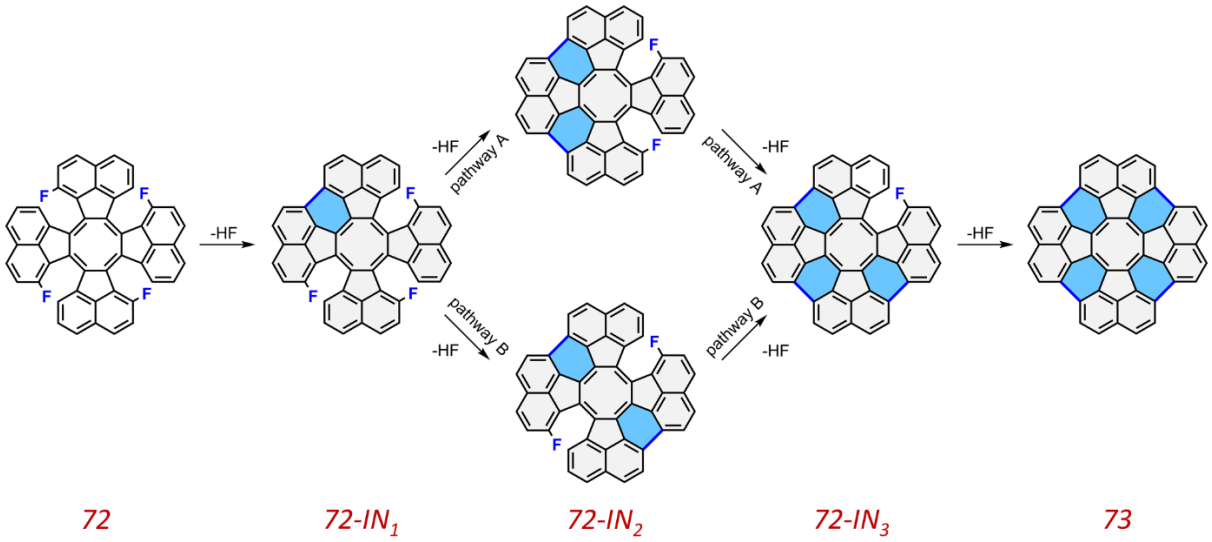

Scheme 45. Possible pathways for cyclodehydrofluorination of 1,7,13,19-tetrafluorotridecacyclene **72**.

Although the 1,7,13-trifluorodecacyclene **70** and 1,7,13,19-tetrafluorotridecacyclene **72** undergo similar fjord region closure, the reaction pathways reveal different behaviours.

3.5.3 On-surface Cyclization of PAHs

The efficient on-surface cyclodehydrogenation of PAHs in fjord region was carried out on Cu(111)[167] and Au(111)[145] surfaces. At the beginning, the cyclodehydrogenation in cove region on Au(111) or Cu(111) appeared to be unsuccessful, hence the Pt(111) surface was used as a stronger catalyst[65]. For instance, the cyclodehydrogenation of fullerene precursor $C_{84}H_{42}$ on Pt(111) resulted in isomer-pure fullerene C_{84}.[168]

In collaboration with Prof. Dr. R. Fasel the cyclodehydrofluorination experiments on atomically clean Au (111) were performed. The Au (111) surface was chosen in order to minimize its catalytic effect on reaction. Here are presented the preliminary results of the conducted investigations.

The deposition of 13,16-difluorobenzo[*s*]picene **30** at the room temperature led to polymers, which were stabilized by weak van der Waals interactions. By annealing at

250 °C a small amount of product **31** was observed. The temperature increase to 280 °C resulted in complete desorption of reagent **30**. Due to a small size of molecules and their easy desorption from the surface, the high conversion to *as*-indaceno[*3,2,1,8,7,6-pqrstuv*]picene **31** failed to complete. We can conclude that the STM experiments on the gold surface at relatively low temperatures allow to provide selective HF-elimination. Similar results were obtained for the cyclodehydrogenation on Cu(111) surface.

The 1,7,13-trifluorotridecacyclene **70**, deposited on the gold surface, showed the complex supramolecular assembling due to its non-planar geometry. The 1,7,13,19-tetrafluorotridecacyclene **72** underwent cyclization via HF elimination already at 280°C. The products of the single-, double- and triple- HF elimination (Scheme 46) were observed by STM, and no direct evidences of the quadruple HF elimination not found. This fact could be explained by non-planar structure of precursor leading to aggregation or desorption from the surface.

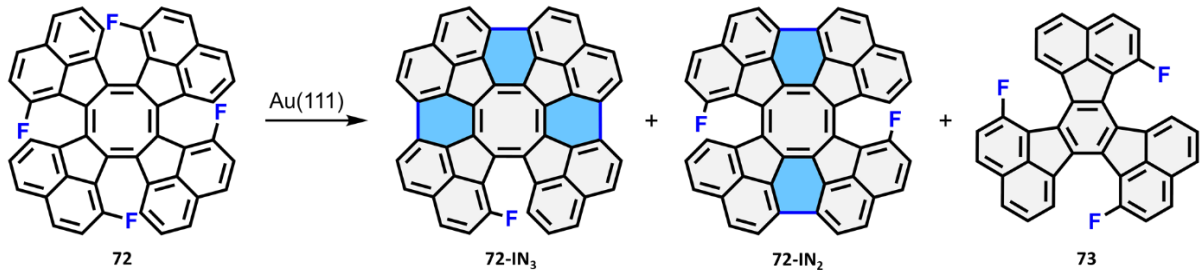

Scheme 46. CDHF of 1,7,13,19-tetrafluorotridecacyclene **72** under STM conditions.

The findings of STM experiments indicate that aromatic C-F bond in cove or fjord regions is active and can undergo the HF elimination at relatively low temperatures.

Apart from the STM experiments we carried out the CDHF of 1,7,13,19-tetrafluorotridecacyclene in presence of aluminium oxide. The mass measurements confirmed the formation of $C_{48}H_{16}$ bowl **73**, although no product peak was detected in the HPLC chromatograms. We can assume that the obtained bowl **73** is instable and undergoes decomposition.

3.5.4 Synthesis of Brominated Decacyclene and Tridecacyclene

The palladium-catalyzed arylation is known as a powerful method for the synthesis of polyarenes, particularly, of geodesic PAHS. Scott *et al.* developed the reaction conditions for the annulation of PAHs employing the Pd(0) complex (*in situ* formation

using $Pd_2(dba)_3$ and PCy_3).[141],[47],[169] Taking this into account, we the prepared precursors for such cyclization and applied the same approach as for synthesis of the 1,7,13-trifluorodecacyclene **70** and 1,7,13,19-tetrafluorotridecacyclene **72**.

The synthesis of the precursors **90** and **91** started with the bromination of the commercially available 3,4-dihydro-1(*2H*)-naphthalenone. The obtained 7-bromo-1-tetralone **82** underwent the same transformations as 7-fluoro-1-tetralone **74** (Scheme 47).

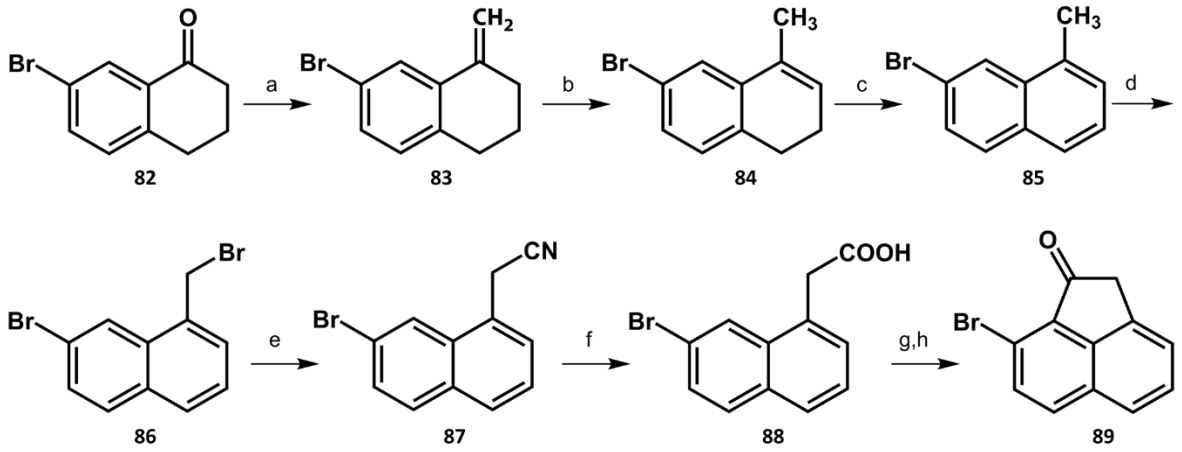

Scheme 47. Reaction pathway to brominated decacyclene **90** and tridecacyclene **91**. a) CH_3PPh_3Br, Et_2O, rt, 15 h, 86 %; b) TsOH, DCM, rt, 15 h, 94 %; c) DDQ, benzene, reflux, 3 h, 27 %; d) NBS, DBPO, CCl_4, 1 h, reflux, 88 % e) KCN, TBAB, DCM, H_2O, rt, 15 h, 98 %; f) H_2SO_4, AcOH, reflux, 3 h, 66 %; h), j) $SOCl_2$, 1 h, reflux, then $AlCl_3$, DCM, rt, 3 h, 43 %.

Brominated tridecacyclene was synthesized according to [170]. Titanium chloride in hot *o*-DCB was used for the aldol polymerisation of 8-bromoacenaphthylen-1(*2H*)-one **89** (Scheme 48).

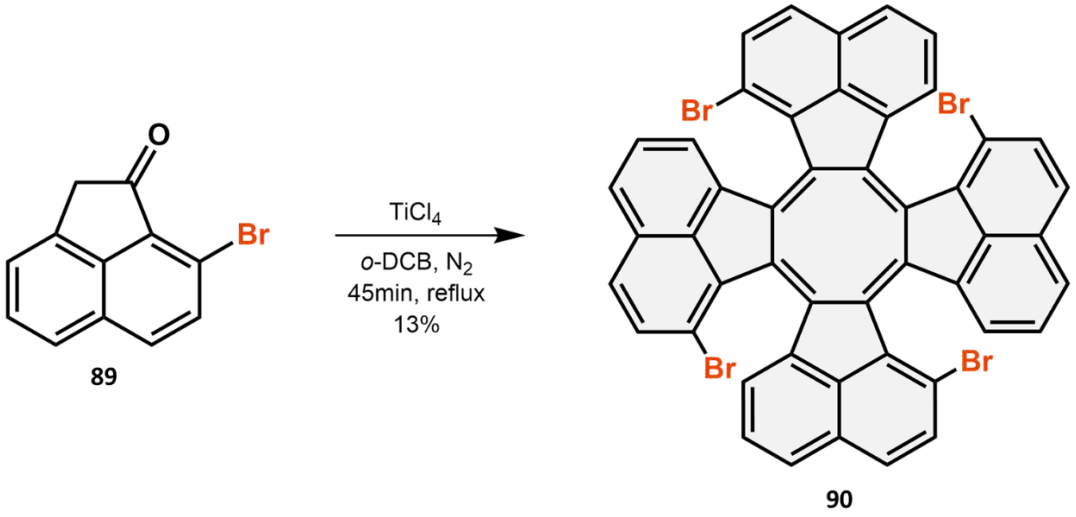

Scheme 48. Reaction pathway to brominated tridecacyclene **90**.

After work-up the product **90** was analyzed by HPLC and NMR-spectroscopy. In the HPLC-chromatograms (Figure 46) the three peaks with different retention times (24.4, 25.9 and 27.3 min) were found that corresponded to the conformational isomers of **90**.

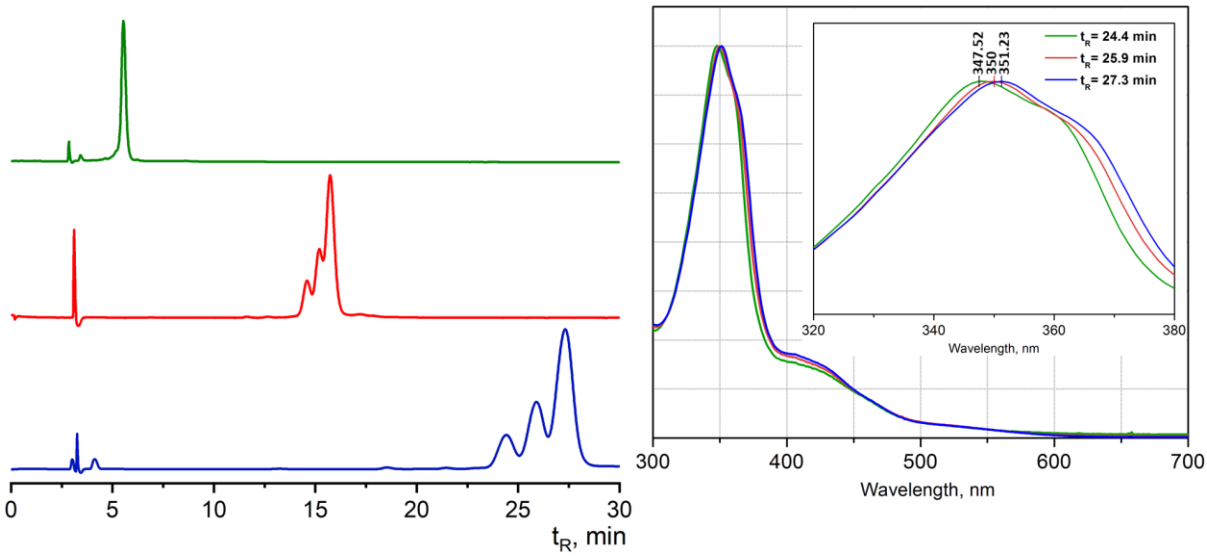

Figure 46. a) HPLC profile of brominated tridecacyclene **90** after purification (detected at 350 nm, PBr column, 1.0 mL min^{-1}). Green: Tol:MeOH:3:1, 40 ºC; blue: Tol:DCM:MeOH:30:20:50, 30 ºC; red: Tol:MeOH:1:1, 40 ºC; b) UV-Vis spectra of **90** isomers in Tol:DCM:MeOH:30:20:50, 35ºC.

^{1}H and ^{13}C NMR spectra were measured at room temperature in 1,1,2,2-tetrachloroethane-d_2 exibit wide range of peaks, corresponding to different conformational isomers.

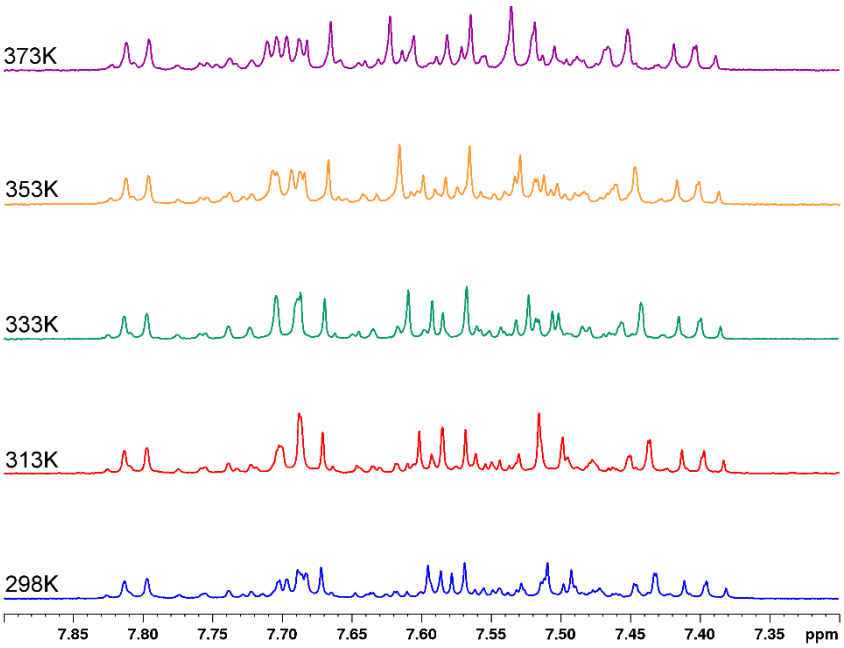

Figure 47. Partial ^{1}H NMR spectra (500 MHz, $C_2D_2Cl_4$) of tridecacyclene **90** at different temperatures.

Compound **90** was investigated by variable-temperature experiments (Figure 47). The temperature growth from 298 to 373 K induced the broadening, shifting towards each other and sharpening of the major peaks. However, even at 373 K an interconversion of isomers was not observed.

3.6 Synthesis of Bowl-Shaped Acene Structures

In recent years there has been an increasing amount of interest in the field of nanographenes and PAHs bearing the zig-zag periphery. The interest to zig-zag PAHs arises from their unique electronic properties, reactivity and stability, which can be applied in the field-effect transistors and spintronic devices.

The aim of this research is to develop a new approach for the synthesis of extended acene-type structures. As an object of the study was selected 2.3,8.9-dibenzathanthene **94** (DBATT).

Our first attempts to synthesize **94** are demonstrated in the Scheme 49. Pd-catalyzed two-fold Suzuki-Miyaura cross-coupling of 1,6-dibromopyrene **24** with 2-formylphenylboronic **92** gave 1,6-bis(2-formylphenyl)pyrene **93** in 60 % yield. To conduct the intramolecular cyclization, we employed the pure sulfuric acid treatment at the different temperatures (from room temperature to 80 ºC). According to the HPLC measurements, the product **94** was obtained in near to 50 % yield. Therefore, this approach can be considered as an appropriate pathway of synthesis.

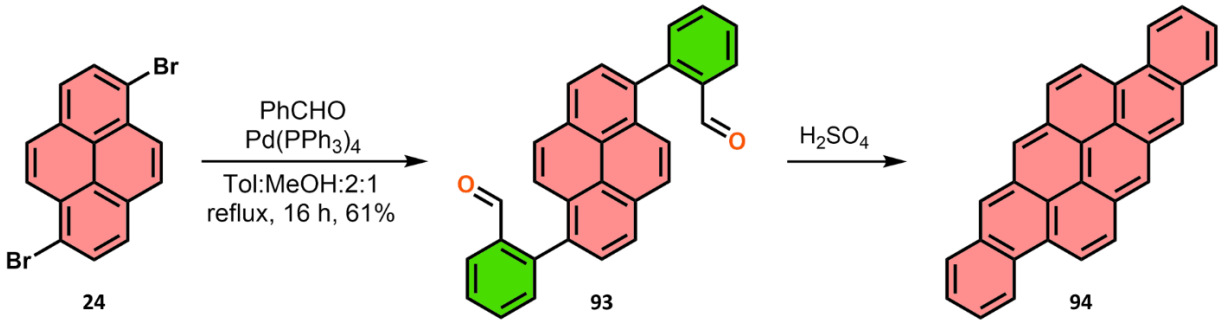

Scheme 49. First attempts to synthesise DBATT **94** by acid-promoted intramolecular cyclization.

Furthermore, the reaction was repeated and scaled up to 55 mg. The product was isolated by HPLC (Figure 48) and characterized by mass spectrometry. However, this approach did not allow to synthesize target product **94** in the yield higher than 50 %.

In cooperation with Dr. D. Lungerich the reaction conditions for acid-promoted reductive intramolecular cyclization of aldehydes were optimized.[171] As a reducing agent for reaction the $SnCl_2*2H_2O$ was chosen. Dichloromethane, which provides the best level of the conversion was used as solvent.

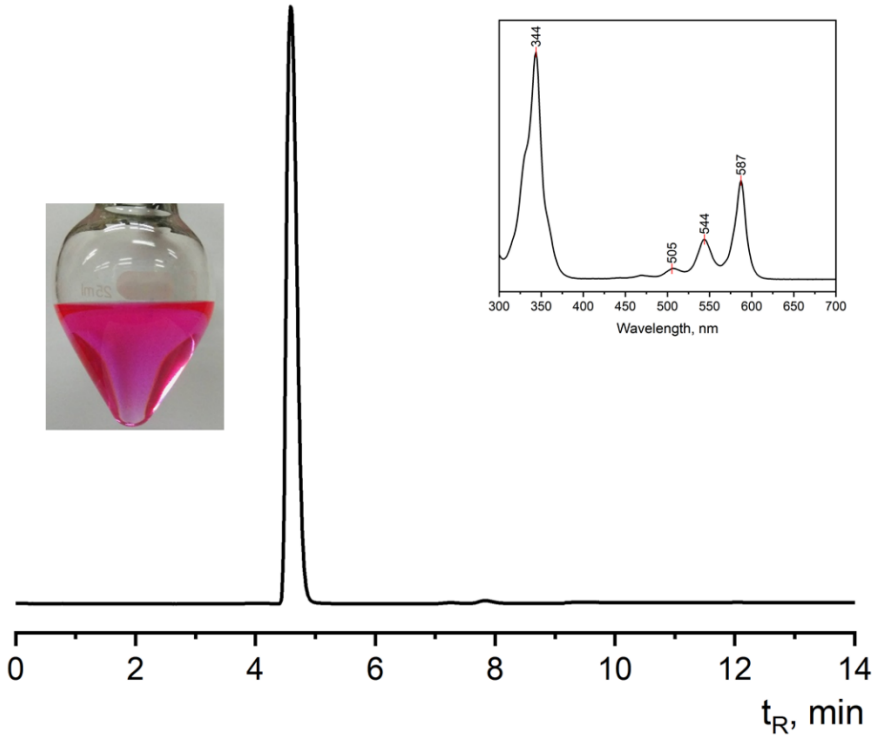

Figure 48. HPLC profile of DBATT **94** after purification detected at 580 nm (5-PBB-R column, Tol as eluent, 5.0 mL min^{-1}, 40 ºC). Inset: UV-Vis spectrum of **94** in toluene solution.

Moreover, the addition of 2 vol% of a saturated $SnCl_2*2H_2O$ solution in *i*-PrOH significantly improved the reaction yields. Thus, presence of *i*-PrOH slows down the conversion and increases the selectivity of reaction.

It was also found out that the 2:1 ratio of the $SnCl_2$/*i*-PrOH to H_2SO_4 is issential for the intramolecular cyclization. The work-up includes the following steps: treatment with a 1 M hydrochloric acid, extraction with DCM and precipitation in MeOH. Pure product was obtained in near-quantitative yields, as determined by the HPLC analysis. It is worth to mention that all reactions were carried out under ambient atmosphere at the room temperature. All solvents do not need any purification or degassing and can be used as obtained. Additionally, the reaction can be scaled-up (0.44 g of DBATT from the 0.50 g of **93**). The only condition, which must be kept, is avoiding of the direct light irradiation due to the decomposition of DBATT under the light.[172]

The optimized conditions of acid-promoted intramolecular cyclization were applied not only for synthesis of **94**, but also for more extended acenes (Figure 49). Bis-pentacene **95** was synthesized from 1,6-bis(3-formylnaphthyl)pyrene **96** precursor in 97 % yield. The functionalization of 1,6-bis(2-formylphenyl)pyrene **93** by introduction of bromine in 3rd and 8th positions allows to synthesize the DBATT's

derivatives. Thus, bis-phenyl- and bis-pyridinyl DBATTs were obtained from 1,6-bis-(2-formylphenyl)-3,8-diphenylpyrene **97** and 1,6-bis(2-formylphenyl)-3,8-bis(4-pyridyl) pyrene **98** in 97 and 95 %yield respectively.[171]

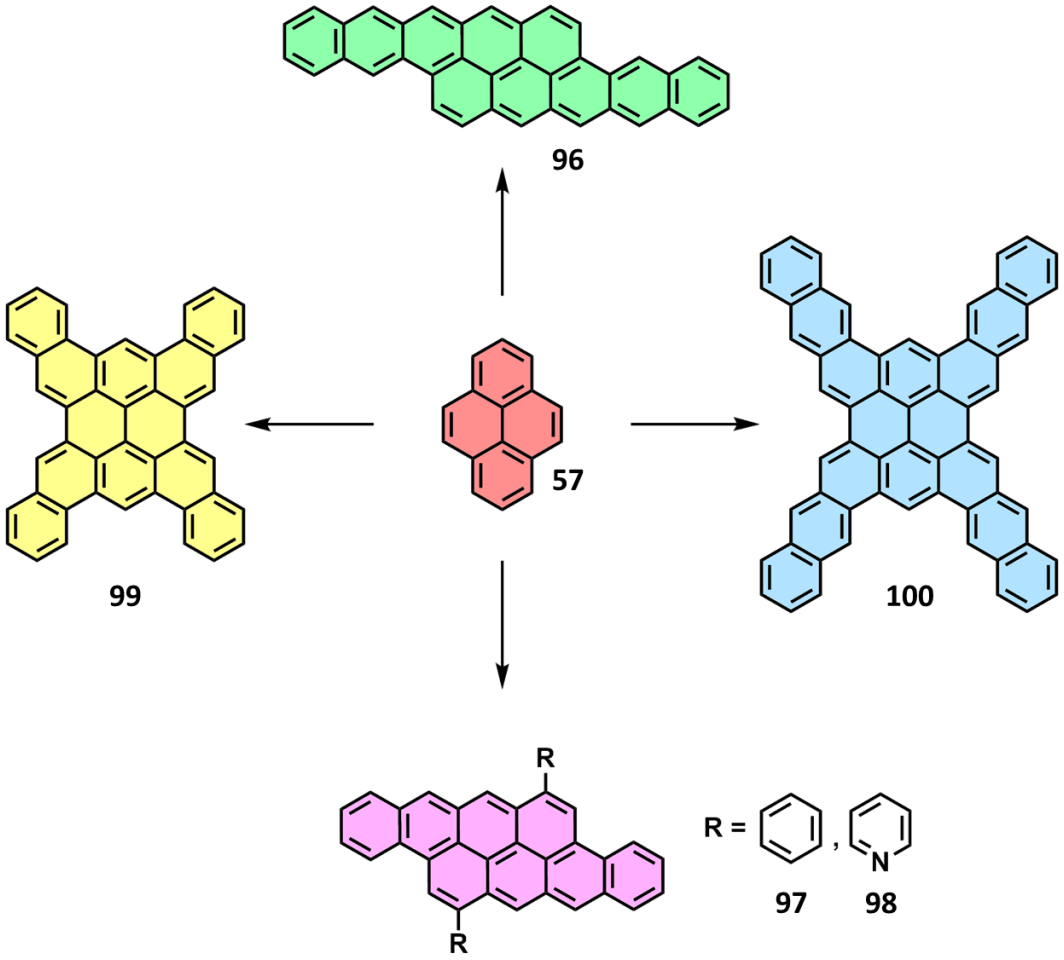

Figure 49. An overview of zig-zag nanographenes formed by acid-promoted reductive intramolecular cyclization.

The intramolecular cyclization of the tetrakis-acene precursors, which were synthesized by four-fold Suzuki cross-coupling of 1,3,6,8-tetrabromopyrene **61** with the corresponding aromatic aldehydes, gave tetrakis-tetracene **99** and tetrakis-pentacene **100** in 96 % yield.

We were facing the difficulties in the structure confirmation since the obtained molecules were highly insoluble, and hence the standard methods of characterization could not be applied. Consequently, the scanning tunneling microscopy (STM) was chosen as an instrument for structure elucidation of products. For this purpose, the samples of polyacenes were were sublimed in ultra-high vacuum at the temperature range 300-395 °C onto metal surface (Au(111) or Ag(111). The STM measurements

confirmed structure of tetrakis-tetracene **99**, tetrakis-pentacene **100** and bis-pentacene **96**. Notably, tetrakis-pentacene and bis-pentacene adsorbed as single molecules on Au(111) and Ag(111), whereas the tetrakis-tetracene formed the self-assembly on Au(111).[171]

The optimized reaction protocol of acid-promoted reductive intramolecular cyclization was applied for the introduction of acene species in the bowl-shaped structures. The 1,6-bis(2-fluorophenyl)pyrene **59** and 3,9-dibromodiindenochrysene **51a** were selected as the building blocks.

1,6-bis(2-fluorophenyl)pyrene **59** was brominated with bromine in chloroform yielding a mixture of mono- and dibrominated products. The recrystallisation of products from xylenes did not lead to the pure dibrominated **101** (Scheme 50).

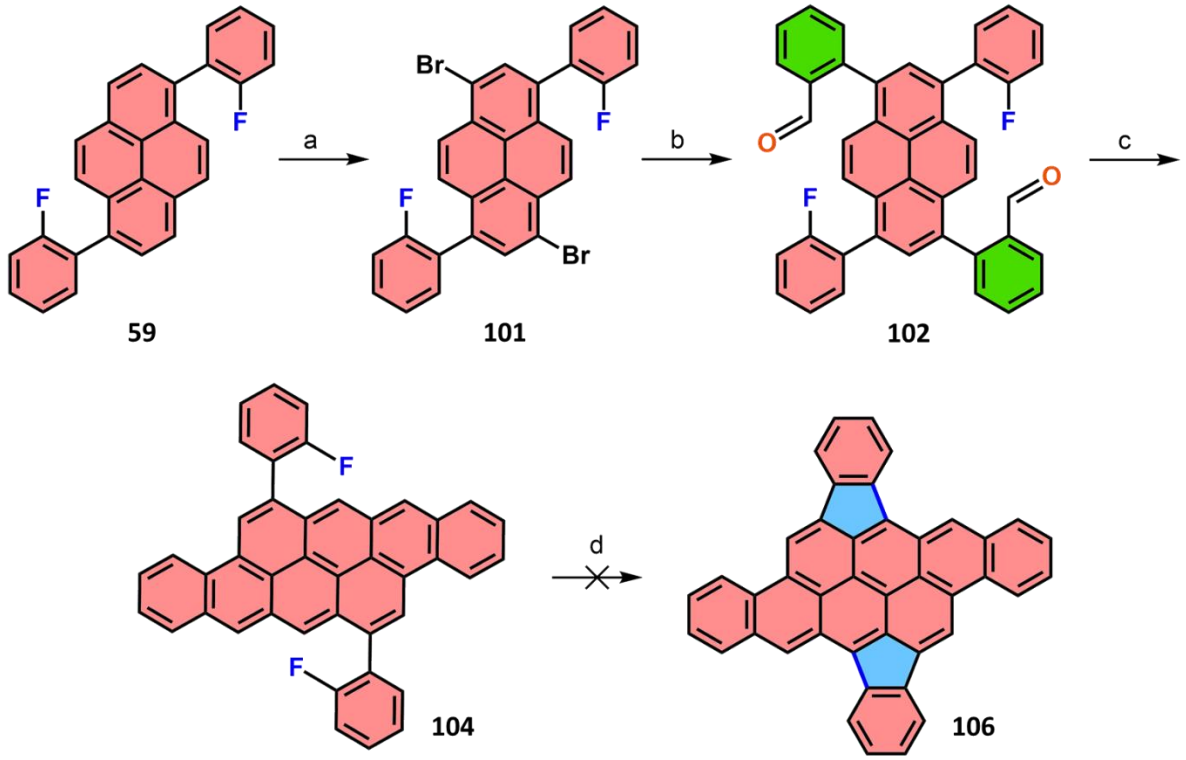

Scheme 50. Synthetic way to indeno[*1,2,3-de*]indeno[*1',2',3':4,5*]tetraceno[*2,1,12,11-opqra*]tetracene **106**. a) Br_2, $CHCl_3$; b) PhCHO, 5 % $Pd(PPh_3)_4$, K_2CO_3, Tol:MeOH:2:1, reflux, N_2, 16 h; c) 2 vol% sat. $SnCl_2$*$2H_2O$/*i*-PrOH, 1 vol% conc. H_2SO_4, DCM, rt, quant.; d) *γ*-Al_2O_3, *o*-DCB, MW, 180ºC.

Nevertheless, both products were converted into 2,2'-(3,8-bis(2-fluorophenyl)pyrene-1,6-diyl)dibenzaldehyde **102** and 2-(3,8-bis(2-fluorophenyl)pyren-1-yl)benzaldehyde **103** by Suzuki cross-coupling with 2-formylphenylboronic acid **92**. The both products – 2,2'-(3,8-bis(2-fluorophenyl)pyrene-1,6-diyl)dibenzaldehyde **104** and 2-(3,8-bis(2-

fluorophenyl)pyren-1-yl)-benzaldehyde **105** – were isolated by HPLC chromatography (Scheme 50).

The intramolecular cyclization of **102** was conducted according to standard protocol giving the product 6,14-bis(2-fluorophenyl)tetraceno[*2,1,12,11-opqra*]tetracene **104** in a near-quantitative yield. The bis-fluorophenyl DBATT was characterized by ^{1}H NMR spectroscopy and mass spectrometry. Aluminium oxide mediated cyclodehydrofluorination of bis-fluorophenyl DBATT into indeno[*1,2,3-de*]-indeno[*1',2',3':4,5*]tetraceno[*2,1,12,11-opqra*]tetracene **106** failed to proceed. The product mixture analysis revealed that neither product nor starting material were detected. The reaction was repeated at the lower temperature (180 ºC), but no improvement was observed. We can conclude that the high reaction temperatures led to the decomposition of the material.

However, the other strategy for synthesis of indeno[*1,2,3-de*]indeno[*1',2',3':4,5*] tetraceno[*2,1,12,11-opqra*]tetracene **106** can be recommended (Scheme 51).

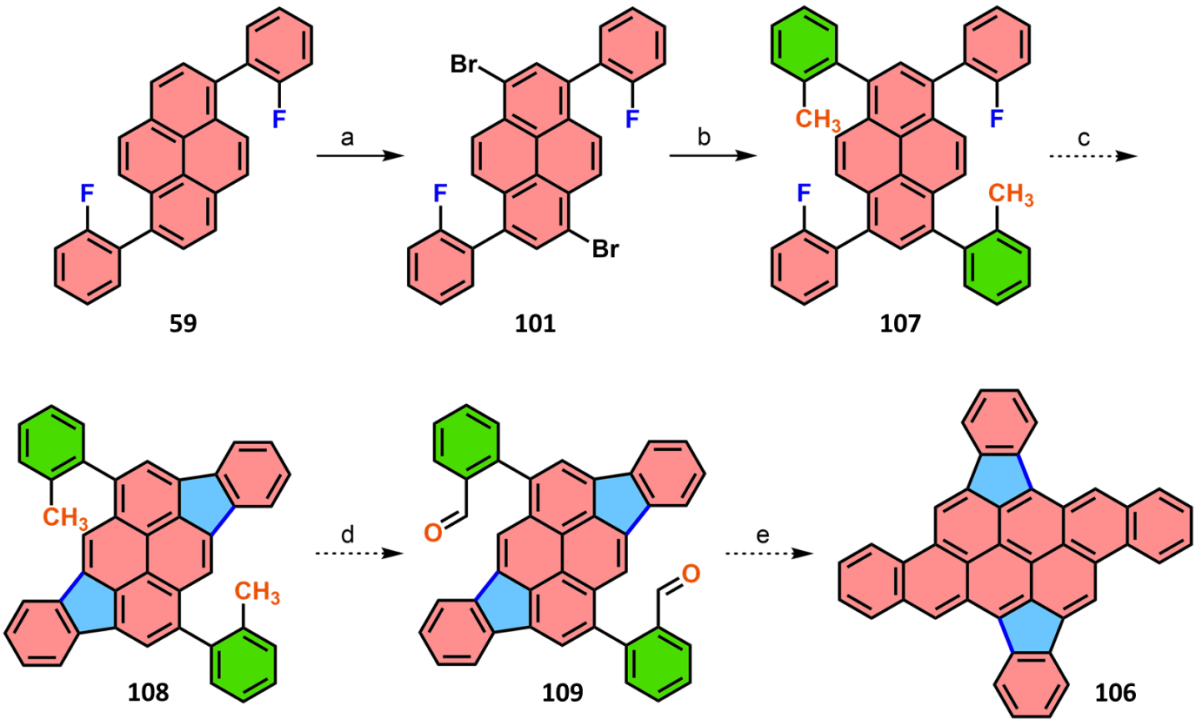

Scheme 51. Alternative synthetic route to indeno[*1,2,3-de*]indeno[*1',2',3':4,5*]tetraceno[*2,1,12,11-opqra*]tetracene **106**.

After the bromination of 1,6-bis(2-fluorophenyl)pyrene **59**, the product **101** can be converted into 1,6-bis(2-fluorophenyl)-3,8-di-*o*-tolylpyrene **107** by Suzuki cross-coupling with 2-methyl-1-phenylboronic acid. The further two-fold HF-elimination of

107 can give 6,13-di-*o*-tolyldiindeno[*1,2,3-cd:1',2',3'-jk*]pyrene **108**. The methyl groups in **108** can be transformed into formyl groups **109**, which undergo the acid-promoted intramolecular further into **106**. Due to time limitations the only Suyuki cross-coupling was carried out. Alternatively, the HF-elimination of brominated 1,6-bis(2-fluorophenyl)pyrene **101** can be conducted. Although, according to our previous investigations the conversion of 1,6-dibromo-3,8-bis(2-fluorophenyl)pyrene into 6,13-dibromodiindeno[*1,2,3-cd:1',2',3'-jk*]pyrene did not succeed.

The synthesis of extended bowl-shaped acene systems based is presented in the Scheme 52. The 2,2'-(4,10-dihydrodiindeno[4,3,2,1-cdef:4',3',2',1'-lmno]chrysene-3,9-diyl)dibenzaldehyde **110** was prepared in a yield of 94 % starting from the 3,9-dibromodiindenochrysene **51a** *via* Suzuki cross-copling. The intramolecular cyclization of **110** by the developed protocol gave the product **111**.

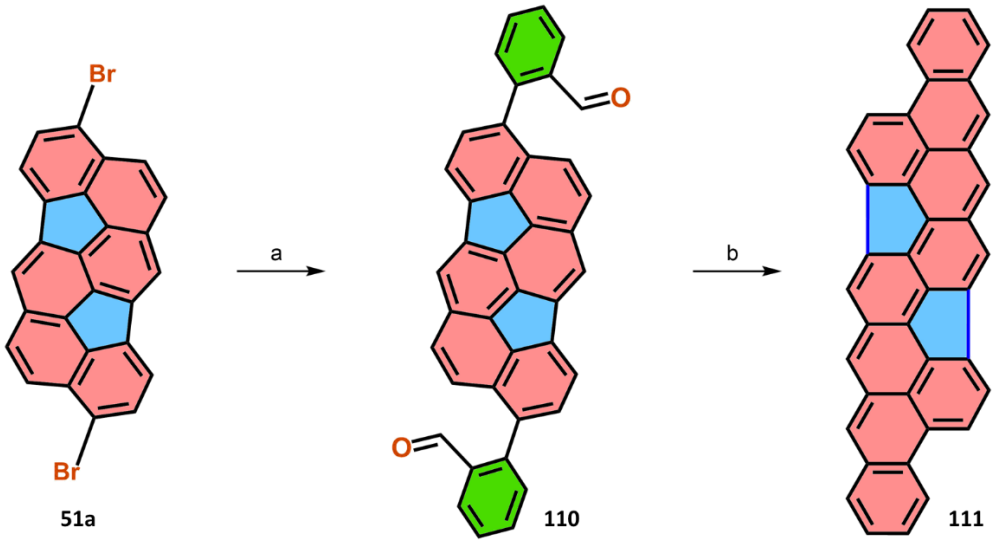

Scheme 52. Two-step synthesis of benzo[*l*]indeno[*5,4,3,2,1-nopqr*]naphtho[*3',2',1':5,6*]acenaphtho[*3,2,1-cde*]tetraphene **111**. a) PhCHO, 5 % $Pd(PPh_3)_4$, K_2CO_3, Tol:MeOH:2:1, reflux, N_2, 16 h, 86 %; b) 2 vol% sat. $SnCl_2$*$2H_2O$/*i*-PrOH, 1 vol% conc. H_2SO_4, DCM, rt.

The mass spectrum of **111** was measured directly after work-up. In the Figure 50 can be seen that there are two major peaks at *m/z* 499.38 and 516.40. This data confirmed the formation of product (*m/z* 499.38) and also its oxidized form (*m/z* 516.40). The MS measurement was repeated after one month resulting in the remarkable changes: the new peak at *m/z* 529.50 appeared. It can be assumed that the product is unstable and undergoes oxidation under ambient conditions.

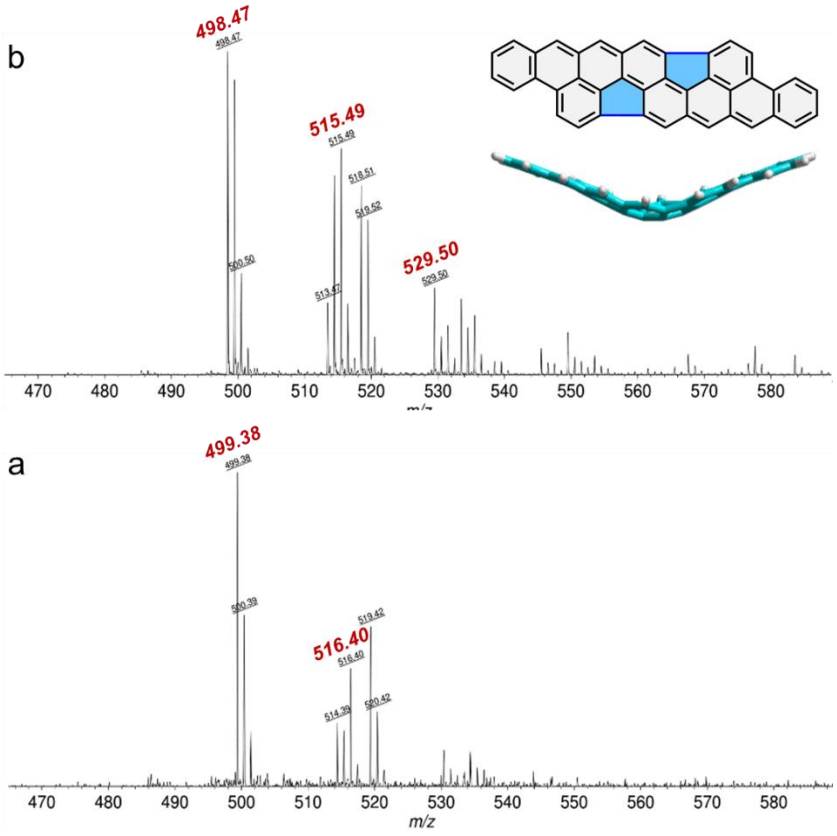

Figure 50. LDI-MS spectra of benzo[*l*]indeno[*5,4,3,2,1-nopqr*]naphtho[*3',2',1':5,6*]acenaphtho[*3,2,1-cde*]tetraphene **111** after synthesis (a) and after one month (b).

We can conclude that acid-promoted intramolecular cyclization is applicable for synthesis of large acenes in near-quantitative yields. This method appears to be tolerant to halogens and heterocycles (e.g. pyridine). Moreover, it is can be scaled up to gram amount and not affected by moistures and air. Worth mentioning that developed approach allows to synthesize highly insoluble acenes and structures combining acene-type inclusions in bowl-shape structures.

4 Summary

The main goal of this thesis was the synthesis of the extended PAHs *via* selective C-F bond activation.

The first part of the thesis is concentrated on the activation of C-F bond in the trifluoromethyl group in the aromatic arenes under mild conditions. We found out that the direct intramolecular cyclization of the CF_3 group on activated alumina allows us to synthesize a range of the cyclic aromatic ketones in appropriate yields. The main advantages of this approach are the scalability, the inexpensive starting materials, the high tolerance of the CF_3 group and the high selectivity of reaction. In addition, the hydrolysis of the CF_3 group was found to be a simple way for the synthesis of carboxylated PAHs.

Furthemore, we demonstrate a facile pathway for synthesis have presented an approach for the synthesis of rationally halogenated bowl-shaped PAHs. We succeeded in the transformation of precursors into the halogenated buckybowls by aryl-aryl coupling in near-quantitative yields. The presented method allowed us to introduce the halogen functionalities at virtually any position and, thus, the obtained halogenated diindenochrysenes and indacenopicenes can be used as building blocks for structures with the complex architecture. The alumina promoted aryl-aryl coupling appeared to be tolerant towards aromatic C-Br and C-Cl bonds. For the first time, the X-ray crystallographic analysis of diindeno[*4,3,2,1-cdef:4',3',2',1'-lmno*]chrysene structure was conducted and the bowl-shaped character of the molecule was confirmed (bowl depth at 1.78 Å).

It is worth to mention that in the alumina-promoted aromatic C-F bond activation a solvent plays a crucial role providing the homogenious distribution of the precursor and influencing the efficiency of HF-elimination. Our finding revealed the ability of *o*-dichlorobenzene to accelerate the reaction up to 200 times yielding a pure target compound.

In the second part of the thesis we present a novel type of molecular receptor based on two indacenopicene units and tolyl as a tether. The binding behaviour of the 9,9'-(5-methyl-1,3-phenylene)di-as-indaceno[*3,2,1,8,7,6-pqrstuv*]picene towards C_{60} or C_{70} in toluene was investigated by fluorescence spectroscopy. The formation of 1:1 complexe in the presence of C_{60} or C_{70} was herewith confirmed. Titration experiments

gave crude estimation of the association constants. The preliminary association constants were found to be 8.65×10^3 M^{-1} for C_{60} and 6.04×10^4 M^{-1} for C_{70} complexes. Thus, the binding affinity to C_{70} is significantly higher than to C_{60}.

The third part of the thesis describes the synthetic approach for the preparation of the highly curved buckybowls from the diindenochrysene precursor. The product obtained by the double-fold Suzuki cross-coupling and subsequent aryl-aryl coupling on the activated alumina exhibits the large bowl depth (5.2 Å). Moreover, in this chapter we illustrated a pyrene-based method for the synthesis of oligoindenopyrenes including the intramolecular cyclization *via* C-F bond activation.

The last part of the thesis highlights the introduction of peripheral zig-zag units into nanographene molecules by acid-promoted intramolecular reductive cyclization. As precursor for acene-type nanographenes were employed aromatic aldehydes. The advantages of such cycloaromatization are effectiveness, availiability of chemicals, scalability and near-quantitative yields. The developed reaction protocol allowed us to synthesize a series of nanographenes and the bowl-shaped acene-type molecule based on diindenochrysene core.

Taken together, these findings suggested the simple and facile ways towards extended bowl-shaped and planar structures, which can be utilized in the synthesis of fullerenes, nanotubes and nanographenes.

5 Zusammenfassung

Das Hauptziel der Dissertation war die Synthese von erweiterten polyzyklischen aromatischen Kohlenwasserstoffen durch die selektive C-F-Bindungsaktivierung.

Der erste Teil der Arbeit konzentriert sich auf die Aktivierung der C-F-Bindung in der Trifluormethylgruppe in den aromatischen Arenen unter milden Bedingungen. Wir fanden heraus, dass die direkte intramolekulare Zyklisierung der CF_3-Gruppe auf aktiviertem Aluminiumoxid es uns ermöglicht, eine Reihe der zyklischen aromatischen Ketone in geeigneten Ausbeuten zu synthetisieren. Die Hauptvorteile dieses Ansatzes sind die Skalierbarkeit, die kostengünstigen Ausgangsstoffe, die hohe Toleranz der CF_3-Gruppe und die hohe Selektivität der Reaktion. Darüber hinaus wurde festgestellt, dass die Hydrolyse der CF_3-Gruppe ein einfacher Weg für die Synthese von carboxylierten PAK ist.

Des Weiteren erarbeiteten wir eine einfache Methode zur Synthese und haben einen Ansatz für die Synthese von rational halogenierten schalenförmigen PAKs vorgestellt. Es ist uns in nahezu quantitativen Ausbeuten gelungen, die Präkursore in halogenierte Buckybowls durch Aryl-Aryl-Kupplung zu transformieren. Die vorgestellte Methode erlaubt es uns, die Halogenfunktionalitäten an beliebiger Stelle einzuführen. Somit können die syntetisierten halogenierten Diindenochrysene und Indacenopene als Bausteine für Strukturen mit einer komplexen Architektur verwendet werden. Die mit Aluminiumoxid geförderte Aryl-Aryl-Kupplung schien tolerant gegenüber aromatischen C-Br- und C-Cl-Bindungen zu sein. Erstmals wurde die röntgenkristallographische Analyse der Diindenochrysenstruktur durchgeführt und der schalenförmige Charakter des Moleküls bestätigt (Schalentiefe von 1.78 Å).

Es gilt zu erwähnen, dass bei der durch Aluminiumoxid produzierten aromatischen C-F-Bindungsaktivierung das Lösungsmittel eine entscheidende Rolle spielt. Es sorgt für eine homogene Verteilung des Präkursors und beeinflusst die Effizienz der HF-Eliminierung. Unser Ergebnis zeigte die Fähigkeit von *o*-Dichlorbenzol, die Reaktion bis zu 200-mal zu beschleunigen, was zu einer reinen Zielverbindung führt.

Im zweiten Teil der Arbeit präsentieren wir einen neuartigen Typ eines molekularen Rezeptors, der auf zwei Indacenopicen-Einheiten und Phenyl als Halteverbindung basiert. Das Bindungsverhalten des 9,9'-(5-Methyl-1,3-phenylen)di-*as*-indaceno[*3,2,1,8,7,6-pqrstuv*]picens gegenüber C_{60} oder C_{70} in Toluol wurde mithilfe von

Fluoreszenzspektroskopie untersucht. Die Bildung eines 1:1-Komplexes in Anwesenheit von C_{60} oder C_{70} wurde hiermit bestätigt. Die Titrationsexperimente gaben eine grobe Einschätzung der Assoziationskonstanten. Die vorläufige Assoziationskonstanten wurden als $8{,}65\times10^{3}$ M^{-1} für C_{60} und $6{,}04\times10^{4}$ M^{-1} für C_{70}-Komplexe definiert. Somit ist die Bindungsaffinität zu C_{70} deutlich höher als zu C_{60}.

Das dritte Kapitel beschreibt einen synthetischen Ansatz für die Herstellung der stark gewölbten Buckybowls aus Diindenochrysen-Präkursoren. Das durch die doppelte Suzuki-Kreuzkupplung und die anschließende Aryl-Aryl-Kupplung auf aktiviertem Aluminiumoxid erhaltene Produkt weist eine sehr große Schalentiefe (5.2 Å) auf. Darüber hinaus veranschaulichen wir in diesem Teil ein pyrenbasiertes Verfahren zur Synthese von Oligoindenopyrenen einschließlich der intramolekularen Zyklisierung über die C-F-Bindungsaktivierung.

Das letzte Kapitel dieser Dissertation widmet sich der Einführung von dezentralen Zickzack-Einheiten in Nanographene-Moleküle mittels säurefördernder intramolekularer reduktiver Zyklisierung. Als Präkursor für die acenartigen Nanographene wurden aromatische Aldehyde eingesetzt. Die Vorteile einer solchen Zykloaromatisierung sind die Effektivität, die gute Verfügbarkeit der Chemikalien, die gute Skalierbarkeit, sowie nahezu quantitative Ausbeuten. Die von uns entwickelte Synthesestrategie erlaubte es, eine Reihe von Nanographenen und das schalenförmige acenartige diindenochrysenbasierte Molekül herzustellen.

Zusammengefasst, zeigen diese Ergebnisse einen einfachen und leichten Wege zu erweiterten schalenförmigen und planaren Strukturen auf, die zur Synthese von Fullerenen, Nanoröhren und Nanographenen genutzt werden können.

6 Experimental Section

6.1 General Information

Solvents and chemicals

All chemicals were purchased from chemPUR, Fluorochem, Sigma-Aldrich®, Acros, Organics®, Fluka®, Fisher Scientific®, Alfa Aesar® and used without any further purification. HPLC grade solvents were purchased from VWR®. Solvents for flash chromatography (hexane) and photocyclization were distilled prior to usage. Aluminium oxide (neutral, 50-200 micron) for C-F bond activation was purchased from (neutral, 50-200 micron), Acros.

Nuclear magnetic resonance spectroscopy

NMR spectra were recorded on Bruker® Avance 300 operating at 300 MHz (^{1}H NMR), 75 MHz (^{13}C NMR) and 282 MHz (^{19}F NMR), Bruker® Avance 400 or Jeol ® EX400, operating at 400 MHz (^{1}H NMR) and 100 MHz (^{13}C NMR), JEOL® Alpha 500 operating at 500 MHz (^{1}H NMR) and 125 MHz (^{13}C NMR) or Bruker® Avance Neo 500 operating at 500 MHz (^{1}H NMR) and 125 MHz (^{13}C NMR), Bruker® Avance Neo 600 operating at 600 MHz (^{1}H NMR) and 151 MHz (^{13}C NMR). Deuterated solvents were purchased from Sigma Aldrich ® and used as received. Signals were referenced to solvent peaks (δ in ppm) CD_2Cl_2: ^{1}H 5.32 ppm, ^{13}C 53.5 ppm; $CDCl_3$: ^{1}H 7.24 ppm, ^{13}C 77.0 ppm; $C_2D_2Cl_4$: ^{1}H 5.92 ppm, ^{13}C 73.7 ppm; C_6D_6: ^{1}H 7.15 ppm, ^{13}C 128.0 ppm; *o*-DCB: ^{1}H ppm, ^{13}C ppm. Resonance peaks were indicated as “s” (singlet), “d” (doublet), “t” (triplet), “q” (quartet) and “m” (multiplet).

Absorption spectroscopy

UV/Vis spectra were recorded on a Varian® Cary 5000 UVvis spectrophotometer at room temperature.

Emission spectroscopy

Fluorescence spectra were recorded on a Shimadzu® RF-5301PC spectrofluorophotometer.

X-ray crystallography

X-ray structure analysis was carried out on Bruker® Smart APEX II CCD area detector diffractometer and Agilent Technologies® SuperNova Dual Wavelength Platform with Atlas detector and Xcalibur E System diffractometer.

High-performance liquid chromatography

HPLC analyses were carried out using analytical Cosmosil 5-PYE (4.6 x 250 mm) column and Cosmosil PBr (4.6 x 250 mm) and purification using semi-preparative PBB-R (10 x 250 mm) column (UV-Vis detection).

Flash liquid chromatography

Automated flash-column chromatography (aFLC) was performed on Intershim® puriflash 430 with flash grade silica gel Kiesegel 60 (0.06-0.2 mm).

Thin layer chromatography

TLC was performed on silica-backed silica plates and visualized by UV-light (254 nm, 366 nm), layer thickness 0.25 mm, medium pore diameter 60 Å, Fluka.

Photocyclization

Photocyclization was carried out in the 500 W water-cooled quartz photochemical reactor.

Mass spectrometry

ESI and APPI mass spectra were recorded on maXis 4G, Bruker® Daltonic GmbH. LDI-TOF mass spectra were recorded on the Axima Confidence, Shimadzu Biotech® Spectrometer, Shimadzu Deutschland GmbH. All spectra are reported as *m/z*.

Microwave assisted experiments

Microwave assisted experiments were carried out using Discover® SP Microwave Synthesizer, CEM and Biotage® initiator+ monomode microwave reactor, Biotage in the respective vials.

Computational methods for the catalyst-free cyclodehydrofluorination

Geometry optimizations were performed at rhe PBE0/cc-pVDZ level of theory. In all cases, no symmetry restrictions were applied. All calculated structures of reactive complexes, intermediates and products correspond to local minima (no imaginary

frequencies) and transition states were located at saddle point with unique imaginary frequencies on the corresponding potential energy surfaces, as determined by calculation of the full Hessian matrix, followed by estimation of frequencies in the harmonic approximation. The nature of transition states was probed through IRC (intrinsic reaction coordinates) technique that showed a directly connection to the target products and reactants. All these calculations were performed using the Firefly program (version 8.1.0).

General procedure for synthesis of ortho-substituted trifluoromethylarenes[100]

1 eq. of respective aryl bromide, 1.2 eq. of respective boronic acid, 1.2 eq. of K_2CO_3 and 5 % of $Pd(PPh_3)_4$ were added to the mixture of Tol:MeOH:2:1 (60 mL). The reaction mixture was degassed and refluxed for 12 h under argon atmosphere. After cooling to the room temperature mixture was washed with water (3x100 mL). The organic layer was dried over Na_2SO_4 and filtered through a silica plug. Resulting mixture and the solvent was removed under reduced pressure. Purification of product was made by column chromatography on silica using hexane.[100]

General procedure for bromination reaction[102]

1 eq. of respective methylarene was dissolved in fluorobenzene or chloroform, then 1.1 eq. of NBS and a catalytic amount of DBPO were added. Reaction was carried out under reflux and monitored by TLC. After cooling to the room temperature reaction mixture was diluted with appropriate solvent (toluene or DCM), filtrated through silica plug and concentrated under reduced pressure. Further, product was purified by column chromatography or aFLC.[102]

General procedure for Wittig reaction[102]

All arylethenes were obtained by Wittig reaction as described in [102]. Prior to carry out Wittig reaction was synthesised phosphonium salt from alkyl bromide (1 eq.) and PPh_3 (1.1 eq) in refluxed toluene during 20 h. After cooling to the room temperature, the precipitate was filtered, washed with toluene and hexane and dried in vacuo. Further, 1 eq. of respective aldehyde 1.1 eq. of respective phosphonium salt and 1.1 eq. *t*-BuOK were added in absolute EtOH. The reaction mixture was degassed under dynamic vacuum and refluxed for 12 h under argon atmosphere. After cooling to the room temperature, the reaction mixture was neutralized, and DCM and H_2O were added. The layers were separated, and the aqueous phase was extracted with DCM

(3 times). Combined organic layers were dried over anhydrous Na_2SO_4 and concentrated under reduced pressure. Product was purified by column chromatography or aFLC.[102]

General procedure for photocylization reaction[31,102]

All arylethenes were used in the form of a *cis/trans* isomer mixture since the isomers interconvert under photocyclization conditions. 1 eq. arylethene, 1 eq. I_2 and 5 eq. propylene oxide were dissolved in distilled cyclohexane or toluene. Reaction was monitored by TLC. Since the reaction was finished, the mixture was washed with sodium thiosulfate solution in water. Organic layer was dried over anhydrous Na_2SO_4 and concentrated under reduced pressure. Product was purified by column chromatography or aFLC.[31,102]

General procedure for Al_2O_3 mediated C-F bond activation for aryl-aryl coupling[98]

γ-Al_2O_3 was preactivated (1 g) in glass ampule at 250 °C under air conditions for 10 min and then activated at 550°C for 15 min in vacuum (10^{-3} mbar). Activated *γ*-Al_2O_3 was added to the microwave glass vial containing 20 mg of fluoroarene dissolved in 3 mL of anhydrous *o*-DCB. 3-5 g of alumina and 10-15 mL of *o*-DCB were used for 100 mg fluoroarene. The glass vial was closed with the cap and placed into microwave oven. The reaction was conducted at 150-240 °C for 0.5-3 h. All steps were carried out under argon atmosphere. After cooling to rt the products were extracted with toluene. Pure products (95-98 % yield) were obtained by direct precipitation with MeOH from the respective concentrated toluene extract.[98]

General procedure for Al_2O_3 mediated condensation of trifluoromethylated arenes[100]

2-3 g of *γ*-Al_2O_3 were placed in a glass ampoule and activated by annealing in vacuum (10^{-2} mbar). The temperature was increased gradually, and kept for 30 min at 600°C. After cooling (rt) the ampoule was filled with argon, and 20-30 mg of the respective trifluoromethyl arene were mixed with activated aluminium oxide. The ampoule was evacuated again and sealed. Condensation was conducted without stirring at 30-250°C. The condensation products were extracted with MeOH (or MeOH/AcOH mixture) and analysed after evaporation.[100]

General procedure for Al_2O_3 mediated hydrolysis of trifluoromethylated arenes[100]

2-3 g of γ-Al_2O_3 were mixed with 20-30 mg of the respective trifluoromethyl arene in glass ampoule under ambient atmosphere. The ampoule was heated to 100-250°C. The hydrolysis products were extractied with MeOH/AcOH mixture and analysed after evaporation.[100]

General procedure for synthesis of nanographenes[171]

20 mg of nanographene precursor was dissolved in 100 mL of DCM. Solution of $SnCl_2$*$2H_2O$ (500 mg, 2.22 mmol) in *i*-PrOH (2.0 mL) was added at rt while stirring. The colour of the solution changed to yellowish. Then, 1.0 mL of conc. H_2SO_4 was added and the mixture was stirred at rt for 18 h (the reaction mixture should be protected from the daylight). The reaction mixture was quenched with 2.0 mL of 1 M HCl by vigorous mixing, diluted with DCM (20 mL) and washed with water (50 mL). The aqueous layer was extracted with DCM (3x20 mL). Organic layers were combined and diluted with MeOH (100 mL). DCM was removed at atmospheric pressure at 50 °C. Obtained precipitate in the MeOH layer was centrifuged, the MeOH layer was decanted and the solid was washed again with MeOH. Following that, the product was dried in vacuo.[171]

6.2 Synthesis of Trifluoromethylated Compounds and Aromatic Ketons

2-Trifluoromethyl-1,1'-biphenyl (1)

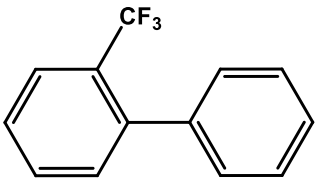

$C_{13}H_9F_3$
M = 222.21

1 was obtained according to general procedure from 2-bromobenzotrifluoride **2** (20.0 mmol) and phenylboronic acid **3** (22.0 mmol).[100]

Colourless liquid, **92 %** yield.

^{1}H NMR spectrum is in accordance with [103].

9H-Fluoren-9-one (4)

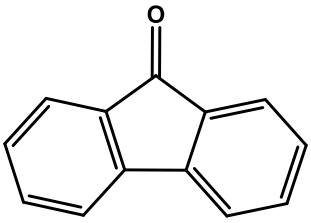

$C_{13}H_8O$
M = 180.21

4 was obtained from **1** according to general procedure for Al_2O_3 mediated condensation.[100]

Yellow solid, **80 %** yield.

^{1}H NMR spectrum is in accordance with [173].

1,1'-Biphenyl-2-carboxylic acid (5)

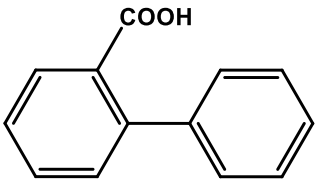

$C_{13}H_{10}O_2$
M = 198.22

5 was obtained from **1** according to general procedure for Al_2O_3 mediated hydrolysis.[100]

White solid, quantitative yield (determined by NMR).

^{1}H NMR spectrum is in agreement with [174].

4'-Methyl-2-(trifluoromethyl)-1,1'-biphenyl (8)

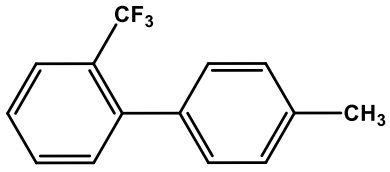

$C_{14}H_{11}F_3$
M = 236.24

8 was obtained according to general procedure from 2-trifluoromethyl phenylboronic acid (16.0 mmol) and arylbromide (14.0 mmol).[100]

Colorless liquid, **94 %** yield.

^{1}H NMR spectrum is in agreement with [175].

2-Methyl-9H-fluoren-9-one (9)

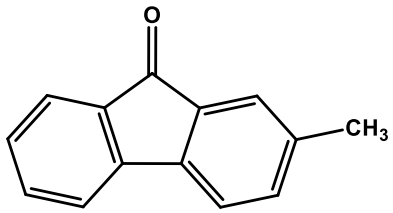

$C_{14}H_{10}O$
M = 194.23

9 was obtained from **8** according to general procedure for Al_2O_3 mediated condensation.[100]

Yellow liquid, **72 %**yield.

^{1}H NMR spectrum is in accordance with [173].

4-Methyl-2'-biphenylcarboxylic acid (10)

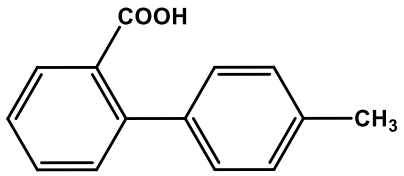

$C_{14}H_{12}O_2$
M = 212.25

10 acid was obtained following to general procedure for Al_2O_3 mediated hydrolysis from **8**.[100]

White solid, **quantitative** yield (determined by NMR).

^{1}H NMR spectrum is in agreement with [176].

1-[2-(Trifluoromethyl) phenyl]-naphthalene (10)

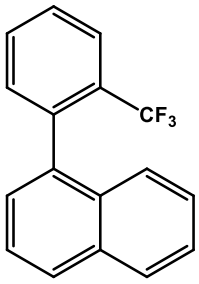

$C_{17}H_{11}F_3$
M = 272.27

10 was obtained according to general procedure from 1-naphthylboronic acid **11** (16.0 mmol) and 2-bromobenzotrifluoride **13** (14.0 mmol).[100]

White solid, **92 %** yield.

^{1}H NMR [400 MHz, $CDCl_3$, 293 K]: *δ* (ppm) 7.91 (s, 1H), 7,89 (s, 1H), 7.4 (d, *J*=7.81 Hz, 1H), 7.63-7.44 (m, 4H), 7.41-7.31 (m, 4H).

^{13}C NMR [100 MHz, CD_2Cl_2, 293 K]: *δ* (ppm) 139.32, 136.74, 133.25, 132.67, 132.41, 131.103, 129.6 (q), 128.18, 128.05, 127.88, 127.68, 127.02, 126.18, 126.10, 126.08, 126.02, 125.97, 124.68, 124.00 (q).

7H-Benz[de]anthracen-7-one (14)

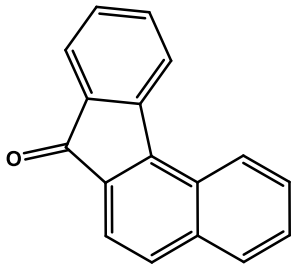

$C_{17}H_{10}O$
M = 230.27

14 was obtained from **10** according to general procedure for Al_2O_3 mediated condensation.[100]

Red solid, **40 %** yield.

^{1}H and **^{13}C NMR** spectra are in accordance with [177].

7H-Benzo[c]fluoren-7-one (15)

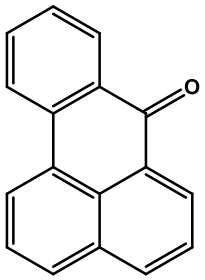

$C_{17}H_{10}O$
M = 230.27

15 was obtained according to general procedure for Al_2O_3 mediated condensation from **10**. Small amounts of *7H*-benzo[*c*]fluoren-7-one and *7H*-benz[de]anthracen-7-one were separated by column chromatography for analysis.[100]

Orange solid, **18 %** yield.

^{1}H and **^{13}C NMR** spectra is in accordance with [178].

2-(1-Naphthalenyl)-benzoic acid (16)

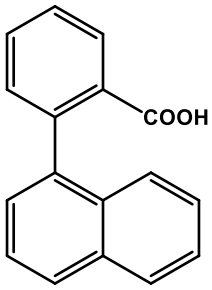

$C_{17}H_{12}O_2$
M = 248.28

16 was obtained from **10** according to general procedure for Al_2O_3 mediated hydrolysis.[100]

White solid, **quantitative** yield (determined by NMR).

^{1}H and **^{13}C NMR** spectra are in agreement with [179].

2-(Trifluoromethyl)-terphenyl (17)

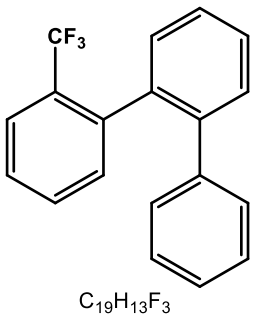

$C_{19}H_{13}F_3$
M = 298.31

17 was obtained according to general procedure from 2-biphenylboronic acid (16.0 mmol) and 2-bromobenzotrifluoride **13** (14.0 mmol).[100]

Colourless oil, **80 %** yield.

^{1}H and **^{13}C NMR** spectra are in accordance with [180].

4-Phenyl-9H-fluoren-9-one (18)

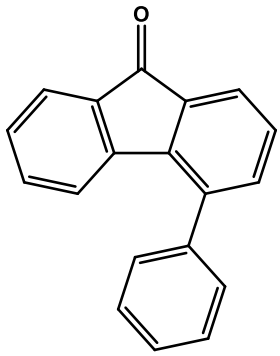

$C_{19}H_{12}O$
M = 256.30

18 was obtained from **17** according to general procedure for Al_2O_3 mediated condensation. Small amounts of 4-phenyl-*9H*-fluoren-9-one and *9H*-tribenzo[*ace*] cyclohepten-9-one for NMR analysis were separated by HPLC (5PYE column, MeOH as eluent).[100]

Orange solid, **8 %** yield.

^{1}H NMR [300 MHz, $CDCl_3$, 293 K]: *δ* (ppm) 7.69-7.59 (m, 2H), 7.53-7.44 (m, 5H), 7.38-7.33 (m, 2H), 7.25-7.15 (m, 2H), 6.77 (m, 1H).

^{13}C NMR [75 MHz, CD_2Cl_2, 293 K]: *δ* (ppm) 193.84 (CO), 144.86, 143.36, 139.85, 137.06, 135.05, 134.80, 134.70, 129.15 (2C), 129.07 (2C), 128.49, 124.21, 123.51, 123.31. One carbon signal is not observed due to overlapping.

9H-Tribenzo[ace]cyclohepten-9-one (19)

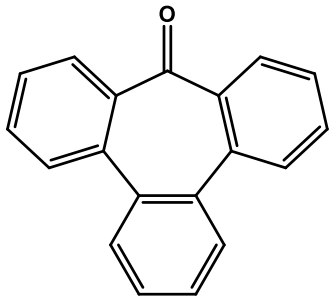

$C_{19}H_{12}O$
M = 256.30

19 was obtained from **17** according to general procedure for Al_2O_3 mediated condensation.[100]

Yellow solid, **52 %** yield.

^{1}H and **^{13}C NMR** spectra are in accordance with [181].

o-Terphenyl-2-carboxylic acid (20)

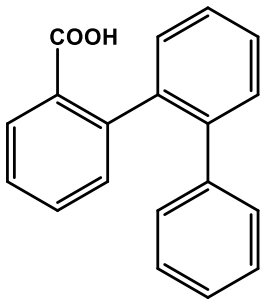

$C_{19}H_{14}O_2$
M = 274.32

20 acid was obtained from **17** according to general procedure for Al_2O_3 mediated hydrolysis.[100]

White solid, **quantitative** yield (determined by NMR).

^{1}H NMR [300 MHz, $CDCl_3$, 293 K]: δ (ppm) 7.8 (d, J=7.46 Hz, 1H), 7.47-7.34 (m, 4H), 7.33-7.28 (m, 2H), 7.19-7.02 (m, 6H).

^{13}C NMR [100 MHz, $CDCl_3$, 293 K]: δ (ppm) 172.05 (CO), 143.14, 141.00, 140.57, 139.93, 132.19, 131.73, 130.31, 129.80, 129.78, 129.69, 128.53, 127.72, 127.63, 126.99, 126.98, 126.81, 126.44. One carbon signal is not observed due to overlapping of signals.

Benzo[c]-phenanthrene-2-carboxylic acid (22)

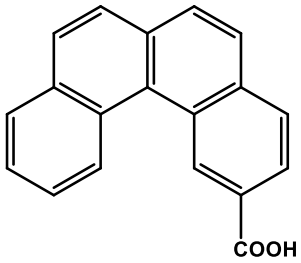

$C_{19}H_{12}O_2$
M = 272.30

22 was obtained from **19** according to general procedure for Al_2O_3 mediated hydrolysis.[100]

White solid, **96 %** yield.

^{1}H and **^{13}C NMR** spectra are in accordance with [182].

1,6-dibromopyrene (24)

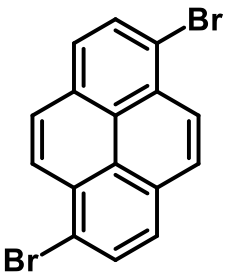

$C_{16}H_8Br_2$
M = 360.05

1,6-dibromopyrene was synthesized according to modified procedure [148]. In two-neck RBF pyrene **57** (30.0 g, 1.48 mol) was dissolved in 1.5 L of chloroform. The solution of Br_2 (15.3 mL, 2.97 mol) in $CHCl_3$ (500 mL) was added dropwise (from dropping funnel) while stirring at rt for 8 h. Precipitated product was collected after 16 h and washed with MeOH. Then, the precipitate was recrystallized from hot xylene (mixture of isomers), yielding the product in 19.0 g (52.8 mmol).[171]

Beige solid, **36 %** yield.

^1H NMR is in agreement with [183].

1,6-Bis(2-(trifluoromethyl)phenyl)pyrene (23)

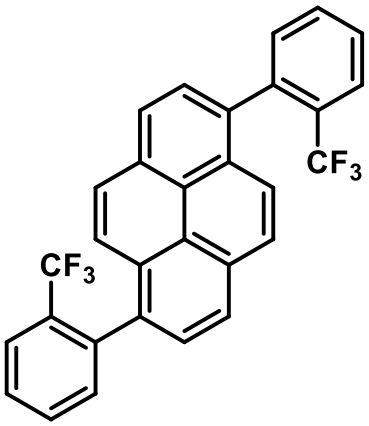

$C_{30}H_{16}F_6$
M = 490.45

0.1 g (0.28 mmol) 1,6-dibromopyrene **24** and 2-(trifluoromethyl)phenylboronic acid **25** 0.14 g (0.73 mmol) were dissolved in Tol:MeOH (2:1) mixture, then potassium carbonate (0.73 mmol) and 5 % mol of $Pd(PPh_3)_4$ as catalyst were added. Reaction mixture was stirred under reflux in nitrogen atmosphere for 15 h. Mixture was washed with water; organic layer was dried over Na_2SO_4 and filtrated through silica plug.

Solvent was removed under reduced pressure. After addition of hexane white precipitate was collected on filter (0.13 g, 0.264 mmol).

White solid, **95.6 %** yield.

^{1}H NMR [300 MHz, CD_2Cl_2, 293 K]: *δ* (ppm) 8.22 (2H, d, *J*=7.86 Hz), 8.04 (2H, d, *J*=9.27 Hz), 7.93 (4H, d, *J*=7.86 Hz), 7.77- 7.65 (m, 4H), 7.63 (2H, d, *J*=9.18 Hz), 7.49 (2H, d, *J*=7.23 Hz).

^{13}C NMR [75 MHz, CD_2Cl_2, 293 K]: *δ* (ppm) 139.84-139.72 (m), 134.86, 133.14, 131.56-131.46 (m), 130.73, 129.82-129.68 (m), 129.39, 128.07, 127.80-127.66 (m), 127.48, 126.30-126.07 (m), 125.59, 124.36, 124.06, 122.49, 118.86.

6.3 Synthesis of Halogenated Buckybowls

6.3.1 Synthesis of Brominated Benzo- and Indacenopicenes

2-Bromo-13,16-difluorobenzo[s]picene (38a)

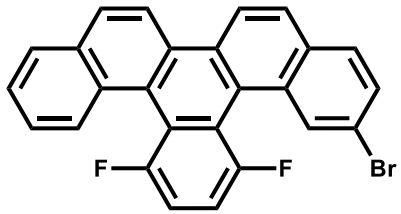

$C_{26}H_{13}BrF_2$
M = 443.29

38a was synthesized according to general procedures (bromination, Wittig reaction, photocylization).[98]

Light-yellow solid, **55 %** yield.

^{1}H NMR [400 MHz, $CDCl_3$, 293 K]: *δ* (ppm) 8.53 (1H, d, *J*=8.80 Hz), 8.50 (1H, d, *J*=8.84 Hz), 8.34 (1H, dd, *J*=1.94, 13.62 Hz), 8,23-8,14 (1H, m), 8.11 (1H, d, *J*=8.80 Hz), 8.05 (1H, d, *J*=8.76 Hz), 7.98-7.93 (1H, m), 7.81 (1H, d, *J*=8.72 Hz), 7.64 (1H, dd, *J*=1.84, 8.60 Hz), 7.62-7.55 (2H, m), 7.45-7.33 (2H, m).

^{13}C NMR [100MHz, $CDCl_3$, 293 K]: *δ* (ppm) 153.90, 153.73, 132.44, 131.97, 131.81, 131.38, 130.68, 130.08, 129.75, 129.71, 129.60, 129.48, 129.30, 128.92, 128.63, 127.13, 126.34, 125.36, 120.23, 119.66, 119.59, 114.72, 114.89-114.40.

^{19}F NMR [282 MHz, $CDCl_3$, 293 K]: *δ* (ppm) -103.55- -103.76 (m), -104.23 - -104.47 (m).

HRMS [APPI]: Chemical Formula: $C_{26}H_{13}BrF_2$ calc. 442.0163, found 442.0166.

4-Bromo-13,16-difluorobenzo[s]picene (38b)

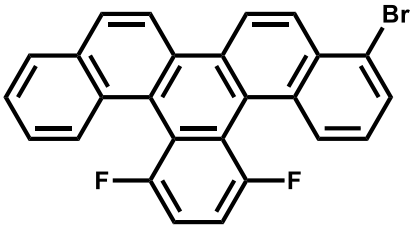

$C_{26}H_{13}BrF_2$
M = 443.29

38b was synthesized according to general procedures (bromination, Wittig reaction, photocylization).[98]

Light-yellow solid, **50 %** yield.

^{1}H NMR [400 MHz, $CDCl_3$, 293 K]: *δ* (ppm) 8.59 (1H, d, *J*=9.28 Hz), 8.51 (1H, d, *J*=8.80 Hz), 8.50 (1H, d, *J*=8.88 Hz), 8.24-8.12 (2H, m), 8.10 (1H, d, *J*=8.64 Hz), 7.98-7.93 (1H, m), 7.84 (1H, dd, *J*=0.64, J=7.40 Hz), 7.62-7.55 (2H, m), 7.43-7.31 (2H, m).

^{13}C NMR [100 MHz, $CDCl_3$, 293 K]: *δ* (ppm) 156.36, 156.21, 153.90, 153.84, 153.74, 132.49, 131.68, 131.63, 130.74, 130.41, 130.13, 130.08, 129.73, 129.66, 129.58, 129.45, 128.11, 127.19, 126.36, 125.45, 125.43, 125.37 125.35, 123.77, 123.75, 123.73, 123.36, 123.34, 123.31, 122.04, 122.02, 121.21, 120.33, 120.30, 120.19, 120.16, 119.99, 119.96, 119.86, 119.82, 119.62, 114.87, 114.77, 114.64, 114.59, 114.54, 114.49, 114.36, 114.26.

^{19}F NMR [282 MHz, $CDCl_3$, 293 K]: *δ* (ppm) -103.50- -103.75 (m), -103.89 - -104.10 (m).

HRMS [APPI]: Chemical Formula: $C_{26}H_{13}BrF_2$ calc. 442.0163, found 442.0163.

5-Bromo-13,16-difluorobenzo[s]picene (45)

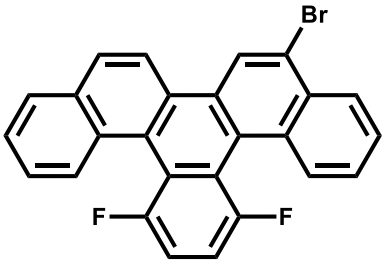

$C_{26}H_{13}BrF_2$
M = 443.29

45 was isolated after bromination of 13,16-difluorobenzo[*s*]picene **30** (side product).

Light-yellow solid, **20 %** yield.

^{1}H NMR [400 MHz, CD_2Cl_2, 293 K]: *δ* (ppm) 8.88 (s,1H), 8.48 (d, *J*=8.96 Hz, 1H), 8.42-8.37 (m, 1H), 8.25-8.17 (m, 2H), 8.15 (d, *J*=8.92 Hz, 1H), 8.03-7.98 (m, 1H), 7.73-7.64 (m, 2H), 7.64-7.59 (m, 2H), 7.48-7.38 (m, 2H).

^{13}C NMR [101 MHz, $CDCl_3$, 293 K]: *δ* (ppm) 154.01, 153.98, 153.79, 153.75, 132.56, 130.60, 130.43, 130.08, 130.04, 129.94, 129.69, 129.66, 129.54, 128.92, 127.41, 127.24, 127.23, 126.51, 126.36, 126.35, 126.10, 126.08, 125.50, 125.48, 124.24, 124.01, 119.52, 115.10-114.50 (m).

HRMS [APPI, Toluene]: Chemical Formula: $C_{26}H_{13}BrF_2$ calc. 442.0163, found 442.0170.

MS [MALDI-TOF, without matrix]: m/z (rel. int.) = 442.0058 [M]+ (100)

MS [MALDI-TOF, DHB]: m/z (rel. int.) = 442.0235 [M]+ (100)

MS [MALDI-TOF, DCTB]: m/z (rel. int.) = 442.0131 [M]+ (100).

1-Bromo-as-indaceno[3,2,1,8,7,6-pqrstuv]picene (39b)

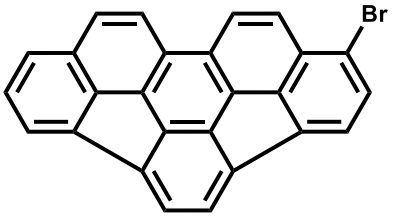

$C_{26}H_{11}Br$
M = 403.28

39b was obtained from 4-bromo-13,16-difluorobenzo[*s*]picene **38b** according to general procedure for Aryl-Aryl coupling *via* C-F bond activation.[98]

Orange solid, **96 %** yield (determined by HPLC).

^{1}H NMR [400 MHz, CD_2Cl_2, 293 K]: *δ* (ppm) 8.13 (1H, d, *J*=8.85 Hz), 8.09 (1H, d, *J*=8.76 Hz), 7.86 (1H, d, *J*=8.85 Hz), 7.79 (1H, d, J=8.76 Hz), 7.70 (1H, d, *J*=6.96 Hz), 7.64 (1H, d, *J*=8.13 Hz), 7.59 (2H, ABq, *J*=7.32 Hz), 7.55 (1H, d, *J*=7.38 Hz), 7.48 (1H, d, *J*=7.38 Hz), 7.40 (1H, dd, *J*=8.18, 6.98 Hz).

^{13}C NMR [100 MHz, CD_2Cl_2, 293 K]: *δ* (ppm) 139.44, 139.25, 138.96, 138.76, 138.37, 138.33, 138.29, 138.05, 138.03, 136.94, 131.90, 130.67, 129.87, 129.65, 129.44, 129.15, 127.44, 127.23, 126.25, 126.22, 126.10, 125.55, 124.75, 124.31, 124.08, 122.16.

HRMS [APPI]: Chemical Formula: $C_{26}H_{11}Br$ calc. 402.0039, found 402.0040.

3-Bromo-as-indaceno[3,2,1,8,7,6-pqrstuv]picene (39a)

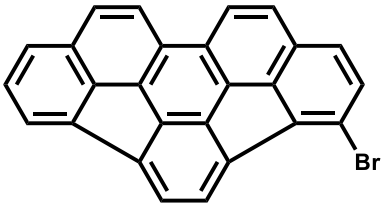

$C_{26}H_{11}Br$
M = 403.28

39a was obtained from 2-bromo-13,16-difluorobenzo[*s*]picene **38a** according to general procedure for Aryl-Aryl coupling *via* C-F bond activation (small amount was collected by analytical HPLC for NMR measurement).[98]

Orange solid, **80 %** yield (determined by HPLC).

^{1}H NMR [300 MHz, $CDCl_3$, 293 K]: *δ* (ppm) 8.10 (1H, dd, *J*=0.78, 8.76 Hz), 7.98 (1H, d, *J*=7.38 Hz), 7.80 (1H, d, *J*=8.79 Hz), 7.77-7,69 (3H, m), 7.65 (1H, d, *J*=8.16 Hz), 7.51-7.37 (3H, m).

HRMS [APPI]: Chemical Formula: $C_{26}H_{11}Br$ calc. 402.0039, found 402.0039.

9-Bromo-as-indaceno[3,2,1,8,7,6-pqrstuv]picene (46)

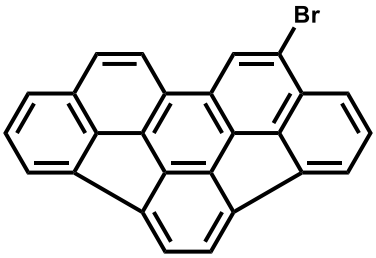

$C_{26}H_{11}Br$
M = 403.28

46 was as obtained according to general procedure for Aryl-Aryl coupling *via* C-F bond activation.

Orange solid, **97 %** yield (determined by HPLC).

^{1}H NMR [400 MHz, CD_2Cl_2, 293 K]: *δ* (ppm) 8.33 (1H, s), 8.02 (1H, d, *J*=8.76 Hz), 7.79 (1H, d, *J*=8.76 Hz), 7.75 (1H, d, *J*=8.32 Hz), 7.72 (2H, dd, *J*=5.22, 6.94 Hz), 7.67 (1H, d, *J*=8.12 Hz), 7.64 (2H, dd, *J*=7.42, 12.34 Hz), 7.46 (1H, dd, *J*=7.00, 8.32 Hz), 7.43 (1H, dd, *J*=6.96, 8.16 Hz).

^{13}C NMR [101 MHz, CD_2Cl_2, 293 K]: *δ* (ppm) 139.16, 138.98, 138.86, 138.37, 138.33, 137.85, 137.62, 137.35, 136.87, 136.60, 130.37, 129.82 (CH), 129.33, 129.15 (CH), 129.09, 128.92, 127.30 (CH), 127.16 (CH), 126.93 (CH), 126.10 (CH), 125.94 (CH), 125.93 (CH), 124.25 (CH), 123.78 (CH).

HRMS [APPI, Toluene]: Chemical Formula: $C_{26}H_{11}Br$ calc. 402.0039, found 402.0041.

5,8-Dibromo-13,16-difluorobenzo[s]picene (44)

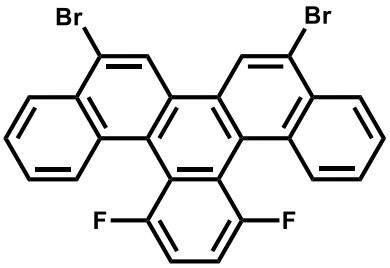

$C_{26}H_{12}Br_2F_2$
M = 522.19

30 (1.0 mmol) was dissolved in 50 mL of chloroform. Bromine (2.2 mmol) in 20 mL of chloroform was added dropwise to the mixture under stirring at room temperature. The reaction was monitored by TLC. After 2 hours the reaction was stopped, and organic phase was washed with aq. $NaHSO_3$ solution, then was dried over Na_2SO_4 and filtrated through silica plug. Solvent was removed under reduced pressure. Purification of product was carried out by HPLC chromatography (5PYE column, Tol:MeOH mixture as eluent).[98]

Light-yellow solid, **60 %** yield

^{1}H NMR [400MHz, $CDCl_3$, 293K]: *δ* (ppm) 8.73 (2H, s), 8.38 (2H, d, *J*=7.93Hz), 8.22-8.12 (2H, m), 7.72-7.61 (4H, m), 7.41-7.36 (2H, m)**.**

^{19}F NMR [282 MHz, $CDCl_3$, 293 K]: *δ* (ppm) -99.75 - -99.93 (m), -11.80 - - 112.96 (m).

HRMS [APPI]: Chemical Formula: $C_{26}H_{12}Br_2F_2$ calc. 519.9268, found 519.9273.

9,12-Dibromo-as-indaceno[3,2,1,8,7,6-pqrstuv]picene (47)

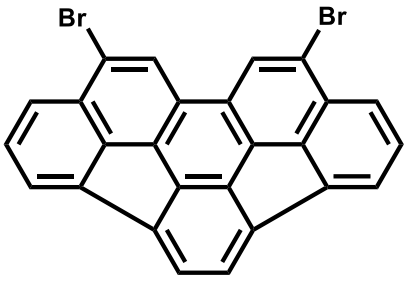

$C_{26}H_{10}Br_2$
M = 482.17

47 was obtained from 5,8-dibromo-13,16-difluorobenzo[*s*]picene **44** according to general procedure for Aryl-Aryl coupling via C-F bond activation.[98]

Orange solid, **92 %** yield (defined by HPLC).

^{1}H NMR [400 MHz, $C_2D_2Cl_4$, 353 K]: δ (ppm) 8.29 (2H, s), 7.78 (2H, d, *J*=8.32 Hz), 7.72 (2H, d, 6.96 Hz), 7.83 (2H, dd, *J*=0.96, 8.80 Hz), 7.65 (2H, s), 7.46 (2H, dd, *J*=7.04, 8.32 Hz).

HRMS [APPI]: Chemical Formula: $C_{26}H_{10}Br_2$ calc. **479**.9144, found 479.9149.

6.3.2 Synthesis of Halogenated Dibenzo- and Diindenochrysenes

1,9-Dibromo-4,12-difluorodibenzo[c,l]chrysene (50a)

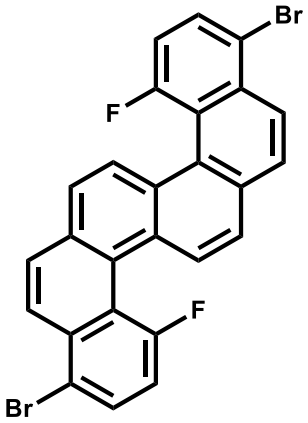

$C_{26}H_{12}Br_2F_2$
M = 522.19

50a was obtained according to general procedures: Wittig reaction, photocylization.[98] Light-yellow solid, **50 %** yield.

^{1}H NMR [400 MHz, $C_2D_2Cl_4$, 353 K]: δ (ppm) 8.40-8.31 (4H, m), 7.96-7.89 (4H, m), 7.83 (2H, d, *J*=9.47 Hz), 7.27 (2H, dd, *J*=11.96, 8.36 Hz).

HRMS [APPI]: Chemical Formula: $C_{26}H_{12}Br_2F_2$ calc. 519.9277, found 519.9268.

1,9-Dichloro-4,12-difluorodibenzo[c,l]chrysene (50b)

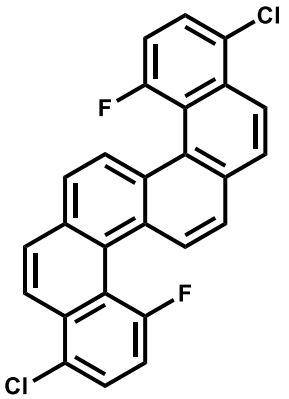

$C_{26}H_{12}Cl_2F_2$
M = 433.28

50b was obtained according to general procedures: Wittig reaction, photocylization.[98] Light-yellow solid, **42 %** yield.

^{1}H NMR [400 MHz, $C_2D_2Cl_4$, 353 K]: *δ* (ppm) 8.41-8.33 (4H, m), 7.96 (2H, d, *J*=8.92 Hz), 7.83 (2H, d, *J*=9.20 Hz), 7.72 (1H, d, *J*=8.36 Hz), 7.71 (1H, d, *J*=8.36 Hz), 6.77 (2H, dd, *J*=11.87, 8.34).

HRMS [APPI]: Chemical Formula: $C_{26}H_{12}Cl_2F_2$ calc. 436.0592, found 436.0599.

1,4,9,12-Tetrafluorodibenzo[c,l]chrysene (50c)

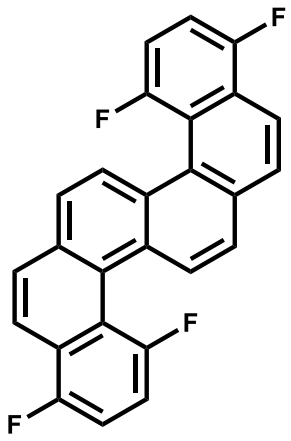

$C_{26}H_{12}F_4$
M = 400.38

50c was obtained according to general procedures: Wittig reaction, photocylization.[98] Light-yellow solid, **47 %** yield.

^{1}H NMR [400 MHz, $C_2D_2Cl_4$, 353 K]: *δ* (ppm) 8.35 (2H, dd, *J*=8.72, 14.05 Hz), 8.14 (2H, dd, *J*=1.64, 8.68 Hz), 7.90 (2H, d, *J*=8.84 Hz), 7.82 (2H, d, *J*=8.88 Hz), 7.31 (4H, m).

^{19}F NMR [282 MHz, $CDCl_3$, 293 K]: *δ* (ppm) -105.41 - -105.70 (m), -125.76 - -125.97 (m).

MS [LDI]: Chemical Formula: $C_{26}H_{12}F_4$ calc. 400.09, found 399.99.

3,9-Dibromodiindeno[4,3,2,1-cdef:4',3',2',1'-lmno]chrysene (51a)

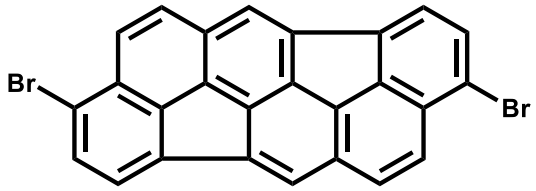

$C_{26}H_{10}Br_2$
M = 482.17

51a was obtained from 1,9-dibromo-4,12-difluorodibenzo[*c,l*]chrysene **50a** according to general procedure for Aryl-Aryl coupling *via* C-F bond activation.[98]
Yellow solid, **95 %** yield.
^{1}H NMR [400 MHz, $C_2D_2Cl_4$, 353 K]: *δ* (ppm) 7.85 (2H, s), 7.53 (2H, d, *J*=7.44 Hz), 7.57 (2H, d, *J*=7.44 Hz), 7.72 (2H, d, *J*=8.88 Hz), 7.79 (2H, d, J=8.92 Hz).
HRMS [APPI]: Chemical Formula: $C_{26}H_{10}Br_2$ calc. 479.9144, found 479.9146.

3,9-Dichlorodiindeno[4,3,2,1-cdef:4',3',2',1'-lmno]chrysene (51b)

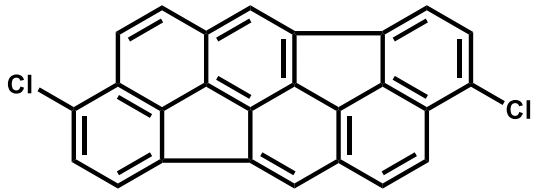

$C_{26}H_{10}Cl_2$
M = 393.27

51b was obtained from 1,9-dichloro-4,12-difluorodibenzo[*c,l*]chrysene **50b** according to general procedure for Aryl-Aryl coupling *via* C-F bond activation.[98]
Yellow solid, **98 %** yield (defined by HPLC).
^{1}H NMR [400 MHz, $C_2D_2Cl_4$, 353 K]: *δ* (ppm) 7.86(2H, s), 7.81 (4H, s), 7.61 (2H, d, *J*=7.52 Hz), 7.37 (2H, d, *J*=7.52 Hz).
HRMS [APPI]: Chemical Formula: $C_{26}H_{10}Cl_2$ calc. 392.0154, found 392.0155.

3,9-Difluorodiindeno[4,3,2,1-cdef:4',3',2',1'-lmno]chrysene (51c)

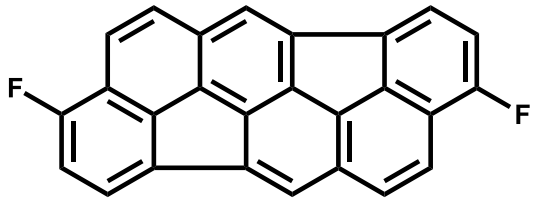

$C_{26}H_{10}F_2$
M = 360.36

51c was obtained from 1,4,9,12-tetrafluorodibenzo[*c,l*]chrysene **50c** according to general procedure for Aryl-Aryl coupling *via* C-F bond activation.[98]
Yellow solid, **63 %** yield (defined by HPLC).
^{1}H NMR [400 MHz, CD_2Cl_2, 293 K]: *δ* (ppm) 7.90 (2H, s), 7.83 (2H, d, *J*=8.91Hz), 7.76 (2H, d, *J*=8.91 Hz), 7.71 (2H, dd, *J*=3.44, 7.68 Hz), 7.01 (2H, dd, *J*=11.33, 7.69 Hz).

^{19}F NMR [282 MHz, CD_2Cl_2, 293 K]: *δ* (ppm) -121.05 - -121.09 (d, J=3.41 Hz), -121.10 - -121.15 (d, J=3.41 Hz).

MS [LDI]: Chemical Formula: $C_{26}H_{10}F_2$ calc. 360.07, found 359.97.

3,9-Diphenyldiindeno[4,3,2,1-cdef:4',3',2',1'-lmno]chrysene (52)

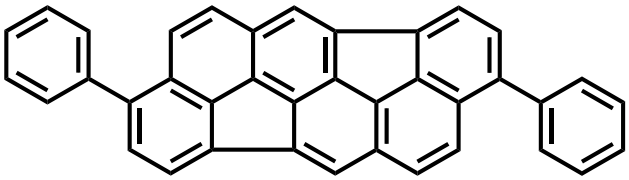

$C_{38}H_{20}$
M = 476.58

51a (1.0 mmol) and phenylboronic acid (2.4 mmol) were dissolved in Tol:MeOH (2:1) mixture, then potassium carbonate (2.4 mmol) and 5 % mol of $Pd(PPh_3)_4$ were added. Reaction mixture was stirred under reflux in nitrogen atmosphere for 15 h. Mixture was washed with water; organic layer was dried over Na_2SO_4 and filtrated through silica plug. Solvent was removed under reduced pressure. Flash chromatography purification of product was made with Hexane:DCM:2.5:1 as eluent.[98]

Yellow solid, **95 %** yield.

^{1}H NMR [400 MHz, CD_2Cl_2, 293 K]: *δ* (ppm) 7.98 (2H, s), 7.85 (2H, d, *J*=7.20 Hz), 7.81 (2H, d, *J*=9.00 Hz), 7.78 (2H, d, *J*=9.00 Hz), 7.69-7.65 (4H, m), 7.56-7.50 (4H, m), 7.49-7.43 (4H, m, *J*=7.20 Hz).

6.4 Synthesis of Buckycatcher and Its Precursors

2-(as-Indaceno[3,2,1,8,7,6-pqrstuv]picen-1-yl)-4,4,5,5-tetramethyl-1,3,2-dioxaborolane (54)

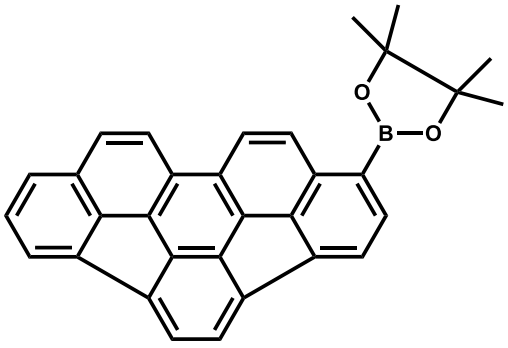

$C_{32}H_{23}BO_2$
M = 450.34

Synthesis of **54** was carried out according to modified procedure [160]. A 5 mL glass vial equipped with a magnetic stir bar was charged with 1-bromo-*as*-indaceno[*3,2,1,8,7,6-pqrstuv*]picene **39b** (90.0 mg, 0.223 mmol, 1.0 eq.), bis(pinacolato)diboron (85.0 mg, 0.335 mmol, 1.5 eq.), CH_3COOK (65.7 mg, 0.669 mmol, 3.0 eq.) and 4 % mol $Pd(dppf)Cl_2$. After addition of 1,4-dioxane:toluene mixture (anh., 1:6, 7 mL), the reaction mixture was degassed by bubbling nitrogen gas. The glass vial was closed with the cap and placed into microwave oven for 3 h (115 °C). After reaction the mixture was quenched with ethyl acetate, then the solvents were removed under reduced pressure. Obtained product was purified by aFLC (Hexane:DCM:2:1 as eluent). Solvents were removed under reduced pressure. Yellow solid was dried in vacuo (75.6 mg, 0.168 mmol).

Yellow solid, **75.3 %** yield.

^{1}H NMR [300 MHz, CD_2Cl_2, 293 K]: *δ* (ppm) 8.50 (d, *J*=8.85 Hz, 1H), 8.18 (dd, *J*=2.61, 8.82 Hz, 2H), 7.97 (d, *J*=6.93 Hz, 1H), 7.85 (d, *J*=8.79 Hz, 1H), 7.80-7.68 (m, 5H), 7.44 (dd, *J*=6.99, 8.19 Hz, 1H), 1.43 (s,12H).

2,2'-(5-Methyl-1,3-phenylene)bis(4,4,5,5-tetramethyl-1,3,2-dioxaborolane) (58)

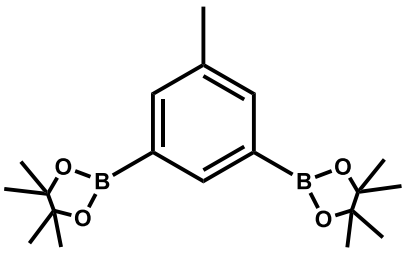

$C_{19}H_{30}B_2O_4$
M = 344.07

A 50 mL two-necked RBF equipped with a magnetic stir bar was charged with 1,3-dibromo-5-methylbenzene (0.3 g, 1.20 mmol), bis(pinacolato)diboron (1.83 mg, 7.2 mmol), potassium acetate (0.71 mg, 7.2 mmol) and 5 % mol of $Pd(dppf)Cl_2$ and dissolved in 1.4-dioxane (anh., 20 mL). The mixture was degassed, and the atmosphere was exchanged by argon. The reaction was brought to reflux for 72 h. The reaction mixture was quenched with water, the aqueous layer was extracted with dichloromethane. Organic layer was dried over Na_2SO_4. Dichloromethane was removed under reduced pressure. Obtained product was purified by aFLC (Hexane:DCM:2:1 as eluent). The solvents were removed under reduced pressure and the product was dried in vacuo (200 mg, 0.58 mmol).

White solid, **48.4 %** yield.

^{1}H NMR [300 MHz, CD_2Cl_2, 293 K]: *δ* (ppm) 7.98-7.90 (m, 1H), 7.71-7.63 (m, 2H), 2.35 (q, *J*=1.31 Hz, 3H), 1.33 (s, 24H).

^{13}C NMR [75 MHz, CD_2Cl_2, 293 K]: *δ* (ppm) 138.97 (C), 138.63 (CH, 2C), 137.05 (CH), 84.34 (O-C-), 25.31 (C-$\underline{C}H_3$), 21.49 (Ar-$\underline{C}H_3$).

1,1'-Bias-indaceno[3,2,1,8,7,6-pqrstuv]picene (55)

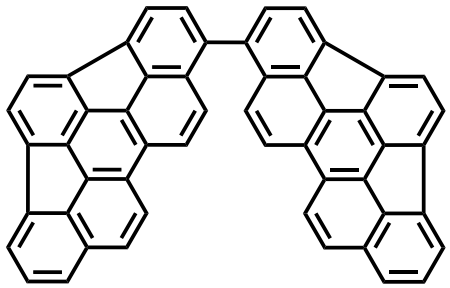

$C_{52}H_{22}$
M = 646.75

55 was obtained as a side product of Miyaura borylation (of **39b**).

^{1}H NMR [400 MHz, $C_2D_2Cl_4$, 293 K]: *δ* (ppm) 8.07 (d, *J*=8.77 Hz, 2H), 8.01 (d, *J*=8.89 Hz, 2H), 7.84 (d, *J*=7.21 Hz, 2H), 7.77 (d, *J*=8.77 Hz, 2H), 7.75-7.68 (m, 8H), 7.63 (d, *J*=8.17 Hz, 2H), 7.53 (d, *J*=7.13 Hz, 2H), 7.39 (t, *J*=7.61 Hz, 2H).

^{13}C NMR [151 MHz, $C_2D_2Cl_4$, 293 K]: *δ* (ppm) 138.99, 138.87, 138.73, 138.49, 138.45, 138.33, 138.27, 138.14, 137.65, 137.13, 136.68, 130.87, 130.15, 129.96, 129.18, 129.15, 128.48, 127.22, 127.02, 126.69, 125.98, 125.88, 124.40, 124.17, 123.87, 123.85, 123.59, 120.36.

MS [LDI]: m/z (rel. int.) = 646.35 [M]+ (100).

HRMS [APPI, Toluene, DCM]: Chemical Formula: $C_{52}H_{22}$ calc. 646.1716, found 646.1709.

9,9'-(5-Methyl-1,3-phenylene)di-as-indaceno[3,2,1,8,7,6-pqrstuv]picene

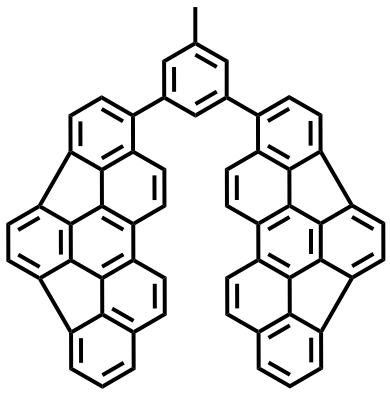

$C_{59}H_{28}$
M = 736.87

A 50 mL RBF equipped with a magnetic stirring bar and a condenser was charged with **39b** (13.5 mg, 0.033 mmol, 2.2 eq.), 2,2'-(5-methyl-1,3-phenylene)bis(4,4,5,5-tetramethyl-1,3,2-dioxaborolane) (5.24 mg, 0.015 mmol, 1.0 eq.), K_2CO_3 (4.21 mg, 0.030 mmol, 2.0 eq) and 5 % mol $Pd(PPh_3)_4$. The solids were suspended in Tol:MeOH:2:1 (30 mL), the reaction mixture was degassed, and the atmosphere was exchanged by N_2. The mixture was brought to reflux for 16 h. The mixture was diluted with toluene (10 mL) and washed with water (2x10 mL). The aqueous layer was extracted with toluene (2x10 mL) and the combined organic layers were dried over $MgSO_4$. The solvent was removed under reduced pressure. Yellow solid was washed with toluene and then product was dried in vacuo (6.0 mg, 8.1 *µ*mol).

Yellow solid, **53 %** yield.

^{1}H NMR [400 MHz, $C_2D_2Cl_4$, 293 K]: *δ* (ppm) 8.09 (dd, *J*=5.81, 8.85 Hz, 4H), 8.00 (d, *J*=8.93 Hz, 2H), 7.80-7.75 (m, 4H), 7.72-7.67 (m, 7H), 7.62 (d, *J*=8.13 Hz, 2H), 7.54-7.51 (m, 2H), 7.49 (d, *J*=7.25 Hz, 2H), 7.37 (dd, *J*=7.11, 8.07 Hz, 2H), 2.54 (s,3H).

^{13}C NMR [151 MHz, $C_2D_2Cl_4$, 293 K]: *δ* (ppm) 140.65, 139.35, 138.89, 138.79, 138.76, 138.41, 138.38, 138.29, 138.28, 138.26, 138.03, 137.30, 136.63, 130.01, 129.92, 129.34, 129.15, 129.11, 128.36, 127.39, 127.17 (CH), 126.96 (CH), 126.44 (CH), 125.92 (CH), 125.70 (CH), 124.49, 124.16, 124.07, 123.81 (CH), 120.36, 21.86 (CH_3).

MS [LDI] m/z (rel. int.) = 736.65 [M]+ (100).

HRMS [APPI, Toluene, DCM] Chemical Formula: $C_{59}H_{28}$ calc. 736.2186, found 736.2195.

6.5 Synthesis of Pyrene and Chrysene Derivatives

1,6-Bis(2-fluorophenyl)pyrene 59

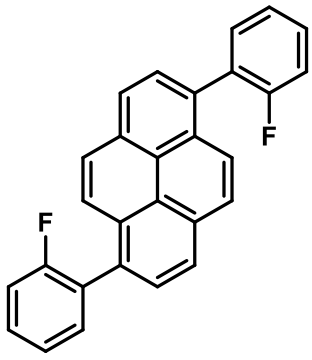

$C_{30}H_{16}F_6$
M = 490.45

A 500 mL RBF equipped with a magnetic stir bar and a condenser was charged with 1.6-dibromopyrene **24** (1.0 g, 2.78 mmol, 1 eq), 2-fluorophenylboronic acid **58** (0.89 g, 6.39 mmol, 2.3 eq), K_2CO_3 (0.88 g, 6.39 mmol, 2.3 eq) and 5% mol $Pd(PPh_3)_4$. The solids were suspended in 2:1 toluene:MeOH (225 mL), the reaction mixture was degassed and the atmosphere was exchanged by nitrogen. The mixture was brought to reflux for 16 h. The mixture was diluted with toluene (30 mL) and washed with water (2x50 mL). The aqueous layer was extracted with toluene (2x50 mL) and the combined organic layers were dried over $MgSO_4$. The solvent was evaporated, and product was dried in vacuo (0.68 g, 1.74 mmol).

White solid, **63 %** yield.

^{1}H NMR [300 MHz, CD_2Cl_2, 293 K]: *δ* (ppm) 8.27 (d, J=7.83 Hz, 2H), 8.11 (d, J=9.27 Hz, 2H), 8.01 (dd, J=0.65, 7.85 Hz, 2H), 7.97 (dd, J=2.46, 9.21 Hz, 2H), 7.61-7.49 (m, 4H), 7.42-7.28 (m, 4H).

^{1}H NMR [400 MHz, $CDCl_3$, 293 K]: *δ* (ppm) 8.22 (d, *J*=7.80 Hz, 2H), 8.06 (d, *J*=9.20 Hz, 2H), 8.00-7.93 (m, 4H), 7.57-7.45 (m, 4H), 7.34 (dt, *J*=1.20, 7.48 Hz, 2H), 7.25-7.31 (m, 2H).

^{1}H NMR [400 MHz, DMSO, 293 K]: *δ* (ppm) 8.40 (d, *J*=7.89 Hz, 2H), 8.25 (d, *J*=9.29 Hz, 2H), 8.06 (d, *J*=7.81 Hz, 2H), 7.87 (dd, *J*=2.42, 9.19 Hz, 2H), 7.66-7.58 (m, 4H), 7.52-7.43 (m, 4H).

^{13}C NMR [101 MHz, DMSO, 293 K]: *δ* (ppm) 159.47 (d, *J*=244.56 Hz, C-F), 132.72 (CH), 131.06 (C), 130.34 (C), 130.31 (d, *J*=6.57 Hz, CH), 128.59 (C), 128.41 (CH), 127.96 (CH), 127.50 (d, *J*=16.05 Hz, C), 125.08 (CH), 124.92 (CH), 124.88 (d, *J*=3.48 Hz, CH), 123.88 (C), 115.86 (d, *J*=22.12 Hz, CH).

^{19}F NMR [377 MHz, DMSO, 293 K]: *δ* (ppm) -114.4-(-114.6).

HRMS [APPI, toluene]: Chemical Formula: $C_{28}H_{16}F_2$ calc. 390.1215, found 390.1220.

MS [MALDI-TOF, without matrix]: m/z (rel. int.) = 390.2013 [M]+ (100)

MS [MALDI-TOF, DHB]: m/z (rel. int.) = 390.1717 [M]+ (100)

MS [MALDI-TOF, DCTB]: m/z (rel. int.) = 390.2115 [M]+ (100).

Diindeno[1,2,3-cd:1',2',3'-jk]pyrene (60)

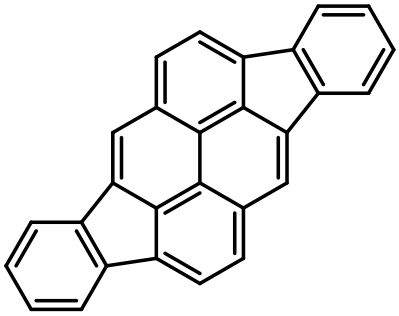

$C_{28}H_{14}$
M = 350.42

1 g of activated aluminium oxide was added to the microwave glass vial containing 100 mg of 1,6-bis(2-fluorophenyl)pyrene **59** dissolved in 3 mL of anhydrous *o*-DCB. The condensation was carried at 240 °C for 1.5 h. After cooling to the room temperature, product precipitated from *o*-dichlorobenzene solution. Collected crystals were analyzed by X-ray crystallography.

^{1}H and **^{13}C NMR** spectra are in accordance with [59].

1,3,6,8-Tetrakis(2-fluorophenyl)pyrene (62)

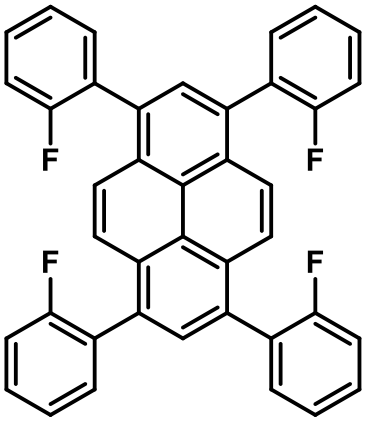

$C_{40}H_{22}F_4$
M = 578.61

A 250 mL RBF equipped with a magnetic stir bar and a condenser was charged with 1,3,6,8-tetrabromopyrene **61** (1.5 g, 2.9 mmol, 1 eq.), 2-fluorophenylboronic acid **58** (2.23 g, 15.93 mmol, 5.5 eq.), K_2CO_3 (1.0 g, 7.24 mmol, 2.5 eq.) and 5% mol $Pd(PPh_3)_4$. The solids were suspended in 2:1:Tol:MeOH (105 mL), the reaction mixture was degassed and the atmosphere was exchanged by nitrogen. The mixture was brought to reflux for 16 h. The mixture was diluted with toluene (30 mL) and

washed with H_2O (2x50 mL). The aqueous layer was extracted with toluene (2x50 mL) and the combined organic layers were dried over $MgSO_4$. The solvent was evaporated, and the product was purified by flash column chromatography in DCM:Hexane:1:1. Solvents were removed under reduced vacuum, and the product was dried in vacuo (1.3 g, 2.25 mmol).

White solid, **75 %** yield.

^{1}H NMR [400 MHz, $CDCl_3$, 293 K]: *δ* (ppm) 8.01-7.96 (m, 6H), 7.62-7.51 (m, 4H), 7.48-7.41 (m, 4H), 7.33-7.21 (m, 8H).

^{13}C NMR [100 MHz, $CDCl_3$, 293 K]: *δ* (ppm) 161.50-161.25 (m),159.06-158.81 (m), 133.14-132.65, 131.11, 131.07, 130.26, 129.68, 129.60, 129.10, 128.16, 128.00, 125.65, 125.17, 124.34-123.98 (m), 116.14-115.49 (m).

^{19}F NMR [282 MHz, $CDCl_3$, 293 K]: *δ* (ppm) -112.7 - (-113.86).

3,9-Bis(2-fluorophenyl)diindeno[4,3,2,1-cdef:4',3',2',1'-lmno]chrysene (65a)

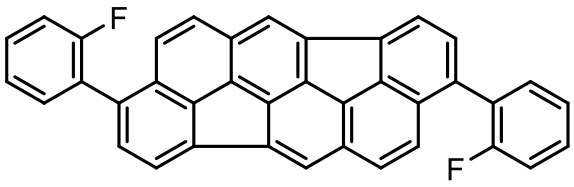

$C_{40}H_{22}F_2$
M = 540.61

A 100 mL RBF equipped with a magnetic stir bar and a condenser was charged with 3,9-dibromodiindenochrysene **51a** (106 mg, 0.220 mmol), 2-fluorophenylboronic acid **58** (74 mg, 0.528 mmol), K_2CO_3 (73 mg, 0.528 mmol) and 5 % mol $Pd(PPh_3)_4$. The solids were suspended in 2:1:toluene:MeOH (45 mL), the reaction mixture was degassed and the atmosphere was exchanged by nitrogen. The mixture was brought to reflux for 16 h. The mixture was diluted with toluene (30 mL) and washed with H_2O (2x30 mL). The aqueous layer was extracted with toluene (2x30 mL) and the combined organic layers were dried over $MgSO_4$. The solvent was removed under reduced pressure and the product was purified by aFLC in hexane:DCM (1:1). Solvents were removed, and product was dried in vacuo (107 mg, 0.209 mmol).

Orange solid, **95 %** yield.

^{1}H NMR [400 MHz, $CDCl_3$, 293 K]: *δ* (ppm) 7.84 (2H, s); 7.75 (2H, d, *J*=7.20 Hz); 7.69 (2H, d, *J*=8.96 Hz); 7.52-7.45 (4H, m); 7.44-7.37 (4H, m); 7.29-7.19 (4H, m).

^{13}C NMR [101 MHz, $CDCl_3$, 293 K]: *δ* (ppm) 161.10; 158.64; 142.35; 139.09; 138.73; 132.22 (d, *J*=3.38 Hz); 130.15 (d, *J*=1.45 Hz); 129.62 (d, *J*=8.04 Hz); 126.66 (d, *J*=15.38 Hz); 125.25 (d, *J*=2.51 Hz); 124.20 (d, *J*=3.67 Hz); 115.99 (d, J=22.41 Hz).
MS [LDI]: m/z (rel. int.) = 512.14 [M]+ (100).
HRMS [APPI, toluene]: Chemical Formula: $C_{38}H_{18}F_2$ calc. 512.1371, found 512.1373.

3,9-Bis(2-fluoro-5-methylphenyl)diindeno[4,3,2,1-cdef:4',3',2',1'-lmno]chrysene (65b)

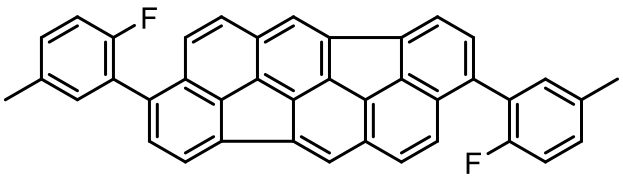

$C_{40}H_{22}F_2$
M = 540.61

A 100 mL round bottom flask equipped with a magnetic stir bar and a condenser was charged with 3,9-dibromodiindenochrysene **51a** (106 mg, 0.220 mmol, 1 eq), 2-fluoro-5-methylphenylboronic acid **64** (81 mg, 0.528 mmol, 2.4 eq), K_2CO_3 (81 mg, 0.528 mmol, 2.4 eq) and 5% mol $Pd(PPh_3)_4$. The solids were suspended in 2:1:toluene:MeOH (45 mL), the reaction mixture was degassed and the atmosphere was exchanged by nitrogen. The mixture was brought to reflux for 16 h. The mixture was diluted with toluene (30 mL) and washed with H_2O (2x 30 mL). The aqueous layer was extracted with toluene (2x 30 mL) and the combined organic layers were dried over $MgSO_4$. The solvent was removed under reduced pressure and the product was purified by aFLC in hexane:DCM (1:1). Solvents were removed, and product was dried in vacuo, yielding the product in 109.3 mg (0.202 mmol).
Orange solid, **92 %** yield.
^{1}H NMR [400 MHz, CD_2Cl_2, 293 K]: *δ* (ppm) 7.87 (2H, s); 7.78 (2H, d, *J*=7.20 Hz); 7.71 (2H, d, *J*=8.96 Hz); 7.51 (2H, dd, *J*=2.46, 8.94 Hz); 7.41 (2H, dd, *J*=0.92, 7.24 Hz); 7.32-7.27 (2H, m); 7.27-7.22 (2H, m); 7.14 (2H, dd, *J*=8.38, 9.90 Hz); 2.41-2.39 (6H, m).
^{13}C NMR [101 MHz, CD_2Cl_2, 293 K]: *δ* (ppm) 159.66; 157.72; 142.86; 139.37 (d, *J*=31.49 Hz); 137.38 (d, *J*=65.27 Hz); 134.70-134.45 (m); 133.27-133.04 (m); 130.79 (d, *J*=9.56 Hz); 128.46 (d, *J*=9.16 Hz); 126.67 (d, *J*=15.49 Hz); 125.89; 125.12; 122.79; 116.11 (d, *J*=22.61 Hz); 20.94.

MS [LDI] m/z (rel. int.) = 540.17 [M]+ (100).

HRMS [APPI, toluene, ACN]: Chemical Formula: $C_{40}H_{22}F_2$ calc. 540.1684, found 540.1691.

Benzo[6,7]-as-indaceno[8,1,2,3-bcdef]benzo[6,7]-as-indaceno[8,1,2,3-klmno]-chrysene (66a)

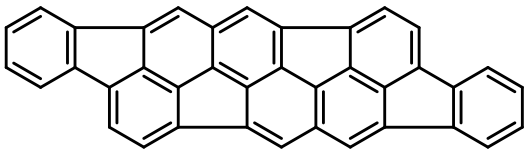

$C_{38}H_{16}$
M = 472.55

6 g of γ-Al_2O_3 were preactivated in glass ampule at 250 °C under air conditions for 30 minutes and then activated at 550 °C for 2 hours in vacuum (10^{-3} mbar). Activated aluminium oxide was added to the microwave glass vial containing 100 mg of **65a** dissolved in 12 mL of anhydrous *o*-DCB. The glass vial was closed with the cap and placed into microwave oven. All preparation steps were performed under argon atmosphere. The condensation was carried out 230 °C for 16 h. After cooling to the room temperature, products were extracted with toluene and separated on semi-preparative HPLC (PBB column, Tol:MeOH:7:3 as eluent, 5.0 ml min^{-1})

^{1}H NMR [300 MHz, CD_2Cl_2, 293 K] : *δ* (ppm) 7.68-7.63 (2H, m); 7.61-7.57 (2H, m); 7.56 (2H, s); 7.41 (2H, s); 7.39 (4H, s); 7.24-7.18 (4H, m).

MS [LDI]: m/z (rel. int.) = 472.12 [M]+ (100).

HRMS [APPI, toluene, DCM]: Chemical Formula: $C_{38}H_{16}$ calc. 472.1247, found 472.1240.

3,11-Dimethylbenzo[6,7]-as-indaceno[8,1,2,3-bcdef]benzo[6,7]-as-indaceno [8,1,2,3-klmno]chrysene (66b)

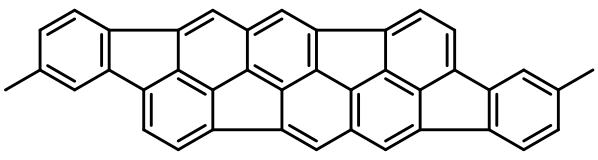

$C_{40}H_{20}$
M = 500.60

6 g of γ-Al_2O_3 were preactivated in glass ampule at 250 °C under air conditions for 30 minutes and then activated at 550 °C for 2 hours in vacuum (10^{-3} mbar). Activated

aluminium oxide was added to the microwave glass vial containing 100 mg of **65b** dissolved in 12 mL of anhydrous *o*-DCB. The glass vial was closed with the cap and placed into microwave oven. All preparation steps were performed under argon atmosphere. The condensation was carried out 230 °C for 16 h. After cooling to the room temperature, products were extracted with toluene and separated on semi-preparative HPLC (PBB column, Tol:MeOH:6:4 as eluent, 5.0 ml min^{-1}).

Red solid, **35 %** yield.

^{1}H NMR [400 MHz, CD_2Cl_2, 293 K]: *δ* (ppm) 7.52 (2H, d, *J*=7.72 Hz); 7.47 (2H, s); 7.42-7.39 (2H, m); 7.38-7.32 (6H, m); 7.04-7.00 (2H, m); 2.36 (6H, s).

^{13}C NMR [101 MHz, CD_2Cl_2, 293 K]: *δ* (ppm) 142.96; 141.92;140.27;139.59;139.24; 138.45; 138.00; 137.53; 137.49; 137.41; 136.88; 136.06; 128.15; 126.29; 123.52; 122.83; 121.96; 121.75; 121.43; 29.25.

MS [LDI]: m/z (rel. int.) = 500.16 [M]+ (100).

HRMS [APPI, toluene]: Chemical Formula: $C_{40}H_{20}$ calc. 500.1560, found 500.1561.

6.6 Synthesis of Halogenated Decacyclene and Tridecacyclene

6.6.1 Synthesis of Fluorinated Decacyclene **70** and Tridecacyclene **72**

7-Fluoro-1-methylene-1,2,3,4-tetrahydronaphthalene (75)

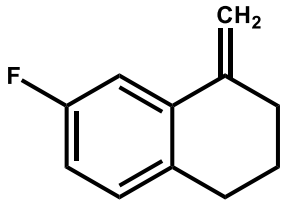

$C_{11}H_{11}F$
M = 162.21

RBF was charged with 0.8 g (4.87 mmol) of 7-fluoro-1-tetralone **74**, 1.9 g (5.4 mmol) of methyltriphenylphosphonium bromide, 0.6 g (5.4 mmol) of *t*-BuOK and 100 mL of distilled Et_2O and was stirred for 48h at rt under nitrogen atmosphere. The reaction mixture was neutralized with HCl, then DCM and H_2O were added, and after extraction the layers were separated. The aqueous phase was extracted with DCM (3x50 mL) and was combined with organic layer, then combined layers were dried over anhydrous Na_2SO_4. DCM was removed under reduced pressure and residue was

purified by column chromatography (SiO_2, hexane) yielding to 0.77 g (4.7 mmol) of product.

Colourless liquid, **97 %** yield.

^{1}H NMR [400 MHz, $CDCl_3$, 293 K]: *δ* (ppm) 7.30 (dd, *J*=2.68, 10.68 Hz, 1H), 7.07-7.00 (m, 1H), 6.86 (td, *J*=2.68, 8.34, 8.34 Hz, 1H), 5.45-5.42 (m, 1H), 5.00-4.98 (m, 1H), 2.78 (t, *J*=6.26 Hz, 2H), 2.55-2.48 (m, 2H), 1.89-1.81 (m, 2H).

^{13}C NMR [101 MHz, $CDCl_3$, 293 K]: *δ* (ppm) 161.26 (d, *J*=242.30 Hz, C-F), 142.64 (d, *J*=2.30 Hz), 136.36 (d, *J*=7.17 Hz), 132.88 (d, *J*=2.89 Hz), 130.52 (d, *J*=7.86 Hz, CH), 114.63 (d, *J*=21.72 Hz, CH), 110.24 (d, *J*=21.50 Hz, CH), 108.98 (d, *J*=0.84 Hz, CH_2), 32.72 (CH_2), 29.73 (CH_2), 23.67 (CH_2).

6-Fluoro-4-methyl-1,2-dihydronaphthalene (76)

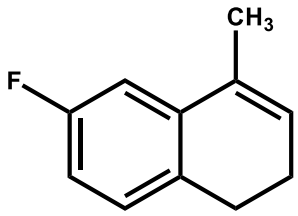

$C_{11}H_{11}F$
M = 162.21

0.57 g (3.5 mmol) of 7-fluoro-1-methylene-1,2,3,4-tetra-hydronaphthalene **75** and catalytic amount of TsOH were dissolved in DCM and stirred for 16 h at rt. The reaction mixture was washed with solution of $NaHCO_3$ in water. Aqueous phase was extracted with DCM. The organic phase was dried over anhydrous Na_2SO_4. After filtration the product was concentrated under reduced pressure (0.56 g, 3.45 mmol). TLC: hexane.

Colourless liquid, **99 %** yield.

^{1}H NMR [400 MHz, $CDCl_3$, 293 K]: *δ* (ppm) 7.08-7.02 (m, 1H), 6.92 (dd, *J*=2.62, 10.34 Hz, 1H), 6.81 (td, *J*=2.66, 8.42, 8.42 Hz, 1H), 5.93-5.87 (m, 1H), 2.70 (t, *J*=8.08 Hz, 2H), 2.28-2.19 (m, 2H), 2.03-2.00 (m, 3H).

^{13}C NMR [101 MHz, $CDCl_3$, 293 K]: *δ* (ppm) 161.84 (d, *J*=241.83 Hz, C-F), 137.63 (d, *J*=7.41 Hz), 131.57 (d, *J*=2.80 Hz), 128.17 (d, *J*=7.87 Hz, CH), 126,62 (CH and C), 112.62 (d, *J*=20.80 Hz, CH), 109.87 (d, *J*=22.19 Hz, CH), 27.42 (CH_2), 23.26 (CH_2), 19.15 (CH_3).

7-Fluoro-1-methylnaphthalene (77)

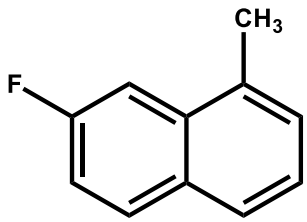

$C_{11}H_9F$
M = 160.19

0.5 g (3.1 mmol) of 6-fluoro-4-methyl-1,2-dihydro-naphthalene **76** and 0.77 g (3.4 mmol) of DDQ were dissolved in DCM. Reaction was carried out at rt and was monitored by HPLC. DCM was removed under reduced pressure and the product was purified by column chromatography (SiO_2, hexane) yielding 0.45 g (2.8 mmol). TLC: hexane (Al_2O_3).

Colourless liquid, **91 %** yield.

^{1}H NMR [400 MHz, CD_2Cl_2, 293 K]: *δ* (ppm) 7.86 (dd, *J*=5.94, 8.98 Hz, 1H), 7.73-7.69 (m, 1H), 7.61 (dd, *J*=2.44, 11.32 Hz, 1H), 7.38-7.32 (m, 2H), 7.27 (td, J=2.55, 8.67, 8.67 Hz, 1H), 2.64 (s, 3H).

^{13}C NMR [101 MHz, CD_2Cl_2, 293 K]: *δ* (ppm) 161.03 (d, *J*=244.03 Hz, C-F), 134.25 (d, *J*=6.14 Hz), 133.91 (d, *J*=8.21 Hz), 133.91 (d, *J*=8.21 Hz), 131.27 (d, *J*=9.16 Hz, CH), 130.97 (d, *J*=1.15 Hz), 127.80 (CH), 126.51 (d, *J*=1.22 Hz, CH), 125.23 (d, *J*=2.54 Hz, CH), 115.98 (d, *J*=25.24 Hz, CH), 108.02 (d, *J*=20.98 Hz, CH), 19.46 (CH_3).

1-(Bromomethyl)-7-fluoronaphthalene (78)

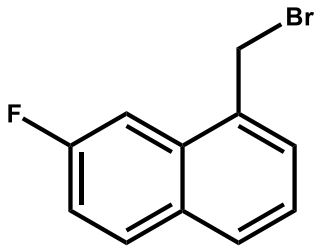

$C_{11}H_8BrF$
M = 239.09

0.45 g (2.8 mmol) of 7-fluoro-1-methylnaphthalene **77** was dissolved in CCl_4, then 3.1 g (0.55 mmol) NBS and catalytic amount of DBPO were added. Reaction was carried out under reflux and monitored by TLC (eluent: hexane). CCl_4 was removed

under reduced pressure, the product mixture contained mono- and dibrominated product was used for the next step without further purification.

2-(7-Fluoronaphthalen-1-yl)acetonitrile (79)

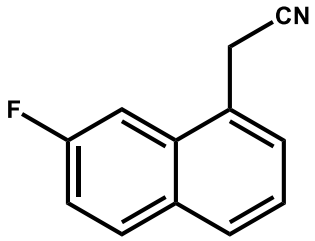

$C_{12}H_8FN$
M = 185.20

2.46 g (10.29 mmol) of 1-(bromomethyl)-7-fluoronaphthalene **78**, 0.55 g (11.2 mmol) of NaCN (dissolved in water) and catalytic amount of TBAB were dissolved in 50 mL DCM. Reaction was carried out at rt for 16 h. Reaction mixture was washed with water (2x30 mL). Organic layer was dried over anhydrous Na_2SO_4, product was concentrated under reduced pressure and purified on aFLC (Hexane:DCM:1:1). (0.56 g, 3.02 mmol).

Light-yellow solid, **29 %** yield.

^{1}H NMR [400 MHz, $CDCl_3$, 293 K]: *δ* (ppm) 7.89 (dd, J=5.82, 9.02 Hz, 1H), 7.84 (d, *J*=8.28 Hz, 1H), 7.64-7.60 (m, 1H), 7.48-7.40 (m, 2H), 4.05 (s,1 H), 7.30 (d, *J*=2.44 Hz, 1 H), 7.32 (dd, *J*=0.72, 2.44 Hz, 1H)

^{13}C NMR [101 MHz, CD_2Cl_2, 293 K]: *δ* (ppm) 161.79 (d, *J*=247.06 Hz, C-F), 132.32 (d, *J*=8.74 Hz), 132.19 (d, *J*=9.30 Hz, CH), 131.34 (d, *J*=1.04 Hz), 129.44 (d, *J*=1.28 Hz, CH), 128.06 (CH), 126.36 (d, *J*=5.70 Hz), 125.40 (d, J=2.58 Hz, CH), 117.98 (CN), 117.11 (d, *J*=25.17 Hz, CH), 107.05 (d, *J*=21.90 Hz, CH), 22.29 (CH_2).

2-(7-Fluoronaphthalen-1-yl)acetic acid (80)

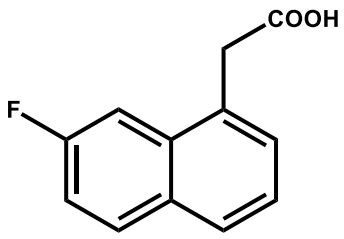

$C_{12}H_9FO_2$
M = 204.20

1.77 g (9.56 mmol) of 2-(7-fluoronaphthalen-1-yl)aceto-nitrile **79** was dissolved in 72 mL AcOH, 48 mL H_2SO_4 and 48 mL H_2O was added. Reaction was carried out 16 h under reflux. After cooling to rt, 400 mL H_2O was added, and the mixture was kept 2-3 hours at the room temperature. The precipitate was filtrated and washed with water (3x50 mL). Product was dried under vacuum for 24 h (1.07 g, 5.24 mmol).

White solid, **55 %** yield.

^{1}H NMR [400 MHz, DMSO, 293 K]: *δ* (ppm) 8.04 (dd, *J*=6.10, 9.02 Hz, 1H), 7.89 (d, *J*=7.80 Hz, 1H), 7.69 (dd, *J*=2.52, 11.53 Hz, 1H), 7.50-7.41 (m, 3H), 4.02 (s,2H).

^{13}C NMR [101 MHz, DMSO, 293 K]: *δ* (ppm) 172.67 (s, COOH), 160.21 (d, *J*=243.33 Hz, C-F), 160.21 (d, *J*=243.33 Hz), 132.86 (d, *J*=8.90 Hz), 131.50 (CH), 131.43 (d, *J*=3.16 Hz, 1 C), 130.57 (d, *J*=0.93 Hz), 129.02 (CH), 127.44 (d, *J*=1.15 Hz, CH), 125.02 (d, *J*=2.43 Hz, CH), 115.87 (d, *J*=25.19 Hz, CH), 107.84 (d, *J*=21.31 Hz, CH), 38.46 (CH_2).

8-Fluoroacenaphthylen-1(2H)-one (81)

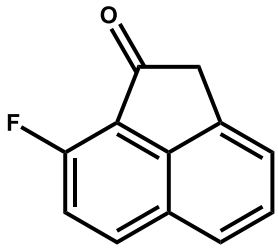

$C_{12}H_7FO$
M = 186.19

0.3 g (1.47 mmol) of 2-(7-fluoronaphthalen-1-yl)acetic acid **80** was dissolved in 1.75 g (14.7 mmol) $SOCl_2$ and was kept while stirring for 1 h at 65ºC. $SOCl_2$ was removed under reduced pressure and the product was diluted with DCM. Then 0.29 g (2.2 mmol) of $AlCl_3$ was added while stirring and the mixture was kept at rt for 3 hours. After reaction the mixture was poured out on ice and 10 % HCl. Product was extracted with DCM, dried over anhydrous Na_2SO_4, concentrated and filtrated. Product was purified on aFLC (DCM:Hexane:2:1) and concentrated under reduced pressure (0.24 g, 1.29 mmol).

Beige solid, **87.8 %** yield.

^{1}H NMR [400 MHz, DMSO, 293 K]: *δ* (ppm) 8.33 (dd, *J*=4.40, 8.80 Hz, 1H), 7.97-7.92 (m, 1H), 7.67-7.54 (m, 4H), 3.88 (s,2H).

^{13}C NMR [101 MHz, DMSO, 293 K]: δ (ppm) 198.18 (d, *J*=1.65 Hz, C=O), 154.43 (d, *J*=263.57 Hz, 1 C-F), 142.05 (d, *J*=4.87 Hz), 135.16 (d, *J*=8.81 Hz, CH), 134.66 (d, *J*=6.03 Hz), 127.47 (d, *J*=2.82 Hz, CH), 127.32 (d, *J*=2.23 Hz), 123.61 (d, *J*=1.40 Hz, CH), 121.84 (CH), 117.98 (d, *J*=1.15 Hz, CH), 117.75 (CH), 41.85 (CH_2).

Synthesis of the fluorinated decacyclene (70) and tridecacyclene (72) was conducted according to modified procedure [164]. Two-necked RBF was equipped with a stirring bar and condenser. 0.35 ml (3.2 mmol) of $TiCl_4$ and 3.9 mL of *o*-DCB ware added to the flask and brought to reflux under N_2 atmosphere. Then 0.1 g of 8-fluoroacenaphthylen-1(*2H*)-one **81** (0.53 mmol) was dissolved in 3.9 mL of *o*-DCB and was added dropwise into refluxing reaction mixture. Reaction was monitored by TLC (DCM:Hexane:1:1). After cooling down the mixture was dissolved in acetone; part of product precipitated. The formed precipitate was collected from filter. Dissolved product was concentrated, dissolved in hexane and filtrated on silica plug. After the concentration product was dissolved in Tol:MeOH mixture and purified on semi-preparative HFLC (Tol:MeOH:1:1 as eluent).

Further work-up of precipitate was carried out according to modified procedure [165]. Precipitate was dissolved in small amount of toluene, adsorbed onto aluminium oxide and placed in the thimble of a Soxhlet extractor. Extraction was carried out in hot dichloromethane. The dark-coloured soluble impurities were collected in the first fraction, whereas the second fraction (18 h of extraction) contained pure product **70**. Both products were analysed by NMR-spectroscopy, HPLC chromatography and mass spectrometry.

***1,7,13-Trifluorodecacyclene* (70)**

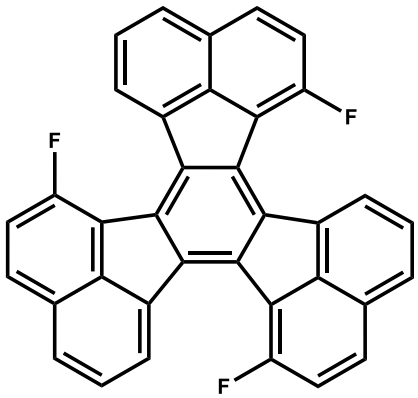

$C_{36}H_{15}F_3$
M = 504.51

Product 6 mg, 0.012 mmol.

Brown-yellow solid, **6.6 %** yield.

^{1}H NMR [400 MHz, $C_2D_2Cl_4$, 293 K]: *δ* (ppm) 8.38 (t, J=6.15 Hz, 3H), 7.97 (dd, J=3.64, 8.73 Hz, 3H), 7.92 (d, J=8.21 Hz, 3H), 7.74 (t, J=7.69 Hz, 3H), 7.48 (dd, J=8.79, 10.83 Hz, 3H).

MS [LDI]: m/z (rel. int.) = 504.35 [M]+ (100).

HRMS [APPI, Toluene, DCM]: Chemical Formula: $C_{36}H_{15}F_3$ calc. 504.1120, found 504.1128.

1,7,13,19-tetrafluorotridecacyclene (72)

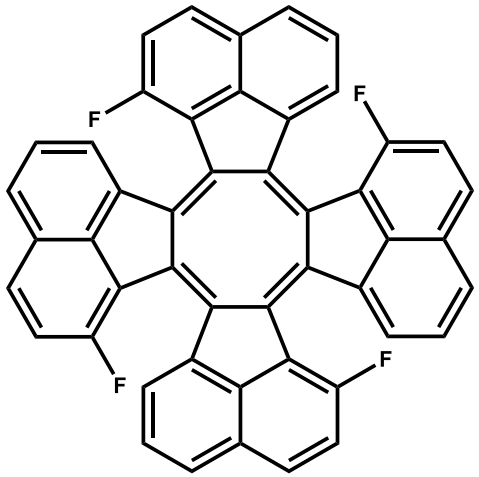

$C_{48}H_{20}F_4$
M = 672.68

Product 12 mg, 0.018 mmol.

Brown solid, **13.5 %** yield.

^{1}H NMR [400 MHz, CD_2Cl_2, 293 K]: *δ* (ppm) 8.58-8.44 (m, 8H), 8.39-8.26 (4H), 8.21-8.11 (4H), 7.92-7.80 (m, 4H).

^{13}C NMR [101 MHz, $CDCl_3$, 293 K]: *δ* (ppm) 154.95, 139.53, 131.31, 131.22, 127.16, 127.10, 125.64, 118.90, 118.64.

MS [LDI]: m/z (rel. int.) = 672.51 [M]+ (100).

HRMS [APPI, Toluene, DCM]: Chemical Formula: $C_{48}H_{20}F_4$ calc. 672.1496, found 672.1502.

6.6.2 Synthesis of Brominated Tridecacyclene **90**

7-Bromo-1-methylene-1,2,3,4-tetrahydro-naphthalene (83)

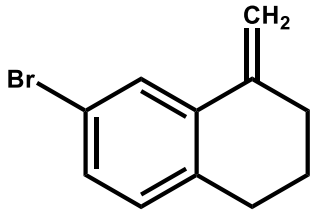

$C_{11}H_{11}Br$
M = 223.11

RBF was charged with 11.2 g (49.7 mmol) of 7-bromotetralone **82**, 19.5 g (54.6 mmol) of methyltriphenylphosphonium bromide, 6.1 g (54.6 mmol) of *t*-BuOK and 300 mL of distilled Et_2O and was stirred for 48 h at rt under nitrogen atmosphere. Reaction mixture was neutralized with HCl, then DCM and H_2O were added. The aqueous phase was extracted with DCM (3x50 mL). The organic layer was dried over anhydrous Na_2SO_4. DCM was removed under reduced pressure and the residue was purified by column chromatography (SiO_2, hexane) yielding to 9.6 g (42.9 mmol) of product. TLC: hexane.

Light-brown liquid, **86 %** yield.

^{1}H NMR [400 MHz, $CDCl_3$, 293 K]: *δ* (ppm) 7.74 (d, *J*=2.04 Hz, 1H), 7.25 (dd, *J*=2.04, 8.17 Hz, 1H), 6.95 (dt, *J*=0.96, 8.17 Hz, 1H), 5.45-4.45 (m, 1H), 5.00-4.96 (m, 1H), 2.76 (t, *J*=6.31 Hz, 2H), 2.53-2.47 (m, 2H), 1.89-1.80 (m, 2H).

^{13}C NMR [101 MHz, $CDCl_3$, 293 K]: *δ* (ppm) 142.22, 136.77, 136.09, 130.81 (CH), 130.31 (CH), 127.06 (CH), 119.63 (C-Br), 109.16 (CH_2), 32.73 (CH_2), 29.92 (CH_2), 23.42 (CH_2).

6-Bromo-4-methyl-1,2-dihydronaphthalene (84)

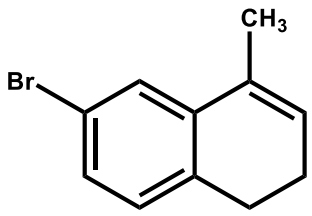

$C_{11}H_{11}Br$
M = 223.11

9.6 g (42.9 mmol) of 7-bromo-1-methylene-1,2,3,4-tetrahydronaphthalene **83** and catalytic amount of TsOH were dissolved in DCM and were stirred for 16 h at rt. Reaction mixture was washed with solution of $NaHCO_3$ in water. Aqueous phase was extracted with DCM. Organic phase was dried over anhydrous Na_2SO_4. After filtration the product was concentrated under reduced pressure (9.0 g, 40.34 mmol). TLC: hexane.

Light-brown liquid, **94 %** yield.

^{1}H NMR [400 MHz, $CDCl_3$, 293 K]: *δ* (ppm) 7.32 (d, *J*=2.08 Hz, 1H), 7.24 (dd, *J*=2.04, 7.93 Hz, 1H), 6.98 (dt, *J*=0.84, 7.93 Hz, 1 H), 5.91-5.85 (m, 1H), 2.68 (t, *J*=8.07 Hz, 2H), 2.27-2.19 (m, 2H), 2.01 (q, *J*=1.71 Hz, 3H).

^{13}C NMR [101 MHz, $CDCl_3$, 293 K]: *δ* (ppm) 137.85, 135.00, 131.30, 129.23 (CH), 128.79 (CH), 126.73 (CH), 125.77 (CH), 120.02 (C-Br), 27.68 (CH_2), 22.99 (CH_2), 19.15 (CH_3).

7-Bromo-1-methylnaphthalene (85)

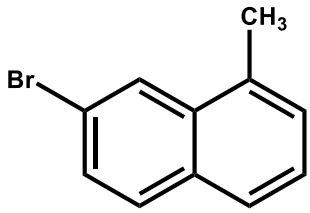

$C_{11}H_9Br$
M = 221.10

9.0 g (40.3 mmol) of 6-bromo-4-methyl-1,2-dihydro-naphthalene **84** and 18.3 g (80.7 mmol) of DDQ were dissolved in benzene. Reaction was carried out under reflux for 3 h. Benzene was removed under reduced pressure, and the product was purified by column chromatography (SiO_2, hexane) yielding 2.4 g (10.9 mmol). TLC hexane (Al_2O_3).

Light-brown liquid, **27 %** yield.

^{1}H NMR [400 MHz, $CDCl_3$, 293 K]: *δ* (ppm) 8.16-8.14 (m, 1H), 7.70 (d, *J*=8.69 Hz, 1H), 7.68-7.64 (m, 1H), 7.55 (dd, *J*=1.94, 8.71 Hz, 1H), 7.38 (dd, *J*=7.05, 8.01 Hz, 1 H), 7.35-7.31 (m, 1H), 2.64 (s, 3H).

^{13}C NMR [101 MHz, $CDCl_3$,293 K]: *δ* (ppm) 133.76, 133.47, 131.89, 130.13 (CH), 128.83 (CH), 127.48 (CH), 126.54 (CH), 126.19 (CH), 125.96 (CH), 119.91 (C-Br), 19.24 (CH_3).

7-Bromo-1-(bromomethyl)naphthalene (86)

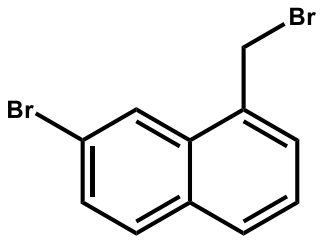

$C_{11}H_8Br_2$
M = 299.99

2.4 g (10.7 mmol) of 7-bromo-1-methylnaphthalene **85** was dissolved in CCl_4, then 2.1 g (11.7 mmol) NBS and catalytic amount of DBPO were added. Reaction was carried out under reflux and monitored by TLC. CCl_4 was removed under reduced pressure, and product was purified by column chromatography (SiO_2, hexane) yielding 2.8 g (9.4 mmol). TLC hexane.

White-yellow crystals, **88 %** yield.

^{1}H NMR [300 MHz, $CDCl_3$, 293 K]: *δ* (ppm) 8.29-8.27 (m, 1H), 7.79 (dt, *J*=1.10, 8.24 Hz, 1H), 7.74 (d, *J*=8.67 Hz, 1H), 7.59 (dd, *J*=1.91, 8.72 Hz, 1H), 7.55 (dd, *J*=1.22, 7.07 Hz, 1H), 7.41 (dd, J=7.08, 8.22 Hz, 1H), 4.88 (s, 2H).

^{13}C NMR [75 MHz, $CDCl_3$, 293 K]: *δ* (ppm) 132.58, 132.42, 132.18, 130.43 (CH), 129.70 (CH), 129.58 (CH), 128.64 (CH), 126.22 (CH), 125.83 (CH), 120.99 (C-Br), 31.03 (CH_2)

2-(7-Bromonaphthalen-1-yl)acetonitrile (87)

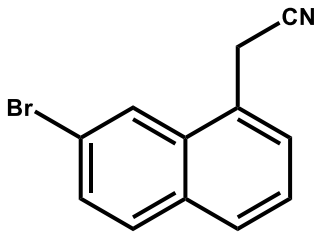

$C_{12}H_8BrN$
M = 246.11

2.4 g (7.8 mmol) of 7-bromo-1-(bromomethyl)naphthalene **86**, 1.0 g (15.7 mmol) of KCN (dissolved in water) and catalytic amount of TBAB were dissolved in 50 mL DCM. Reaction was carried out at rt for 16 h. Reaction mixture was washed with water (2x30 mL). Organic layer was dried over anhydrous Na_2SO_4, obtained product was concentrated under reduced pressure and purified on aFLC (Hexane: DCM:1:1) (1.9 g, 7.7 mmol).

Light-yellow solid, **98 %** yield.

^{1}H NMR [300 MHz, $CDCl_3$, 293 K]: *δ* (ppm) 8.00-7.98 (m, 1H), 7.81 (d, *J*=8.28 Hz, 1H), 7.76 (d, *J*=8.73 Hz, 1H), 7.65-7.59 (m, 2H), 7.48 (dd, *J*=7.20, 8.19 Hz, 1H), 4.08 (s, 2H).

^{13}C NMR [75 MHz, $CDCl_3$, 293 K]: *δ* (ppm) 132.10, 131.89, 130.64 (CH), 129.85 (CH), 129.00 (CH), 127.37 (CH), 125.94 (CH), 124.98, 124.87 (CH), 121.44 (C-Br), 117.23 (CN), 21.62 (CH_2).

2-(7-Bromonaphthalen-1-yl)acetic acid (88)

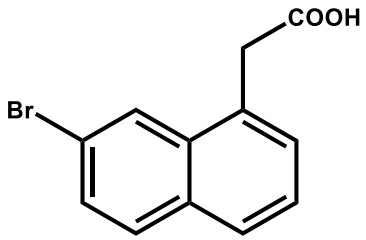

$C_{12}H_9BrO_2$
M = 265.11

1.9 g (7.7 mmol) of 2-(7-bromonaphthalen-1-yl)acetonitrile **87** was dissolved in 60 mL AcOH, 10 mL H_2SO_4 and 10 mL H_2O was added. Reaction was carried out 16 h under reflux. After cooling to rt, 400 mL H_2O was added, and the mixture was kept 2-3 hours at the room temperature. The precipitate was filtrated and washed with water (3x50 mL). Then the product was dried under vacuo for 24 h (1.34 g, 5.05 mmol).

White solid, **66 %** yield.

^{1}H NMR [400 MHz, DMSO, 293 K]: *δ* (ppm) 12.49 (s, 1H), 8.19-8.16 (m, 1H), 7.92 (d, *J*=8.77 Hz, 1H), 7.87 (dd, *J*=2.48, 6.85 Hz, 1H), 7.65 (dd, *J*=1.96, 8.73 Hz, 1H), 7.53-7.42 (m, 2H), 4.06 (s, 2H).

^{13}C NMR [101 MHz, DMSO, 293 K]: *δ* (ppm) 172.57 (C=O), 133.12, 131.88, 131.18, 130.74 (CH), 129.15 (CH), 128.73 (CH), 127.43 (CH), 126.37 (CH), 126.21 (CH), 119.67 (C-Br), 38.30 (CH_2).

8-Bromoacenaphthylen-1(2H)-one (89)

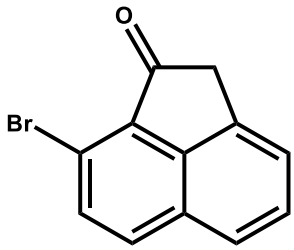

$C_{12}H_7BrO$
M = 247.09

0.7 g (2.83 mmol) of 2-(7-bromonaphthalen-1-yl)acetic acid **88** was dissolved in 2.02 g (17 mmol) $SOCl_2$ and was kept while stirring for 1 h at 65ºC. $SOCl_2$ was removed under reduced pressure and product was diluted with DCM. Then was 0.4 g of (3.2 mmol) $AlCl_3$ was added and the reaction mixture was kept at rt for 3 hours. After reaction the mixture was poured out on ice and 10 % HCl. Product was extracted with DCM and dried over anhydrous Na_2SO_4, then concentrated and filtrated. The obtained product was purified on aFLC (DCM:Hexane:2:1) and concentrated under reduced pressure (0.3 g, 1.21 mmol).

Beige solid, **43 %** yield.

^{1}H NMR [300 MHz, $CDCl_3$, 293 K]: *δ* (ppm) 7.84 (d, J=8.55 Hz, 1H), 7.77-7.71 (m, 1H), 7.69 (d, J=8.52 Hz, 1H), 7.57 (dd, J=6.90, 8.34 Hz, 1H), 7.46-7.42 (m, 1H), 3.80-3.77 (m, 2H).

^{13}C NMR [75 MHz, $CDCl_3$, 293 K]: *δ* (ppm) 200.06 (C=O), 144.06, 133.40, 132.91 (CH), 132.33 (CH), 131.94, 129.65, 128.59 (CH), 124.03 (CH), 121.65 (CH), 116.80 (C-Br), 42.28 (CH_2).

1,7,13,19-Tetrabromotridecacyclene (90)

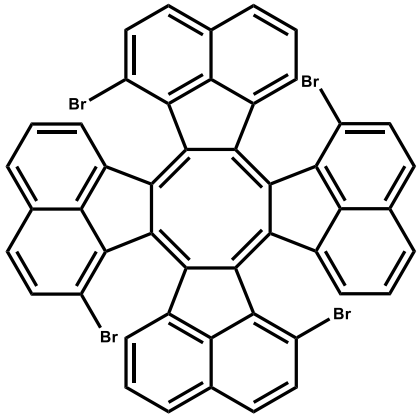

$C_{48}H_{20}Br_4$
M = 916.30

Brominated tridecacyclene **90** was synthesized according to modified procedure [170]. Two-necked RBF was equipped with a stirring bar and condenser. 0.113 ml (1.03 mmol) of $TiCl_4$ and 10 mL of *o*-DCB were added to the flask and brought to reflux under N_2 atmosphere. Then 0.042 g of 8-bromoacenaphthylen-1(*2H*)-one **89** (0.17 mmol) was dissolved in 10 mL of *o*-DCB and was added dropwise into refluxing reaction mixture. After 45 min the reaction mixture was poured into a flask containing crushed ice (100 g) and concentrated $HCl_{(aq)}$ (10 mL). The product was extracted with dichloromethane (3x25 mL) and dried over Na_2SO_4. Dichloromethane was removed under reduced pressure. Product was dissolved in 2 mL of toluene and placed in the thimble of a Soxhlet extractor after adsorption onto aluminium oxide. Extraction was carried out in hot dichloromethane. In first (after 30 min) and second fraction (after 2 h) was collected dark-coloured product, which was analysed by HPLC chromatography. In both fractions the brominated tridecacyclene was detected. Both fractions were combined and concentrated under reduced pressure. Then, 0.2 mL of acetone and MeOH were added. The pure product precipitated in MeOH/Acetone mixture after centrifugation and then was dried in vacuo (5 mg, 0.00546 mmol).

Brown solid, **13 %** yield.

^{1}H NMR [400 MHz, $C_2D_2Cl_4$, 293 K]: *δ* (ppm) 7.82-7.36 (m, 20H).

^{13}C NMR [101 MHz, $CDCl_3$, 293 K]: *δ* (ppm) 142.12, 139.88, 139.69, 139.65, 139.60, 139.50, 139.34, 139.11, 138.88, 138.71, 138.45, 137.30, 137.27, 136.50, 133.54, 133.41, 133.07, 132.94, 132.63, 132.47, 131.19, 131.12, 131.03, 129.28, 129.11, 129.02, 128.92, 128.75, 128.47, 128.39, 127.92, 127.84, 127.77, 127.67, 127.58, 127.51, 127.43, 127.37, 127.31, 127.26, 127.24, 127.08, 125.63, 125.51, 125.23, 125.06, 124.77, 124.53, 124.39, 120.10, 120.02, 119.43, 119.19, 119.09.

MS [LDI]: m/z (rel. int.) = 915.90 [M]+ (100).

HRMS [APPI, Toluene, DCM]: Chemical Formula: $C_{48}H_{20}Br_4$ calc. 911.8293, found 911.8298.

6.7 Synthesis of Bowl-Shaped Stuctures with Zig-Zag Periphery

1,6-Bis(2-formylphenyl)pyrene (93)

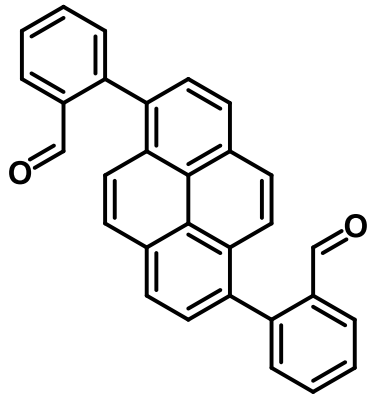

$C_{30}H_{18}O_2$
M = 410.47

In 100 mL round bottom flask 1,6-dibromopyrene (1.00 g, 2.78 mmol), 2-formylphenylboronic acid (1.00 g, 6.67 mmol), K_2CO_3 (2.00 g, 14.5 mmol) and $Pd(PPh_3)_4$ (80.0 mg, 69.0 µmol) were suspended in 2:1:Tol:MeOH mixture (30 mL). Flask was equipped with magnetic stir bar and condenser. Further, flask was degassed, and the atmosphere was exchanged by nitrogen. After 16 h under reflux, reaction mixture was diluted with toluene (100 mL) and washed with water (2x50 mL). Aqueous layer was extracted with toluene (1x50 mL); both organic layers were combined and dried over $MgSO_4$. Solvent was evaporated under reduced vacuum and the product was precipitated from DCM:hexane mixture. Product was filtered, washed with hexane and dried in vacuo (0.7 g, 1.71 mmol).[171]

Pale yellow solid, **61 %** yield.

^{1}H NMR [400 MHz, $CDCl_3$, 293 K]: *δ* (ppm) 9.66 (1H, s); 9.65 (1H, s), 8.24 (2H, d, J=7.80 Hz); 8.18 (2H, d, J=7.84 Hz), 8.07 (2H, d, J=9.24 Hz), 7.97 (2H, d, J=7.76 Hz), 7.82 (2H, dd, J=2.04, 9.20 Hz), 7.77 (2H, m), 7.65 (2H, dd, J=7.56, 7.56 Hz), 7.57 (2H, d, J=7.52 Hz).

^{13}C NMR [75 MHz, $CDCl_3$, 293 K]: *δ* (ppm) 191.83; 191.79; 144.52; 144.48; 135.10; 135.06; 133.7; 133.6; 133.5; 132.20; 132.16; 131.0; 130.3; 128.7; 128.4; 128.3; 127.5; 127.4; 125.3; 124.7; 124.60; 124.58.

HRMS [APPI; toluene]: Chemical Formula: $C_{30}H_{18}O_2$ calc. 410.1301, found 410.1308.

1,6-dibromo-3,8-bis(2-fluorophenyl)pyrene) (101)

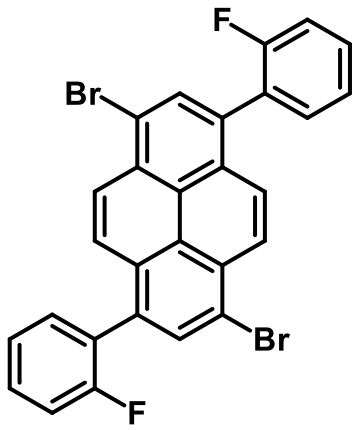

$C_{28}H_{14}Br_2F_2$
M = 548.22

0.5 g of 1,6-bis(2-fluorophenyl)pyrene **59** was dissolved in 100 mL of DMF in 250 mL two-neck RBF. Bromine (0.47 g, 2.95 mmol) was dissolved in 25 mL of DMF and added dropwise at rt (from dropping funnel). Then the mixture was stirred at rt for 16 h. Precipitated product was collected and washed with MeOH and hexane. Then, the precipitate was recrystallized from hot xylene (mixture of isomers), yielding the mixture of mono- and dibrominated products in 0.65 g, which was used without further characterization and purification.
Beige solid.

2,2'-(3,8-bis(2-fluorophenyl)-pyrene-1,6-diyl)dibenzaldehyde (102)

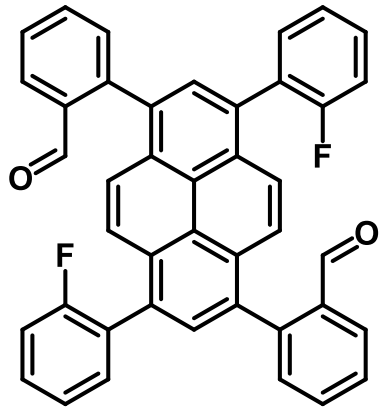

$C_{42}H_{24}F_2O_2$
M = 598.65

A 100 mL RBF equipped with a magnetic stir bar and a condenser and was charged with 1,6-dibromo-3,8-bis(2-fluorophenyl)pyrene **101** (100 mg), 2-formylphenylboronic acid **92** (65 mg, 0.44 mmol), K_2CO_3 (61 mg, 0.44 mmol) and 5% mol $Pd(PPh_3)_4$. The

solids were suspended in Tol:MeOH:2:1 (45 mL), the reaction mixture was degassed and the atmosphere was exchanged by nitrogen. The mixture was brought to reflux for 16 h. After reaction the mixture was diluted with toluene (30 mL) and washed with H_2O (2x30 mL). The aqueous layer was extracted with toluene (2x30 mL), the organic layers were combined and dried over $MgSO_4$. The solvent was removed under reduced pressure. The product **102** was purified by HPLC chromatography (Tol:MeOH:2:8 as eluent). After purification the solvents were removed under reduced pressure, and the products were dried in vacuo.

Yield 55 mg (0.092 mmol).

^{1}H NMR [400 MHz, DMSO, 293 K]: *δ* (ppm) 9.75-9.65 (2H, m); 8.14-8.08 (2H, m); 8.07-8.03 (2H, m); 7.97-7.86 (4H, m); 7.85-7.74 (4H, m); 7.74- 7.64 (4H, m); 7.63-7.56 (2H, m); 7.50-7.38 (4H, m).

^{13}C NMR [101 MHz, DMSO, 293 K]: *δ* (ppm) 191.61; 191.41; 160.67; 155.03; 142.57; 134.51; 134.14; 133.55; 132.94; 132.79; 132.46; 130.74; 130.61; 130.53; 129.12; 128.89; 128.34; 128.21; 128.04; 126.89; 126.73; 125.96; 125.37; 124.91; 124.15.

^{19}F NMR [282 MHz, DMSO, 293 K]: *δ* (ppm) -113÷-113.5 (m).

MS [MALDI-TOF, without matrix]: m/z (rel. int.) = 598.3122 [M]+ (100).

MS [MALDI-TOF, DHB]: m/z (rel. int.) = 598.3011 [M]+ (100).

MS [MALDI-TOF, DCTB]: m/z (rel. int.) = 598.3352 [M]+ (100).

HRMS [APPI, toluene]: Chemical Formula: $C_{42}H_{24}F_2O_2$ calc. 598.1739, found 598.1744.

2-(3,8-bis(2-fluorophenyl)pyren-1-yl)benzaldehyde (103)

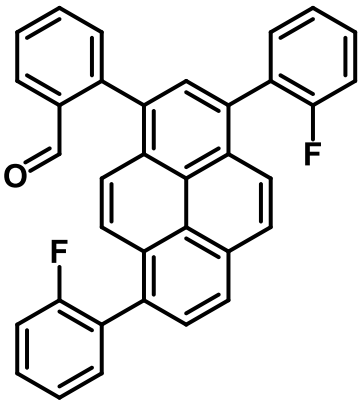

$C_{35}H_{20}F_2O$
M = 494.54

Yield 44 mg (0.089 mmol).

^{1}H NMR [400 MHz, DMSO, 293 K]: *δ* (ppm) 9.71-9.64 (1H, m); 8.34 (1H, d, *J*=9.28 Hz), 8.48 (1H, d, *J*=7.92 Hz); 8.13-8.05 (2H, m); 8.03-7.99 (1H, m), 7.98-7.93 (1H, m); 7.91-7.82 (2H, m); 7.79-7.65 (4H, m), 7.65-7.55 (3H, m).

^{13}C NMR [101 MHz, DMSO, 293 K]: *δ* (ppm) 154.37; 134.48; 134.09; 132.86; 132.46; 130.65; 130.52; 130.40; 128.82; 128.68; 128.45; 125.79; 124.98; 124.85; 115.98; 115.77.

^{19}F NMR [282 MHz, DMSO, 293 K]: *δ* (ppm) -113.80÷-113.45 (m); -113.5÷-113.80 (m).

MS [MALDI-TOF, without matrix]: m/z (rel. int.) = 494.2225 [M]+ (100)

MS [MALDI-TOF, DHB]: m/z (rel. int.) = 494.2752 [M]+ (100)

MS [MALDI-TOF, DCTB]: m/z (rel. int.) = 494.2304 [M]+ (100).

HRMS [APPI, toluene]: Chemical Formula: $C_{35}H_{20}F_2O$ calc. 494.1477, found 494.1475.

6,14-bis(2-fluorophenyl)tetraceno[2,1,12,11-opqra]tetracene (104)

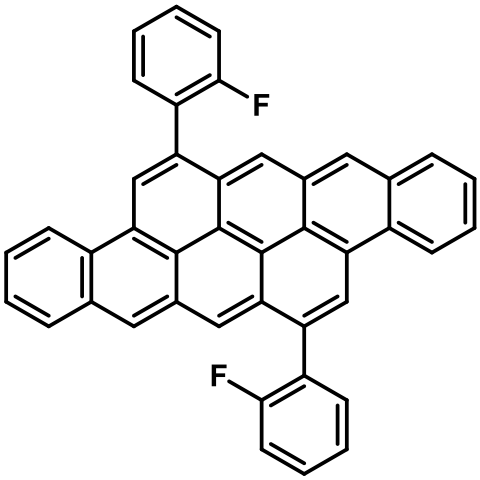

$C_{42}H_{22}F_2$
M = 564.63

The reaction was conducted according to procedure for synthesis of nanographenes. As a precursor was used 2,2'-(3,8-bis(2-fluorophenyl)-pyrene-1,6-diyl)dibenzaldehyde **102** (12 mg; 0.02 mmol).

HRMS [APPI; toluene, DCM]: Chemical Formula: $C_{44}H_{22}F_2$ calc. 564.1684, found 564.1677.

2,2'-(diindeno[4,3,2,1-cdef:4',3',2',1'-lmno]chrysene-3,9-diyl)dibenzaldehyde (110)

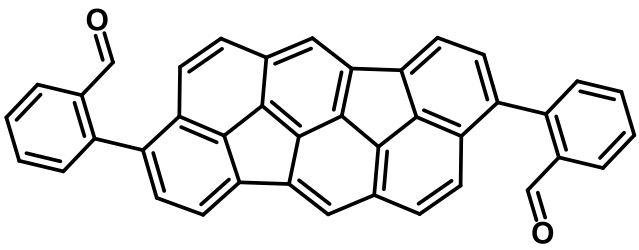

$C_{40}H_{20}O_2$
M = 532.60

A 100 mL RBF equipped with a magnetic stir bar and a condenser was charged with mixture of 80 mg 3,9-dibromodiindeno[4,3,2,1-*cdef*:4',3',2',1'-*lmno*]chrysene **51a** (0.17 mmol), 2-formylphenyl-boronic acid (65 mg, 0.43 mmol), K_2CO_3 (60 mg, 0.43 mmol) and 5% mol $Pd(PPh_3)_4$. The solids were suspended in Tol:MeOH:2:1 (45 mL), the reaction mixture was degassed and the atmosphere was exchanged by nitrogen. The mixture was brought to reflux for 16 h. The mixture was diluted with toluene (30 mL) and washed with H_2O (2x30 mL). The aqueous layer was extracted with toluene (2x30 mL); organic layers were combined and dried over Na_2SO_4. The solvent was removed under reduced pressure. The product **110** was purified by aFLC (DCM as eluent) and dried in vacuo (76 mg, 0.14 mmol).

86 % yield.

^{1}H NMR [400 MHz, CD_2Cl_2, 293 K]: *δ* (ppm) 9.83 (2H, d, *J*=3.40 Hz); 8.09 (2H, ddd, *J*=0.51, 1.45, 7.81 Hz); 8.00 (2H, s); 7.87 (2H, d, *J*=7.12 Hz); 7.79 (2H, d, *J*=8.96 Hz); 7.74 (2H, ddd, *J*=1.47, 7.51, 7.51 Hz); 7.62 (2H, dddd, *J*=0.86, 1.27, 7.42, 7.80 Hz); 7.57 (2H, d, *J*=7.88 Hz); 7.38 (2H, d, *J*=7.24 Hz); 7.38 (2H, d, *J*=8.80 Hz).

^{13}C NMR [101 MHz, CD_2Cl_2, 293 K]: *δ* (ppm) 192.14; 143.18; 143.00; 139.85; 139.47; 137.70; 136.93; 136.34; 135.40; 134.16; 133.44; 132.36; 131.70; 129.23; 129.18; 128.96; 128.00; 125.52; 125.33; 122.62.

HRMS [APPI, ACN, toluene]: Chemical Formula: $C_{40}H_{20}O_2$ calc. 532.1458, found 532.1464.

Benzo[l]indeno[5,4,3,2,1-nopqr]naphtho[3',2',1':5,6]acenaphtho[3,2,1-cde]tetraphene (111)

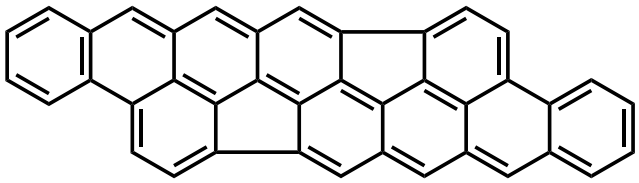

$C_{40}H_{18}$
M = 498.58

The reaction was conducted according to procedure for synthesis of nanographenes. As a precursor was used 2,2'-(diindeno[*4,3,2,1-cdef:4',3',2',1'-lmno*]chrysene-3,9-diyl)dibenzaldehyde **110** (12 mg; 37.5 mmol).

MS [LDI]: m/z (rel. int.) = 498.47 [M]+ (100).

7 Appendix A – Spectra (NMR, MS)

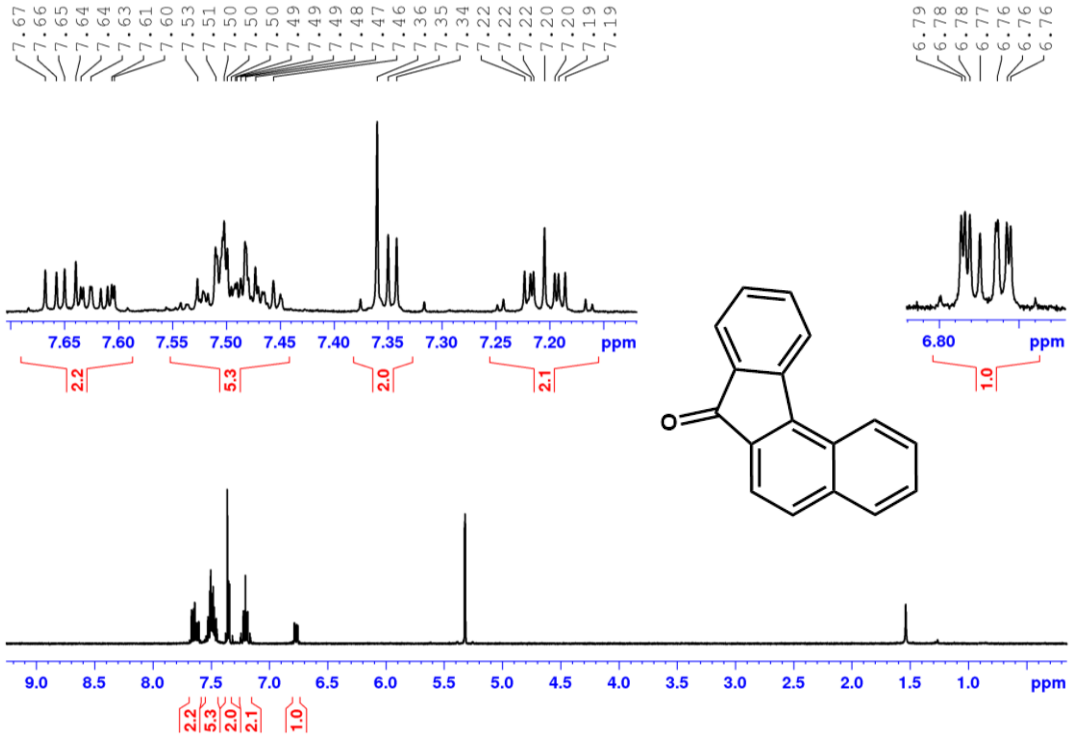

Figure A1. ^{1}H NMR (300 MHz, CD_2Cl_2, 293 K) spectrum of *7H*-benz[*de*]anthracen-7-one **14**.

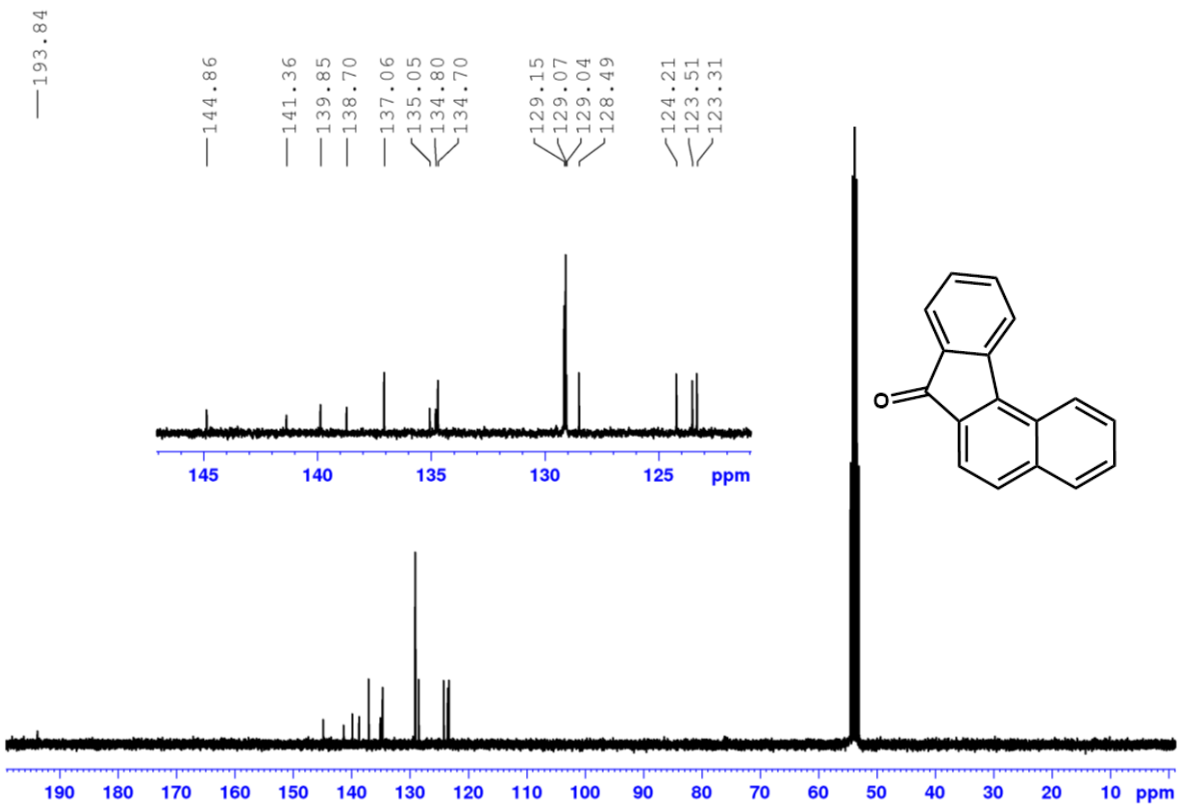

Figure A2. ^{13}C NMR (75 MHz, CD_2Cl_2, 293 K) spectrum of *7H*-benz[*de*]anthracen-7-one **14**.

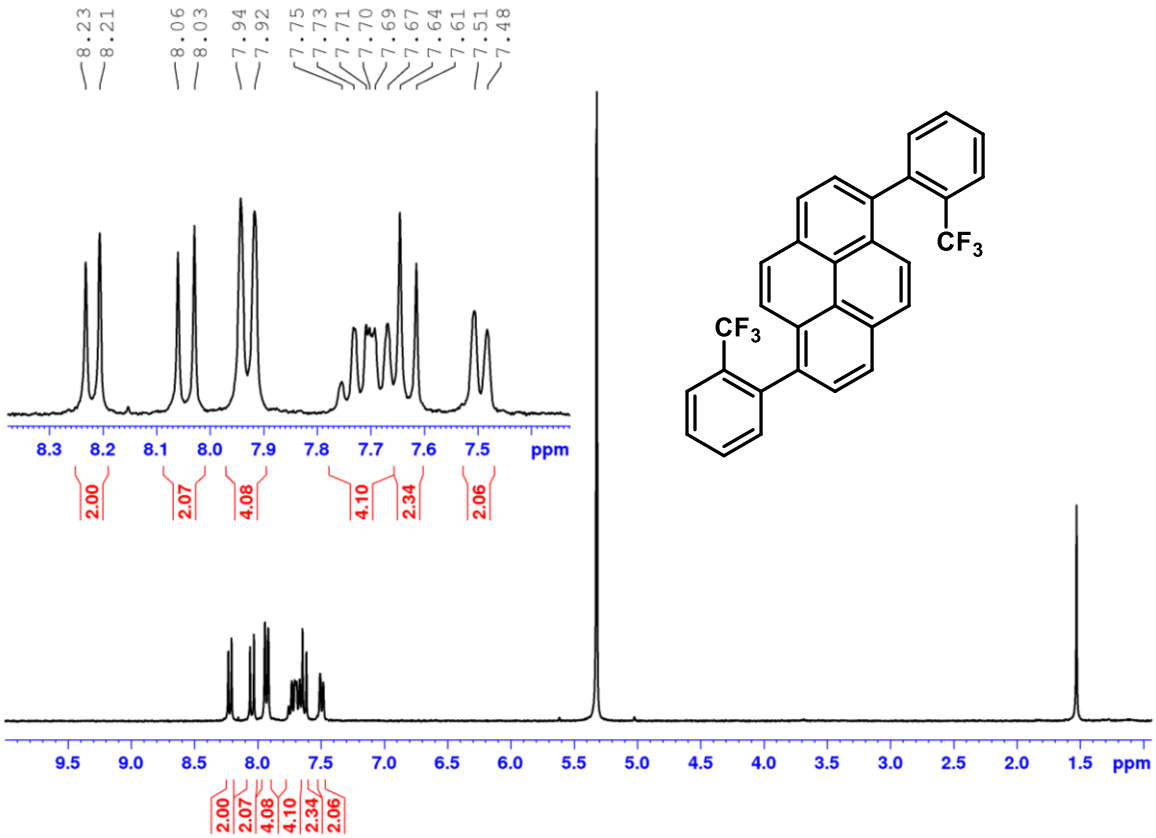

Figure A3. ^{1}H NMR (300 MHz, CD_2Cl_2, 293 K) spectrum of 1,6-bis(2-(trifluoromethyl)phenyl)pyrene **23**.

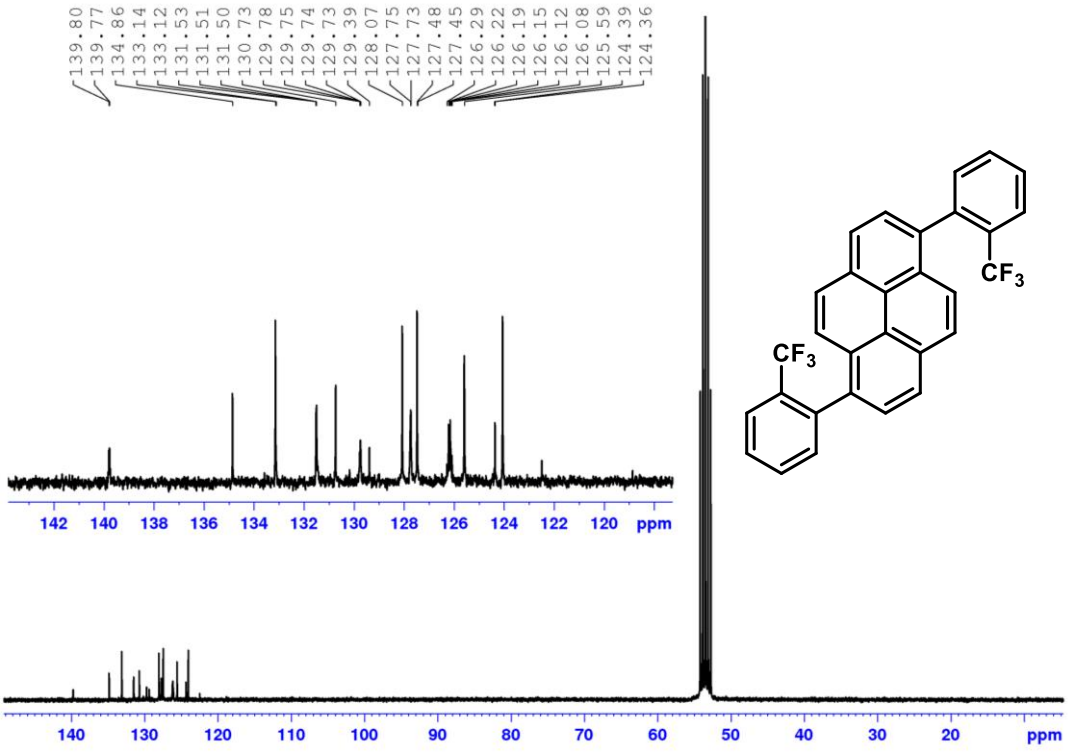

Figure A4. ^{13}C NMR (75 MHz, CD_2Cl_2, 293 K) spectrum of 1,6-bis(2-(trifluoromethyl)phenyl)pyrene **23**.

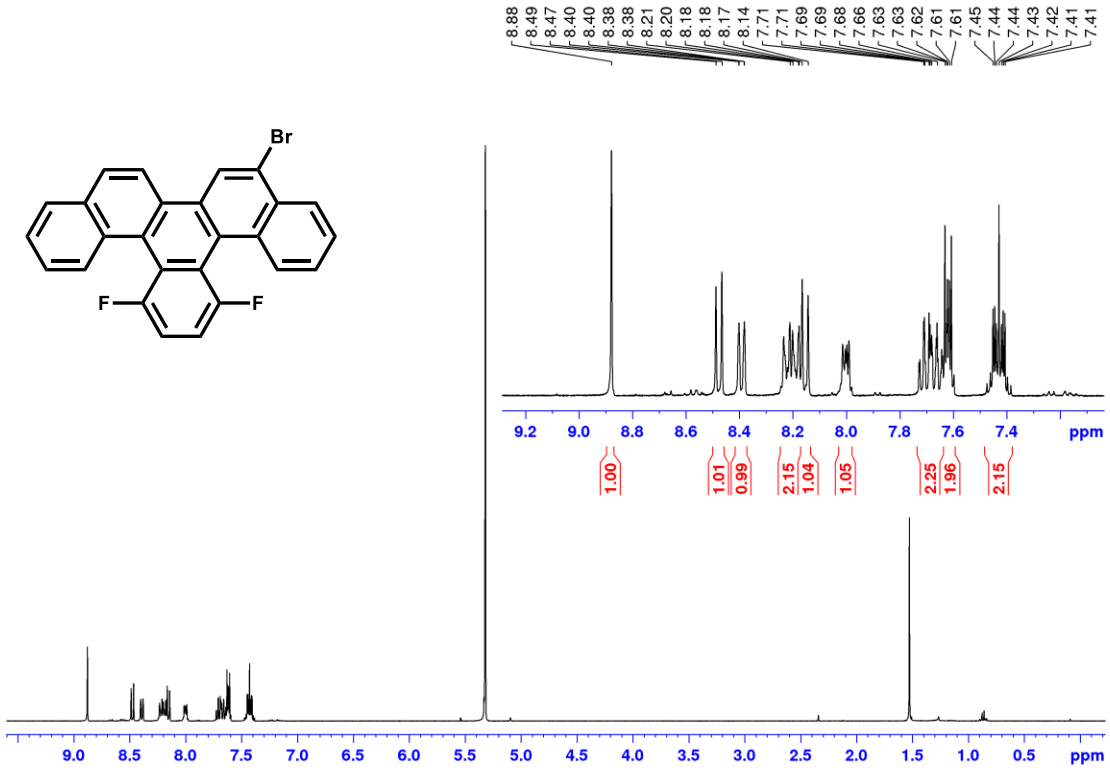

Figure A5. ^{1}H NMR (400 MHz, CD_2Cl_2, 293 K) spectrum of 5-bromo-13,16-difluoro-benzo[*s*]picene **45**.

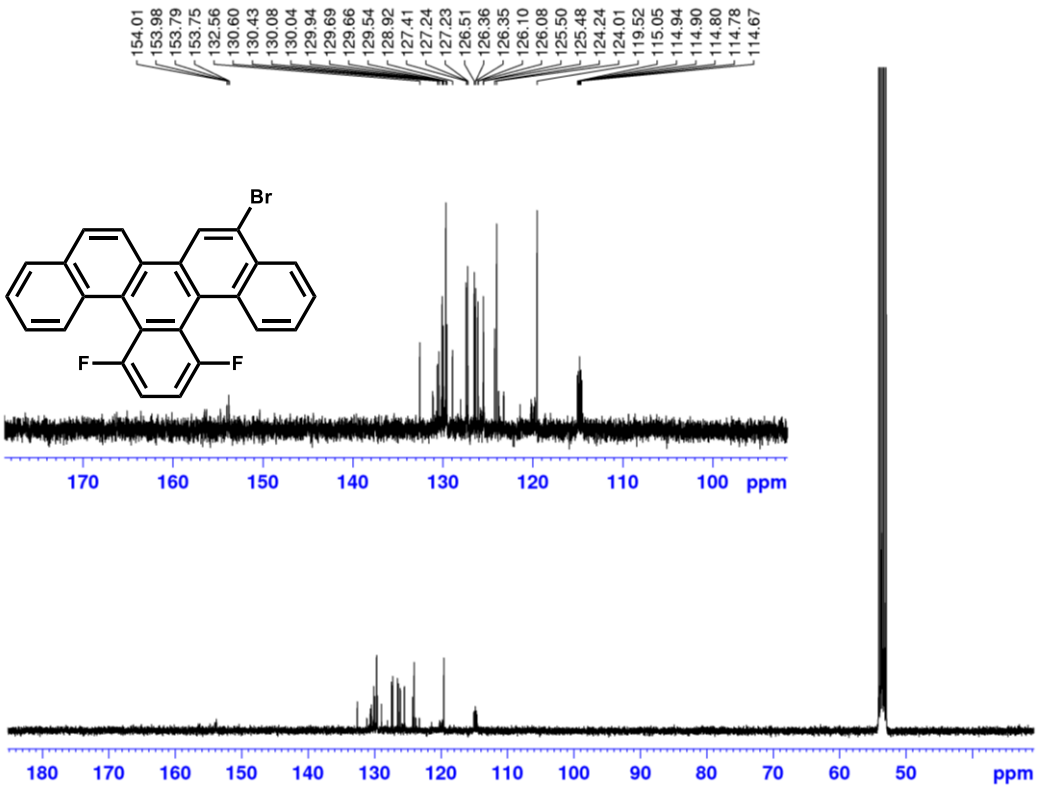

Figure A6. ^{13}C NMR (101 MHz, CD_2Cl_2, 293 K) spectrum of 5-bromo-13,16-difluoro-benzo[*s*]picene **45**.

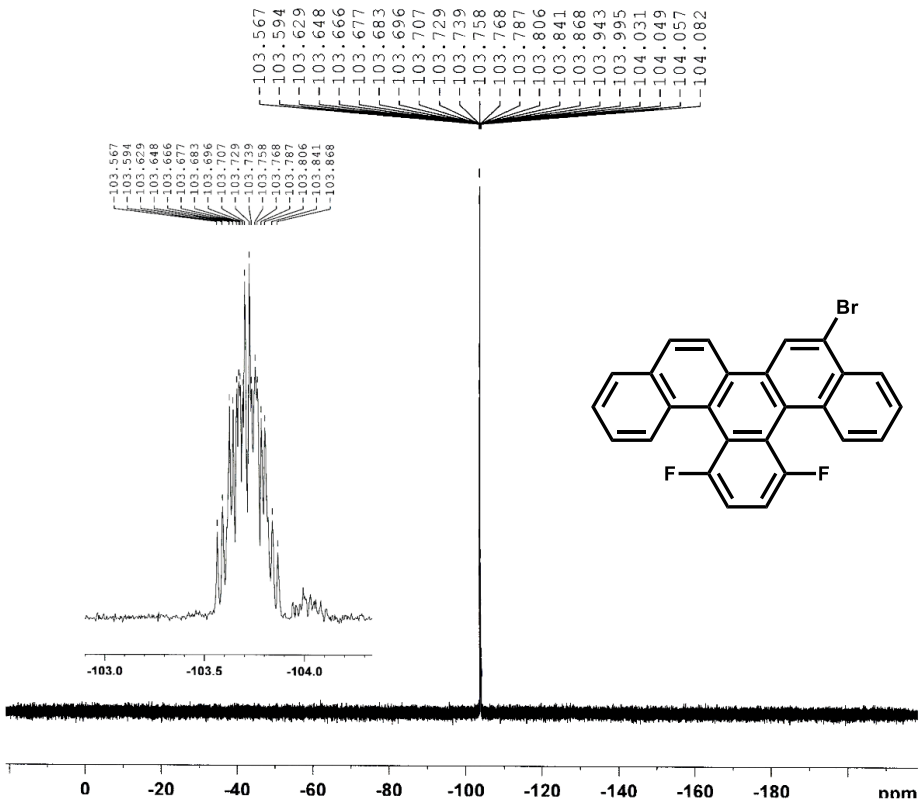

Figure A7. ^{19}F NMR (282 MHz, CD_2Cl_2, 293 K) spectrum of 5-bromo-13,16-difluoro-benzo[*s*]picene **45**.

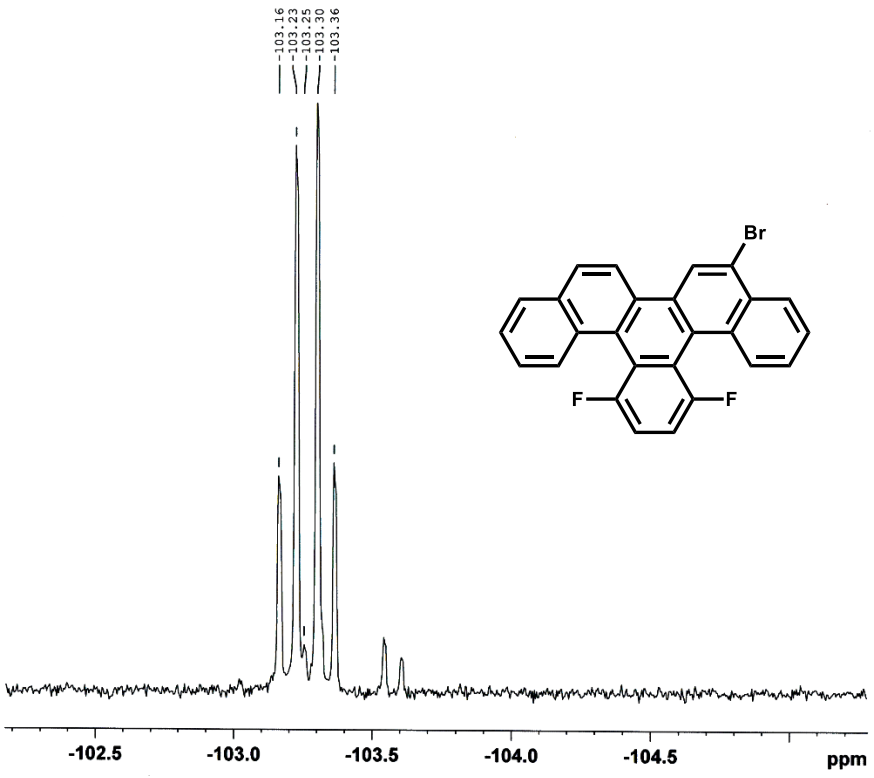

Figure A8. ^{19}F-^{1}H NMR (282 MHz, CD_2Cl_2, 293 K) spectrum of 5-bromo-13,16-difluoro-benzo[*s*]picene **45**.

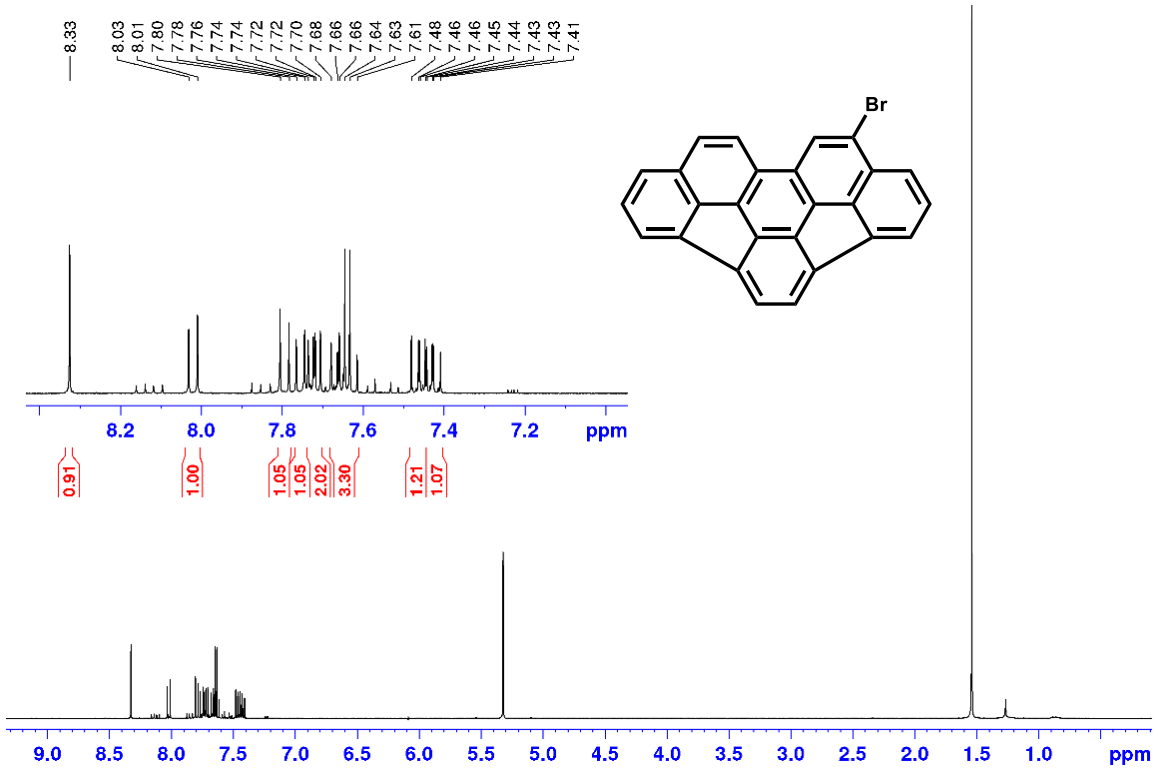

Figure A9. ^{1}H NMR (400 MHz, CD_2Cl_2, 293 K) spectrum of 9-bromo-*as*-indaceno[*3,2,1,8,7,6-pqrstuv*] picene **46**.

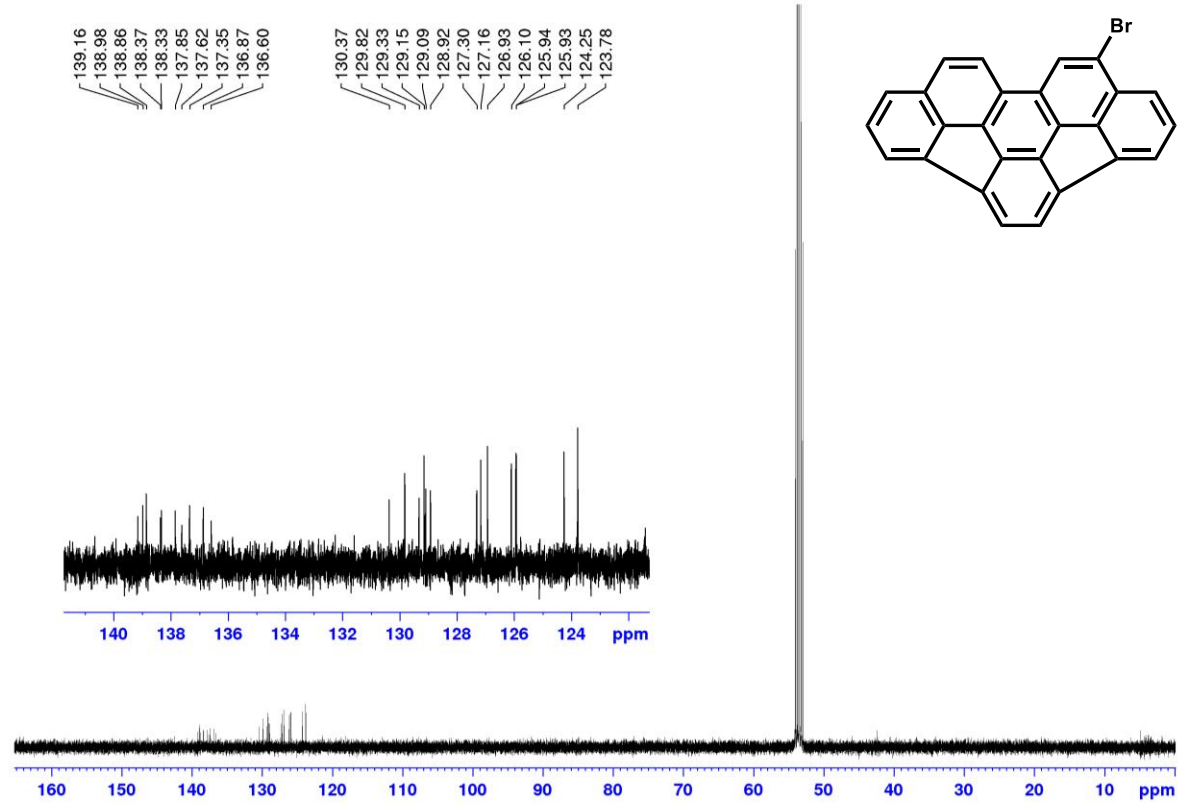

Figure A10. ^{13}C NMR (100 MHz, CD_2Cl_2, 293 K) spectrum of 9-bromo-*as*-indaceno[*3,2,1,8,7,6-pqrstuv*] picene **46**.

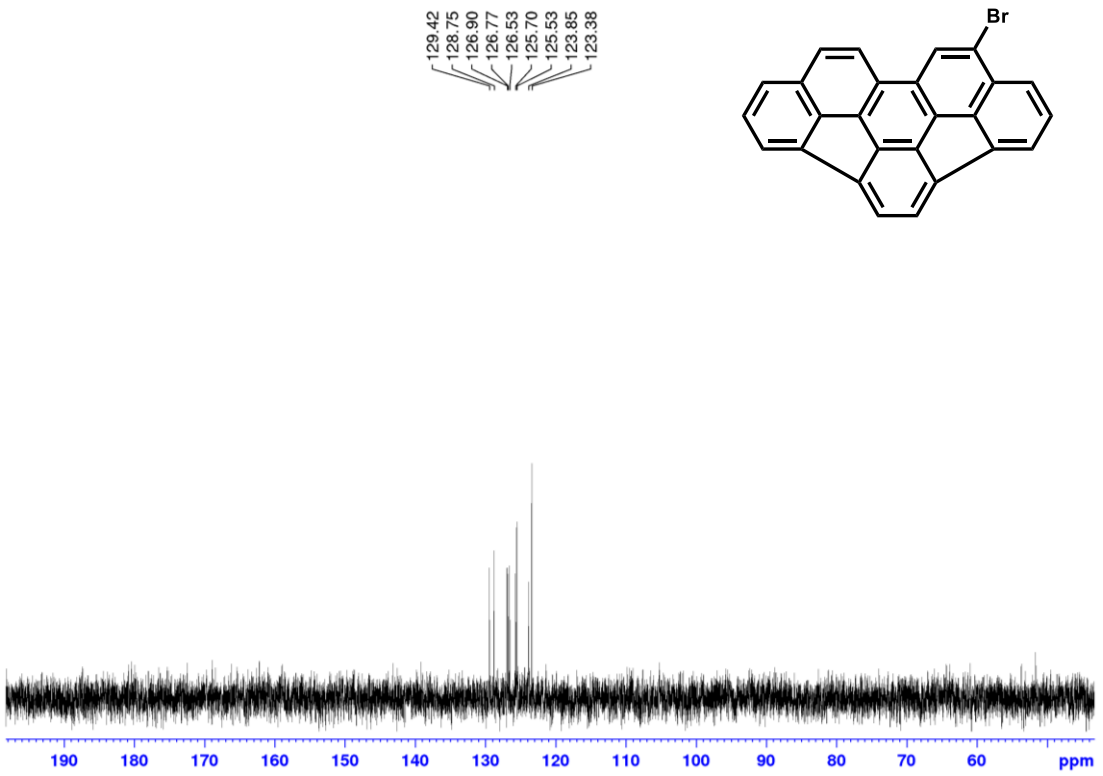

Figure A11. DEPT90 (101 MHz, CD_2Cl_2, 293 K) spectrum of 9-bromo-as-indaceno[*3,2,1,8,7,6-pqrstuv*] picene **46**.

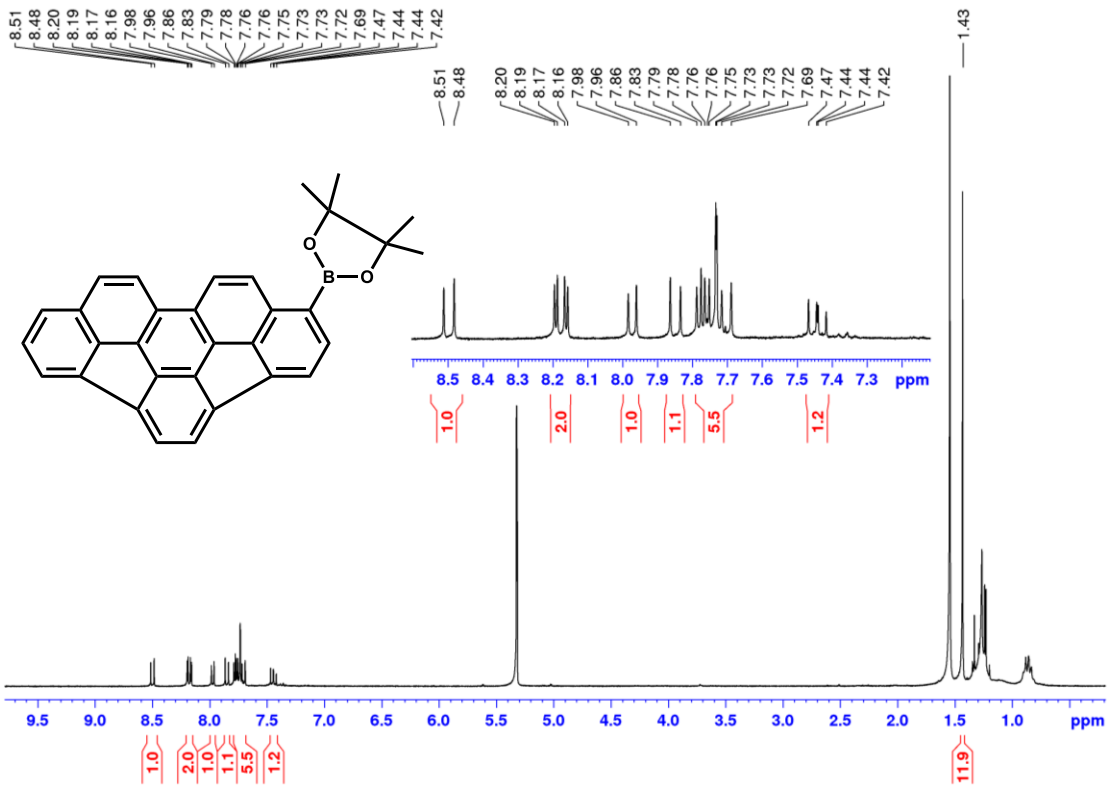

Figure A12. ^1H NMR (300 MHz, CD_2Cl_2, 293 K) spectrum of 2-(*as*-indaceno[*3,2,1,8,7,6-pqrstuv*]picen-1-yl)-4,4,5,5-tetramethyl-1,3,2-dioxaborolane **54**.

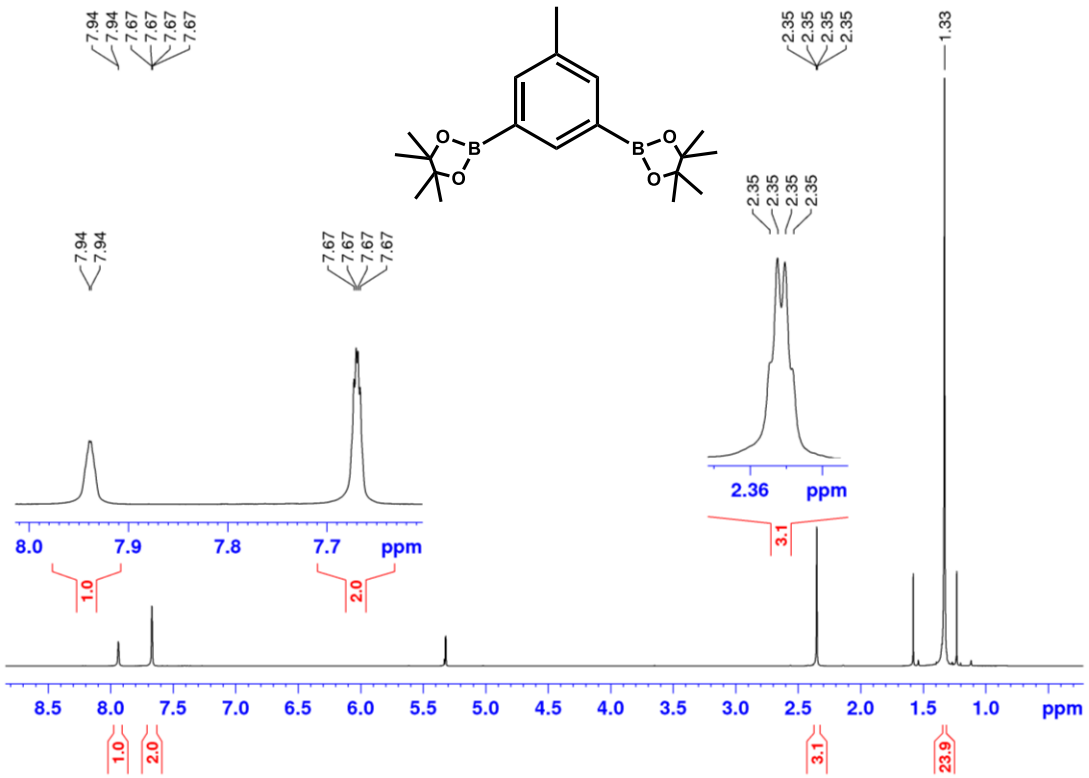

Figure A13. ^{1}H NMR (300 MHz, CD_2Cl_2, 293 K) spectrum of 2,2'-(5-methyl-1,3-phenylene)bis(4,4,5,5-tetra-methyl-1,3,2-dioxaborolane) **58**.

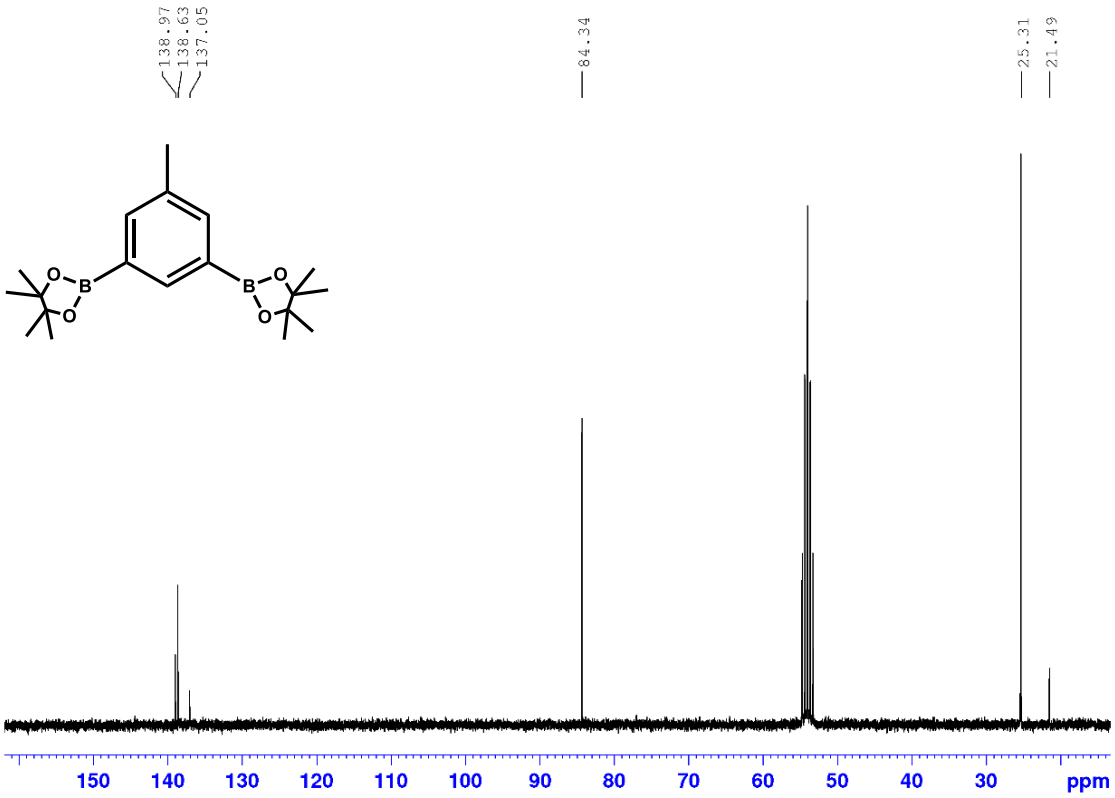

Figure A14. ^{13}C NMR (101 MHz, CD_2Cl_2, 293 K) spectrum of 2,2'-(5-methyl-1,3-phenylene)bis(4,4,5,5-tetra-methyl-1,3,2-dioxaborolane) **58**.

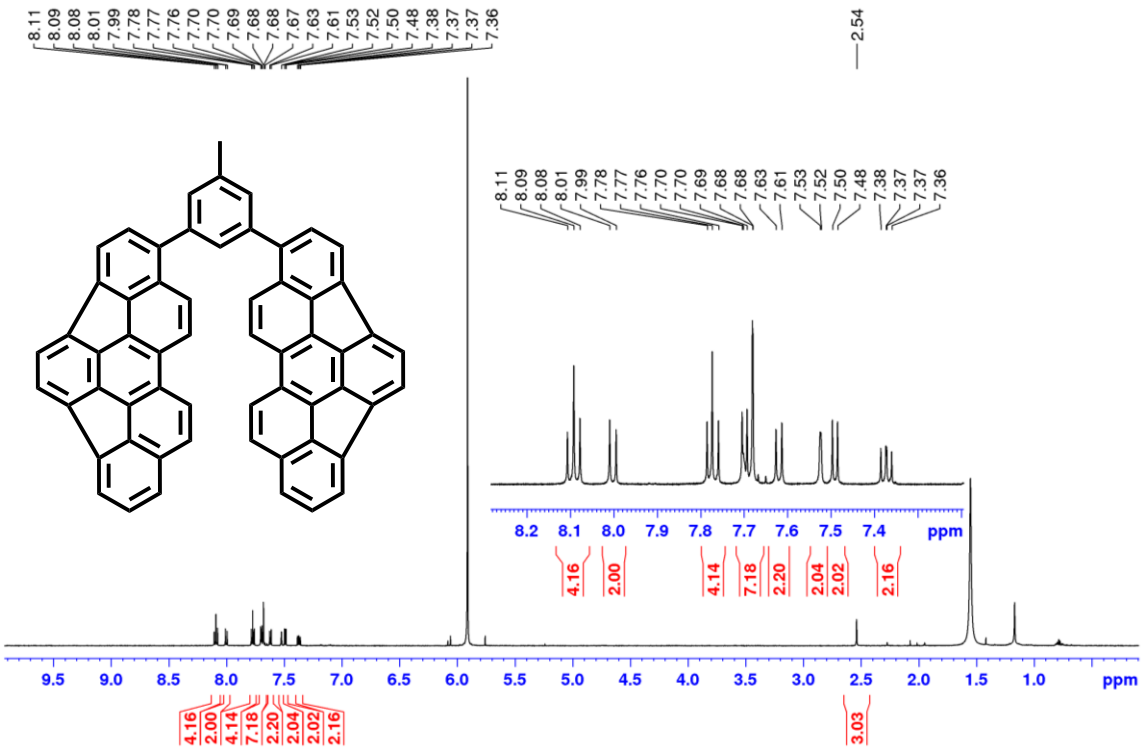

Figure A15. ^{1}H NMR (600 MHz, $C_2D_2Cl_4$, 293 K) spectrum of 9,9'-(5-methyl-1,3-phenylene)di-*as*-indaceno[*3,2,1,8,7,6-pqrstuv*]picene **56**.

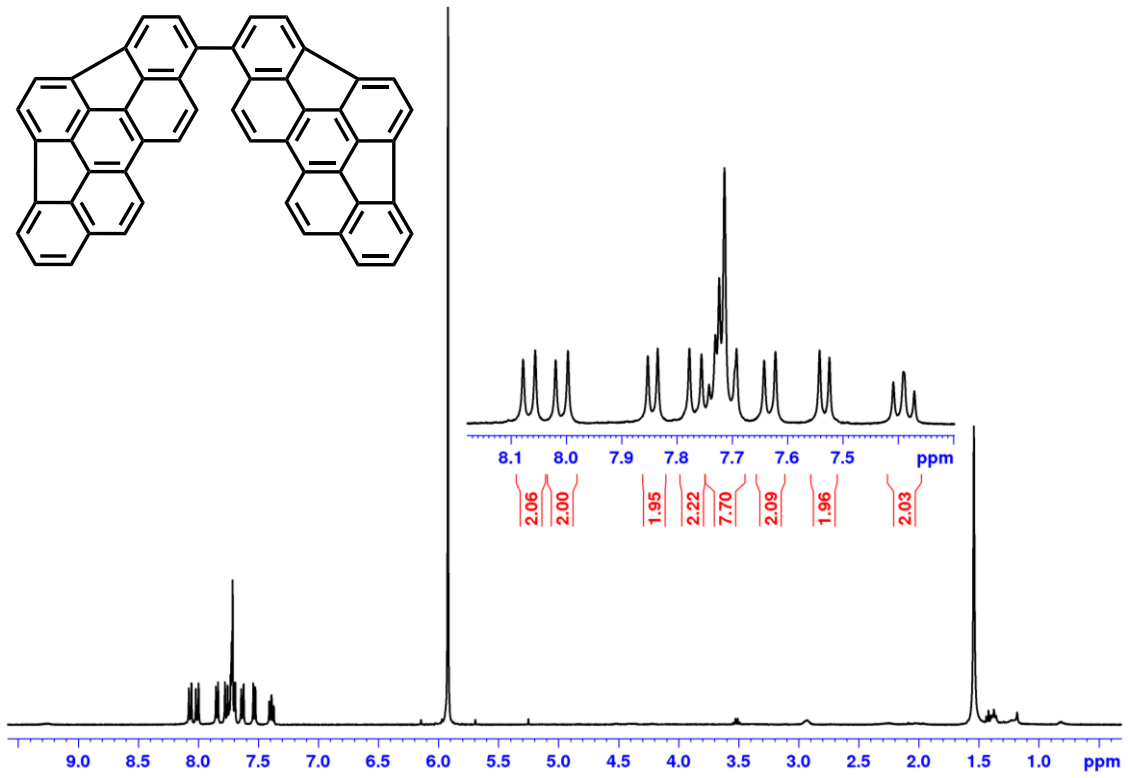

Figure A16. ^{1}H NMR (600 MHz, $C_2D_2Cl_4$, 293 K) spectrum of 1,1'-bias-indaceno[*3,2,1,8,7,6-pqrstuv*] picene **55**.

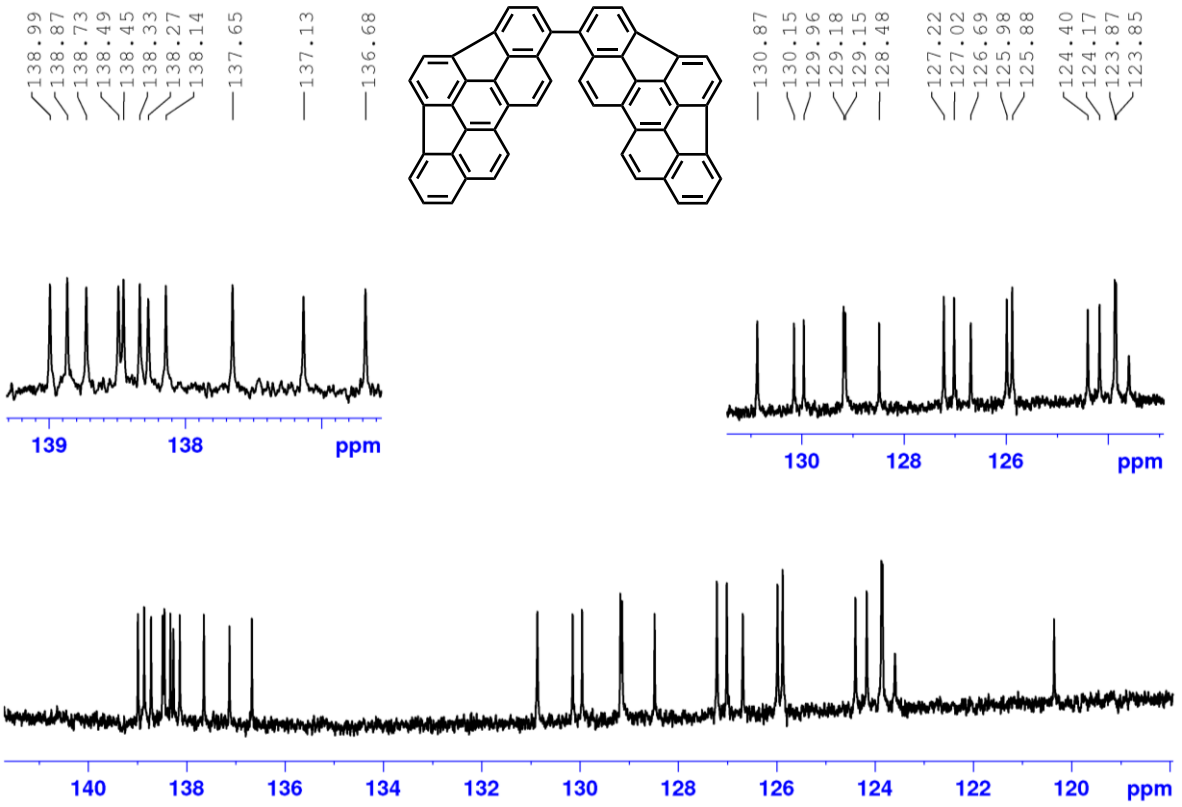

Figure A17. ^{13}C NMR (150 MHz, $C_2D_2Cl_4$, 293 K) spectrum of 1,1'-bias-indaceno[*3,2,1,8,7,6-pqrstuv*] picene **55**.

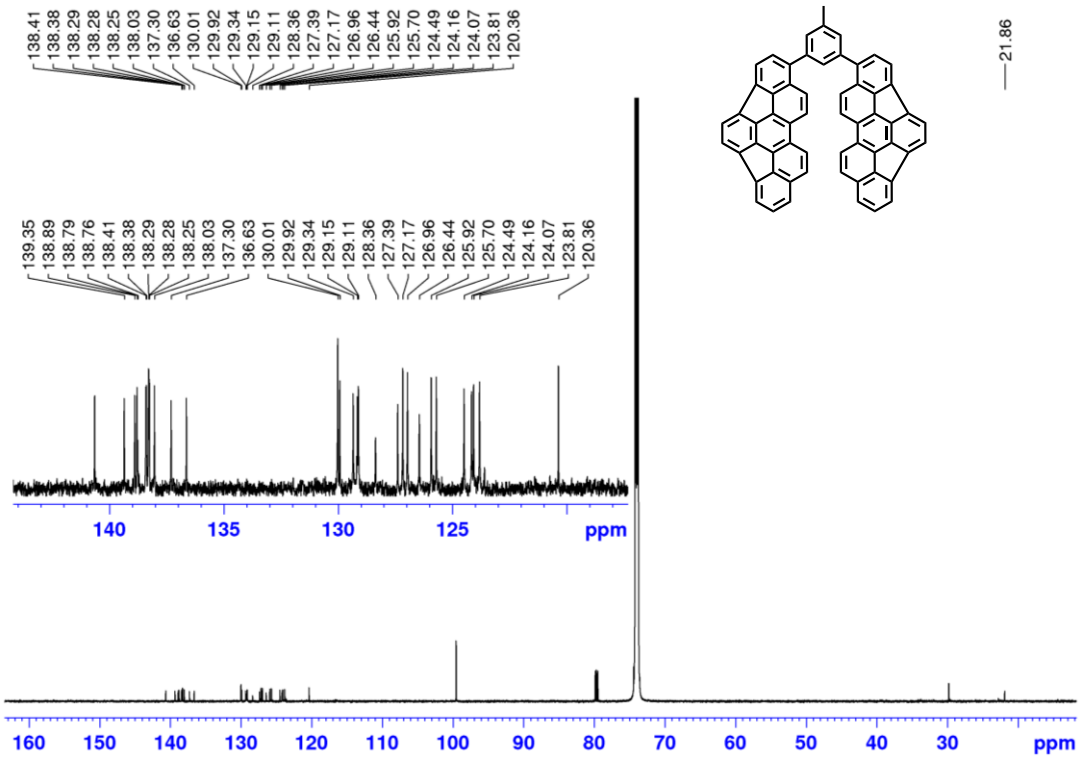

Figure A18. ^{13}C NMR (150 MHz, $C_2D_2Cl_4$, 293 K) spectrum of 9,9'-(5-methyl-1,3-phenylene)di-*as*-indaceno[*3,2,1,8,7,6-pqrstuv*]picene **56**.

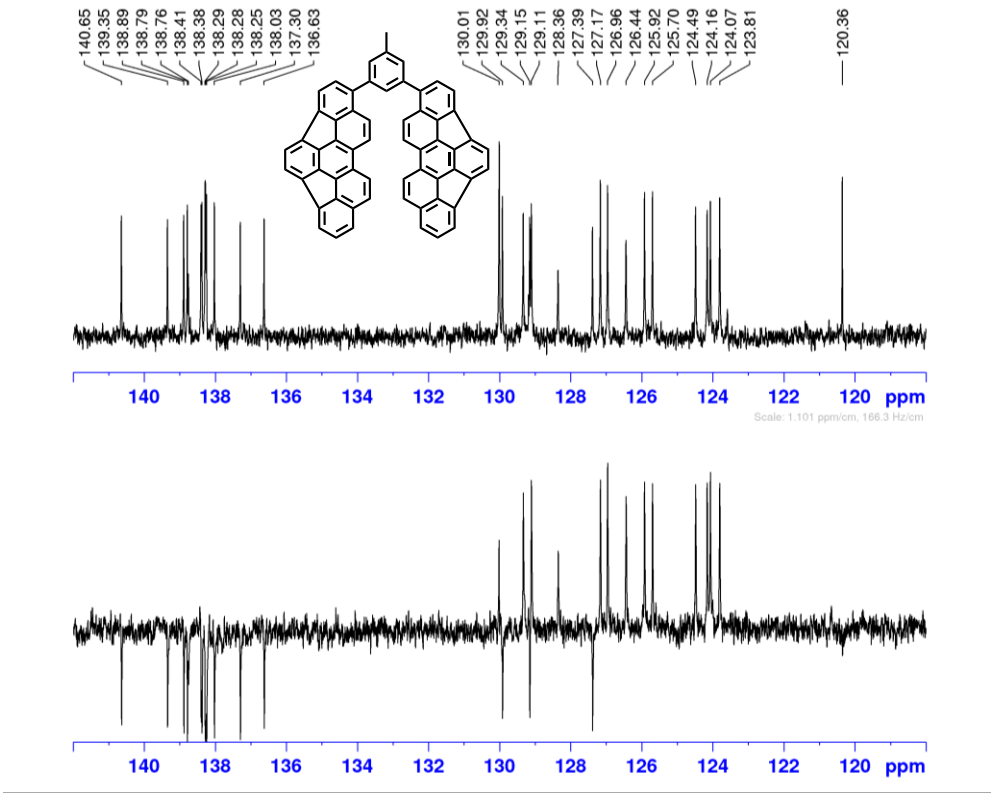

Figure A19. DEPT (150 MHz, $C_2D_2Cl_4$, 293 K) spectrum of 9,9'-(5-methyl-1,3-phenylene)di-*as*-indaceno[*3,2,1,8,7,6-pqrstuv*]picene **56**.

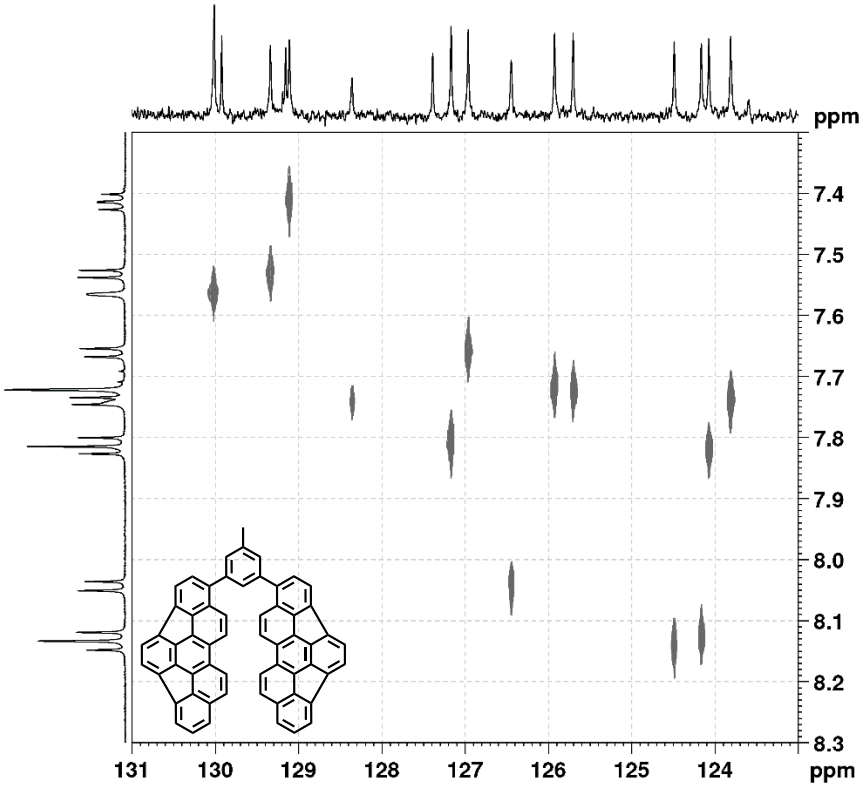

Figure A20. ^{13}C-^{1}H HETCOR (150 MHz, $C_2D_2Cl_4$, 293 K) spectrum of 9,9'-(5-methyl-1,3-phenylene)-di-*as*-indaceno[*3,2,1,8,7,6-pqrstuv*]picene **56**.

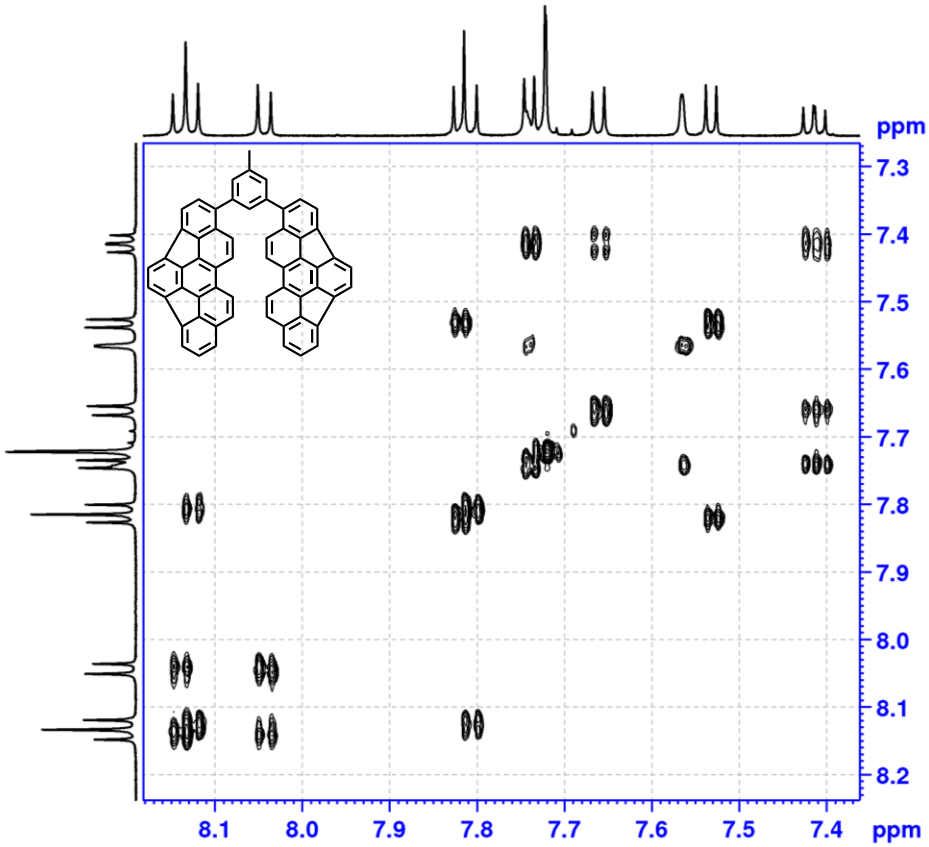

Figure A21. ^{1}H-^{13}C HMBC (400 MHz, DMSO, 293 K) spectrum of of 9,9'-(5-methyl-1,3-phenylene)-di-*as*-indaceno[*3,2,1,8,7,6-pqrstuv*]picene **56**.

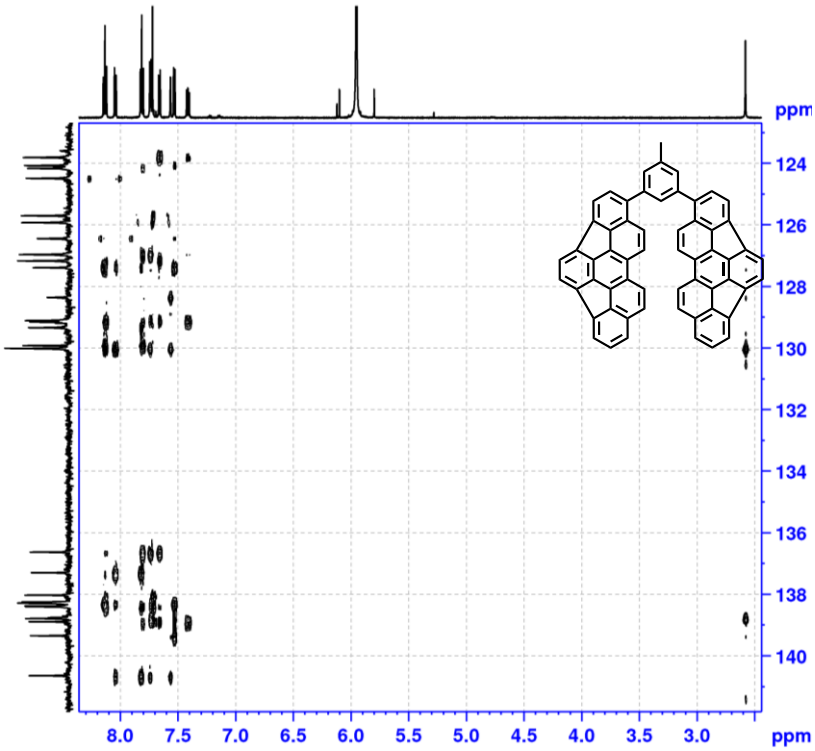

Figure A22. ^{1}H-^{1}H COSY (400 MHz, DMSO, 293 K) spectrum of of 9,9'-(5-methyl-1,3-phenylene)-di-*as*-indaceno[*3,2,1,8,7,6-pqrstuv*]picene **56**.

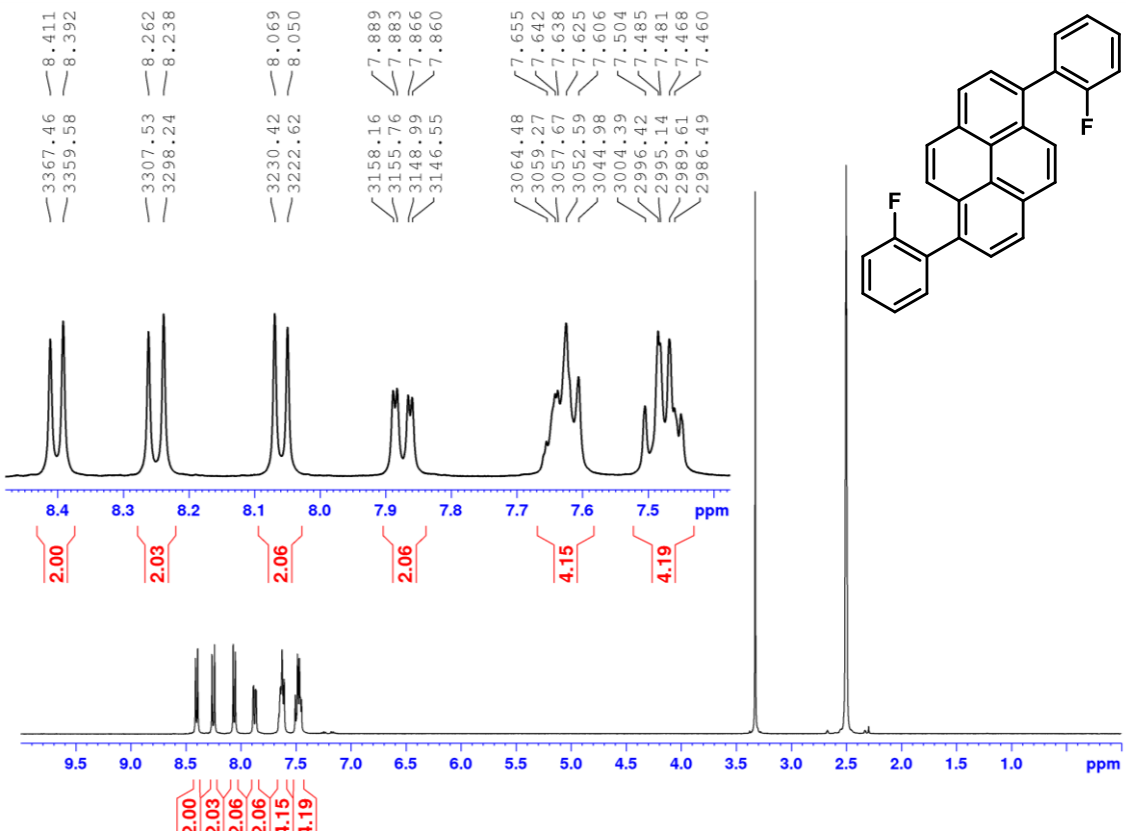

Figure A23. [1]H NMR (400 MHz, DMSO, 293 K) spectrum of 1,6-bis(2-fluorophenyl)pyrene **59**.

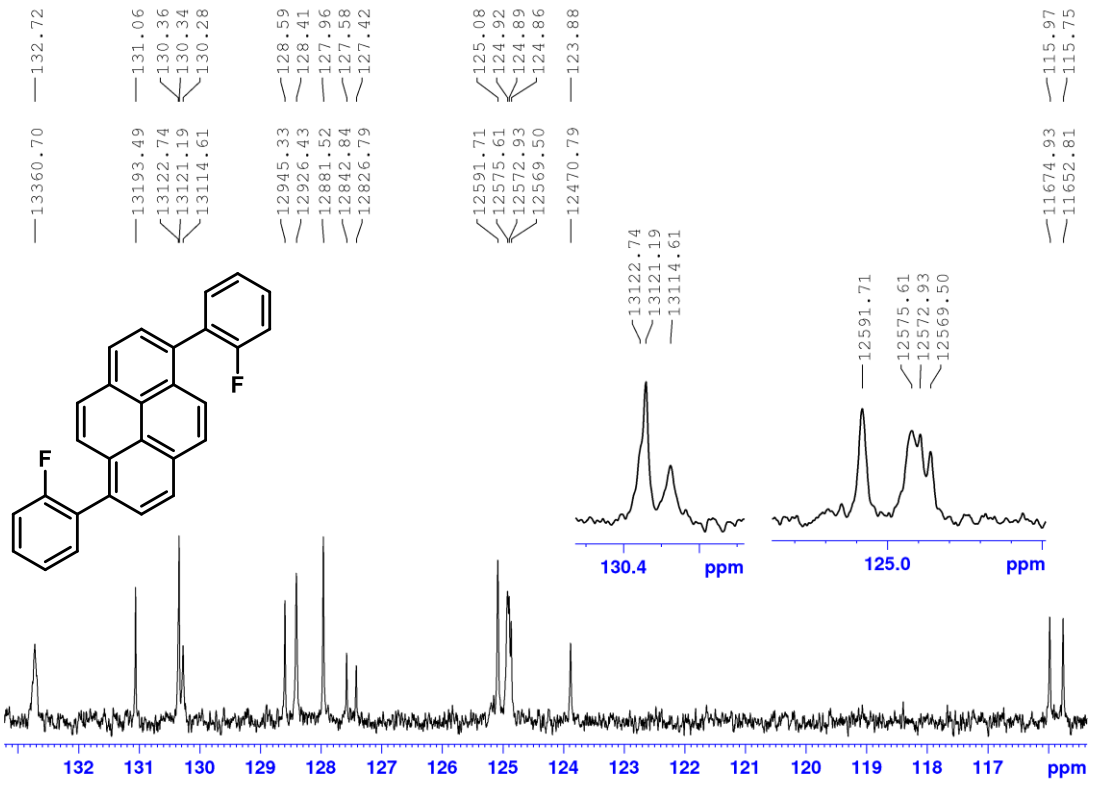

Figure A24. [13]C NMR (101 MHz, DMSO, 293 K) spectrum of 1,6-bis(2-fluorophenyl)pyrene **59**.

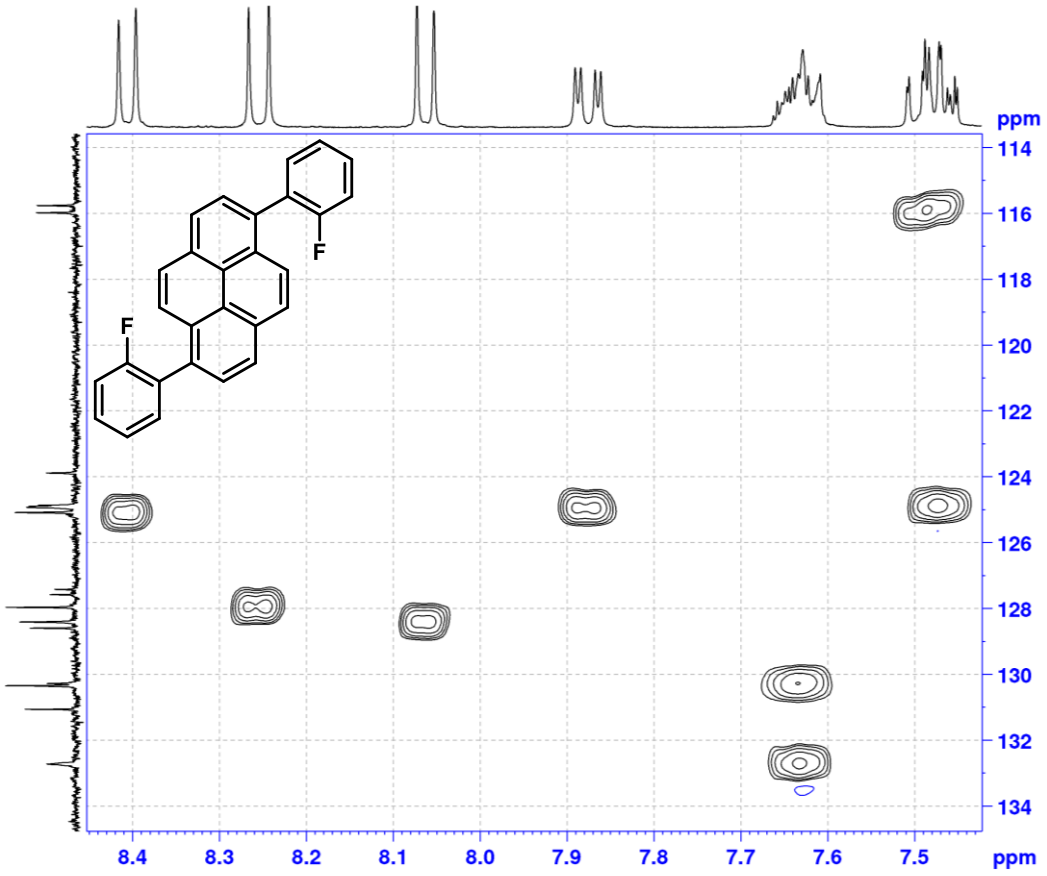

Figure A25. ^{1}H-^{13}C HSQC NMR (101 MHz, DMSO, 293 K) spectrum of 1,6-bis(2-fluorophenyl)pyrene **59**.

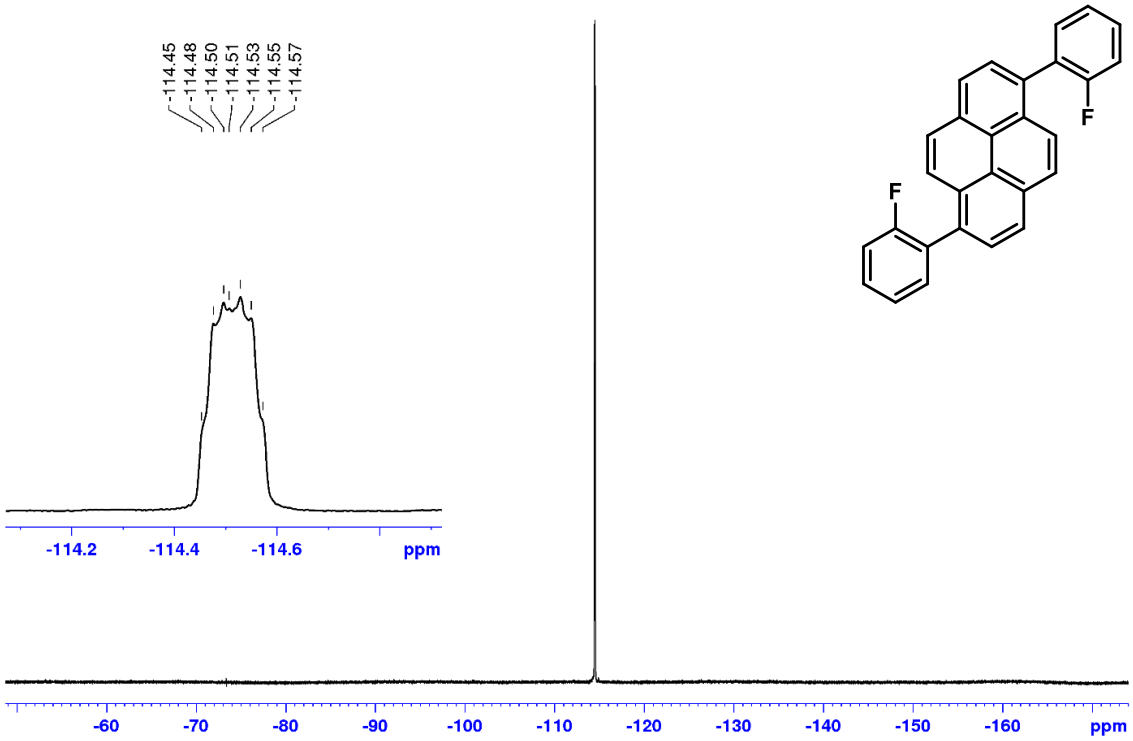

Figure A26. ^{19}F NMR (377 MHz, DMSO, 293 K) spectrum of 1,6-bis(2-fluorophenyl)pyrene **59**.

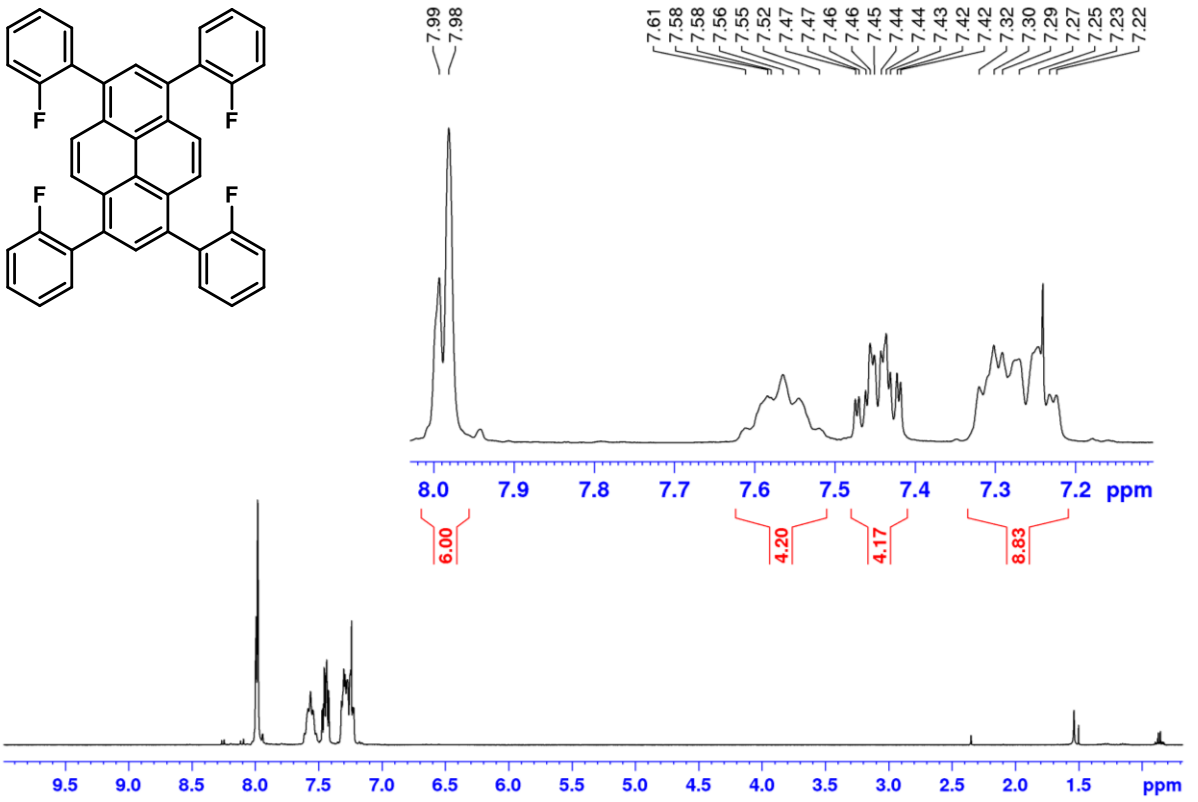

Figure A27. ^{1}H NMR (400 MHz, $CDCl_3$, 293 K) spectrum of 1,3,6,8-tetrakis(2-fluorophenyl)pyrene **62**.

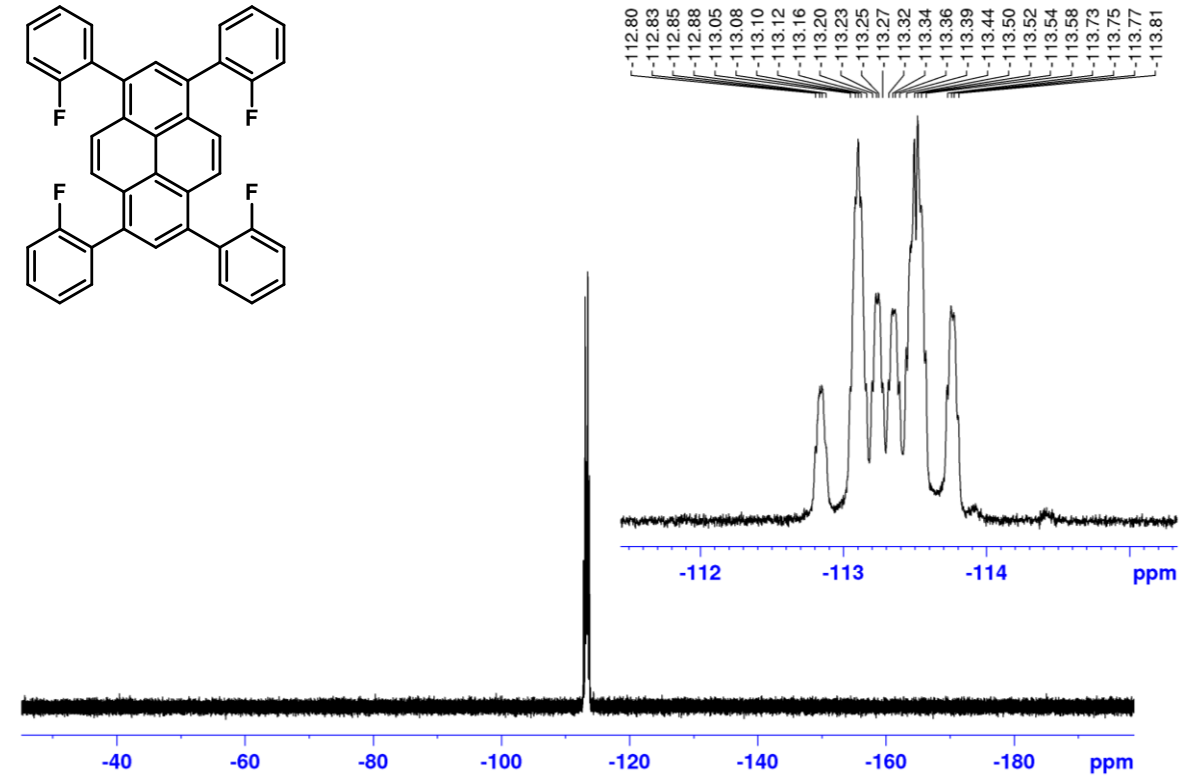

Figure A28. ^{19}F NMR (282 MHz, $CDCl_3$, 293 K) spectrum of 1,3,6,8-tetrakis(2-fluorophenyl)pyrene **62**.

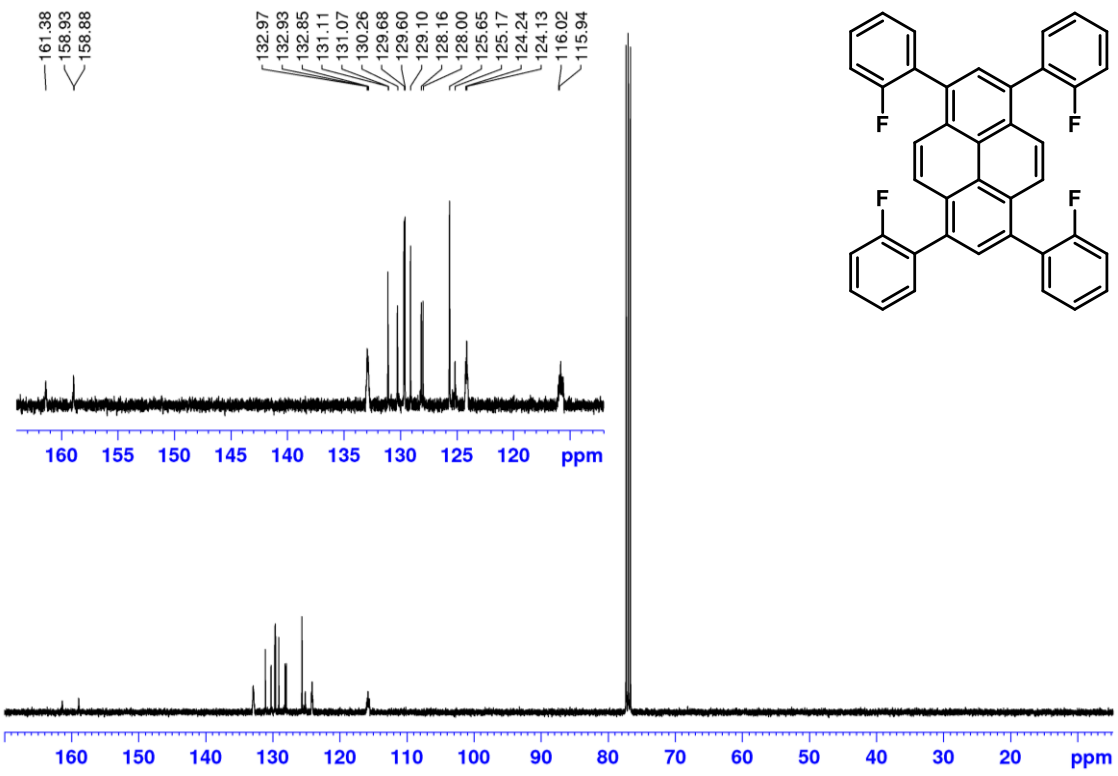

Figure A29. ^{13}C NMR (101 MHz, $CDCl_3$, 293 K) spectrum of 1,3,6,8-tetrakis(2-fluorophenyl)pyrene **62**.

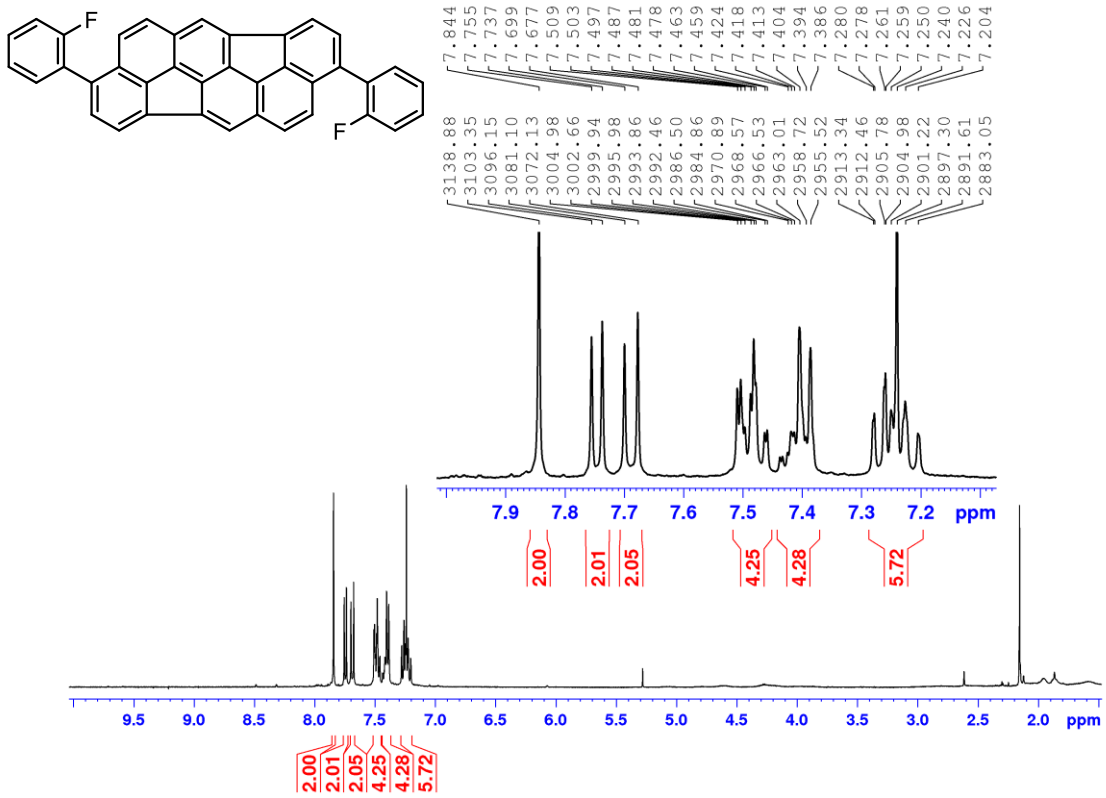

Figure A30. ^{1}H NMR (400 MHz, $CDCl_3$, 293 K) spectrum of 3,9-bis(2-fluorophenyl)diindeno[*4,3,2,1-cdef:4',3',2',1'-mno*]chrysene **65a**.

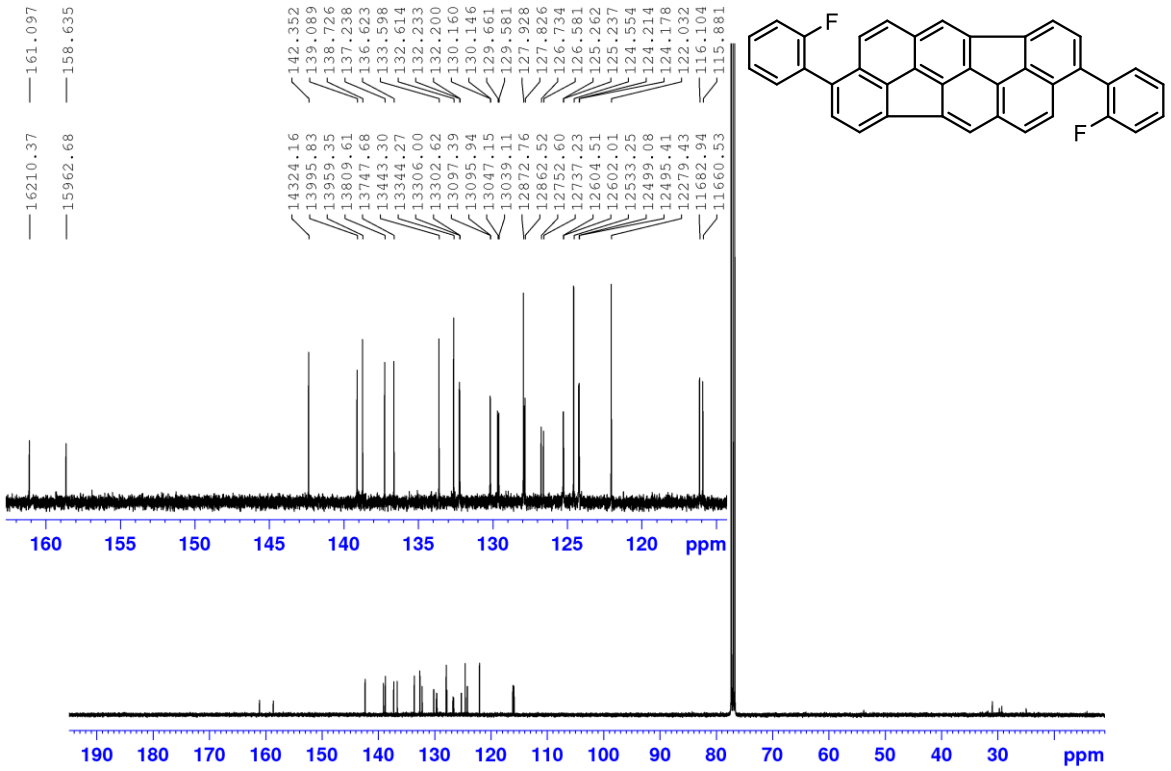

Figure A31. ^{13}C NMR (101 MHz, $CDCl_3$, 293 K) of 3,9-bis(2-fluorophenyl)diindeno[4,3,2,1-*cdef*:4',3',2',1'-*mno*]chrysene **65a**.

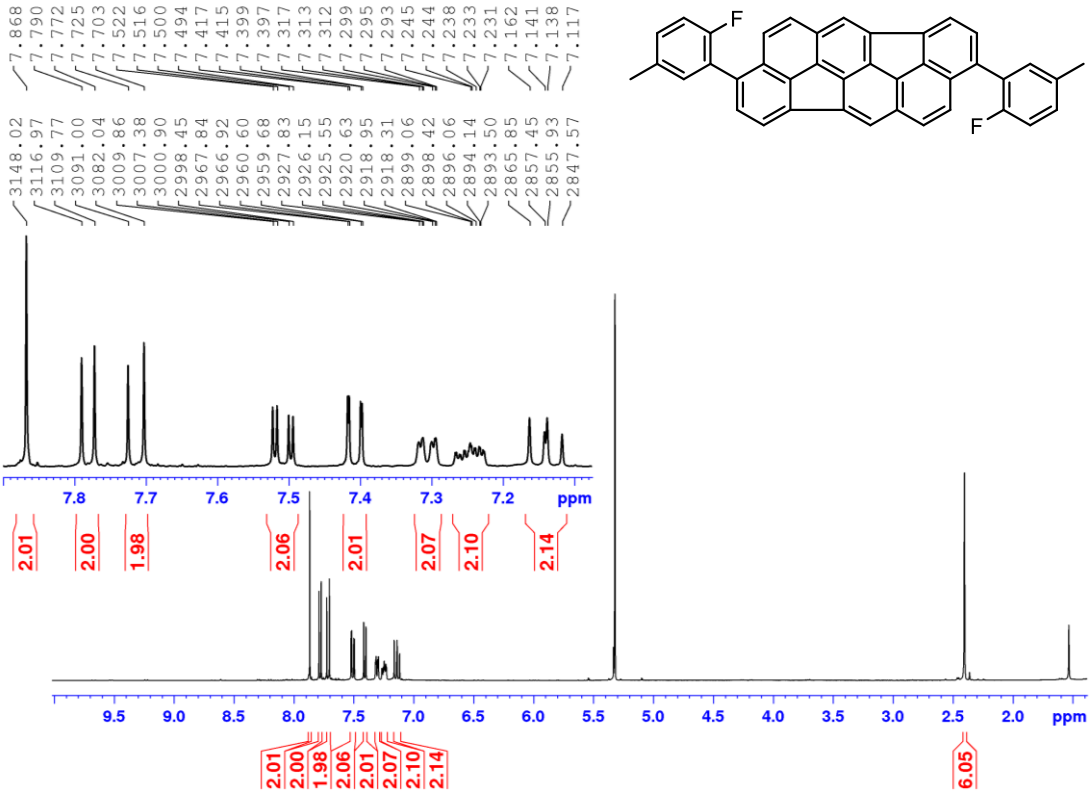

Figure A32. ^{1}H NMR (400 MHz, CD_2Cl_2, 293 K) of 3,9-bis(2-fluoro-5-methylphenyl)diindeno[*4,3,2,1-cdef:4',3',2',1'-lmno*]chrysene **65b**.

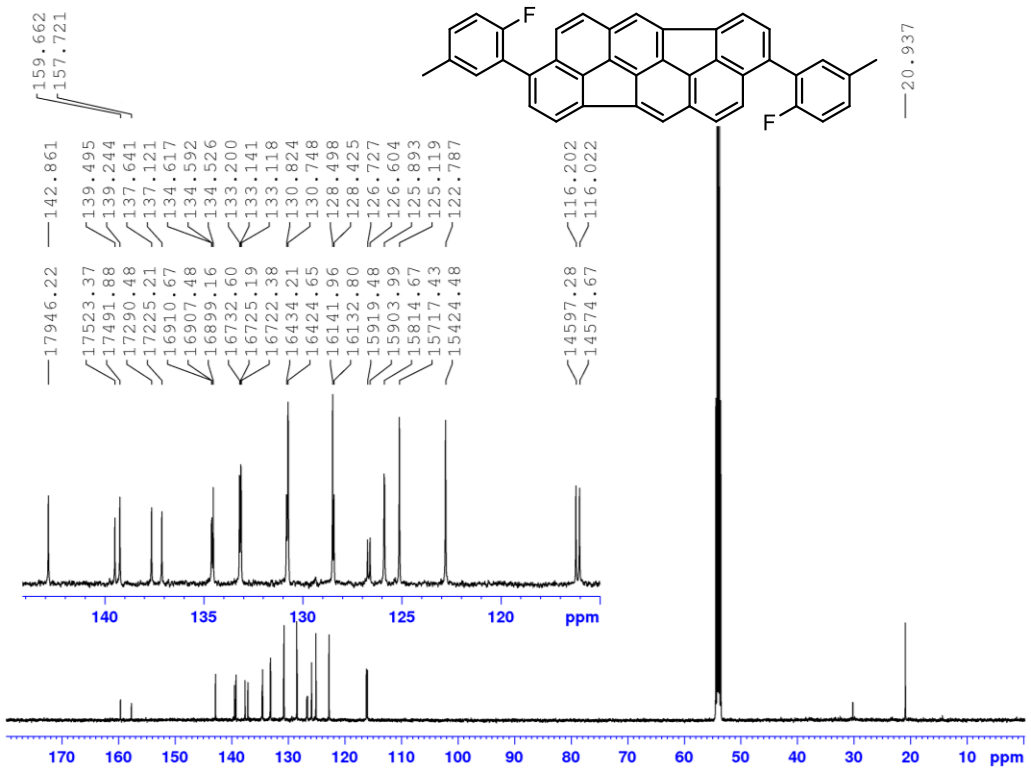

Figure A33. ^{13}C NMR (101 MHz, CD_2Cl_2, 293 K) of 3,9-bis(2-fluoro-5-methylphenyl)diindeno[4,3,2,1-*cdef*:4',3',2',1'-*lmno*]chrysene **65b**.

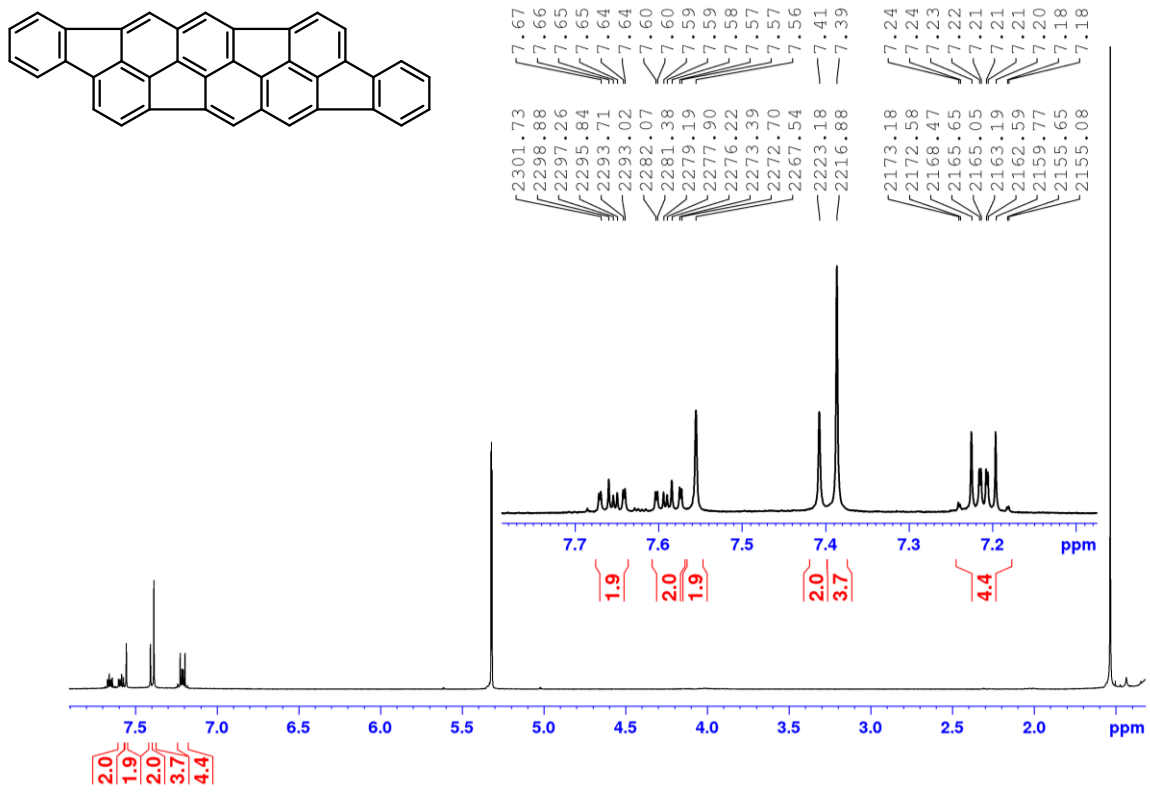

Figure A34. ^{1}H NMR (300 MHz, CD_2Cl_2, 293 K) of benzo[*6,7*]-*as*-indaceno[*8,1,2,3-bcdef*]benzo[*6,7*]-*as*-indaceno[*8,1,2,3-klmno*]chrysene **66a**.

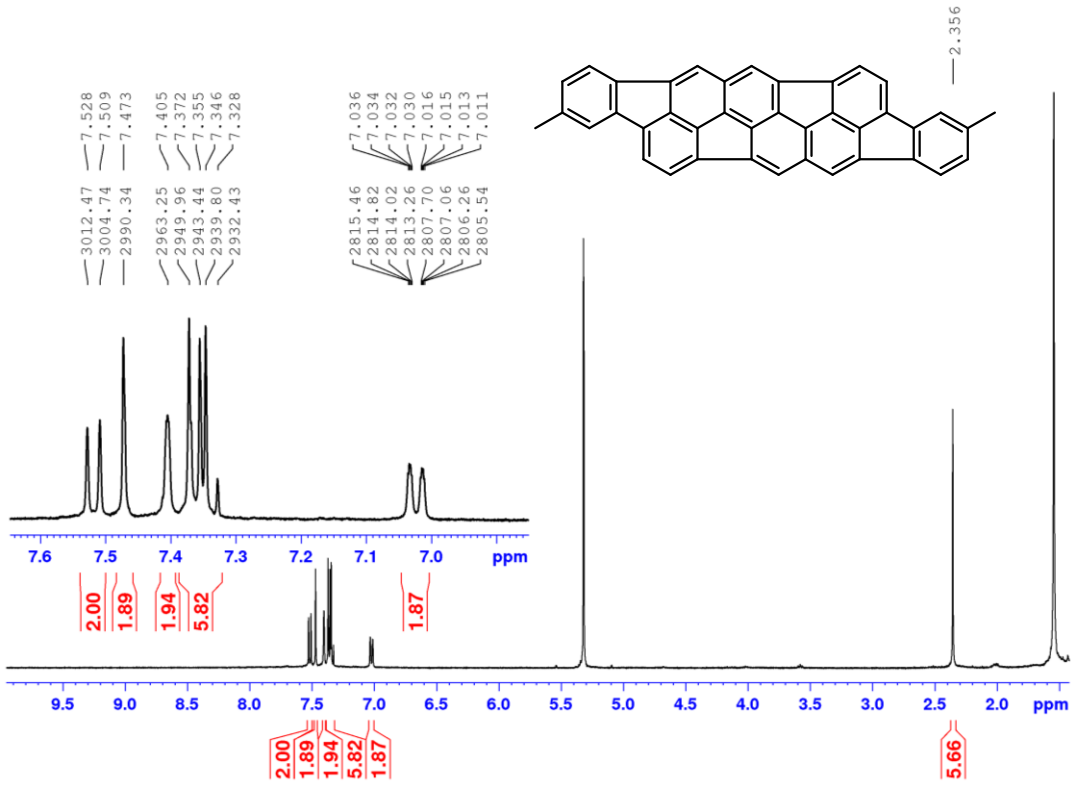

Figure A35. ^{1}H NMR (400 MHz, CD_2Cl_2, 293 K) of 3,11-dimethylbenzo[*6,7*]-*as*-indaceno[*8,1,2,3-bcdef*]benzo[*6,7*]-*as*-indaceno[*8,1,2,3-klmno*]chrysene **66b**.

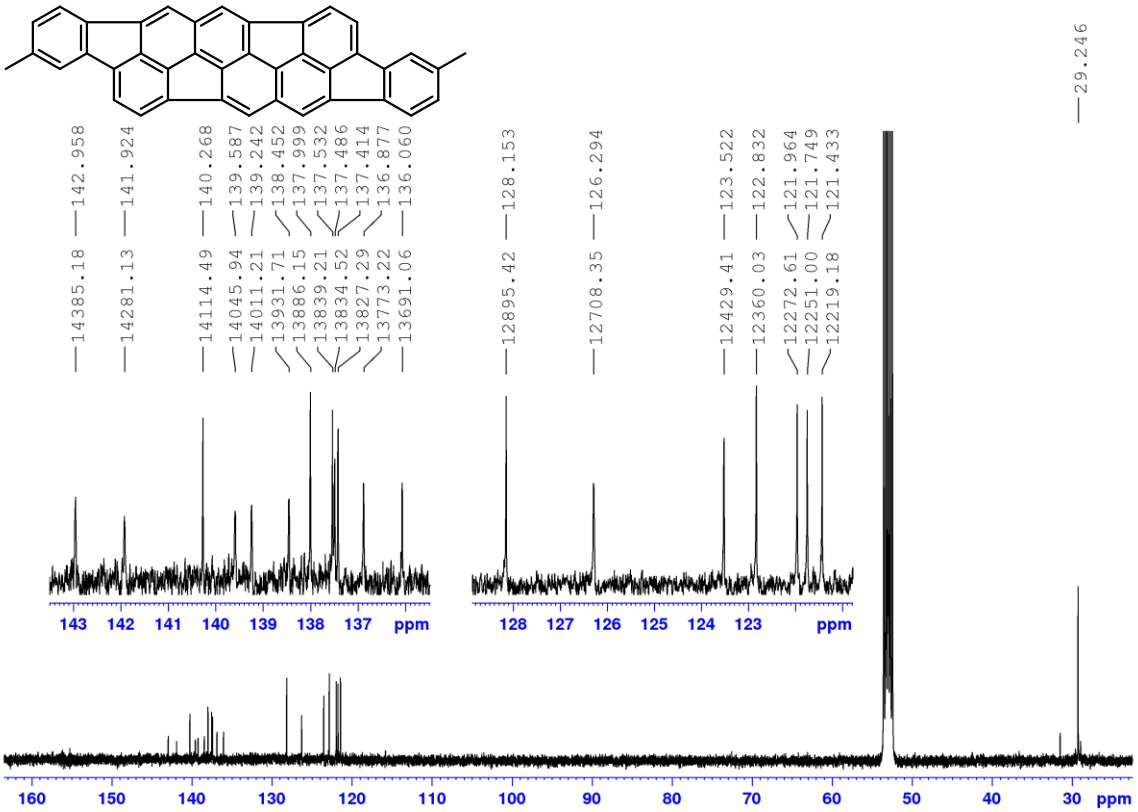

Figure A36. ^{13}C NMR (101 MHz, CD_2Cl_2, 293 K) spectrum of 3,11-dimethylbenzo[*6,7*]-*as*-indaceno[*8,1,2,3-bcdef*]benzo[*6,7*]-*as*-indaceno[*8,1,2,3-klmno*]chrysene **66b**.

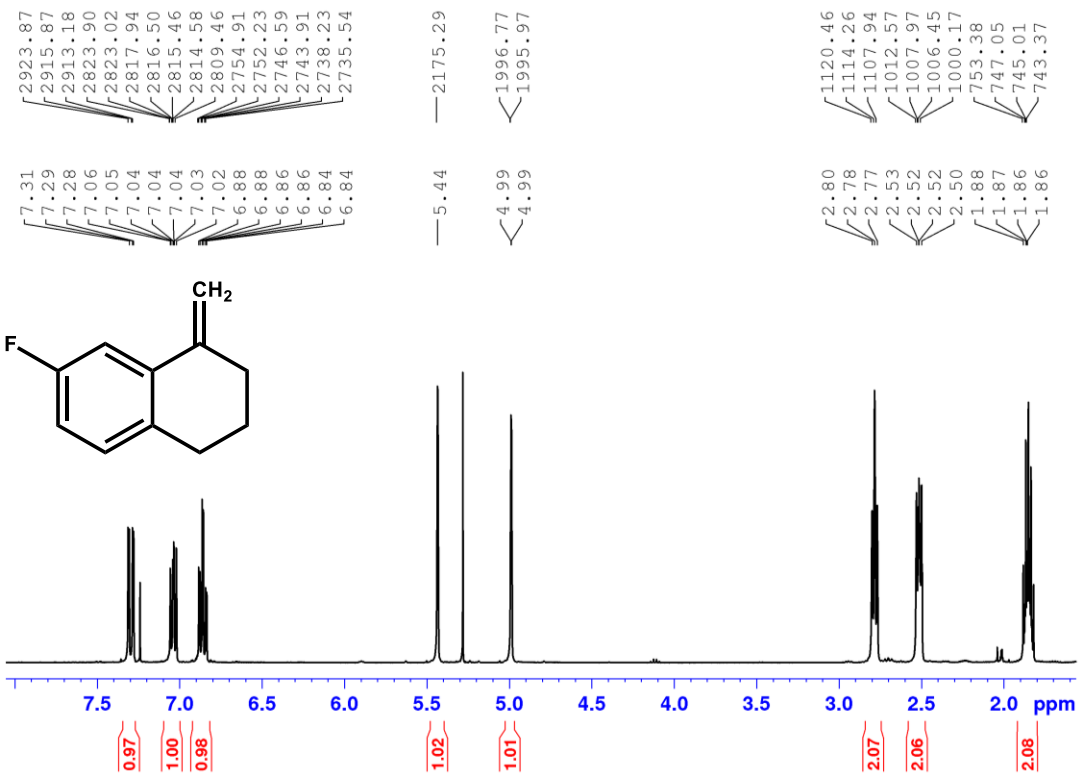

Figure A37. ^{1}H NMR (400 MHz, $CDCl_3$, 293 K) spectrum of 7-fluoro-1-methylene-1,2,3,4-tetrahydro-naphthalene **75**.

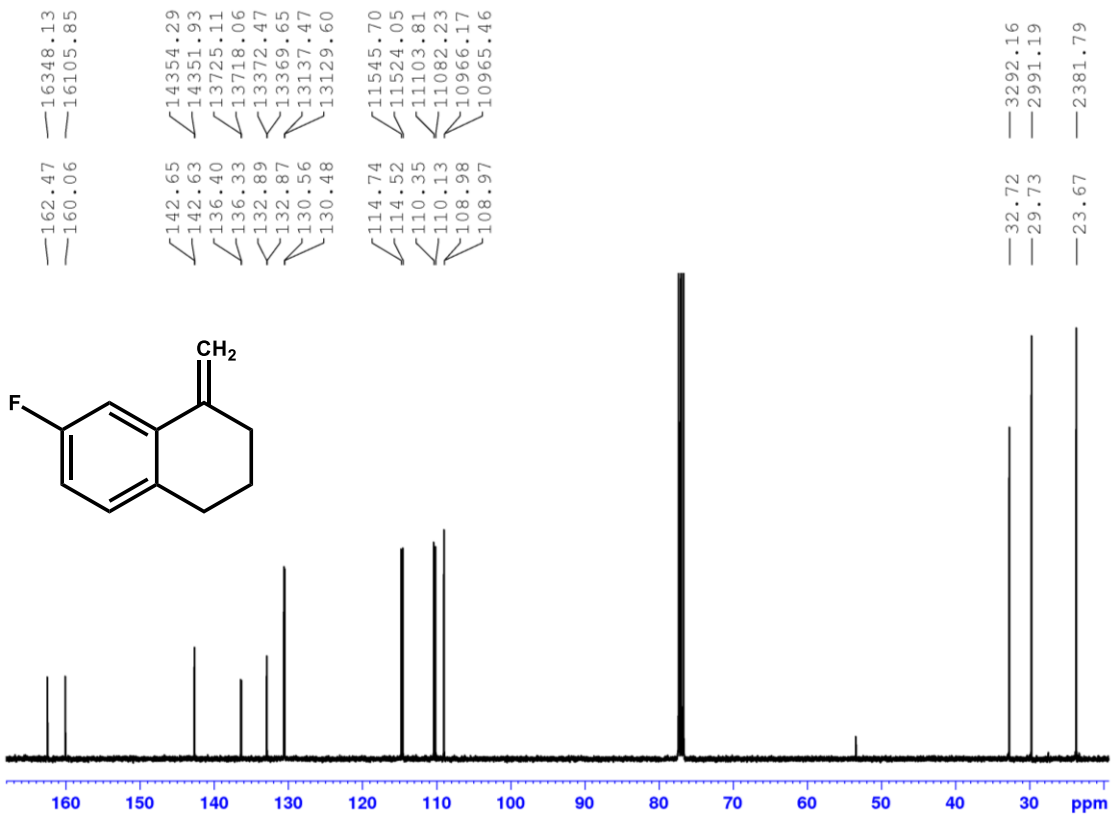

Figure A38. ^{13}C NMR (101 MHz, $CDCl_3$, 293 K) spectrum of 7-fluoro-1-methylene-1,2,3,4-tetrahydro-naphthalene **75**.

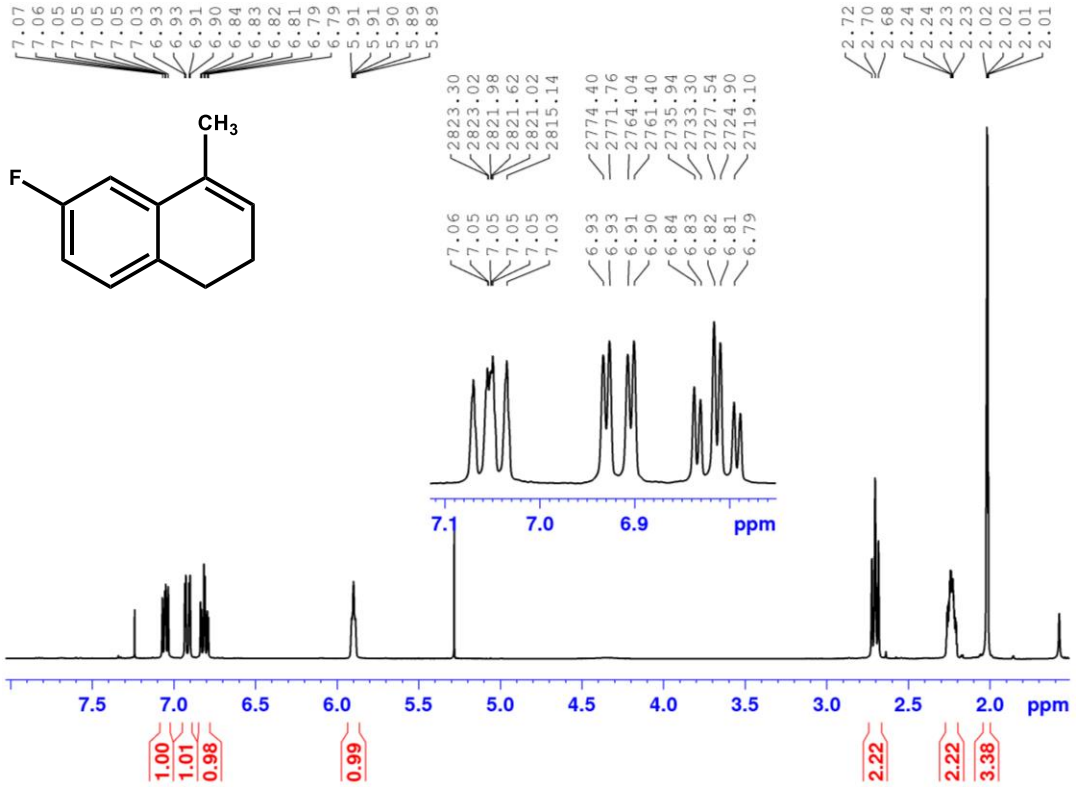

Figure A39. ^{1}H NMR (400 MHz, $CDCl_3$, 293 K) spectrum of 6-fluoro-4-methyl-1,2-dihydronaphthalene **76**.

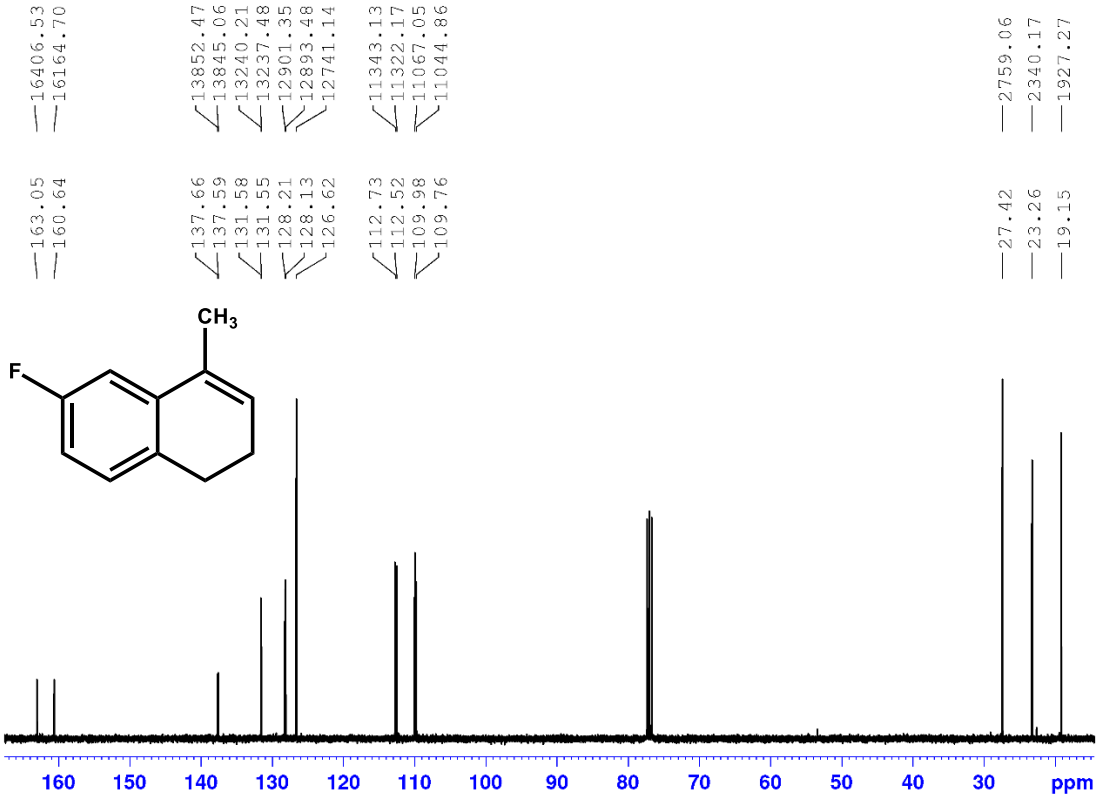

Figure A40. ^{13}C NMR (101 MHz, $CDCl_3$, 293 K) spectrum of 6-fluoro-4-methyl-1,2-dihydronaphthalene **76**.

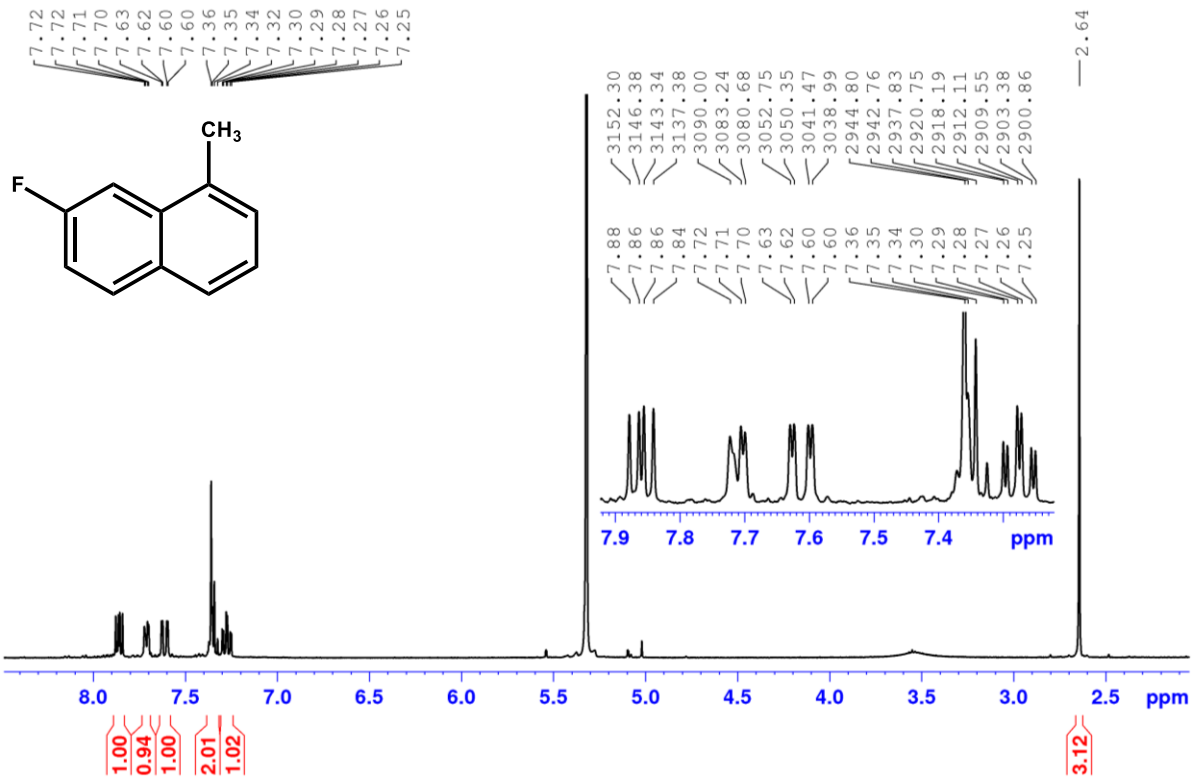

Figure A41. ^{1}H NMR (400 MHz, $CDCl_3$, 293 K) spectrum of 7-fluoro-1-methylnaphthalene **77**.

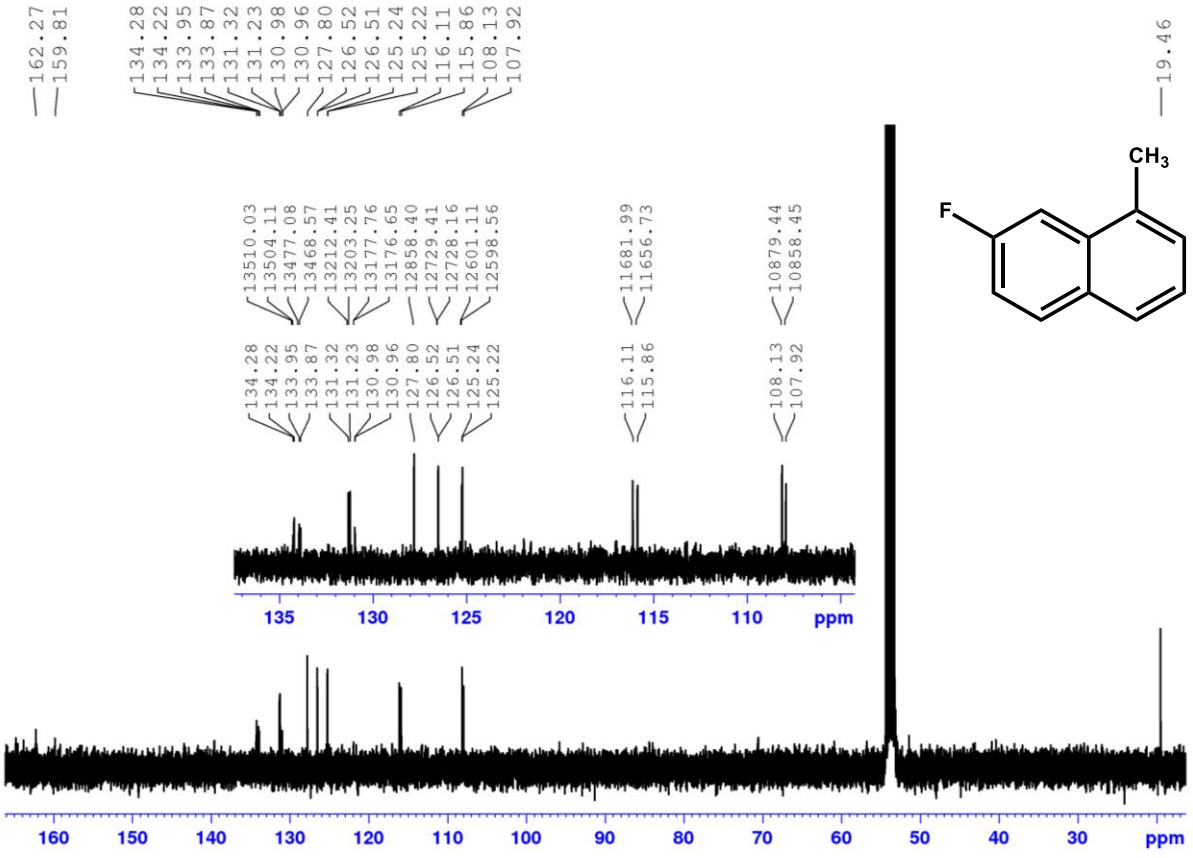

Figure A42. ^{13}C NMR (101 MHz, CD_2Cl_2, 293 K) spectrum of 7-fluoro-1-methylnaphthalene **77**.

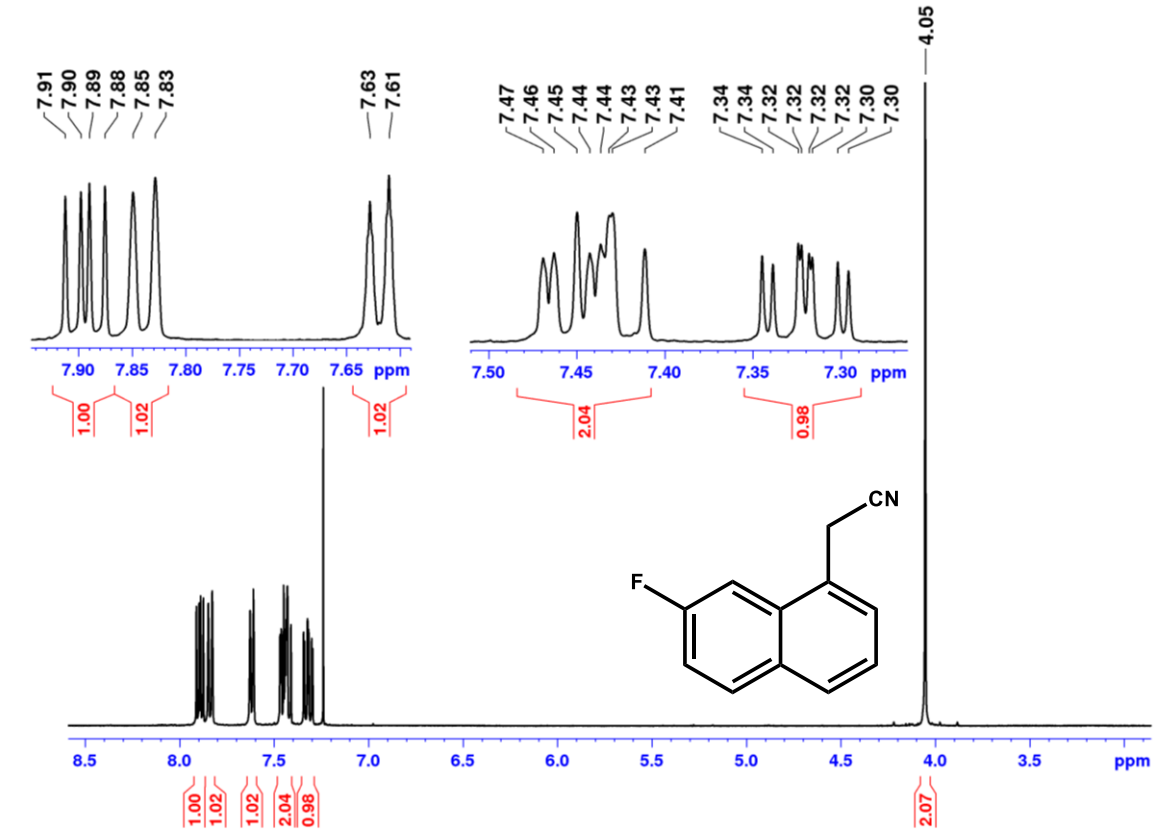

Figure A43. ^{1}H NMR (400 MHz, $CDCl_3$, 293 K) spectrum of 2-(7-fluoronaphthalen-1-yl)acetonitrile **79**.

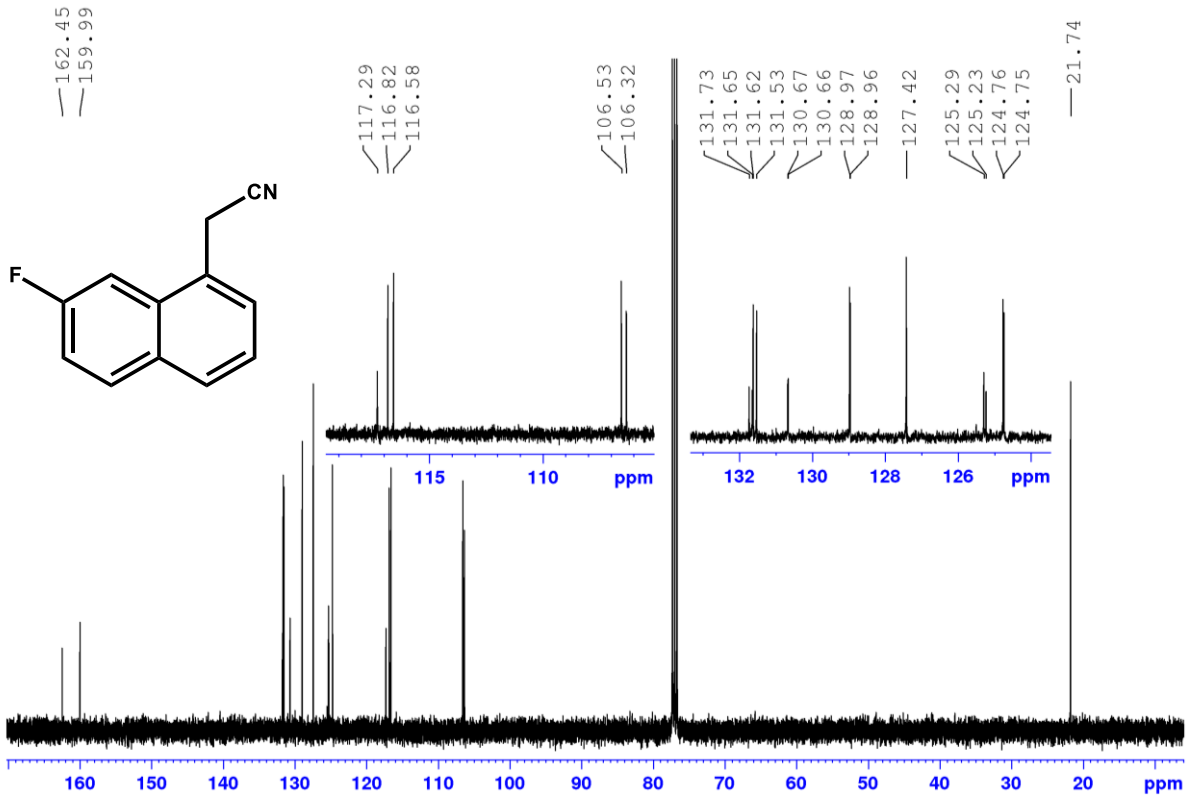

Figure A44. ^{13}C NMR (101 MHz, $CDCl_3$, 293 K) spectrum of 2-(7-fluoronaphthalen-1-yl)acetonitrile **79**.

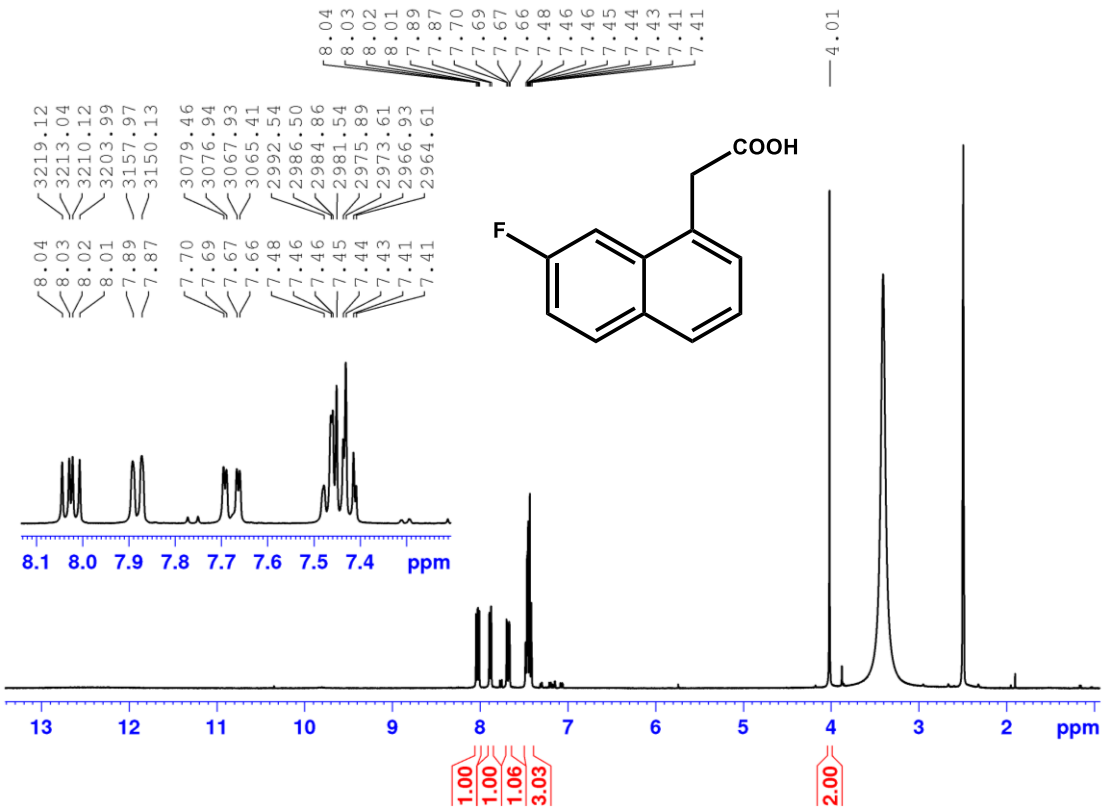

Figure A45. ^{1}H NMR (400 MHz, DMSO, 293 K) spectrum of 2-(7-fluoronaphthalen-1-yl)acetic acid **80**.

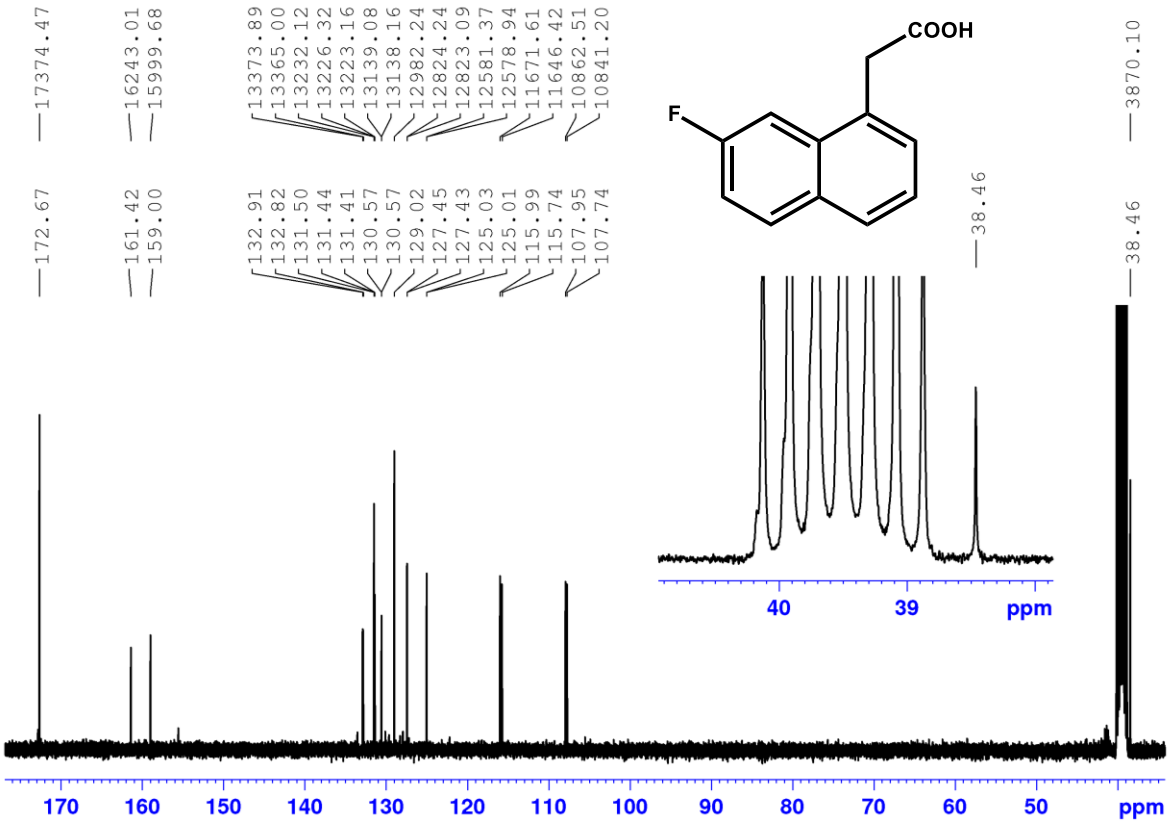

Figure A46. ^{13}C NMR (101 MHz, $CDCl_3$, 293 K) spectrum of 2-(7-fluoronaphthalen-1-yl)acetic acid **80**.

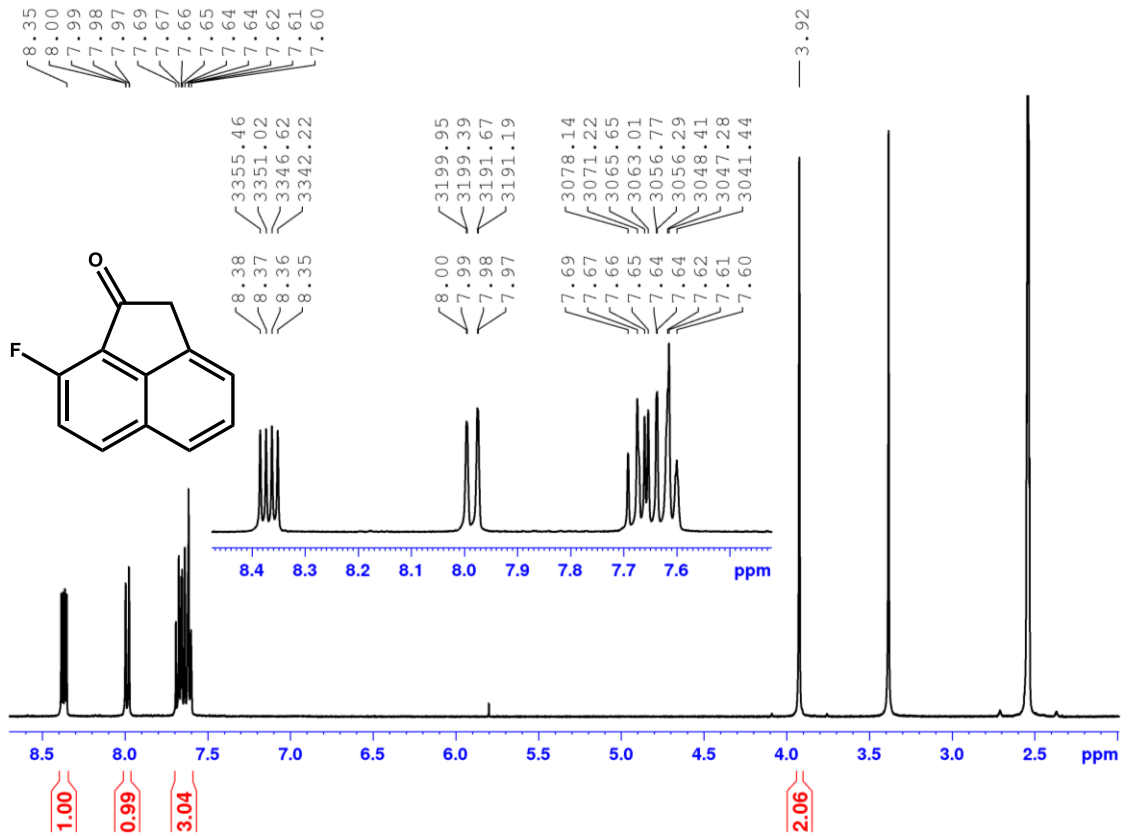

Figure A47. ^{1}H NMR (400 MHz, DMSO, 293 K) spectrum of 8-fluoroacenaphthylen-1(*2H*)-one **81**.

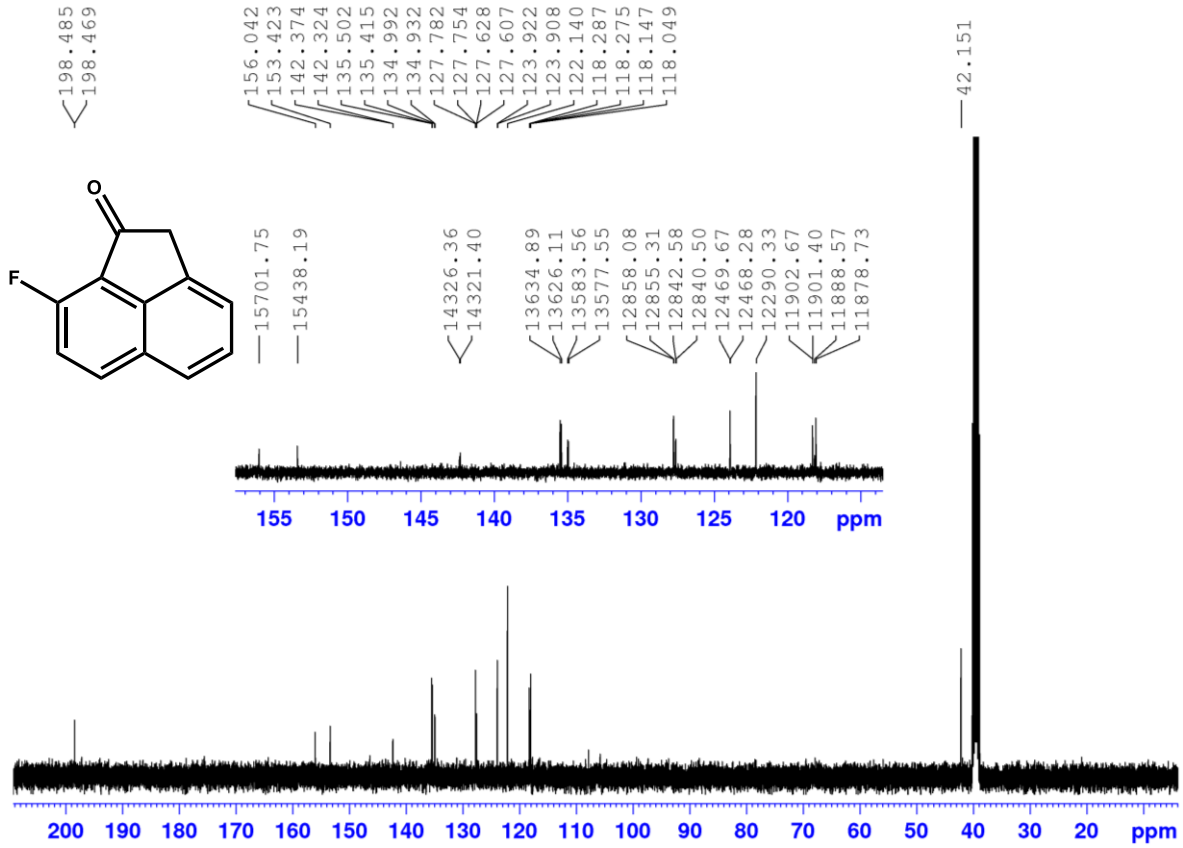

Figure A48. ^{13}C NMR (101 MHz, DMSO, 293 K) spectrum of 8-fluoroacenaphthylen-1(*2H*)-one **81**.

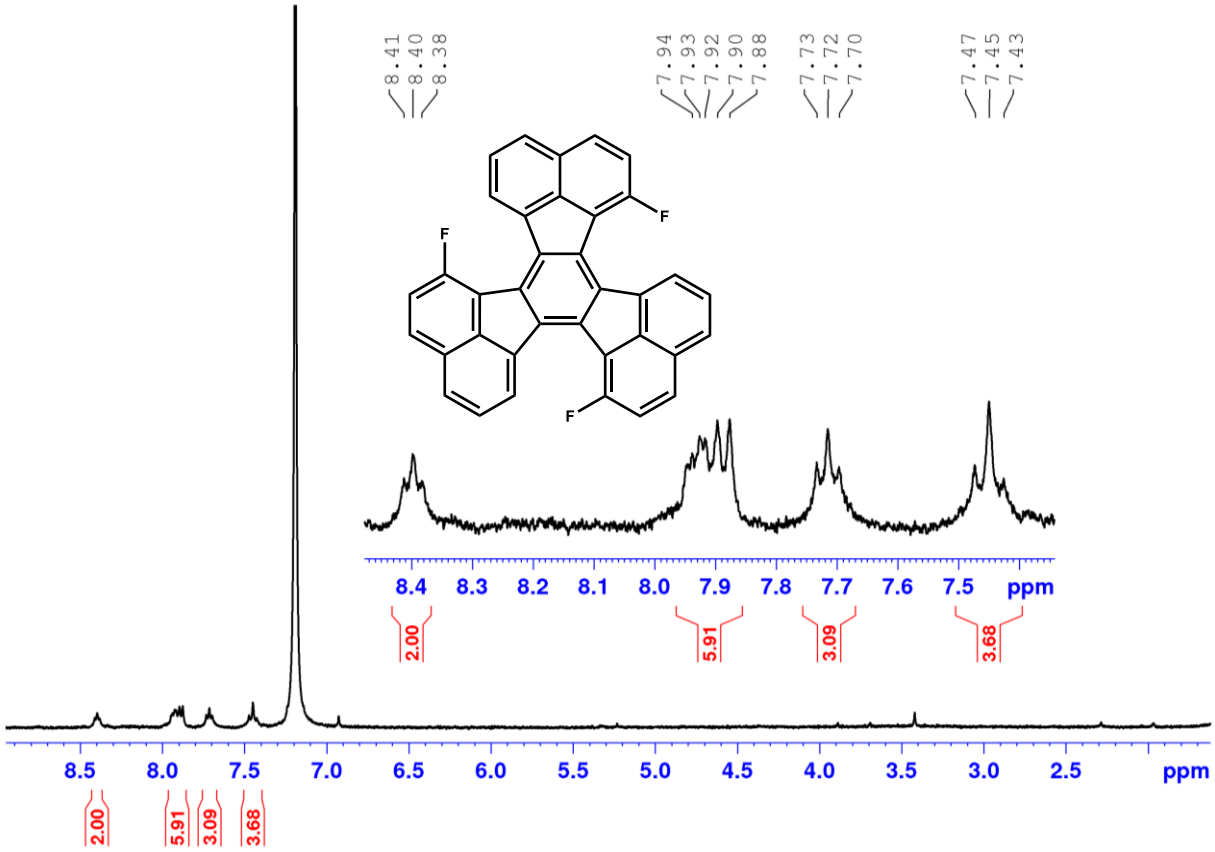

Figure A49. ^{1}H NMR (400 MHz, $C_2D_2Cl_4$, 293 K) spectrum of 1,7,13-trifluorodecacyclene **70**.

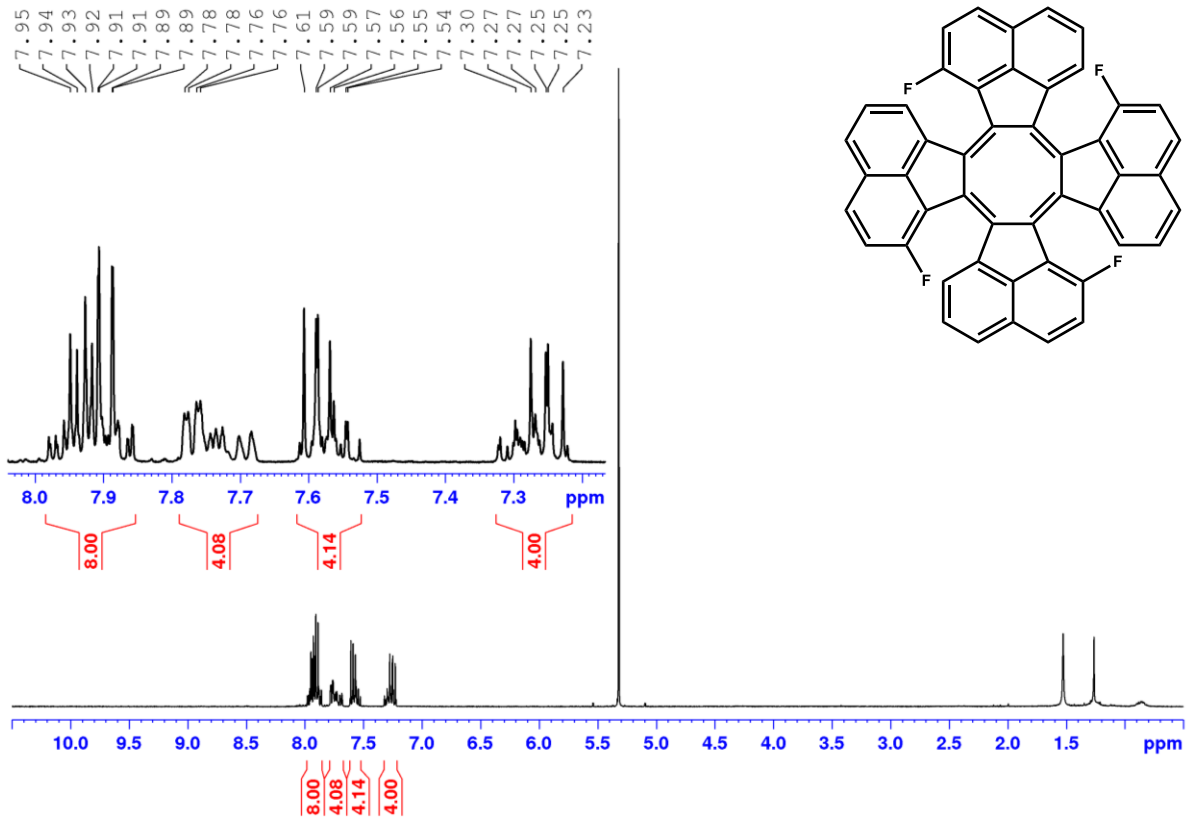

Figure A50. ^{13}C NMR (101 MHz, CD_2Cl_2, 293 K) spectrum of 1,7,13,19-tetrafluorotridecacyclene **72**.

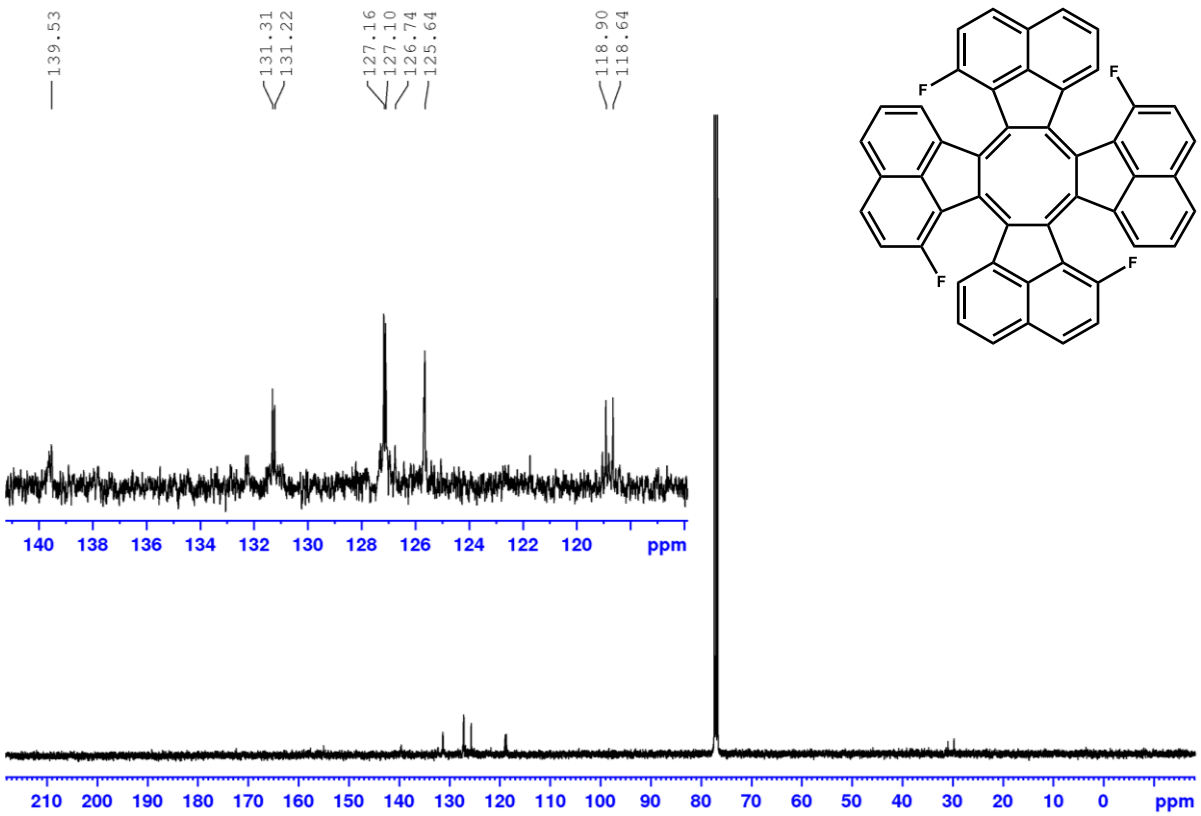

Figure A51. ^{13}C NMR (101 MHz, $CDCl_3$, 293 K) spectrum of 1,7,13,19-tetrafluorotridecacyclene **72**.

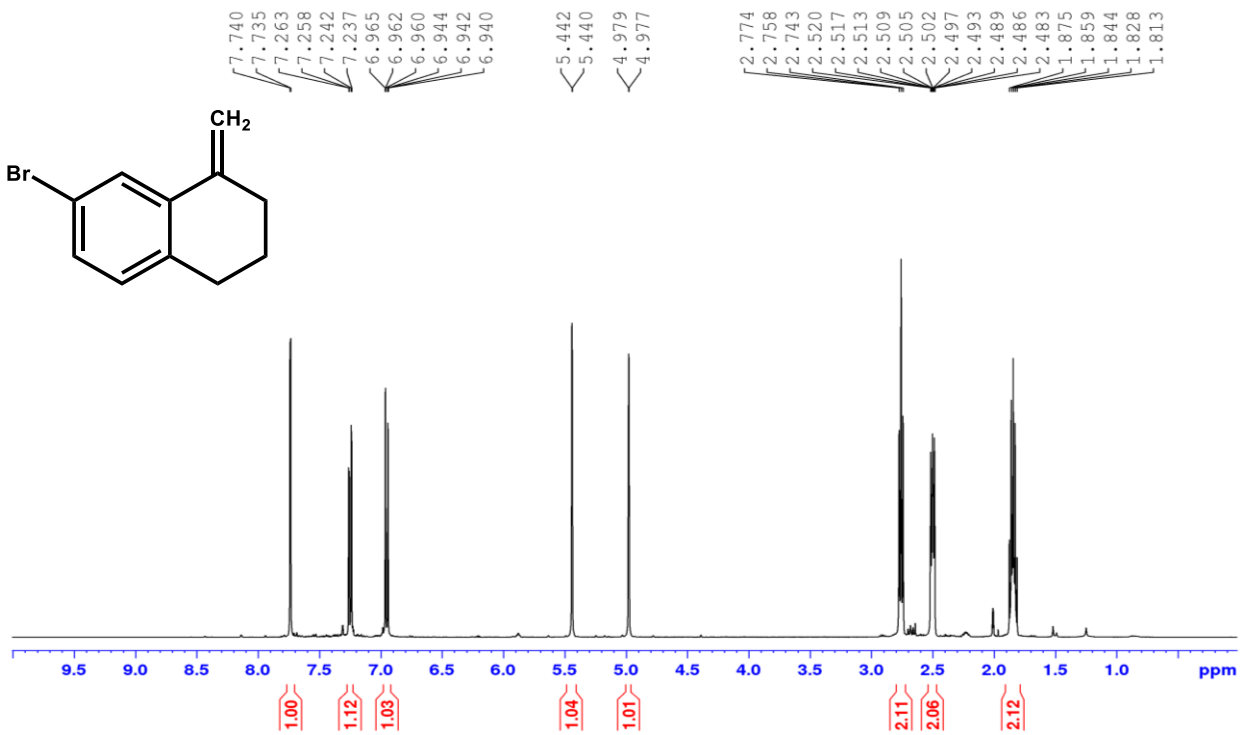

Figure A52. ^{1}H NMR (400 MHz, $CDCl_3$, 293 K) spectrum of 7-bromo-1-methylene-1,2,3,4-tetrahydro-naphthalene **83**.

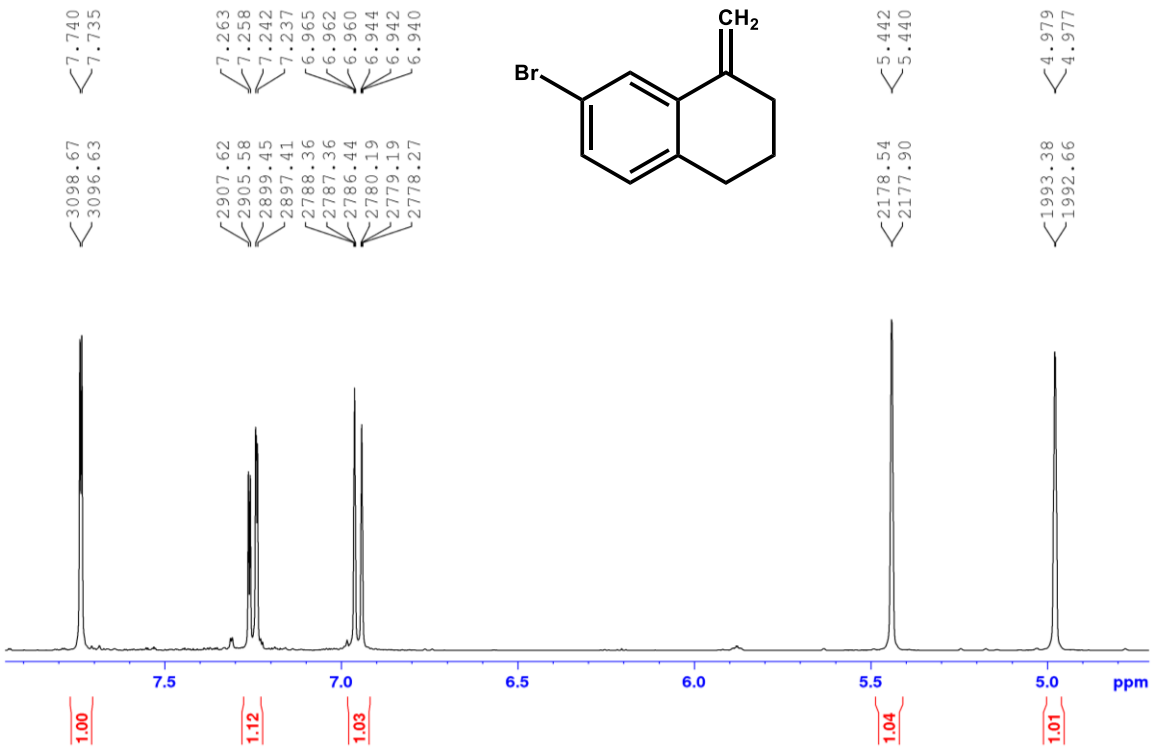

Figure A53. ^{1}H NMR (400 MHz, $CDCl_3$, 293 K) spectrum of 7-bromo-1-methylene-1,2,3,4-tetrahydro-naphthalene **83**.

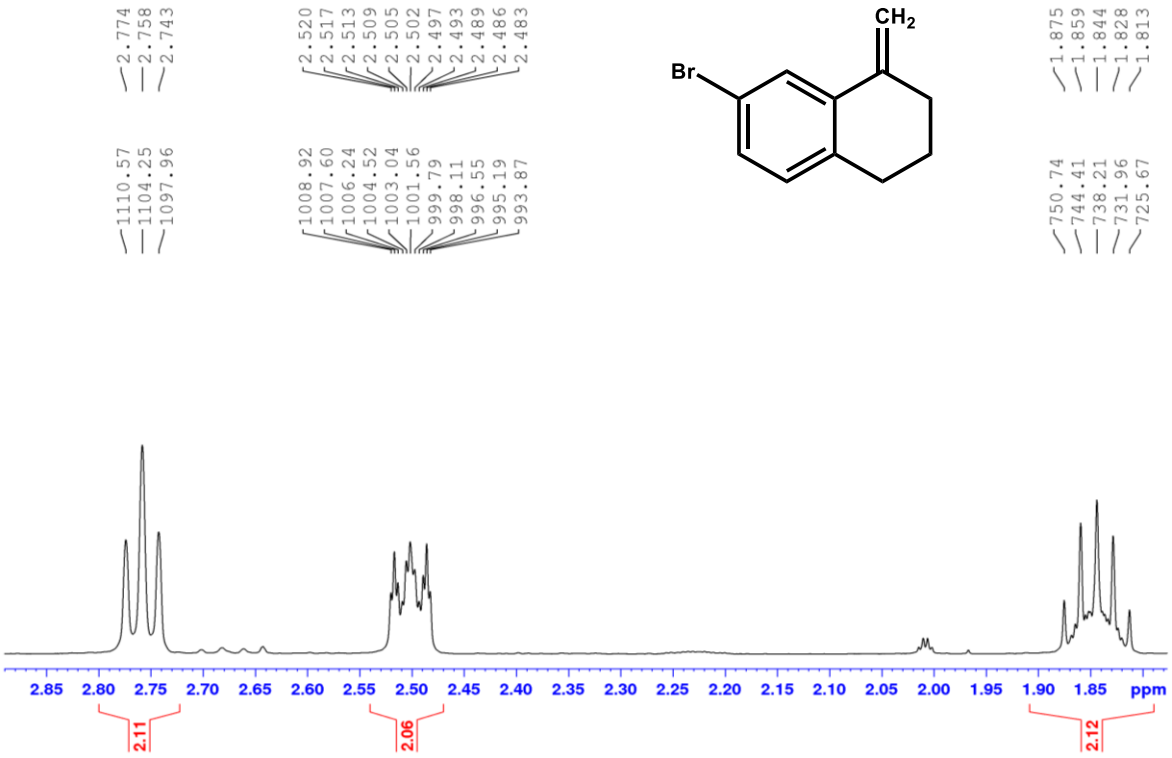

Figure A54. ^{1}H NMR (400 MHz, $CDCl_3$, 293 K) spectrum of 7-bromo-1-methylene-1,2,3,4-tetrahydro-naphthalene **83**.

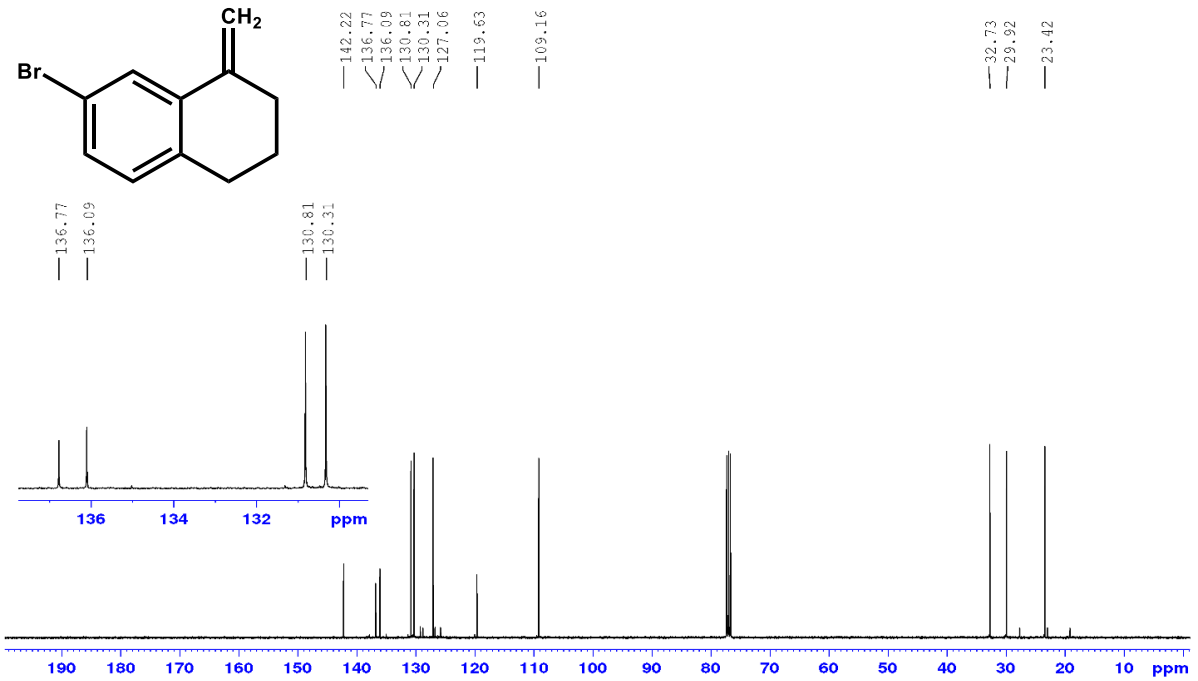

Figure A55. ^{13}C NMR (101 MHz, $CDCl_3$, 293 K) spectrum of 7-bromo-1-methylene-1,2,3,4-tetrahydro-naphthalene **83**.

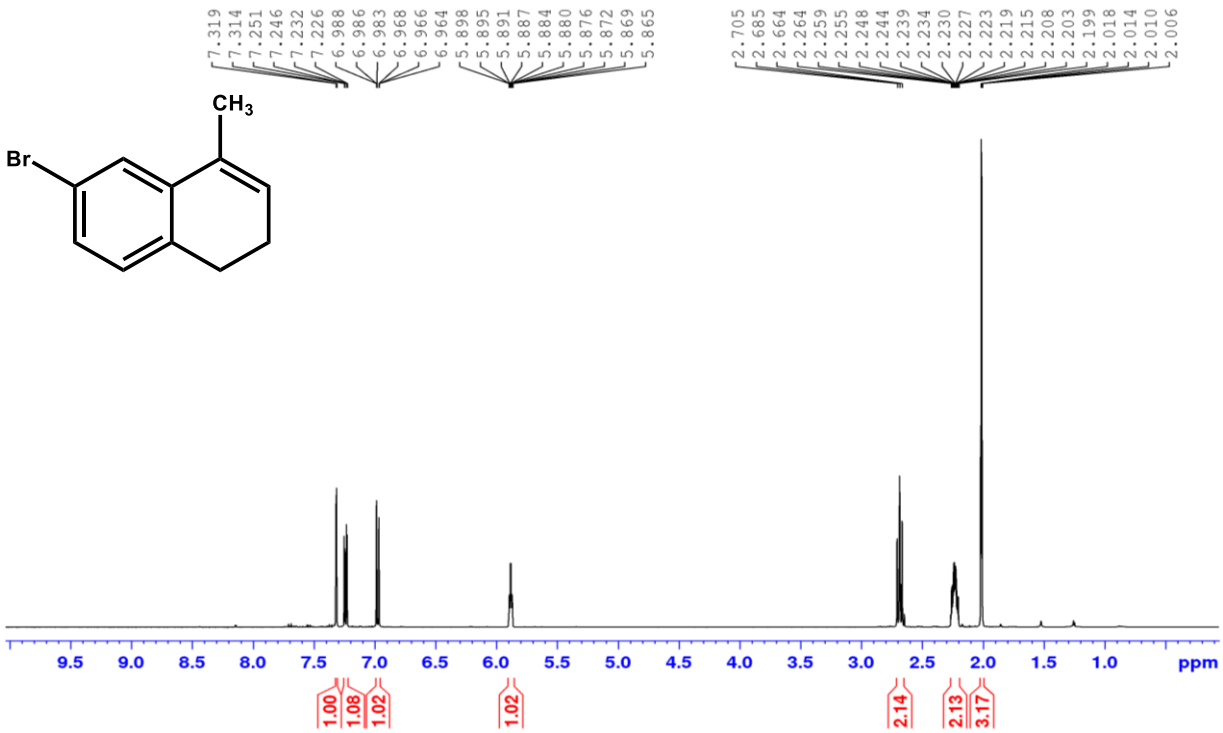

Figure A56. ^{1}H NMR (400 MHz, $CDCl_3$, 293 K) spectrum of 6-bromo-4-methyl-1,2-dihydronaphthalene **84**.

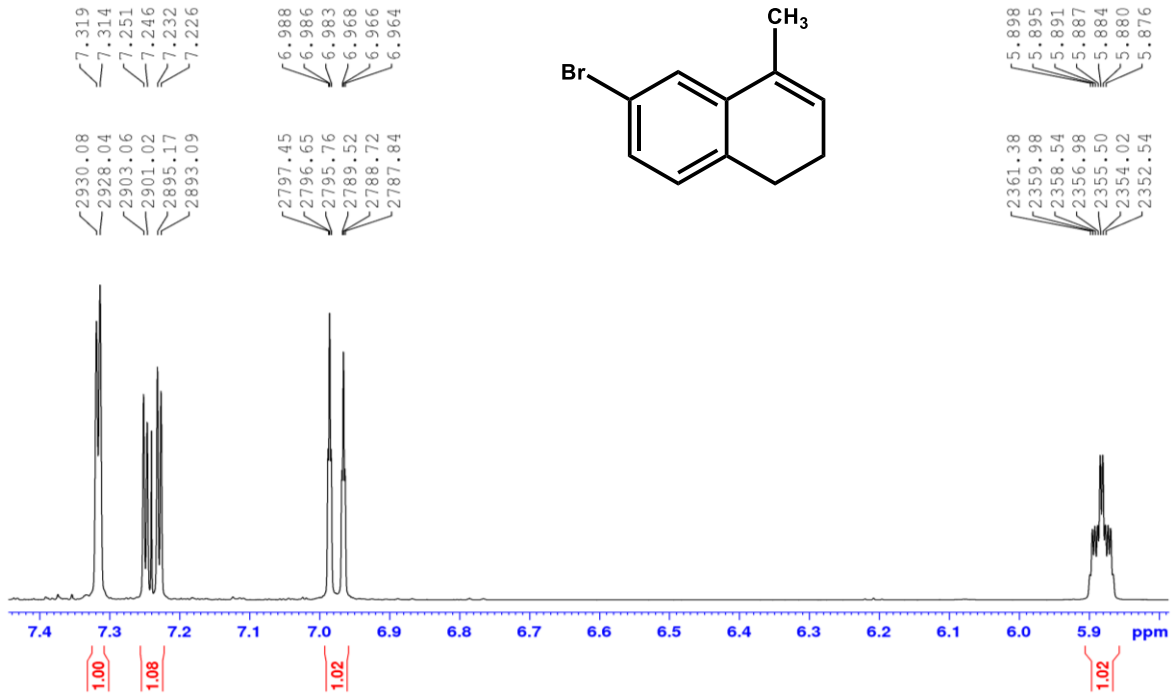

Figure A57. ^{1}H NMR (400 MHz, $CDCl_3$, 293 K) spectrum of 6-bromo-4-methyl-1,2-dihydronaphthalene **84**.

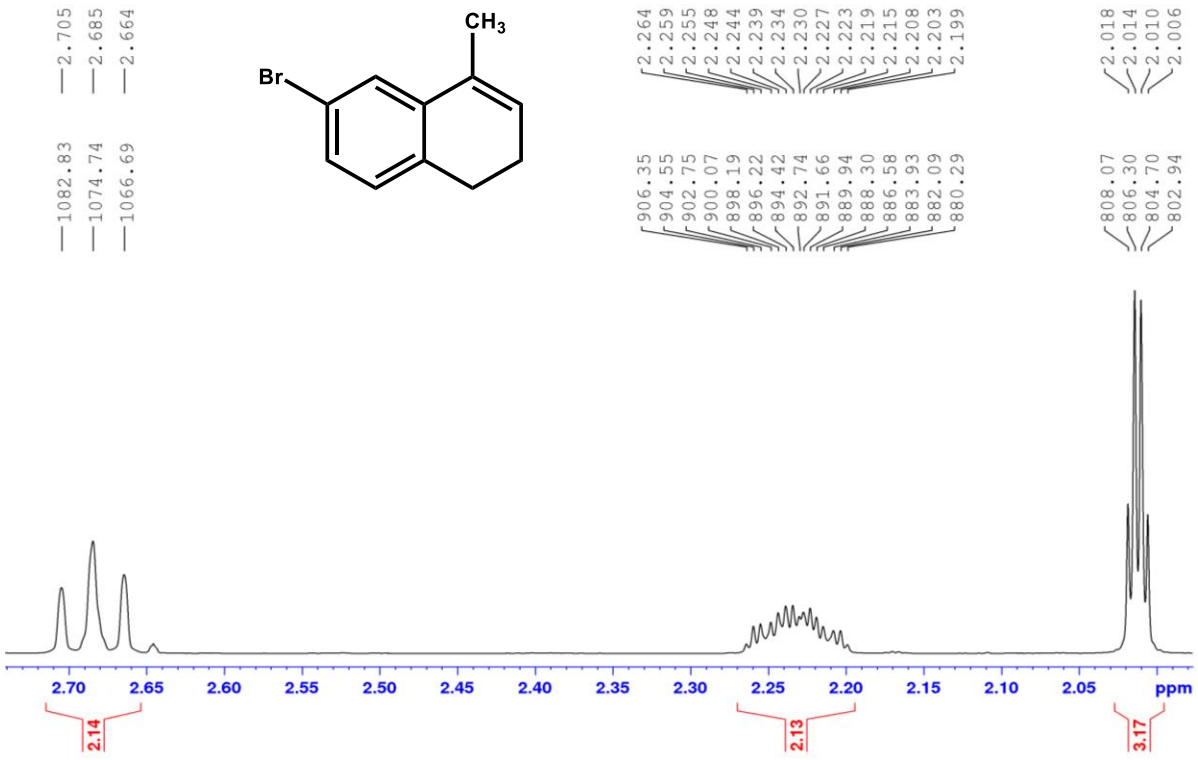

Figure A58. ^{1}H NMR (400 MHz, $CDCl_3$, 293 K) spectrum of 6-bromo-4-methyl-1,2-dihydronaphthalene **84**.

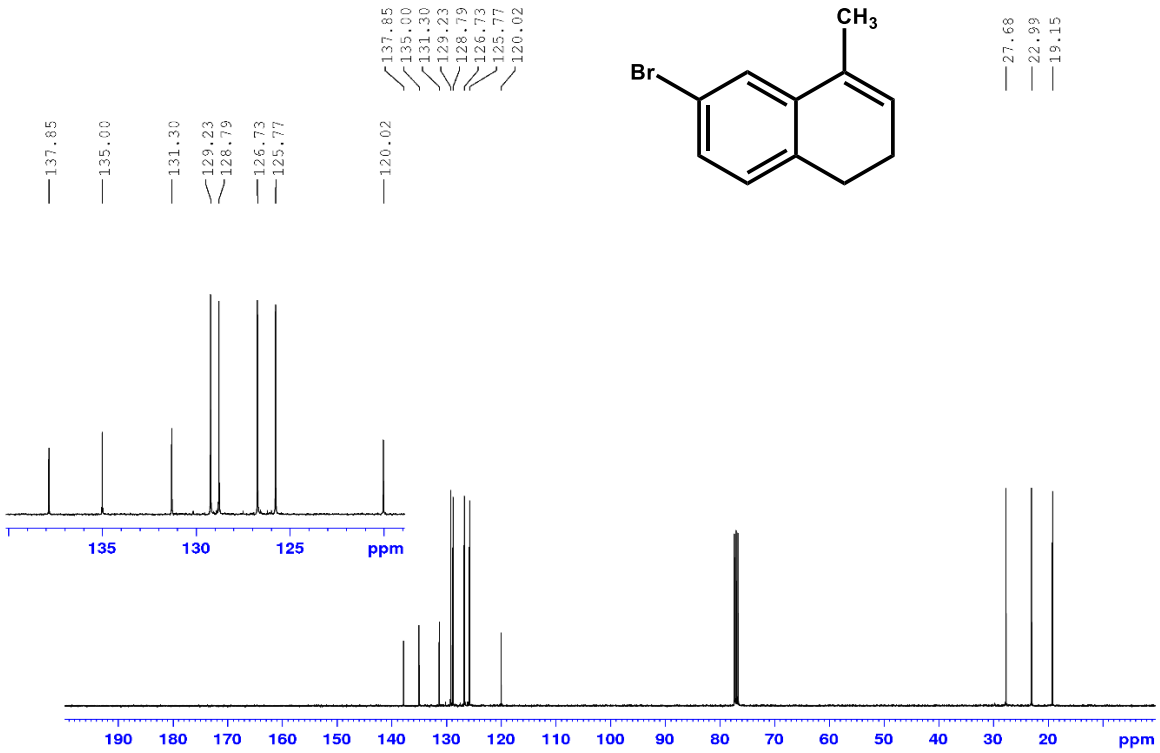

Figure A59. ^{13}C NMR (100 MHz, $CDCl_3$, 293 K) spectrum of 6-bromo-4-methyl-1,2-dihydronaphthalene **84**.

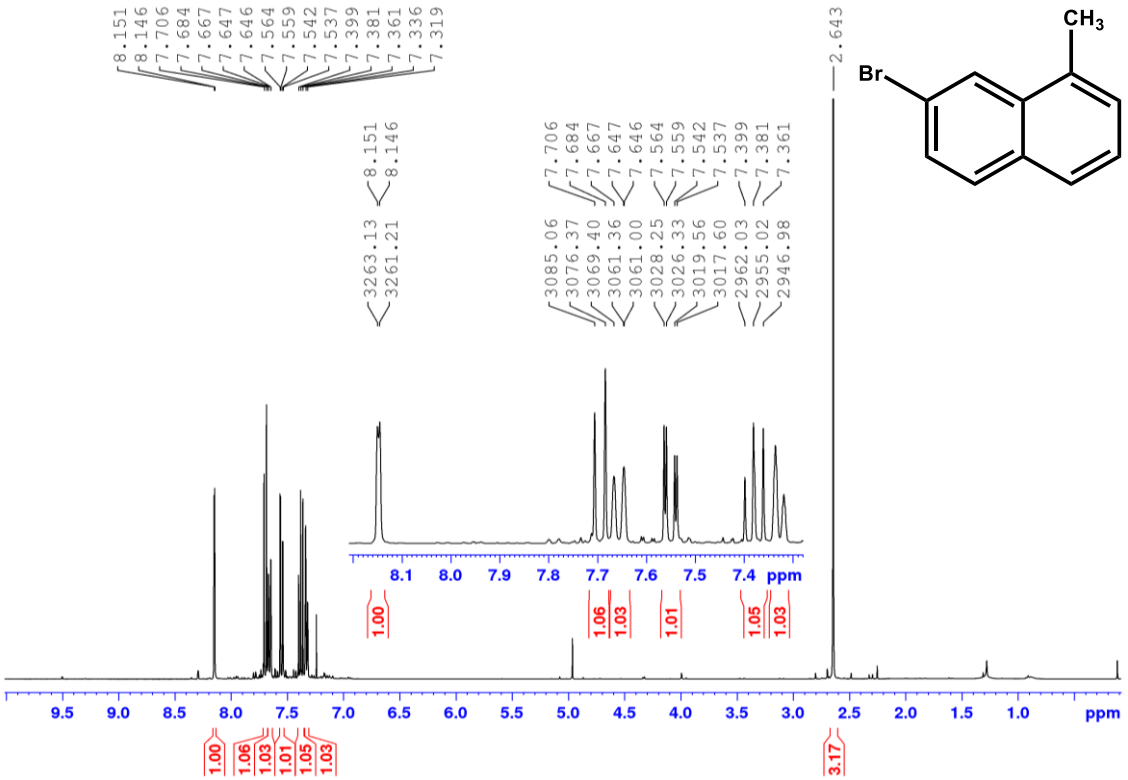

Figure A60. ^{1}H NMR (400 MHz, $CDCl_3$, 293 K) spectrum of 7-bromo-1-methylnaphthalene **85**.

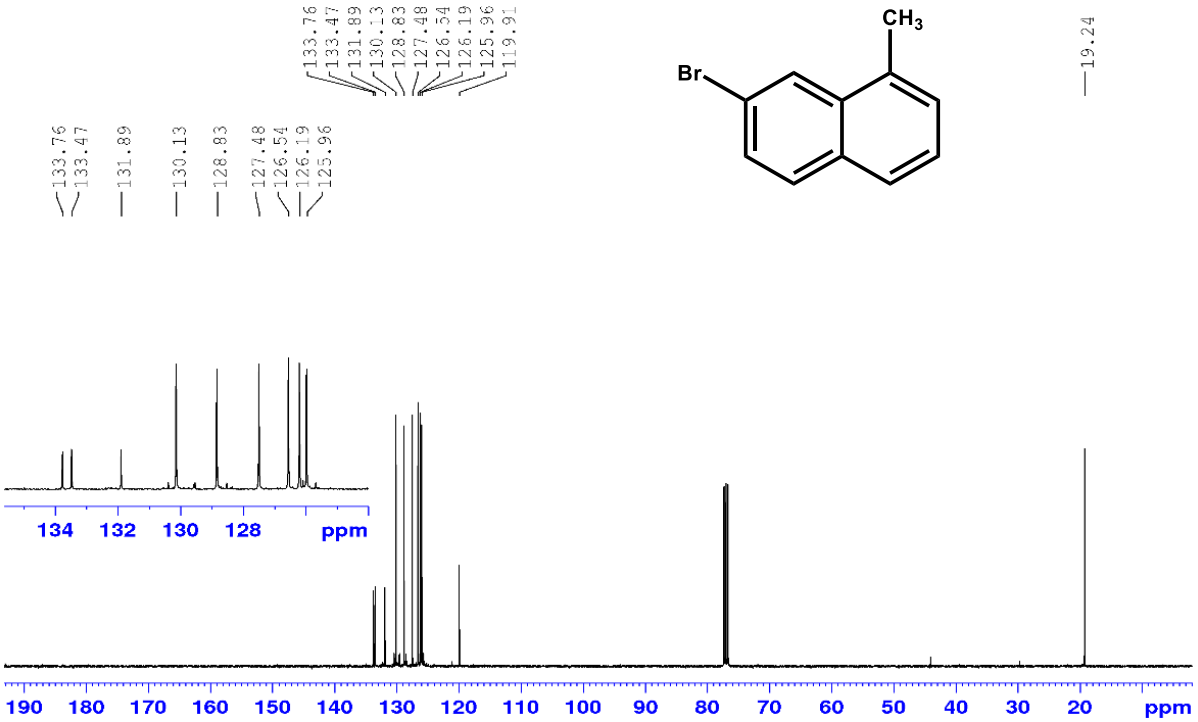

Figure A61. ^{13}C NMR (100 MHz, $CDCl_3$, 293 K) spectrum of 7-bromo-1-methylnaphthalene **85**.

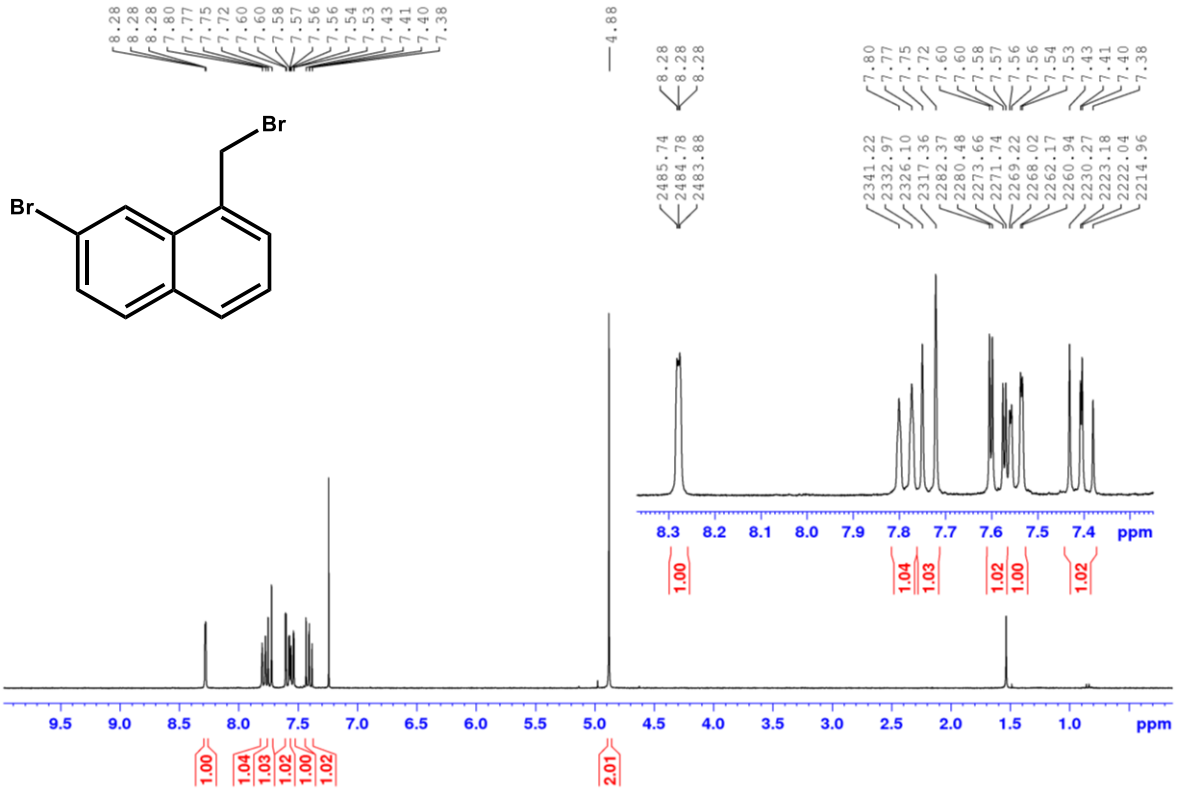

Figure A62. ^{1}H NMR (300 MHz, $CDCl_3$, 293 K) spectrum of 7-bromo-1-(bromomethyl)naphthalene **86**.

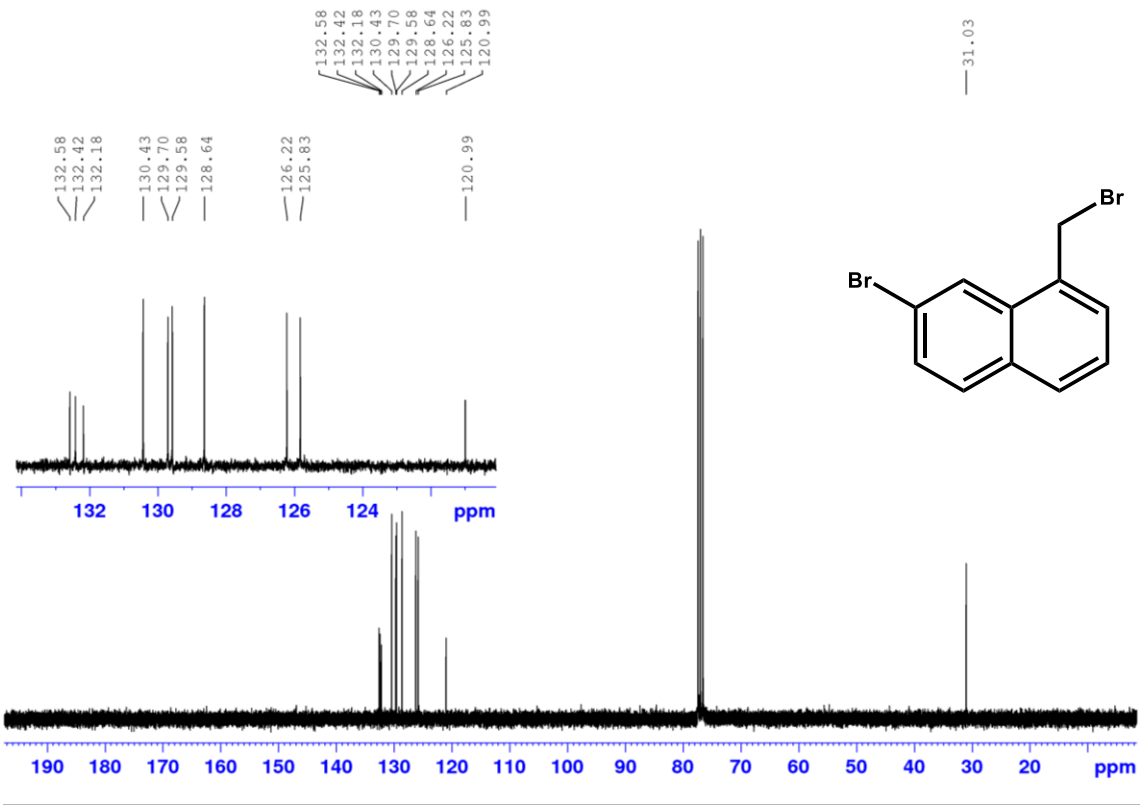

Figure A63. ^{13}C NMR (75 MHz, $CDCl_3$, 293 K) spectrum of 7-bromo-1-(bromomethyl)naphthalene **86**.

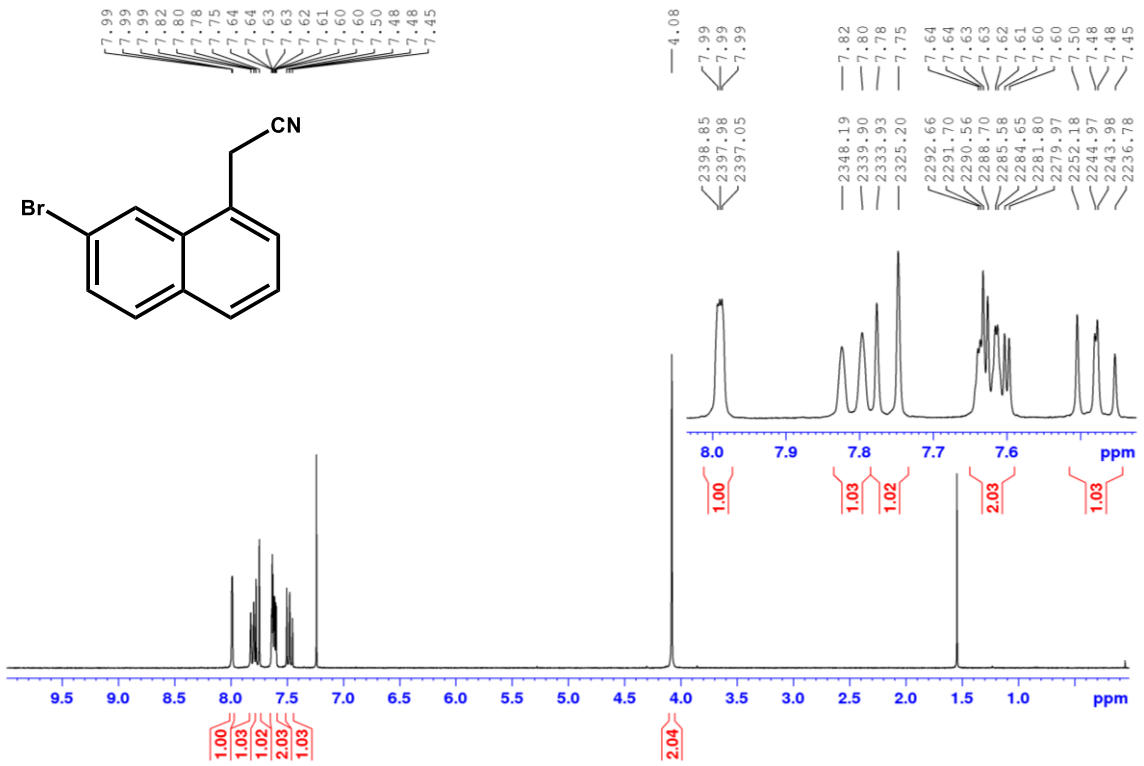

Figure A64. ^{1}H NMR (300 MHz, $CDCl_3$, 293 K) spectrum of 2-(7-bromonaphthalen-1-yl)acetonitrile **87**.

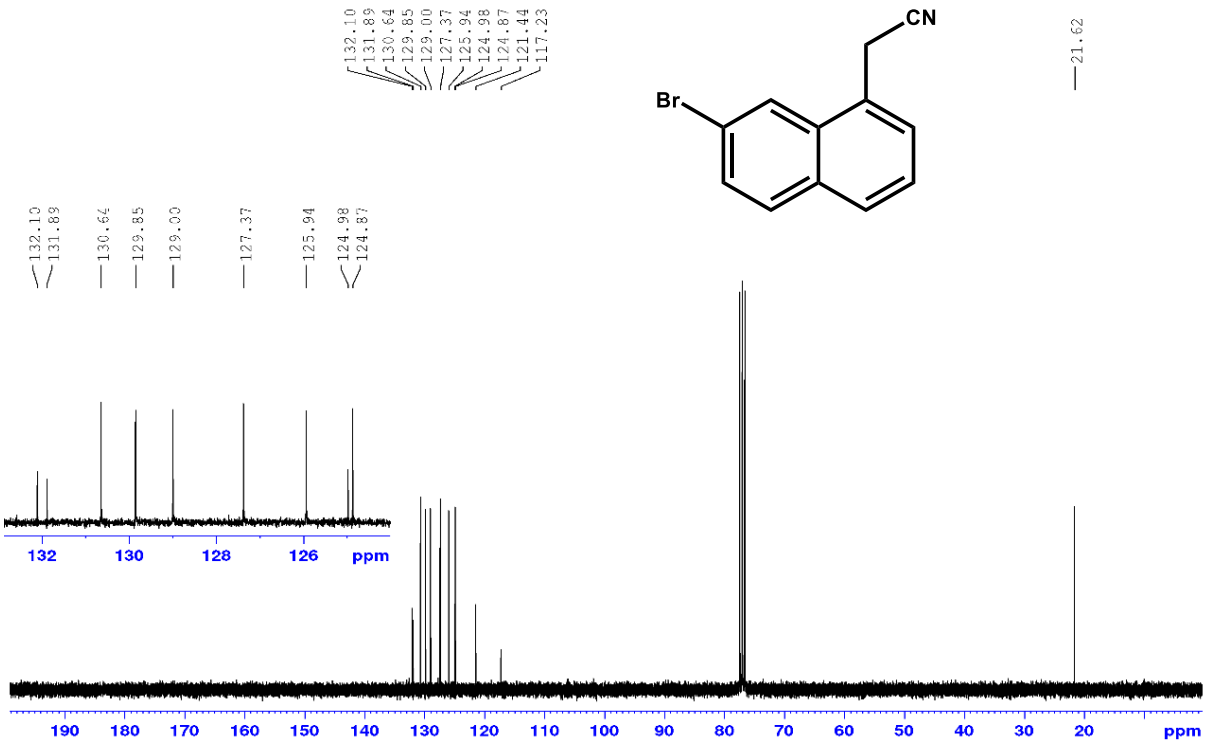

Figure A65. ^{13}C NMR (75 MHz, $CDCl_3$, 293 K) spectrum of 2-(7-bromonaphthalen-1-yl)acetonitrile **87**.

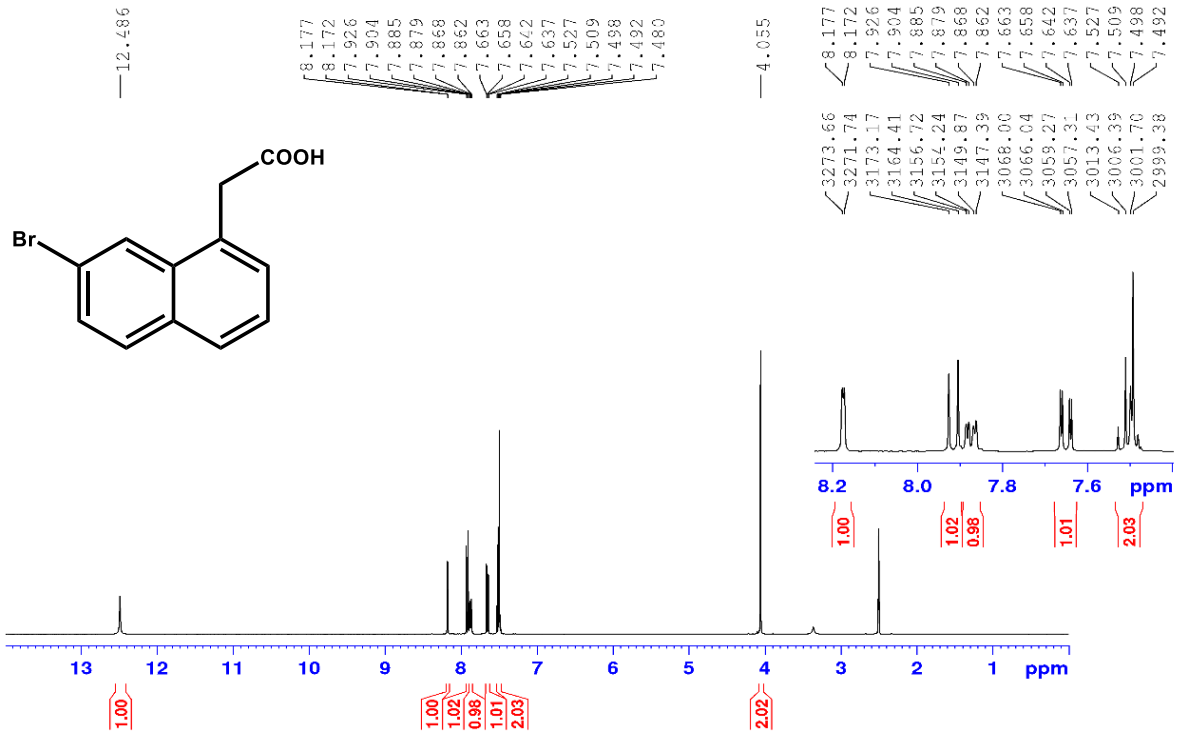

Figure A66. ^{1}H NMR (400 MHz, DMSO, 293 K) spectrum of 2-(7-bromonaphthalen-1-yl)acetic acid **88**.

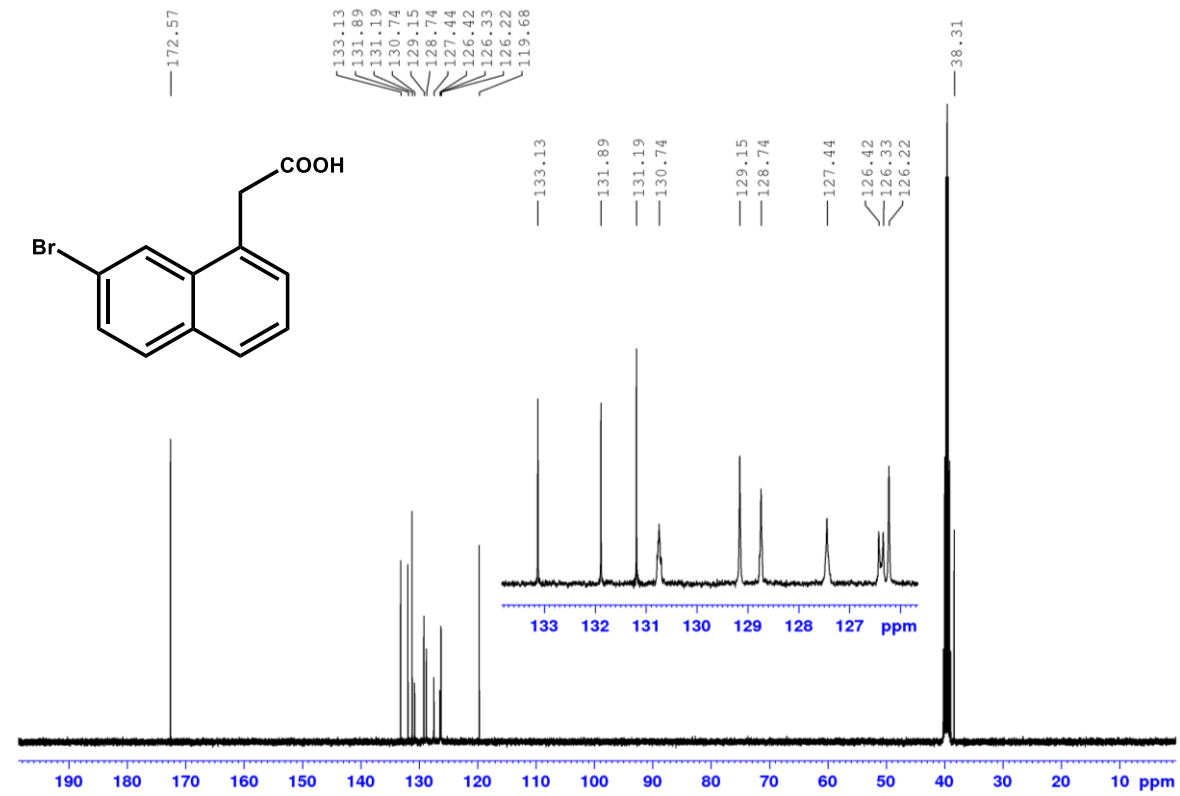

Figure A67. ^{13}C NMR (100 MHz, DMSO, 293 K) spectrum of 2-(7-bromonaphthalen-1-yl)acetic acid **88**.

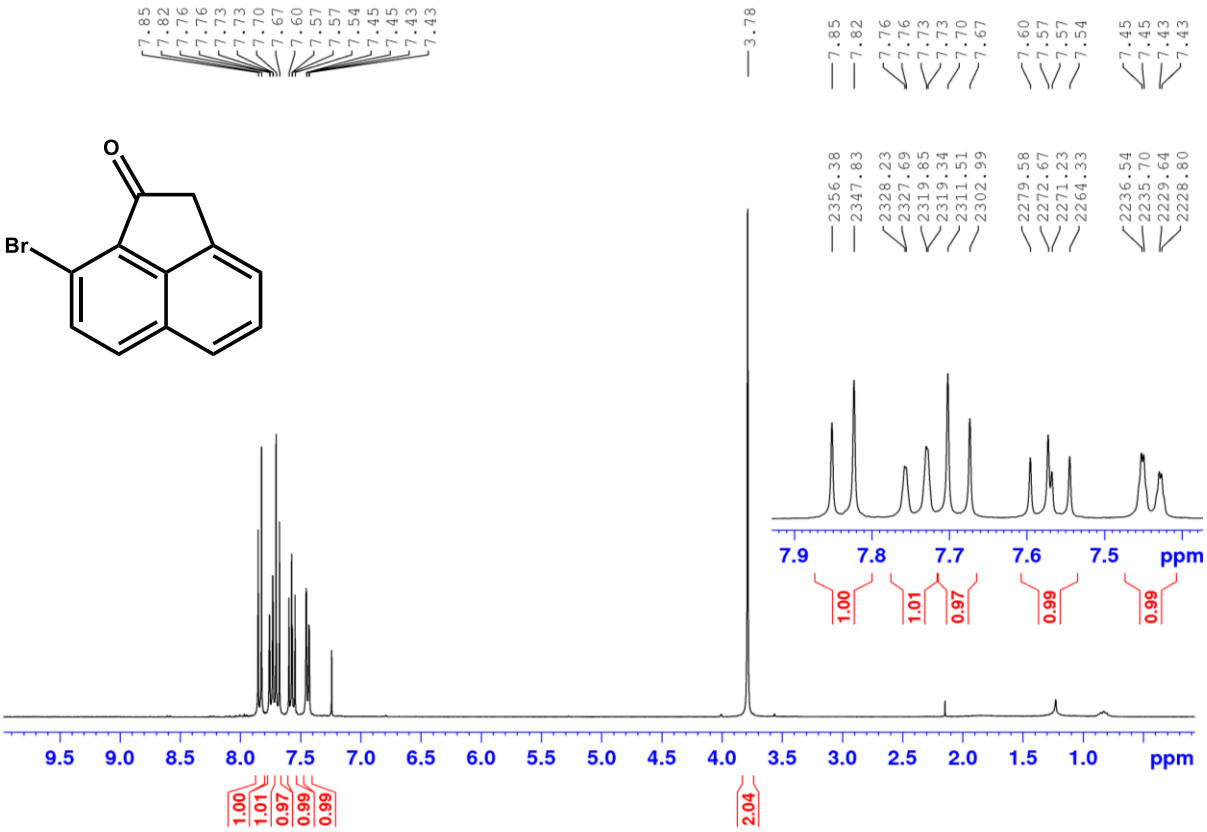

Figure A68. ^{1}H NMR (300 MHz, $CDCl_3$, 293 K) spectrum of 8-bromoacenaphthylen-1(*2H*)-one **89**.

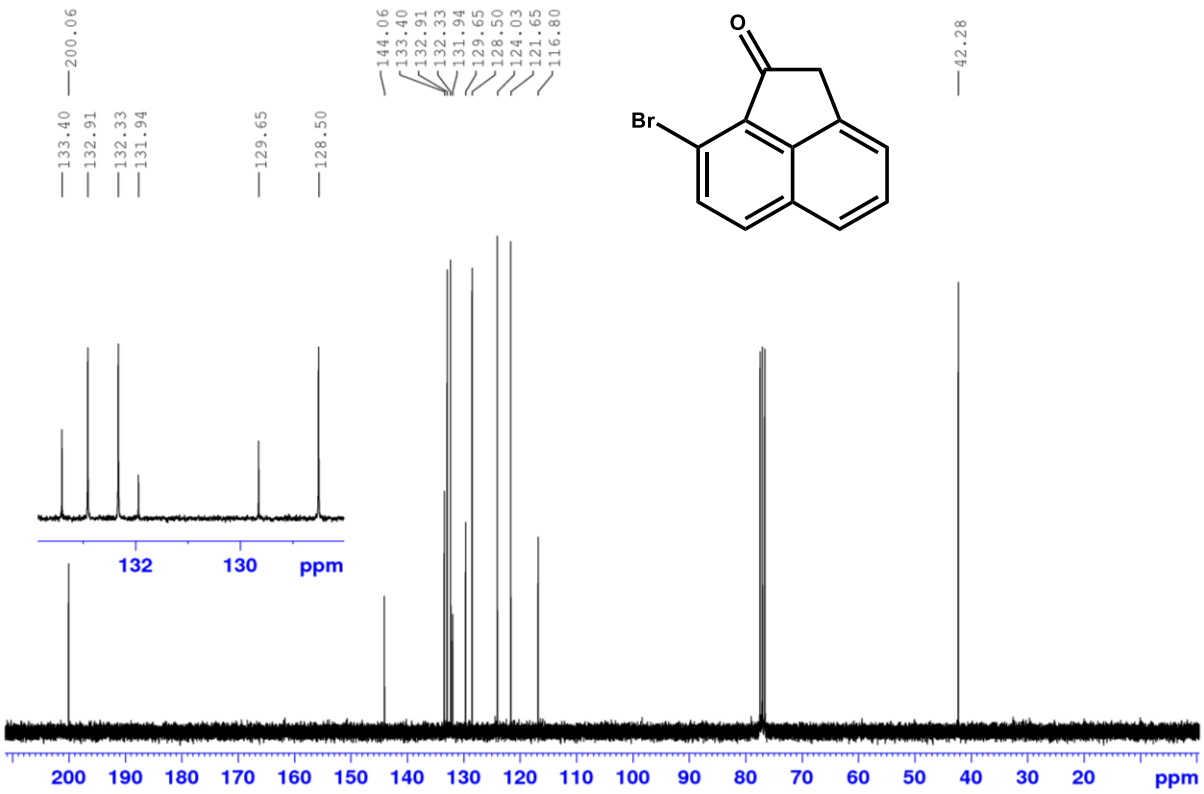

Figure A69. ^{13}C NMR (75 MHz, $CDCl_3$, 293 K) spectrum of 8-bromoacenaphthylen-1(*2H*)-one **89**.

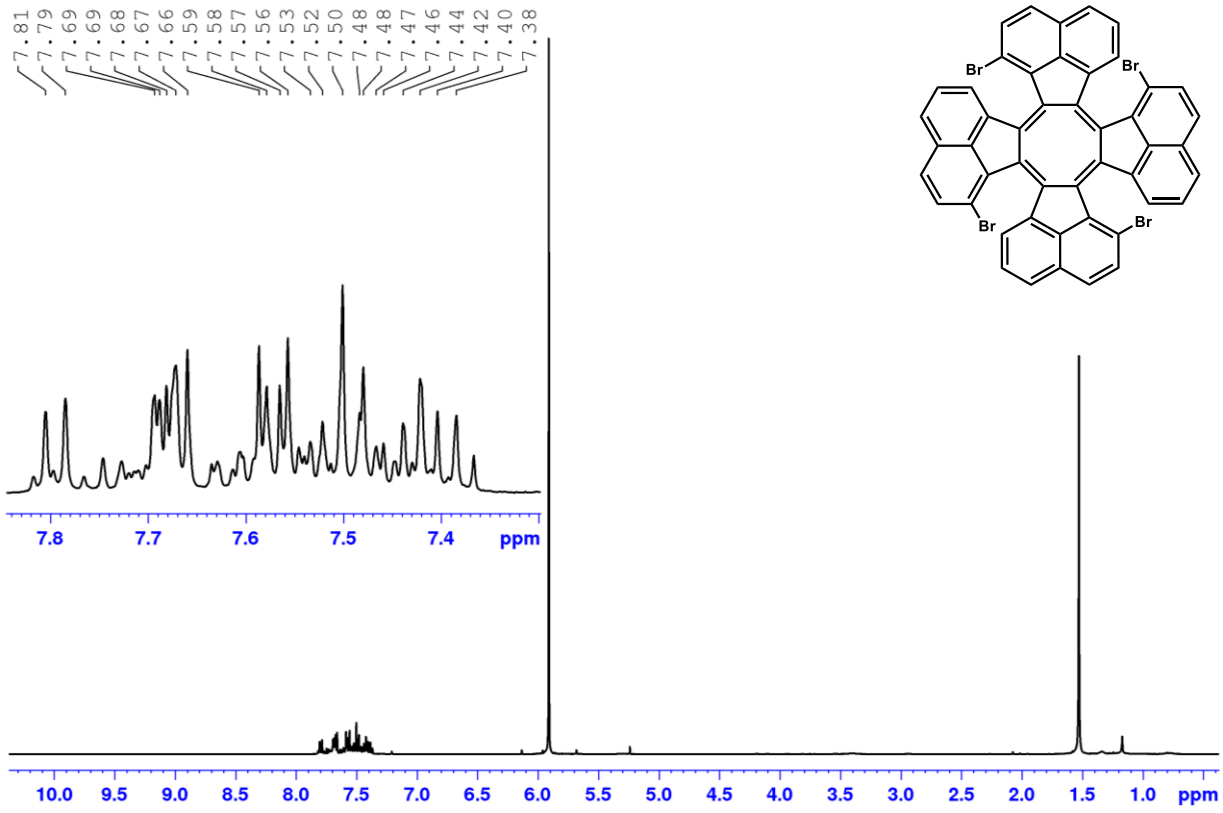

Figure A70. ^{1}H NMR (400 MHz, $C_2D_2Cl_4$, 293 K) spectrum of 1,7,13,19-tetrabromotridecacyclene **90**.

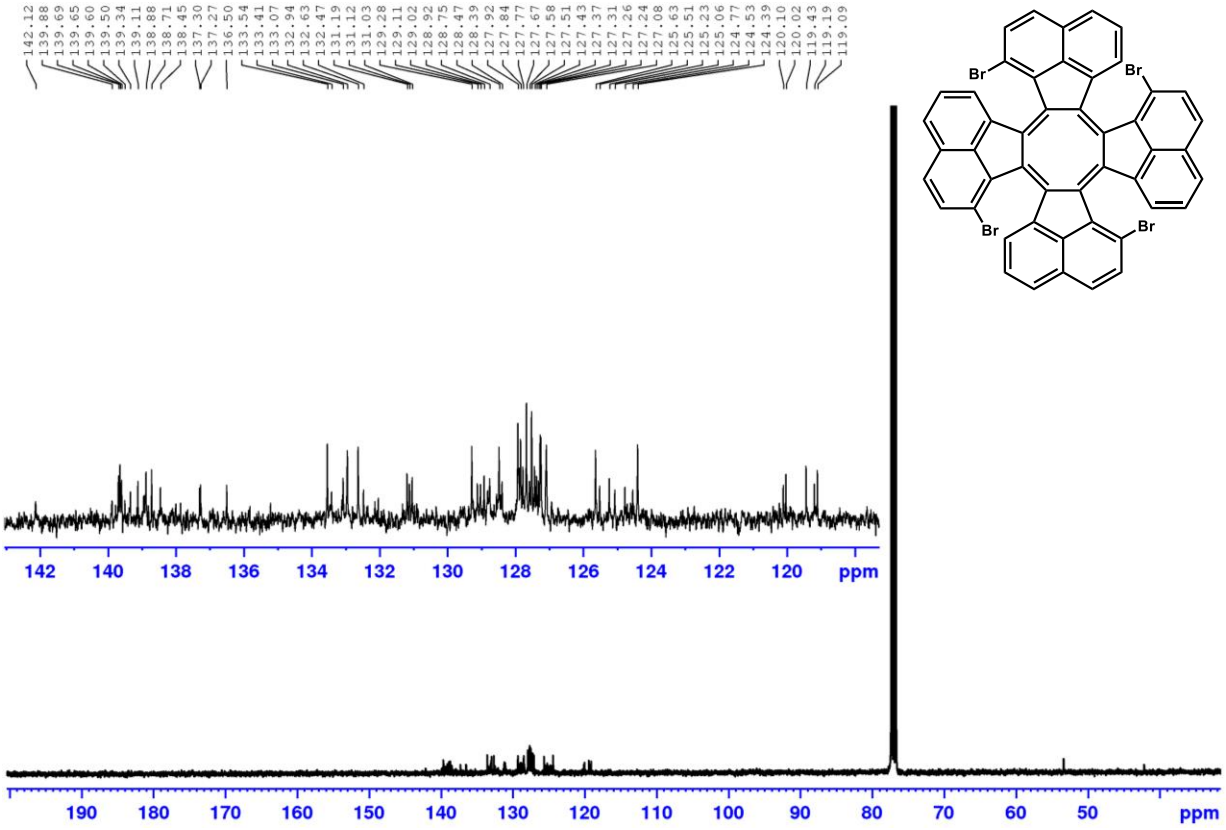

Figure A71. ^{13}C NMR (101 MHz, $CDCl_3$, 293 K) spectrum of 1,7,13,19-tetrabromotridecacyclene **90**.

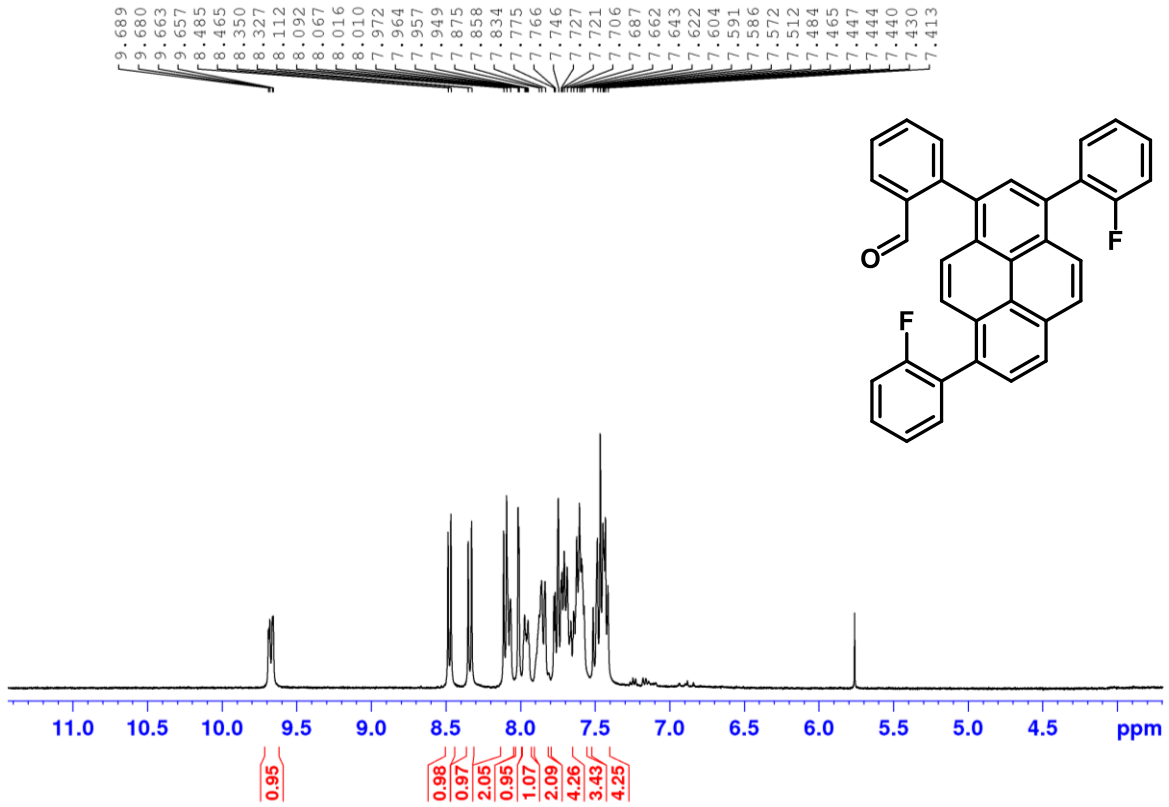

Figure A72. ^{1}H NMR (400 MHz, DMSO, 293 K) spectrum of 2-(3,8-bis(2-fluorophenyl)pyren-1-yl)benz aldehyde **103**.

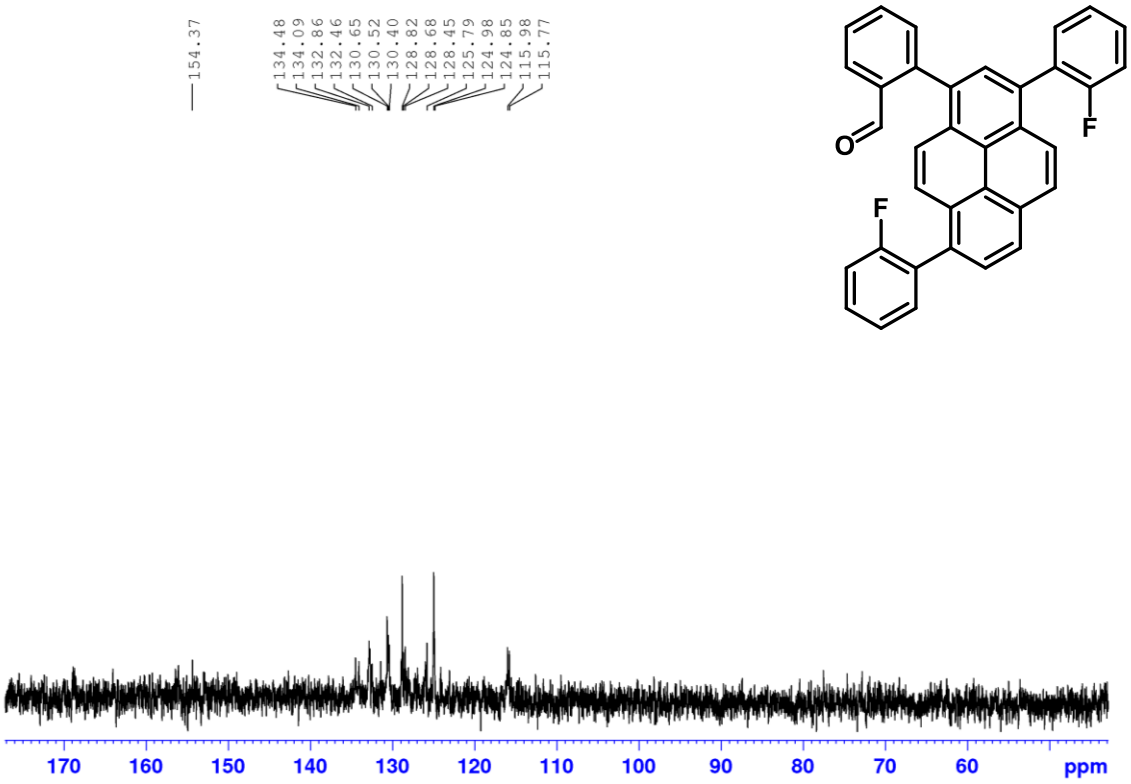

Figure A73. ^{13}C NMR (101 MHz, DMSO, 293 K) spectrum of 2-(3,8-bis(2-fluorophenyl)pyren-1-yl)benz aldehyde **103**.

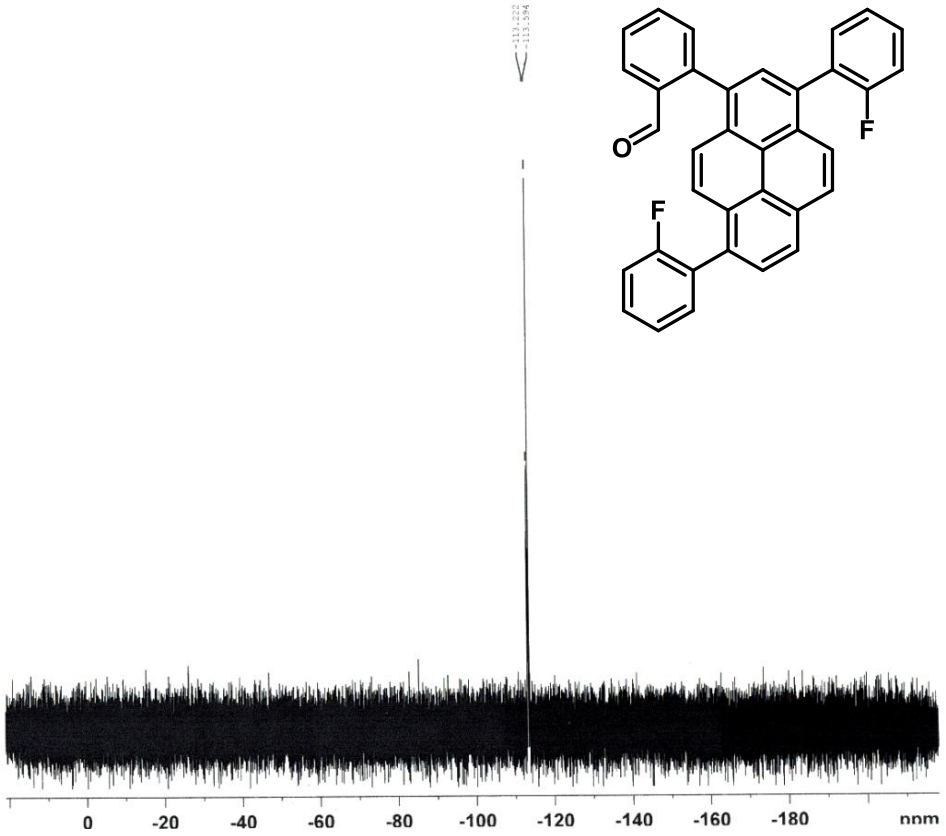

Figure A74. ^{19}F NMR (282 MHz, DMSO, 293 K) spectrum of 2-(3,8-bis(2-fluorophenyl)pyren-1-yl)benz aldehyde **103**.

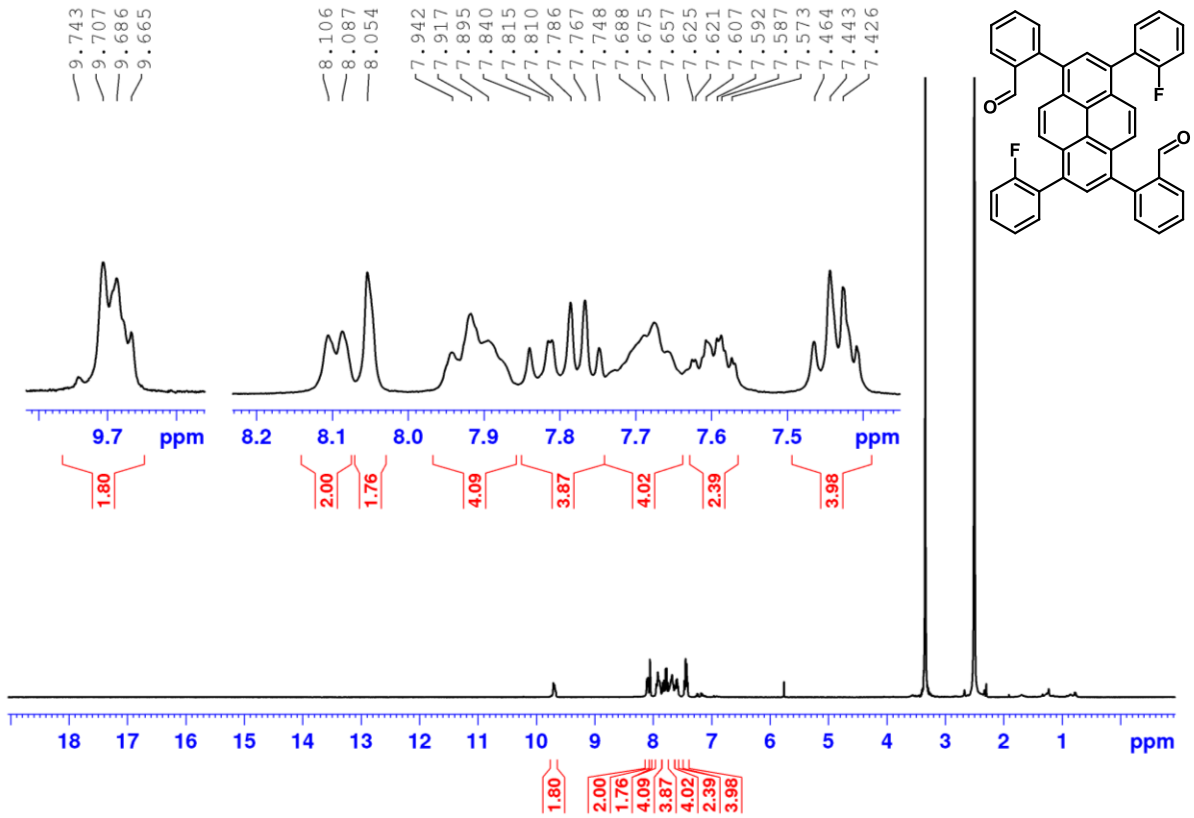

Figure A75. ^{1}H NMR (400 MHz, DMSO, 293 K) spectrum of 2,2'-(3,8-bis(2-fluorophenyl)-pyrene-1,6-diyl)dibenzaldehyde **102**.

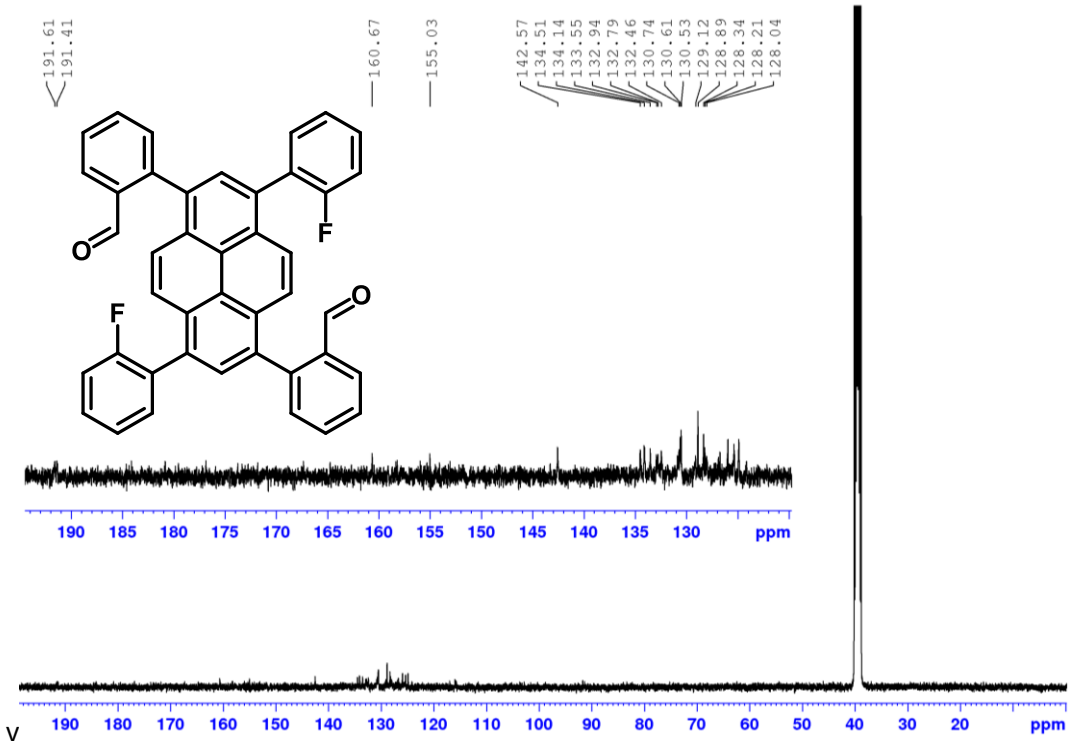

Figure A76. ^{13}C NMR (101 MHz, DMSO, 293 K) spectrum of 2,2'-(3,8-bis(2-fluorophenyl)-pyrene-1,6-diyl)dibenzaldehyde **102**.

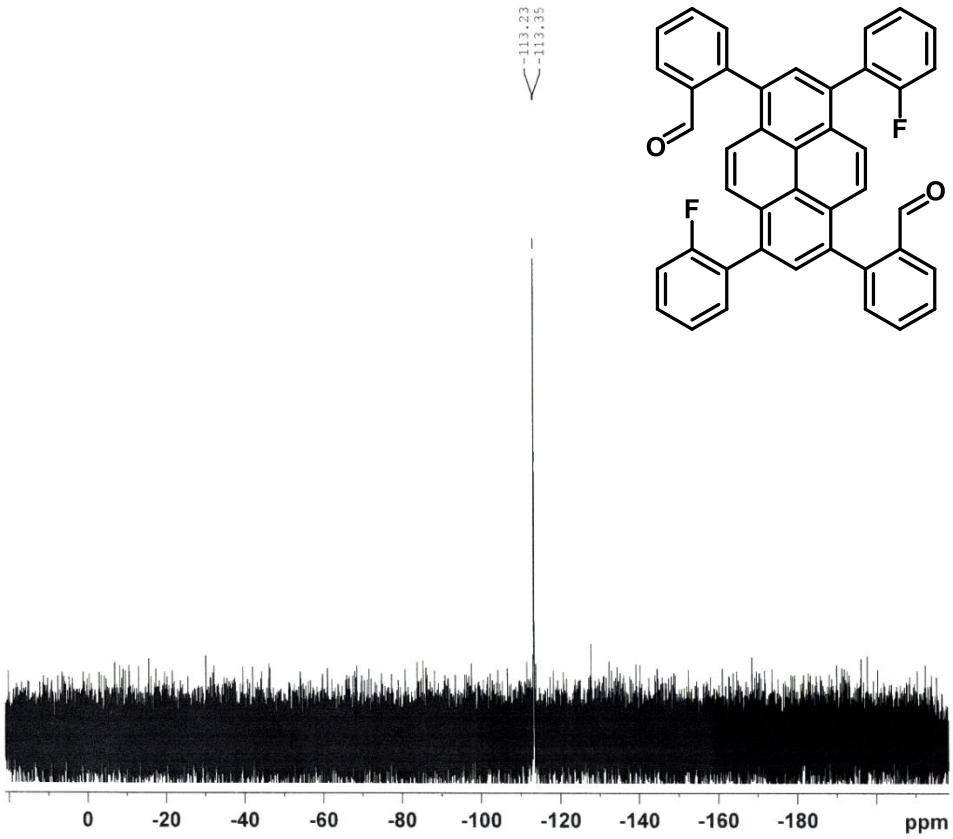

Figure A77. ^{19}F NMR (282 MHz, DMSO, 293 K) spectrum of 2,2'-(3,8-bis(2-fluorophenyl)-pyrene-1,6-diyl)dibenzaldehyde **102**.

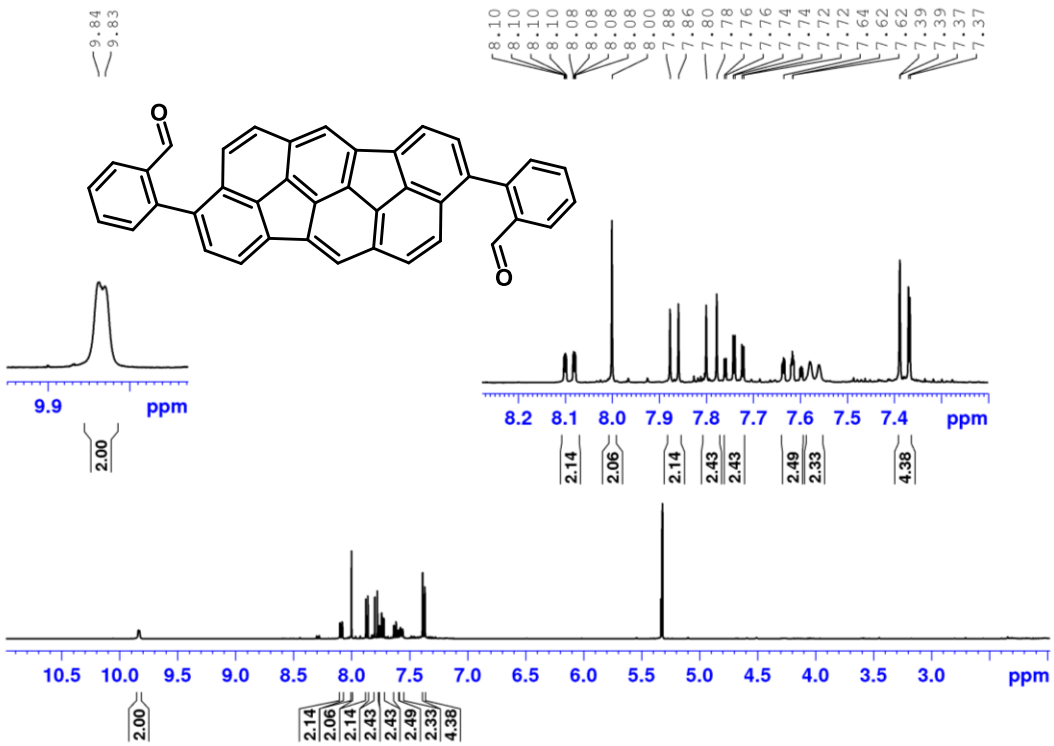

Figure A78. ^{1}H NMR (400 MHz, CD_2Cl_2, 293 K) spectrum of 2,2'-(diindeno[*4,3,2,1-cdef:4',3',2',1'-lmno*]chrysene-3,9-diyl)dibenzaldehyde **110**.

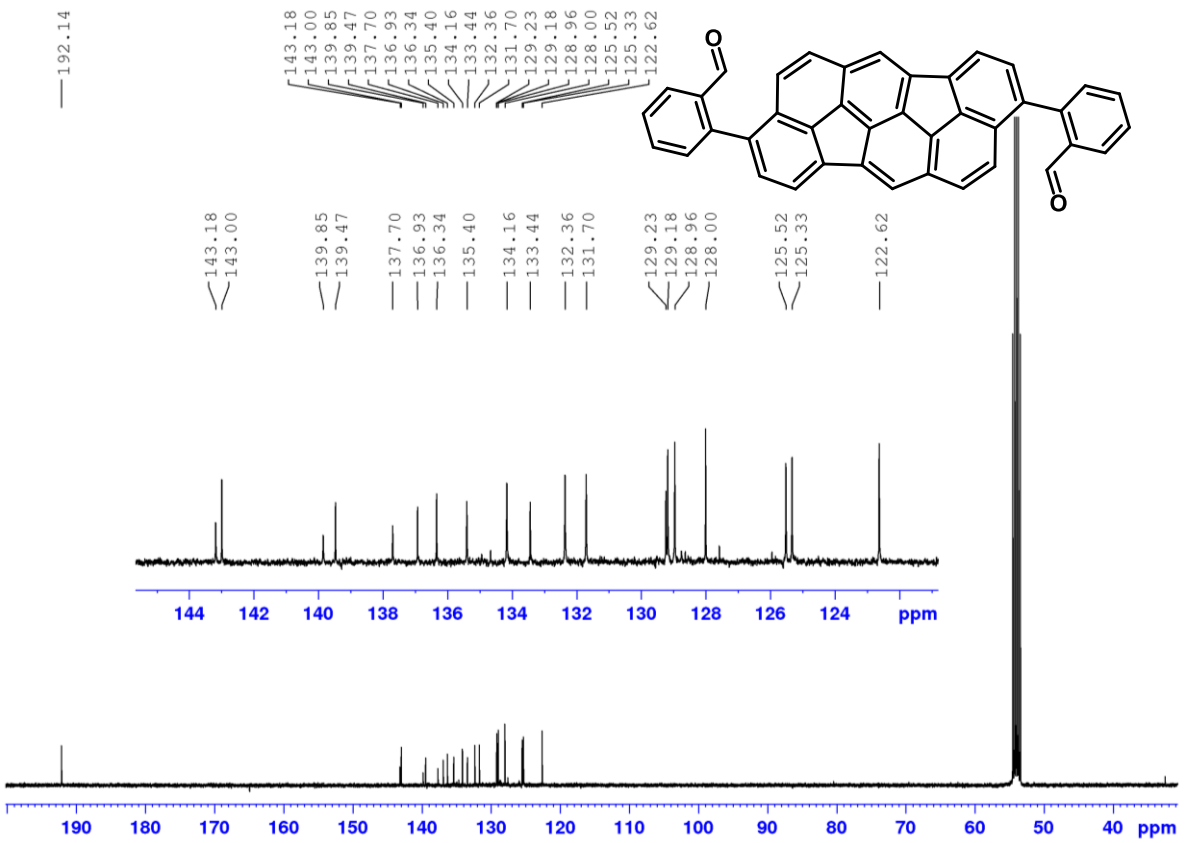

Figure A79. ^{13}C NMR (101 MHz, CD_2Cl_2, 293 K) spectrum of 2,2'-(diindeno[*4,3,2,1-cdef:4',3',2',1'-lmno*]chrysene-3,9-diyl)dibenzaldehyde **110**.

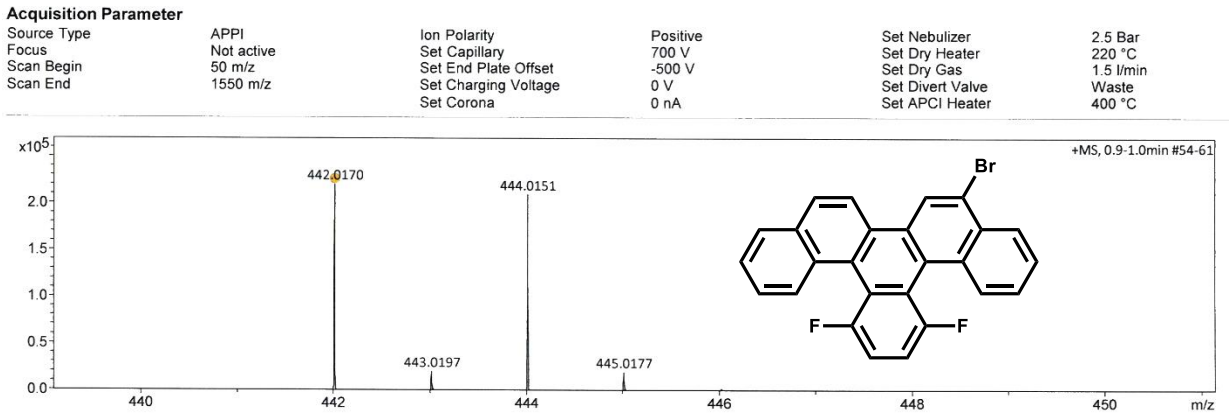

Figure A80. Mass spectrum (HRMS, APPI, toluene) of 5-bromo-13,16-difluoro-benzo[*s*]picene **45**.

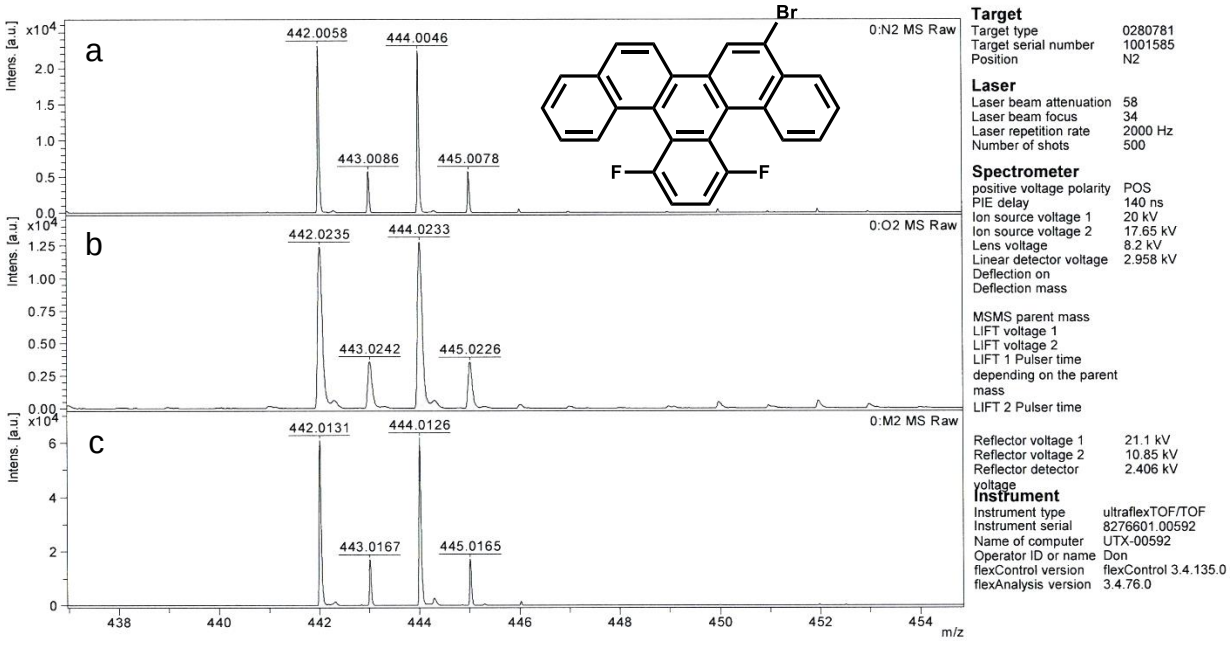

Figure A81. Mass spectrum (MALDI-TOF) of 5-bromo-13,16-difluoro-benzo[*s*]picene **45**: a) without matrix; b) with DHB matrix; c) with DCTB matrix.

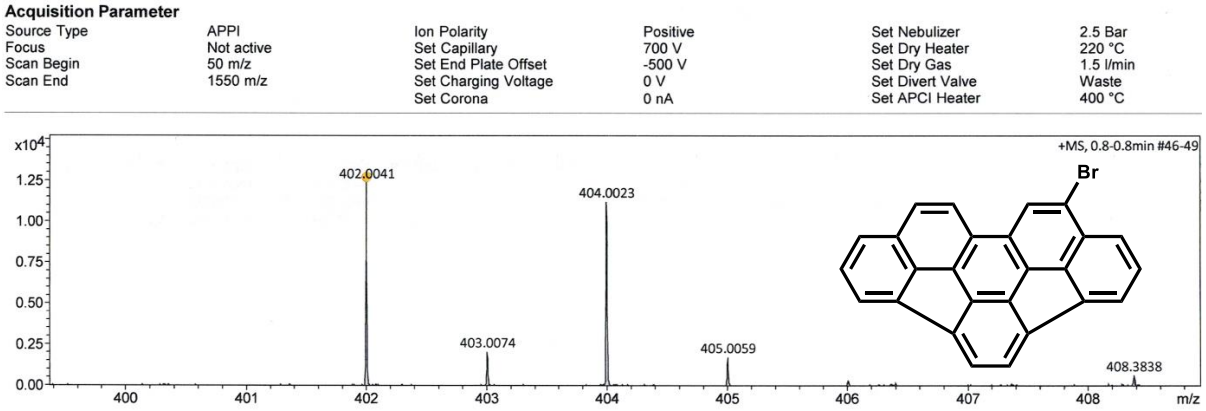

Figure A82. Mass spectrum (HRMS, APPI, toluene) of 9-bromo-*as*-indaceno[*3,2,1,8,7,6-pqrstuv*]-picene **46**.

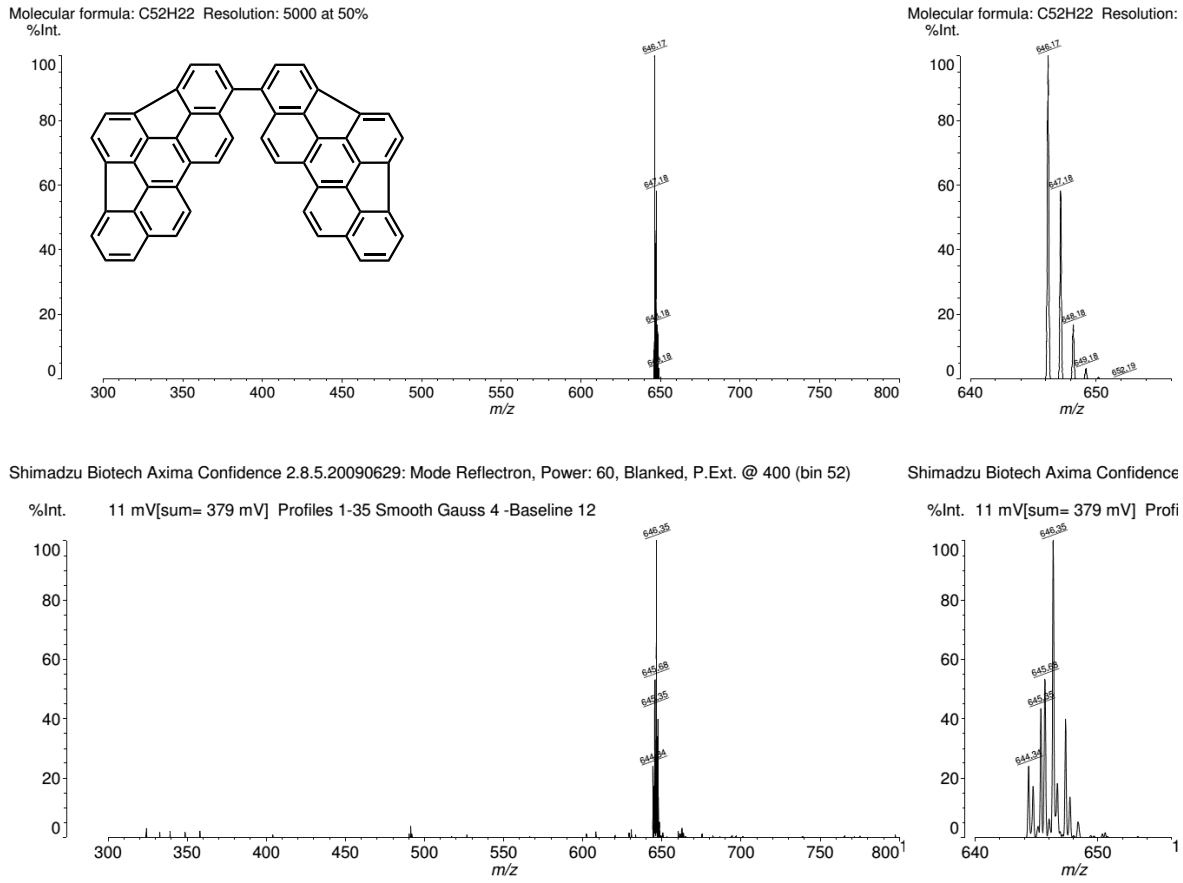

Figure A83. Mass spectrum (LDI) of 1,1'-bias-indaceno[*3,2,1,8,7,6-pqrstuv*]picene **55**.

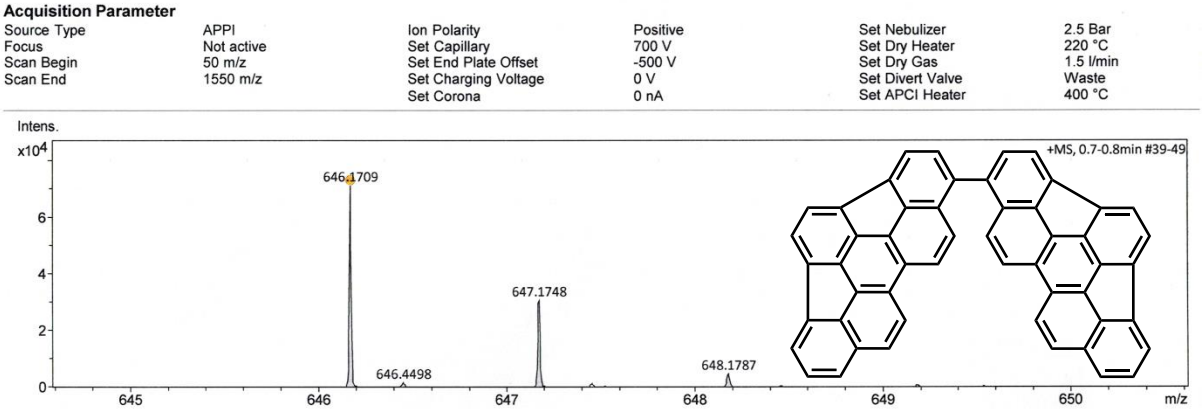

Figure A84. Mass spectrum (HRMS, APPI) of 1,1'-bias-indaceno[*3,2,1,8,7,6-pqrstuv*]picene **55**.

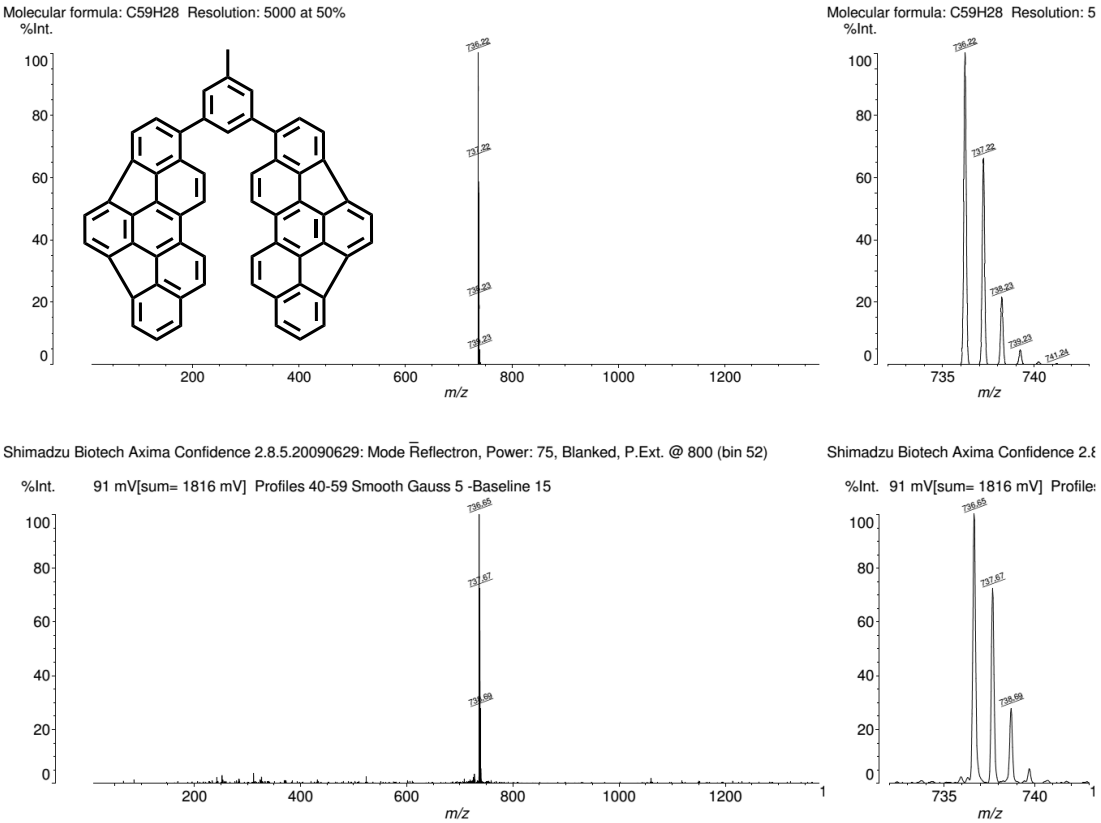

Figure A85. Mass spectrum (LDI) of 9,9'-(5-methyl-1,3-phenylene)di-as-indaceno[3,2,1,8,7,6-*pqrstuv*] picene **56**.

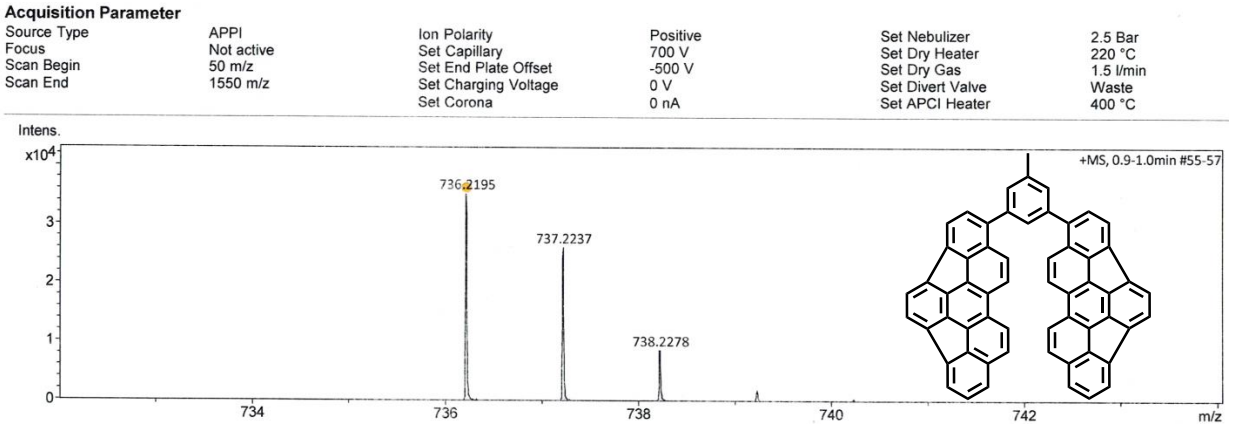

Figure A86. Mass spectrum (HRMS, APPI) of 9,9'-(5-methyl-1,3-phenylene)di-as-indaceno[*3,2,1,8,7,6-pqrstuv*]picene **56**.

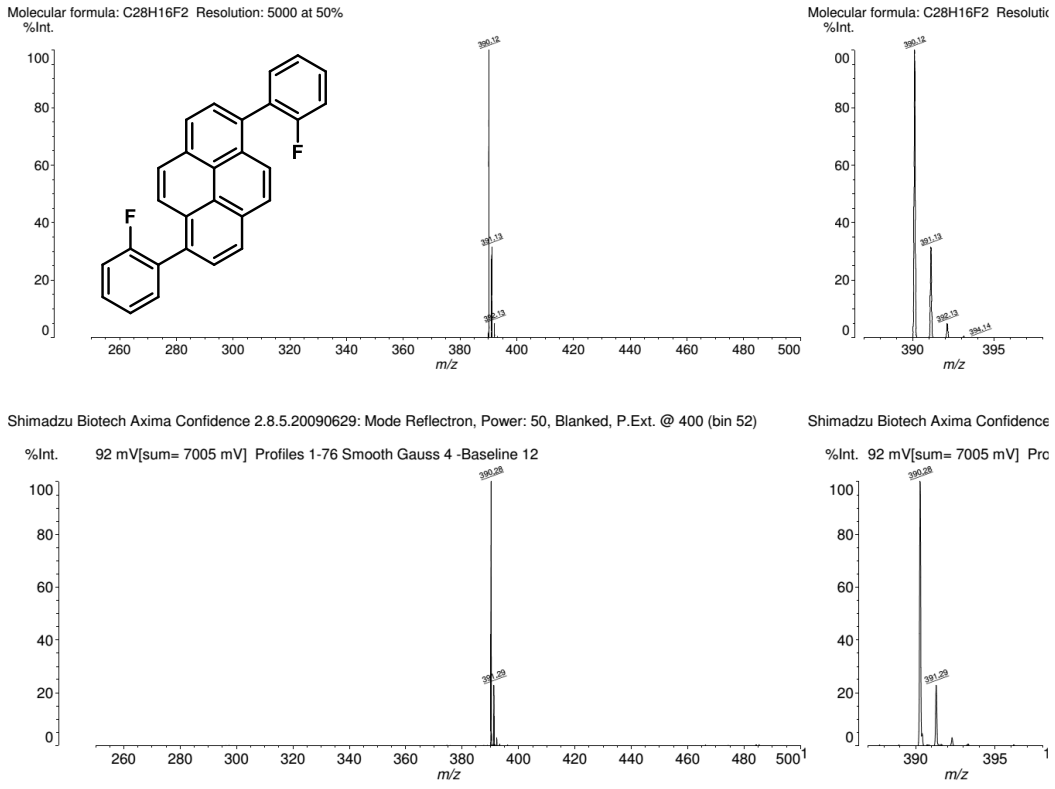

Figure A87. Mass spectrum (LDI) of 1,6-bis(2-fluorophenyl)pyrene **59**.

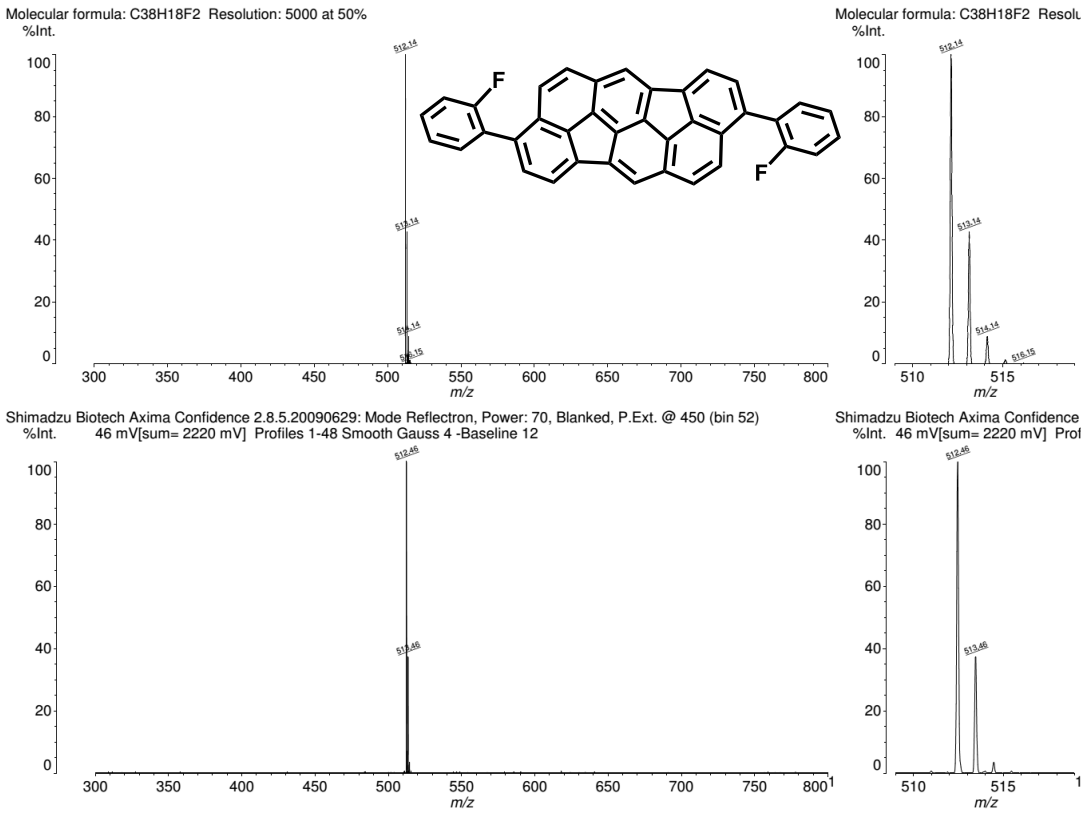

Figure A88. Mass spectrum (LDI) of 3,9-bis(2-fluorophenyl)diindeno[*4,3,2,1-cdef:4',3',2',1'-lmno*]-chrysene **65a**.

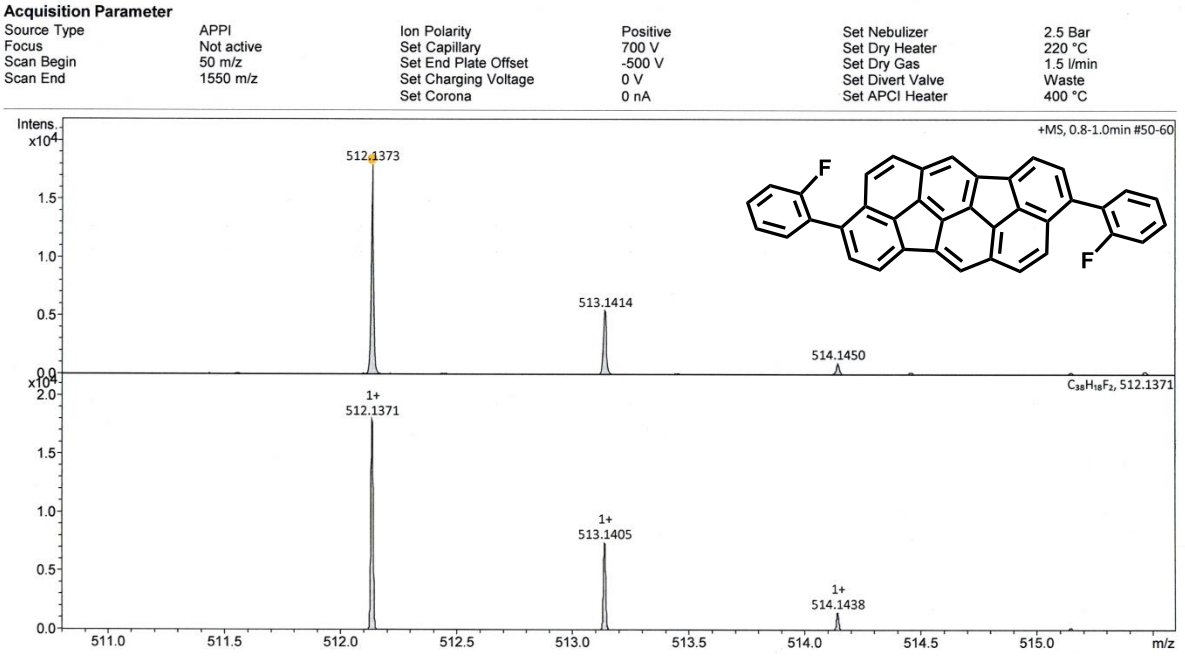

Figure A89. Mass spectrum (HRMS, APPI) of 3,9-bis(2-fluorophenyl)diindeno[*4,3,2,1-cdef:4',3',2',1'-lmno*]chrysene **65a**.

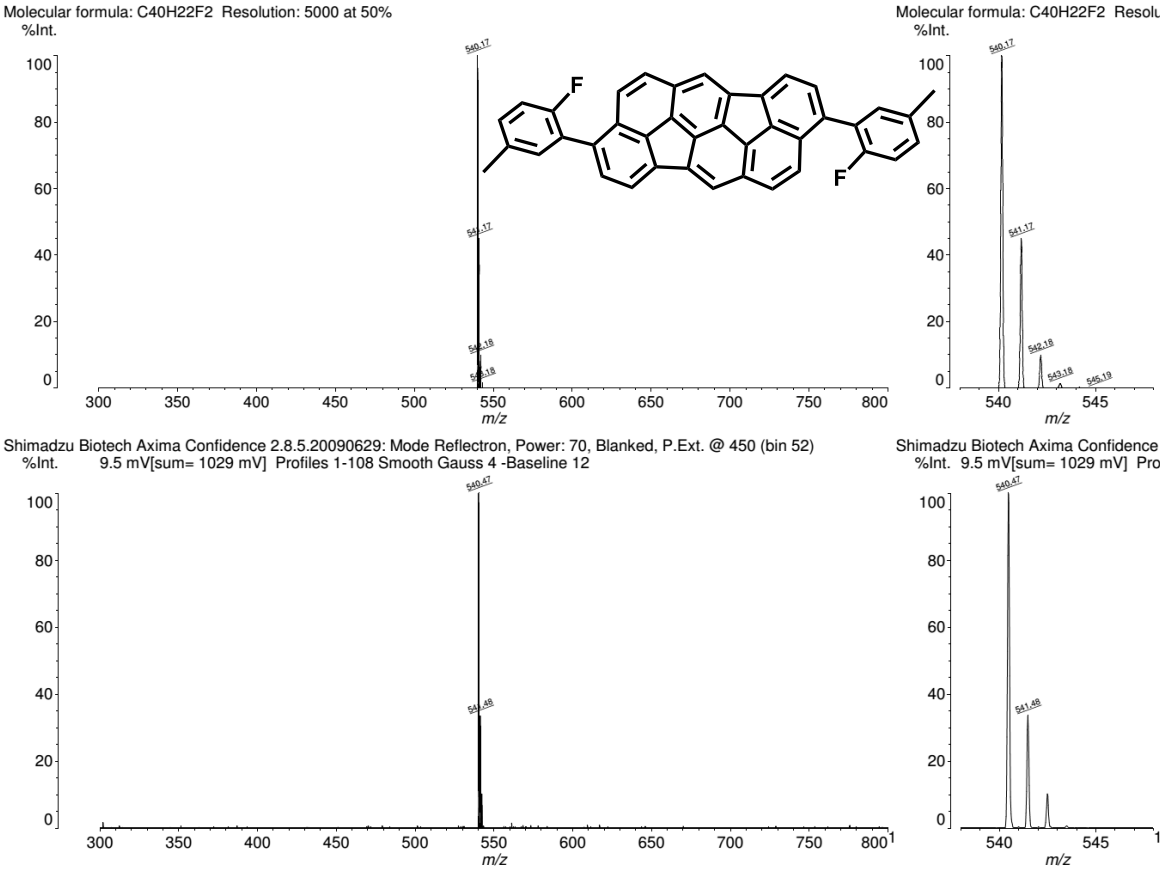

Figure A90. Mass spectrum (LDI) of 3,9-bis(2-fluoro-5-methylphenyl)diindeno[*4,3,2,1-cdef: 4',3',2',1'-lmno*]chrysene **65b**.

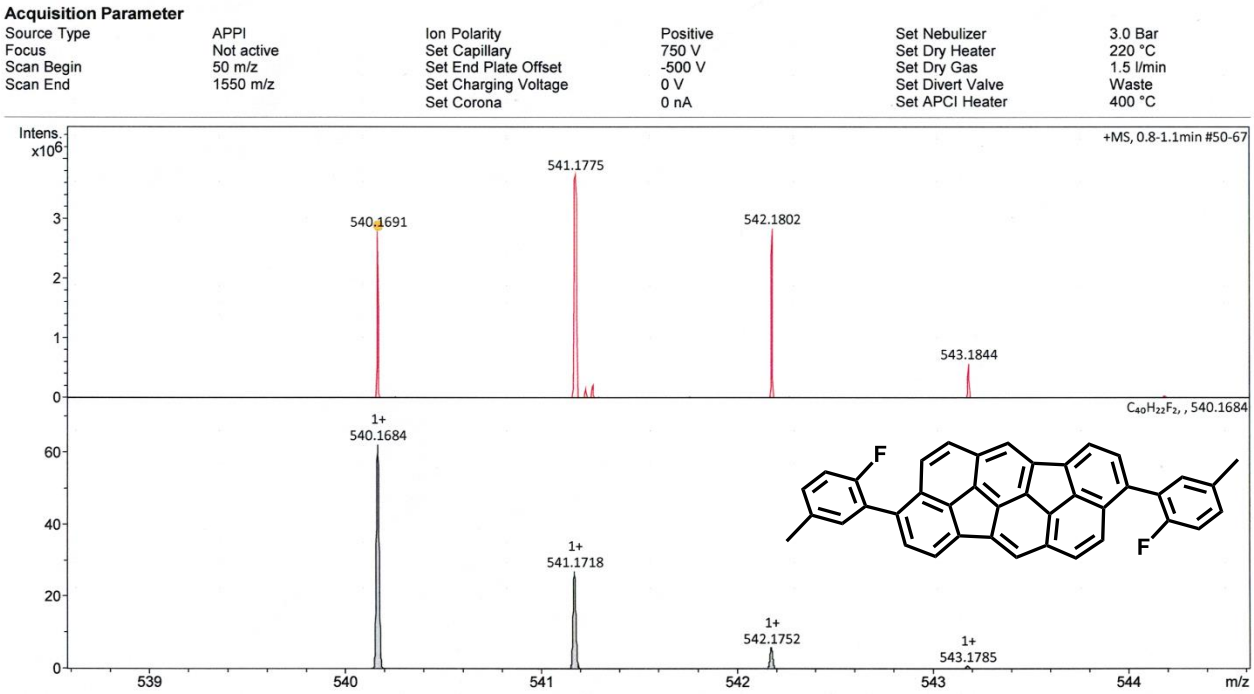

Figure A91. Mass spectrum (HRMS, APPI) of 3,9-bis(2-fluoro-5-methylphenyl)diindeno[*4,3,2,1-cdef:4',3',2',1'-lmno*]chrysene **65b**.

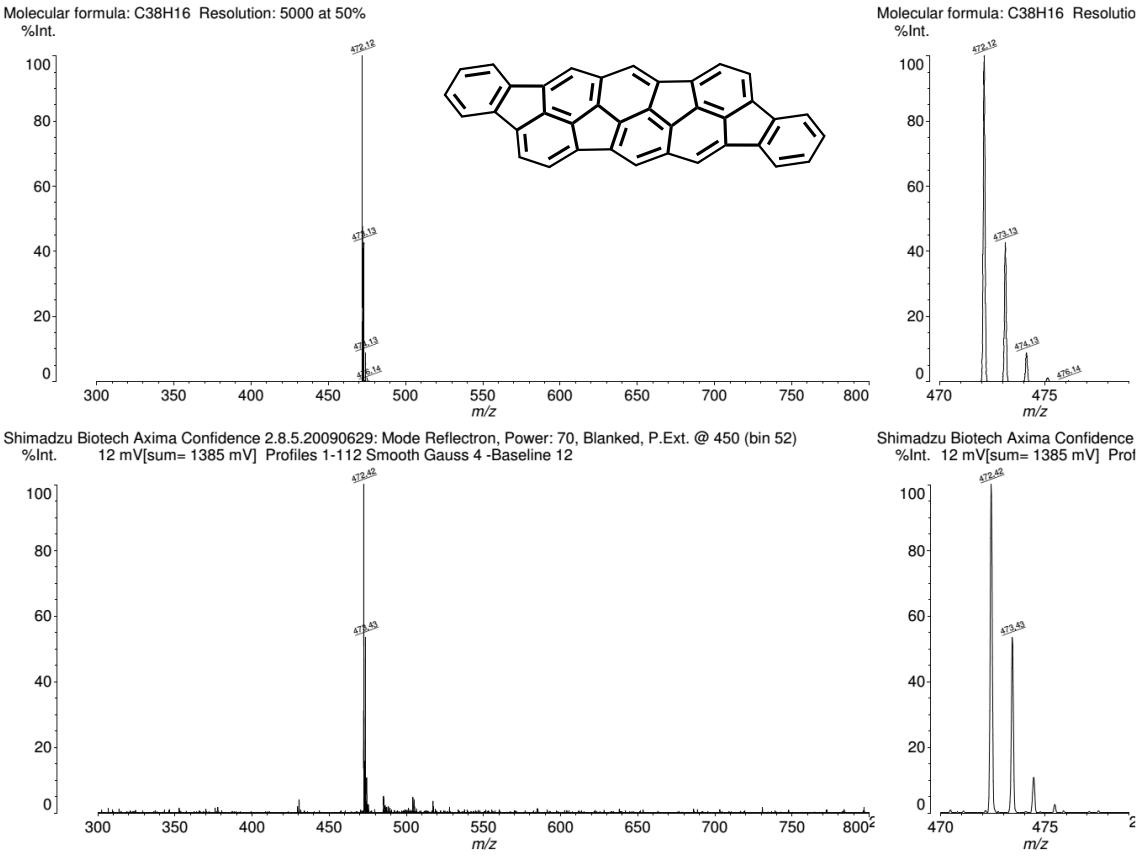

Figure A92. Mass spectrum (LDI) of benzo[*6,7*]-*as*-indaceno[*8,1,2,3-bcdef*]benzo[*6,7*]-*as*-indaceno-[*8,1,2,3-klmno*]chrysene **66a**.

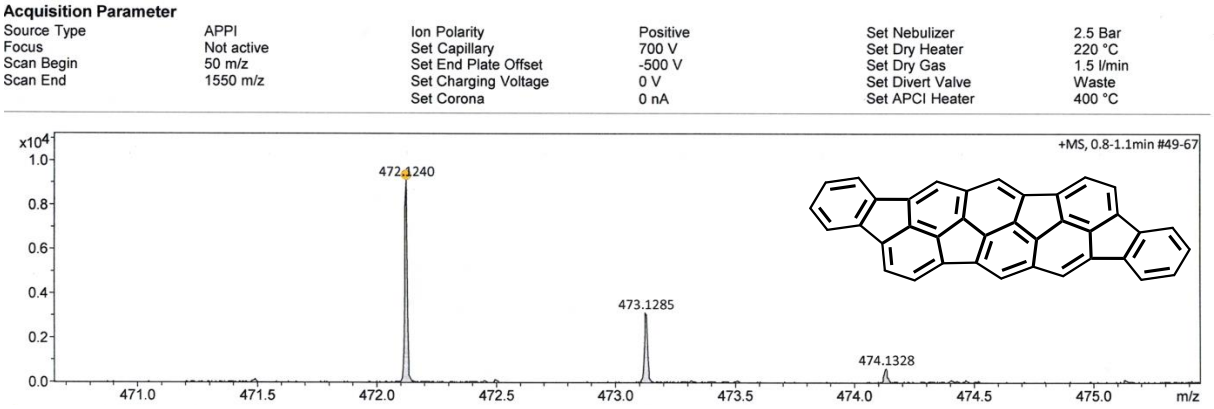

Figure A93. Mass spectrum (HRMS, APPI) of benzo[*6,7*]-*as*-indaceno[*8,1,2,3-bcdef*]benzo[*6,7*]-*as*-indaceno[*8,1,2,3-klmno*]chrysene **66a**.

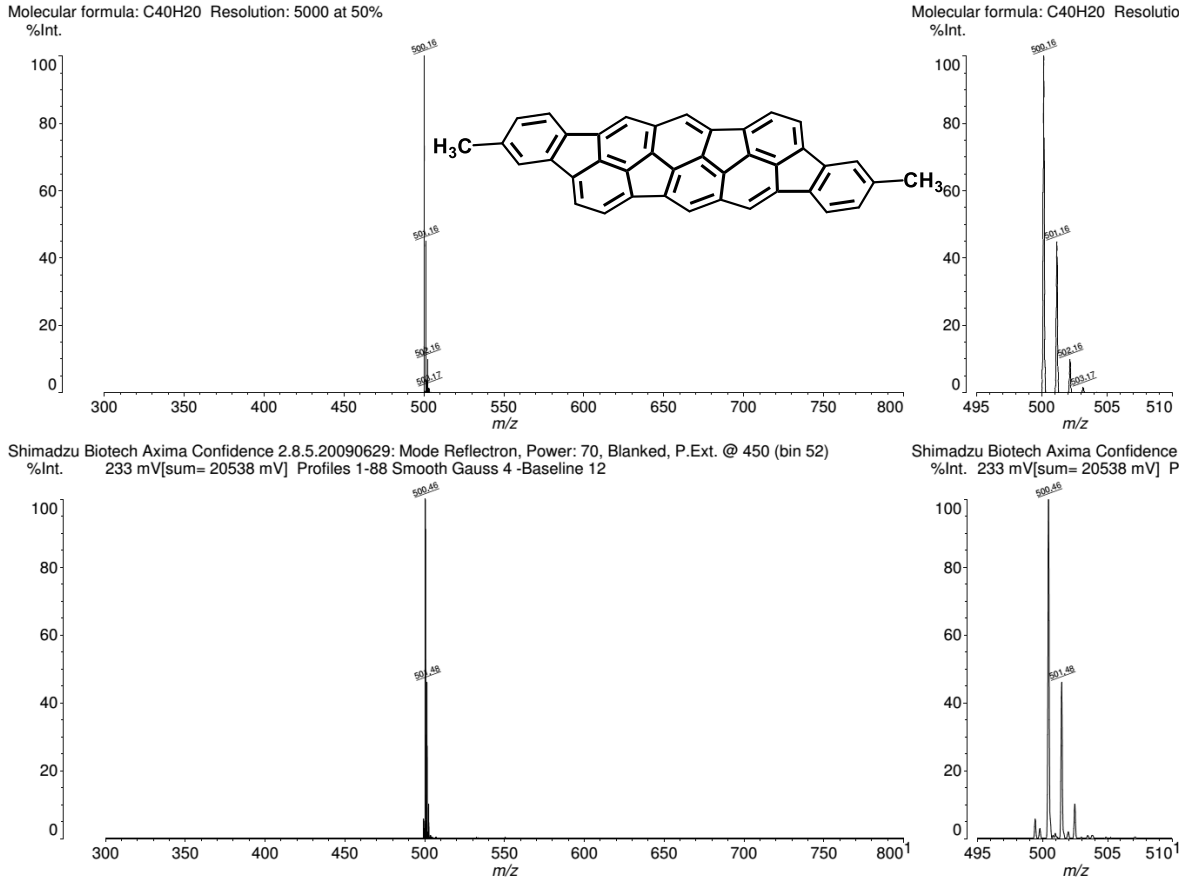

Figure A94. Mass spectrum (LDI) of 3,11-dimethylbenzo[*6,7*]-*as*-indaceno[*8,1,2,3-bcdef*]benzo[*6,7*]-*as*-indaceno[*8,1,2,3-klmno*]chrysene **66b**.

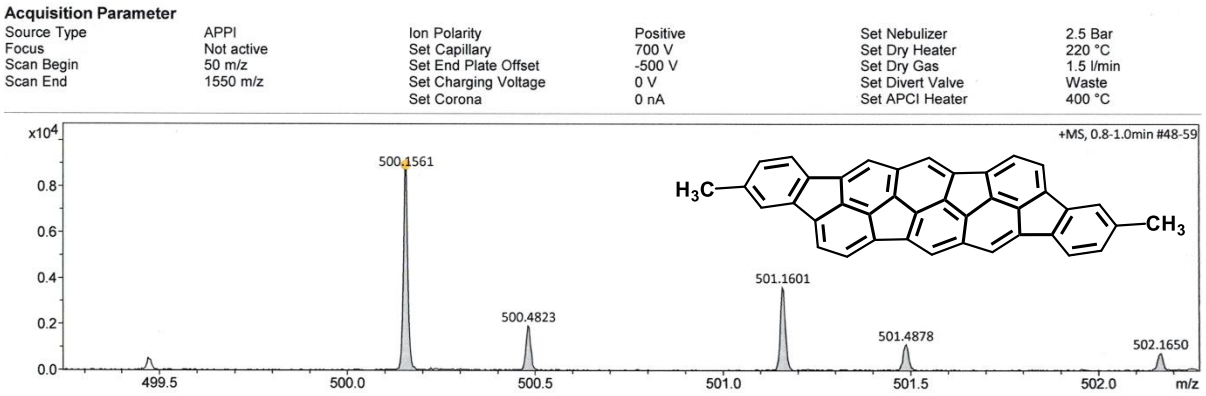

Figure A95. Mass spectrum (HRMS, APPI) of 3,11-dimethylbenzo[*6,7*]-*as*-indaceno[*8,1,2,3-bcdef*]-benzo[*6,7*]-*as*-indaceno[*8,1,2,3-klmno*]chrysene **66b**.

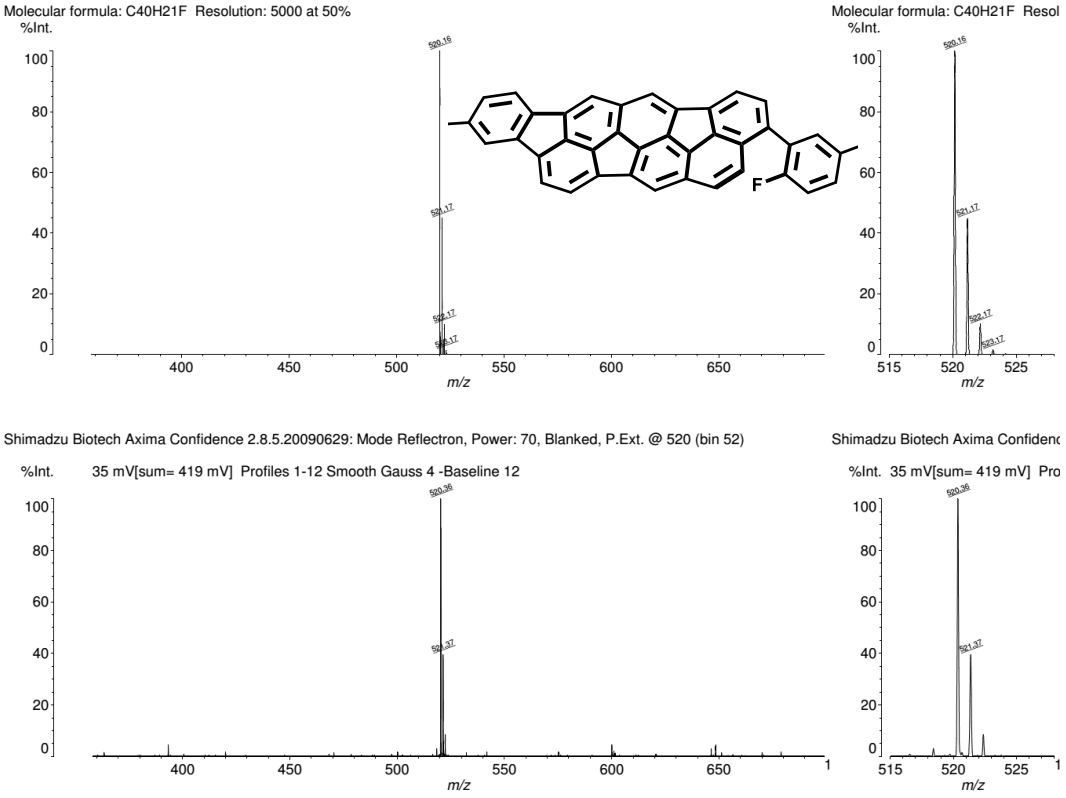

Figure A96. Mass spectrum (LDI) of 3-(2-fluoro-5-methylphenyl)-10-methylbenzo[*6,7*]-*as*-indaceno [*8,1,2,3-bcdef*] indeno[*4,3,2,1-lmno*]chrysene.

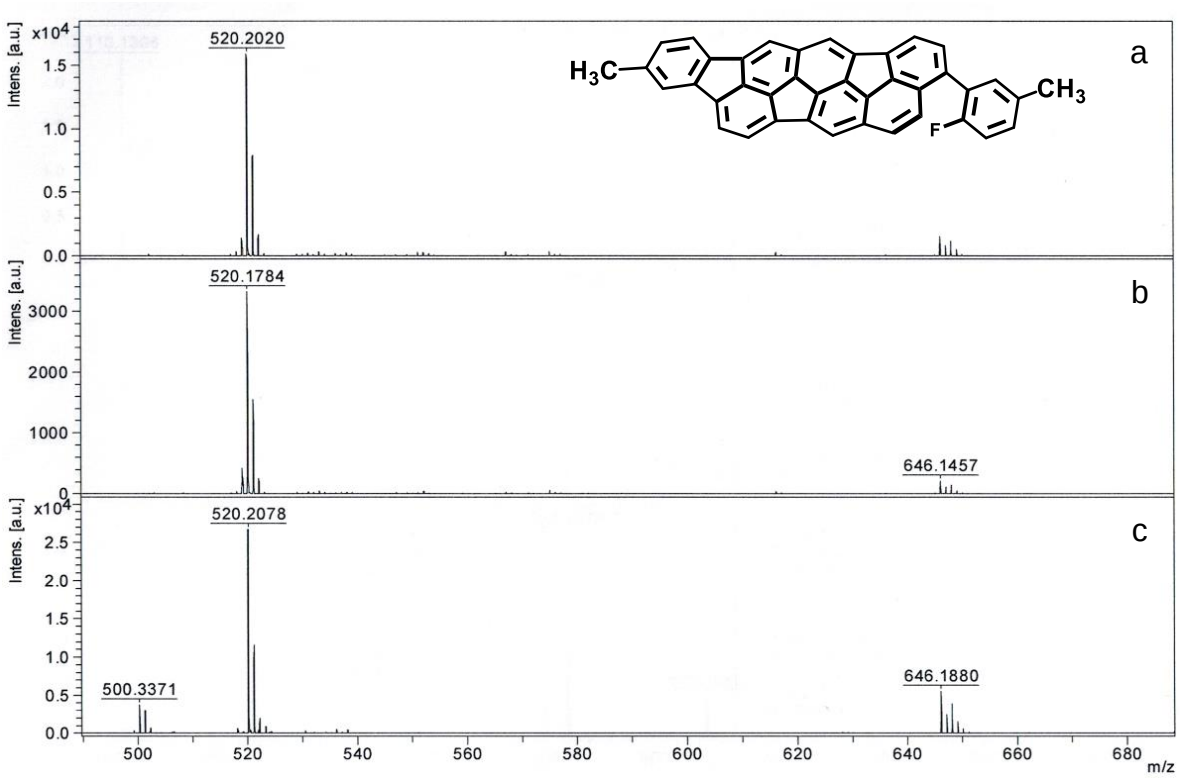

Figure A97. Mass spectrum (MALDI) of 3-(2-fluoro-5-methylphenyl)-10-methylbenzo[*6,7*]-*as*-indaceno[*8,1,2,3-bcdef*]indeno[*4,3,2,1-lmno*]chrysene: a) without matrix; b) with DHB matrix; c) with DCTB matrix.

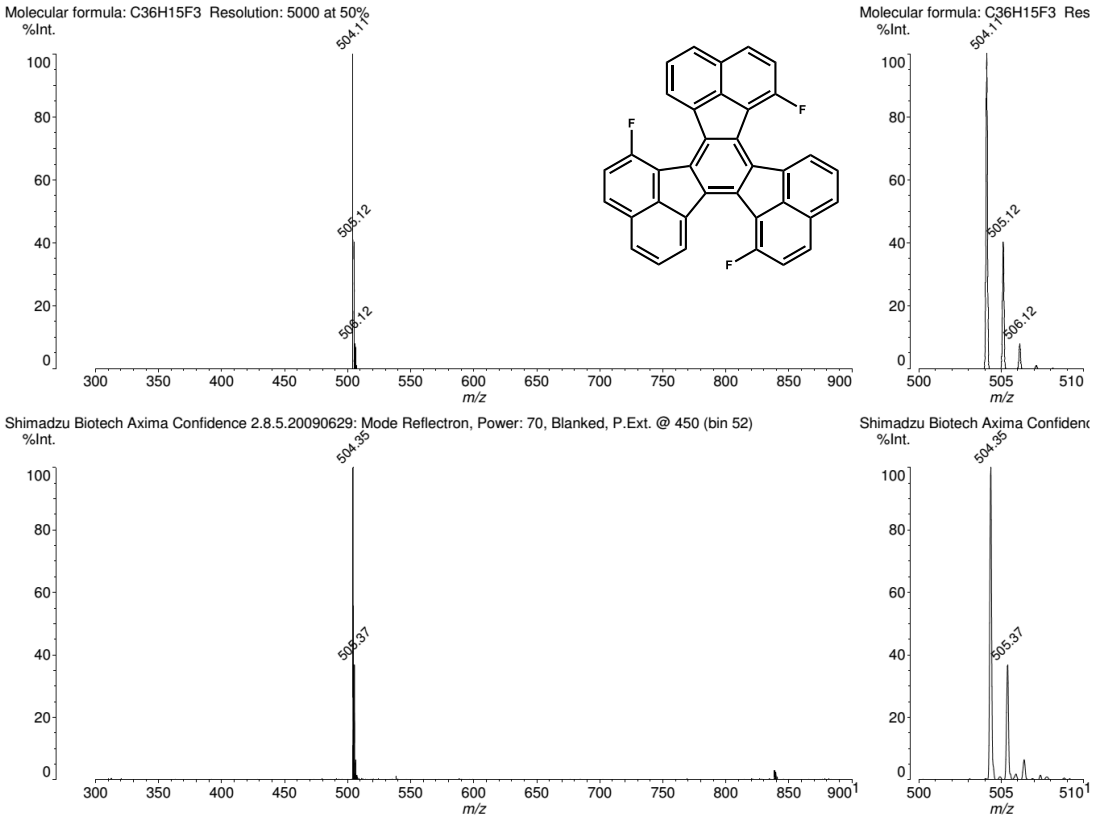

Figure A98. Mass spectrum (LDI) of 1,7,13-trifluorodecacyclene **70**.

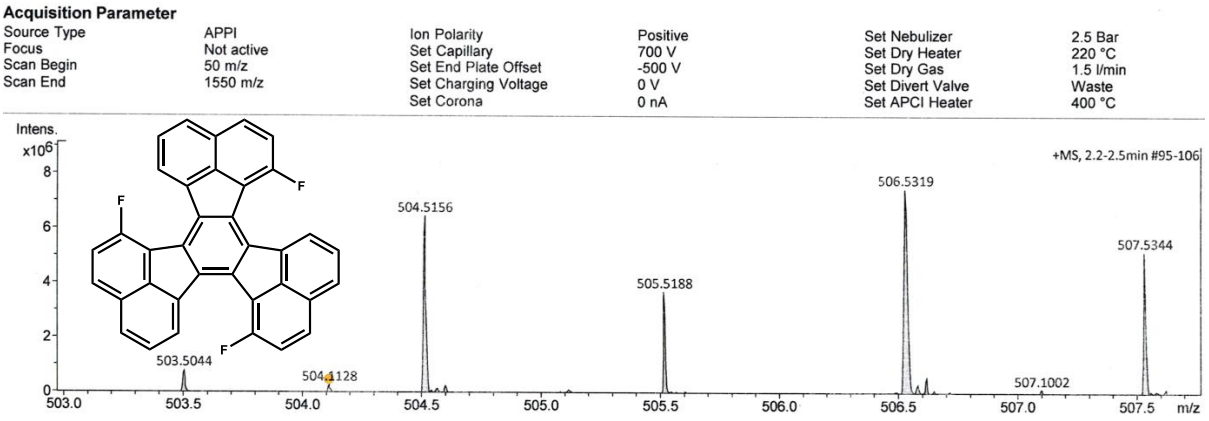

Figure A99. Mass spectrum (HRMS, APPI) of 1,7,13-trifluorodecacyclene **70**.

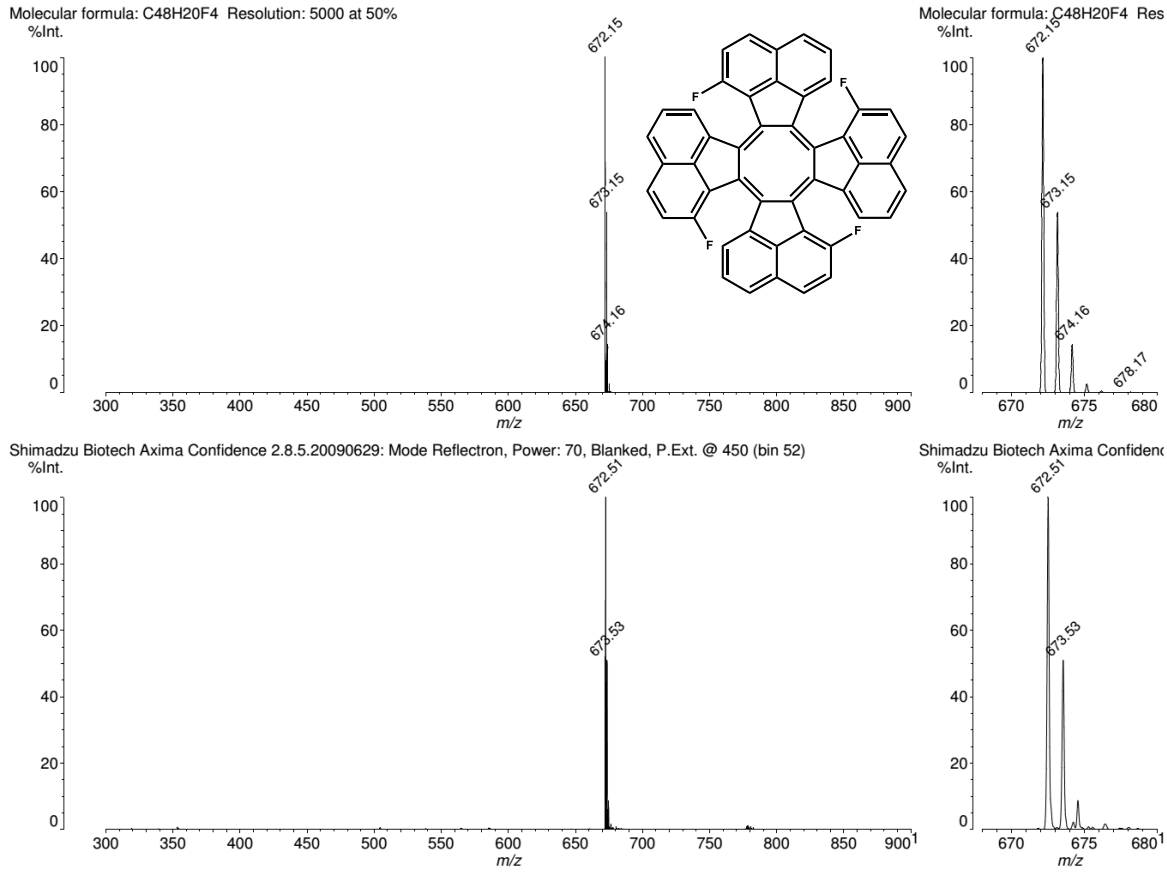

Figure A100. Mass spectrum (LDI) of 1,7,13,19-tetrafluorotridecacyclene **72**.

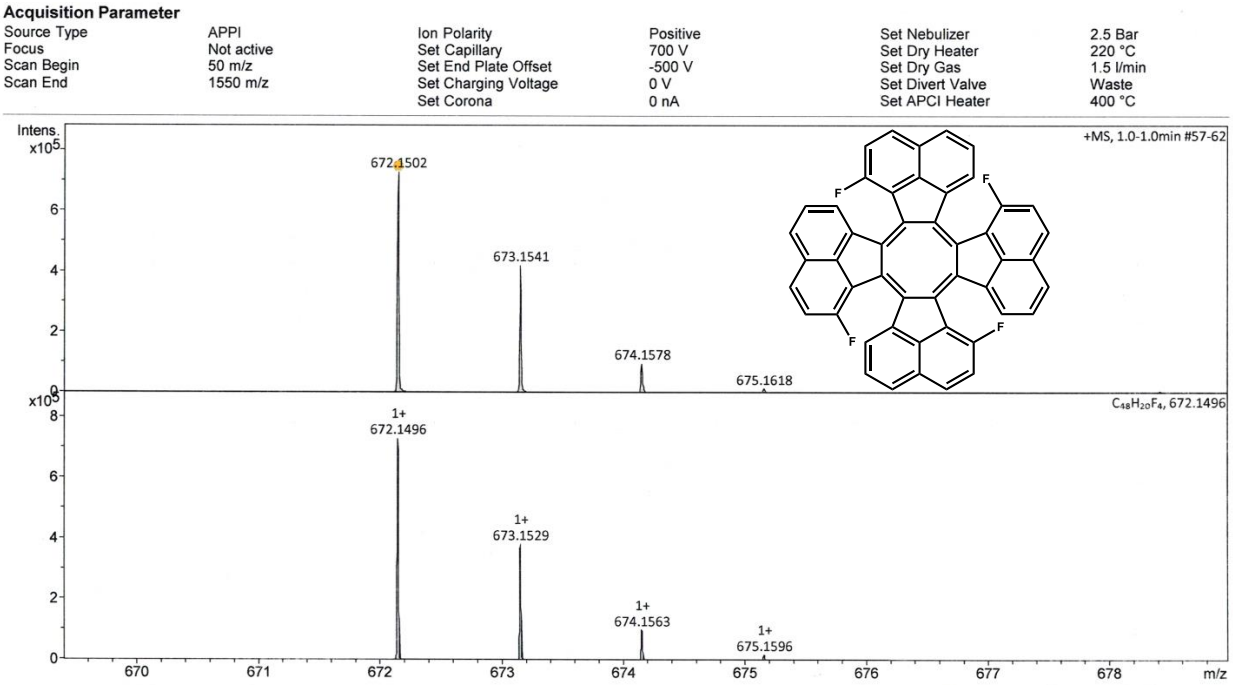

Figure A101. Mass spectrum (HRMS, APPI) of 1,7,13,19-tetrafluorotridecacyclene **72**.

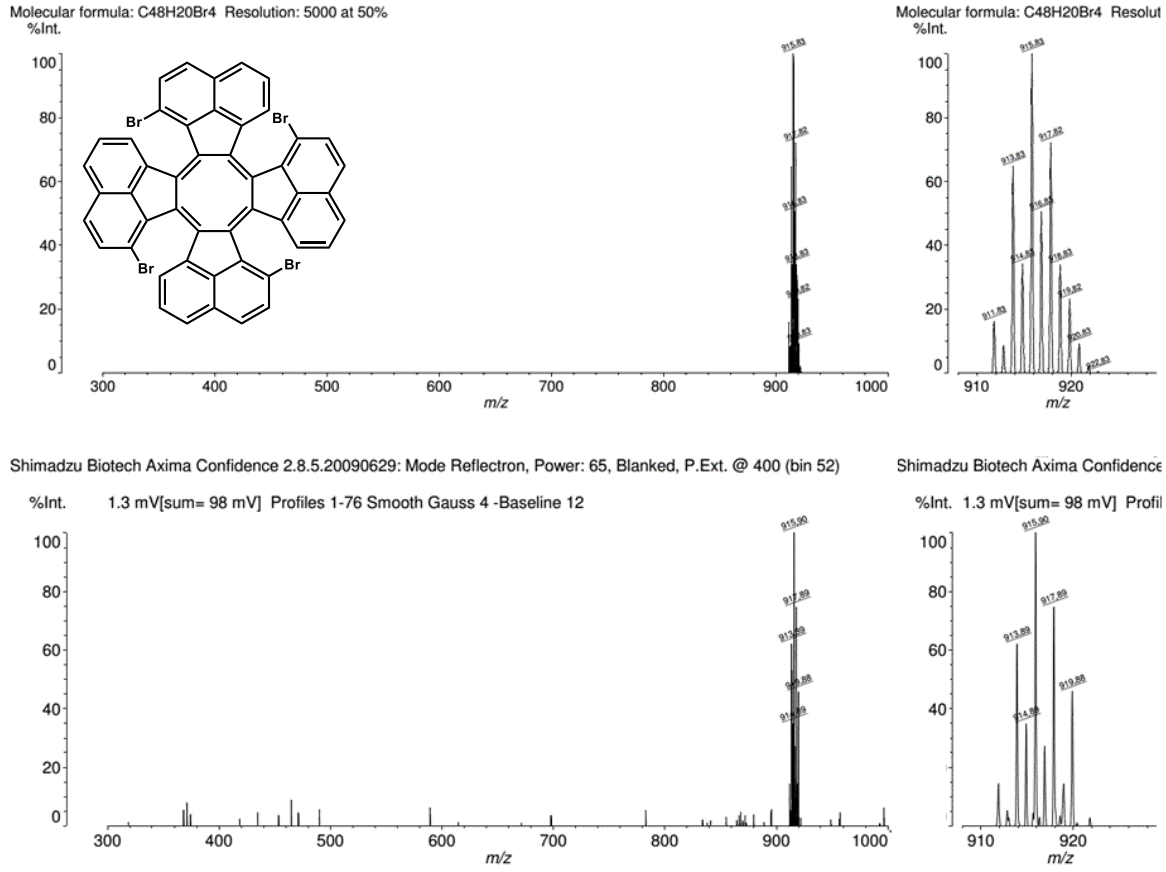

Figure A102. Mass spectrum (LDI) of 1,7,13,19-tetrabromotridecacyclene **90**.

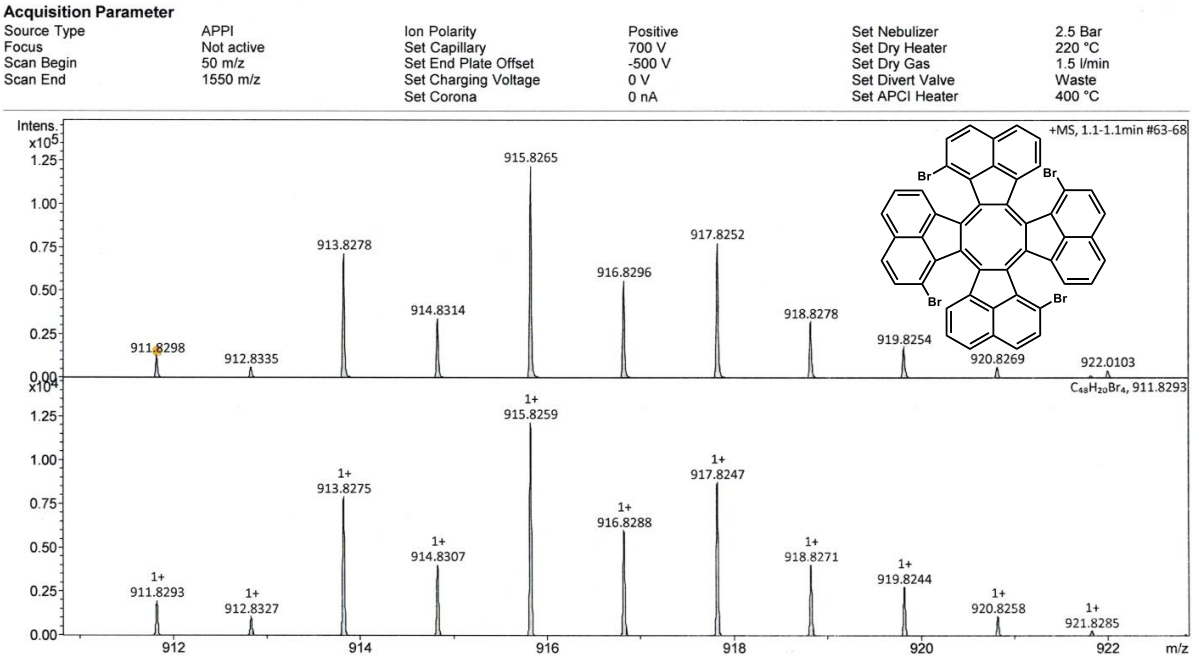

Figure A103. Mass spectrum (HRMS, APPI) of 1,7,13,19-tetrabromotridecacyclene **90**.

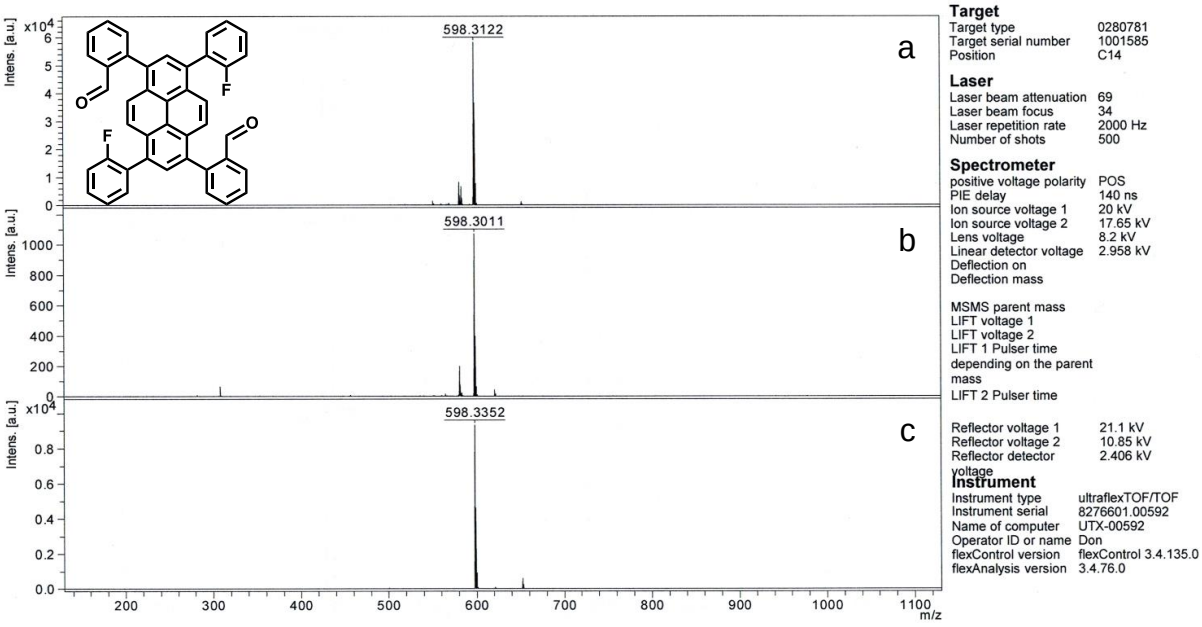

Figure 104. Mass spectrum (MALDI-TOF) of 2,2'-(3,8-bis(2-fluorophenyl)-pyrene-1,6-diyl)dibenzaldehyde **102**: a) without matrix; b) with DHB matrix; c) with DCTB matrix.

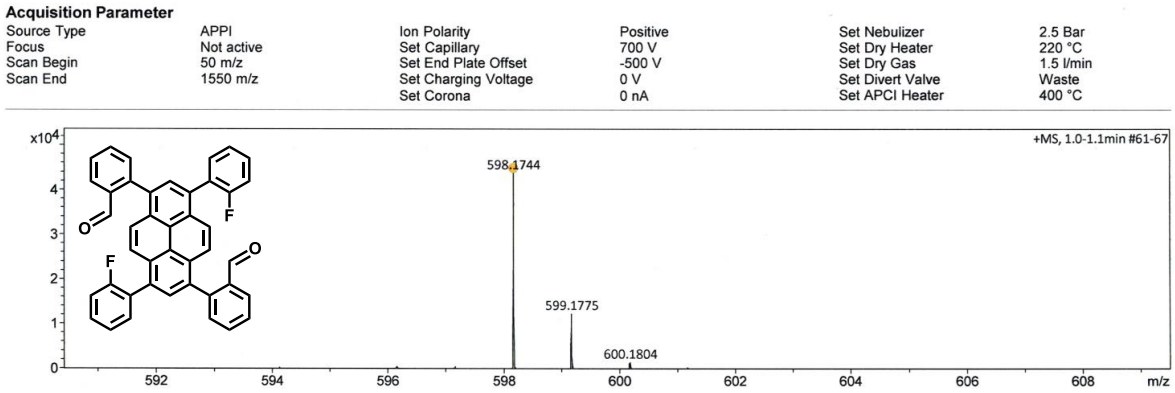

Figure A105. Mass spectrum (HRMS, APPI) of 2,2'-(3,8-bis(2-fluorophenyl)-pyrene-1,6-diyl)dibenz aldehyde **102**.

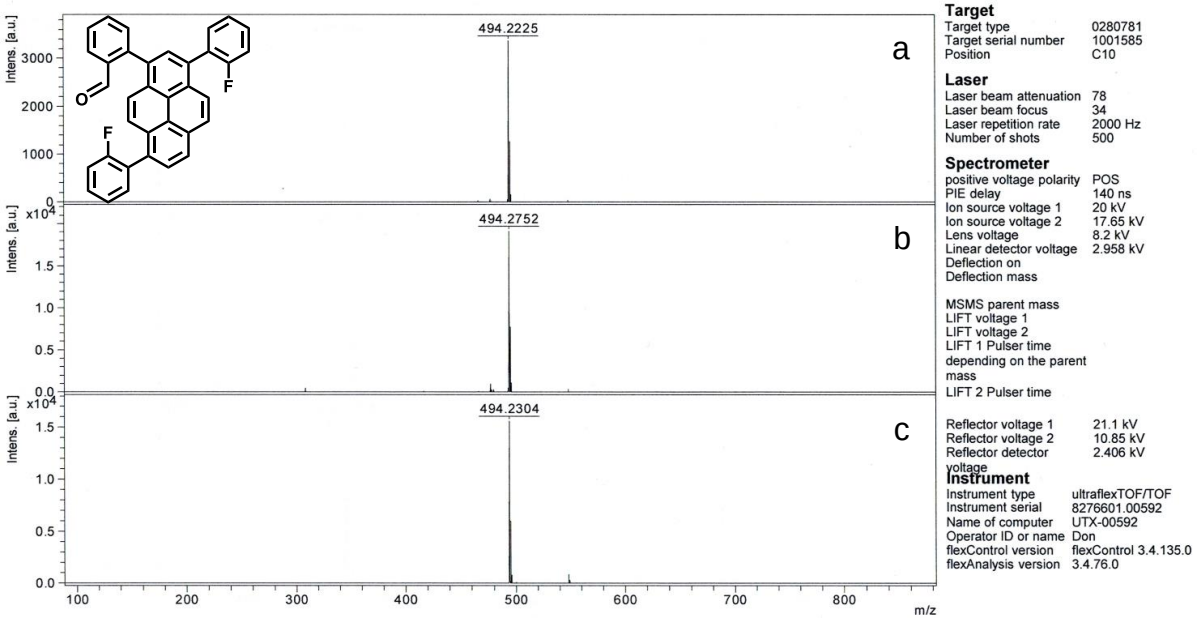

Figure A106. Mass spectrum (MALDI-TOF) of 2-(3,8-bis(2-fluorophenyl)pyren-1-yl)benzaldehyde **103**: a) without matrix; b) with DHB matrix; c) with DCTB matrix.

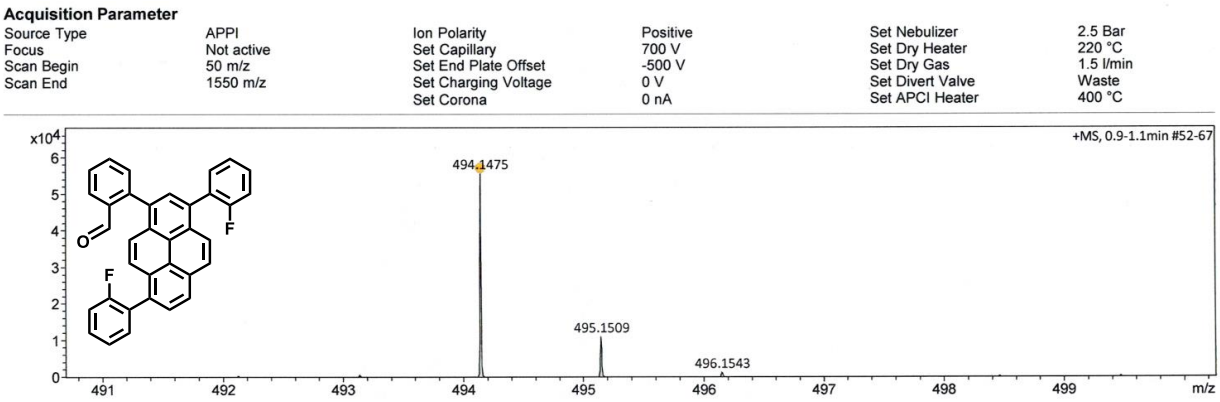

Figure A107. Mass spectrum (HRMS, APPI) of 2-(3,8-bis(2-fluorophenyl)pyren-1-yl)benzaldehyde **103**.

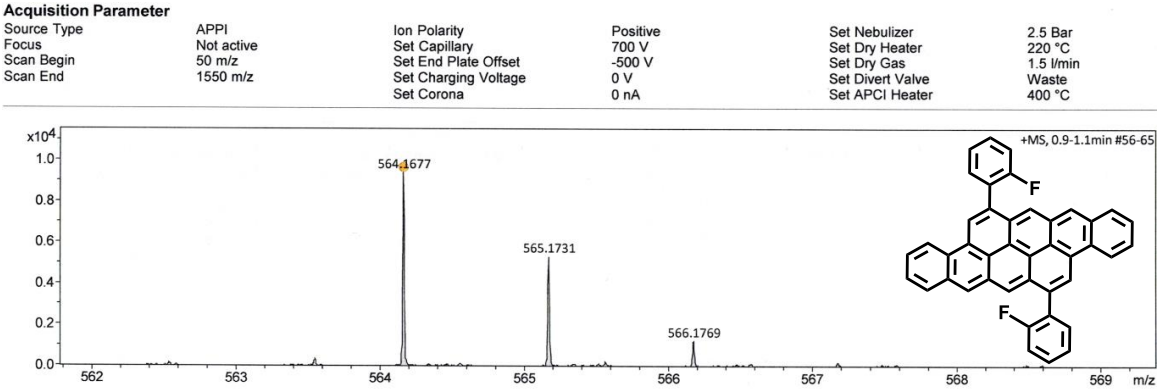

Figure A108. Mass spectrum (HRMS, APPI) of 6,14-bis(2-fluorophenyl)tetraceno[*2,1,12,11-opqra*]-tetracene **104**.

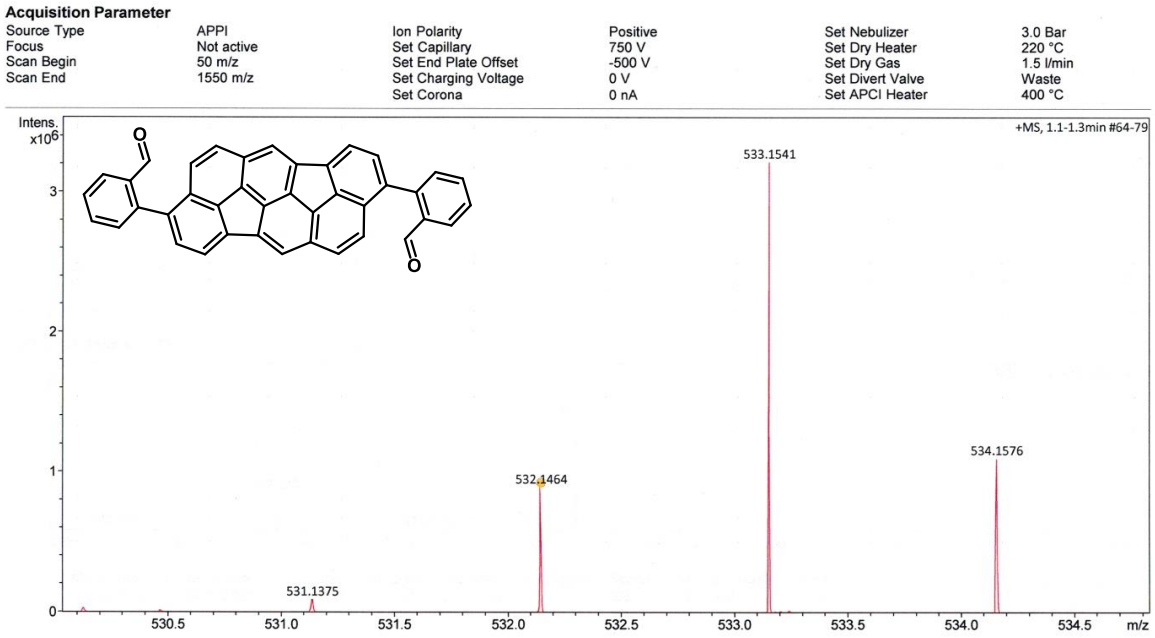

Figure A109. Mass spectrum (HRMS, APPI) of 2,2'-(diindeno[*4,3,2,1-cdef:4',3',2',1'-lmno*]chrysene-3,9-diyl)dibenzaldehyde **110**.

8 Appendix B – HPLC Chromatograms (UV-spectra)

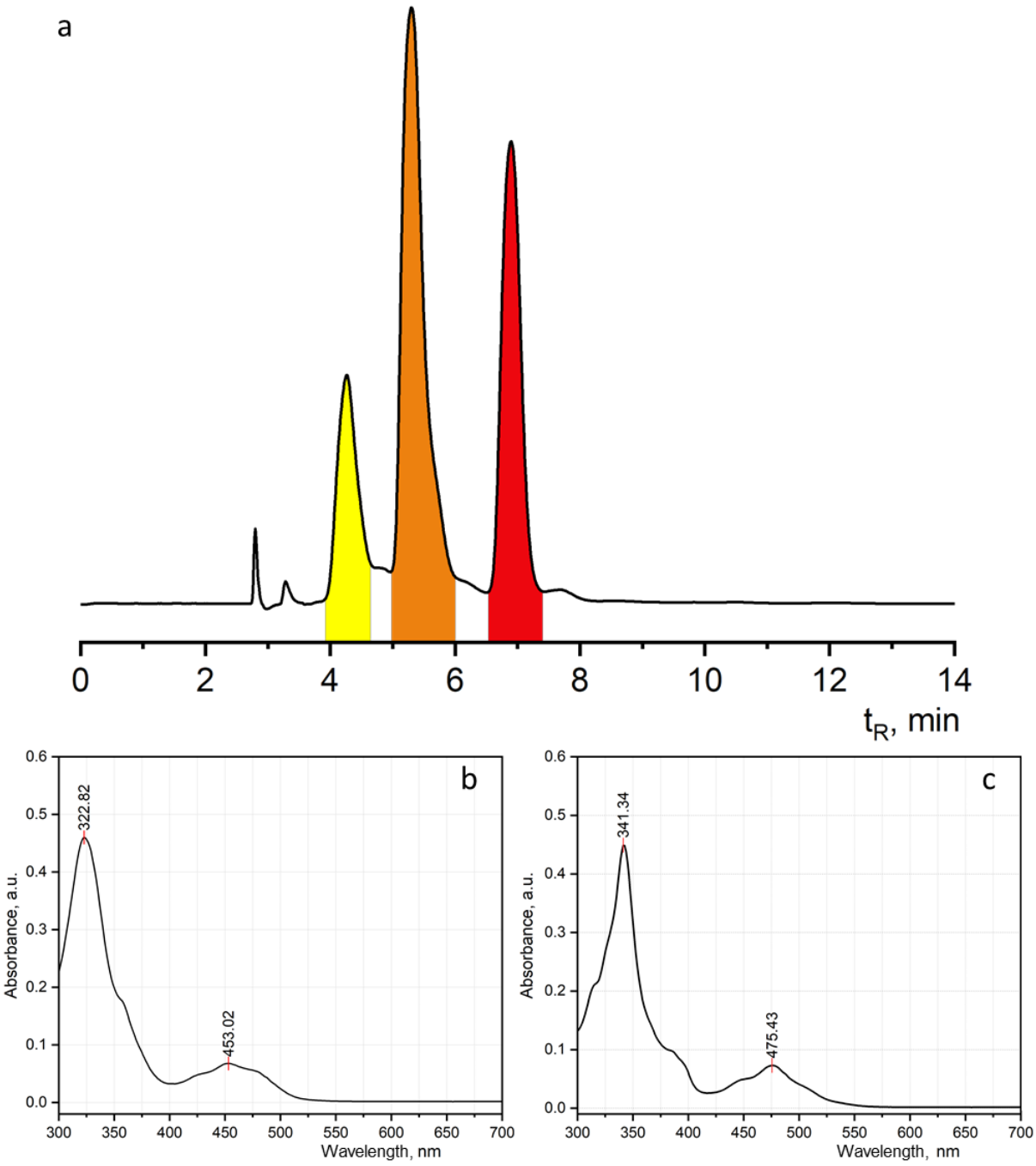

Figure B1. HPLC profile (**a**) as obtained after reaction CDHF of 3,9-bis(2-fluorophenyl)diindeno[*4,3,2,1-cdef:4',3',2',1'-lmno*]chrysene **65a** on *γ*-Al_2O_3 (230 ºC, 16 h, *o*-DCB), detected at 360 nm (PBr column, Tol:MeOH:7:3 as eluent, 1.0 ml min^{-1}, 35 ºC). UV-Vis spectrum of 3-(2-fluorophenyl)-10-methylbenzo[*6,7*]-*as*-indaceno[*8,1,2,3-bcdef*]indeno[*4,3,2,1-lmno*]chrysene (**b**) and 3-methylbenzo[*6,7*]-*as*-indaceno[*8,1,2,3-bcdef*]benzo[*6,7*]-*as*-indaceno[*8,1,2,3-klmno*]chrysene (**c**) in Tol:MeOH 7:3.

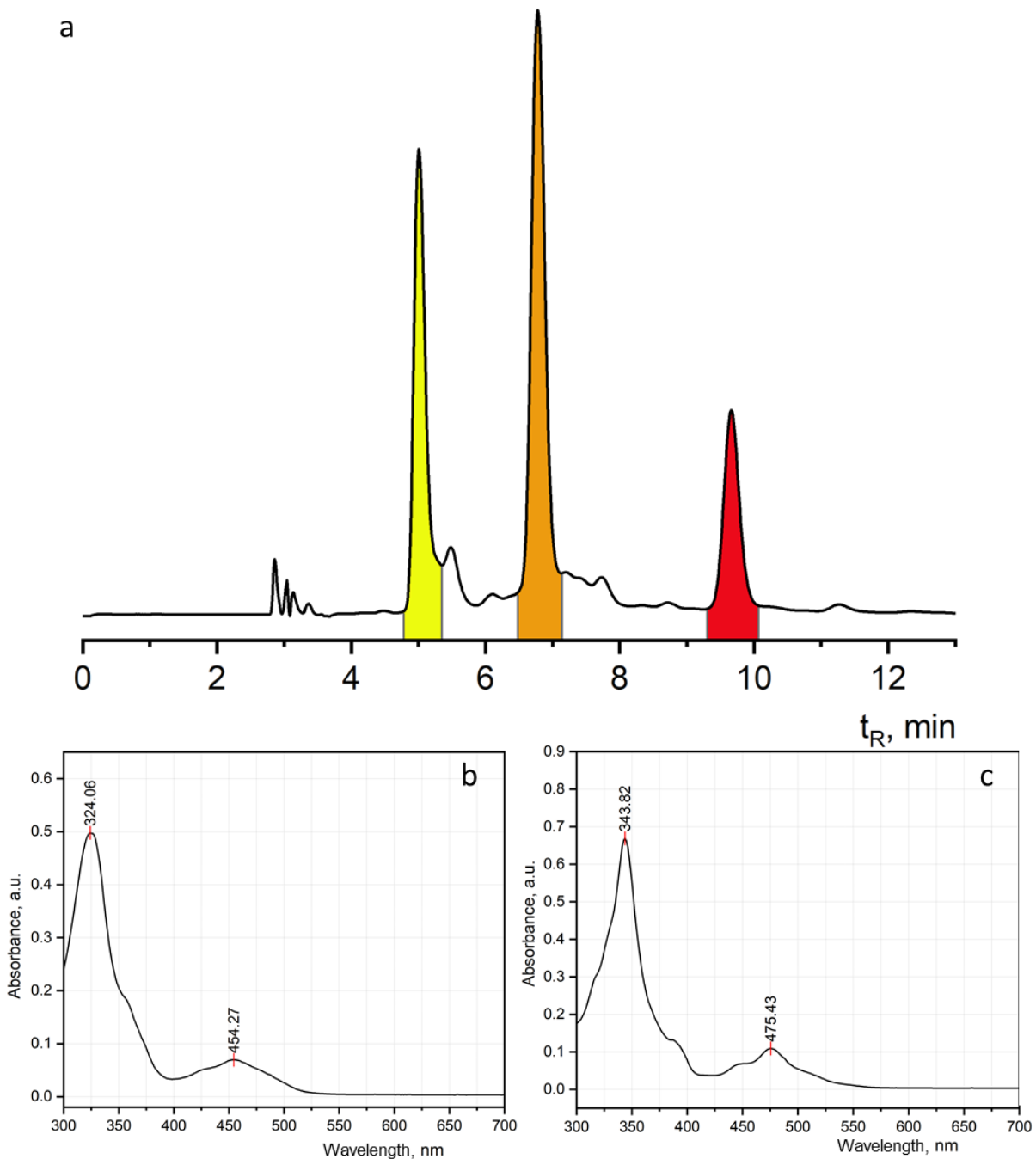

Figure B2. HPLC profile (**a**) as obtained after reaction CDHF of 3,9-bis(2-fluoro-5-methylphenyl)-diindeno[*4,3,2,1-cdef:4',3',2',1'-lmno*]chrysene **65b** on *γ*-Al_2O_3 (230 ºC, 16 h, *o*-DCB), detected at 360 nm (PBr column, Tol:MeOH:6:4 as eluent, 1.0 ml min^{-1}, 40 ºC). UV-Vis spectrum of 3-(2-fluoro-5-methylphenyl)-10-methylbenzo[*6,7*]-*as*-indaceno[*8,1,2,3-bcdef*]indeno[*4,3,2,1-lmno*]chrysene (**b**) and 3,11-dimethylbenzo[*6,7*]-as-indaceno[*8,1,2,3-bcdef*]benzo[*6,7*]-as-indaceno[*8,1,2,3-klmno*]chrysene (**c**) in Tol:MeOH 6:4.

9 Appendix C – X-Ray Crystallographic Data

9,12-Dibromo-as-indaceno[3,2,1,8,7,6-pqrstuv]picene (47)

Empirical formula	$C_{26}H_{10}Br_2$
Formula weight	482.16
Temperature (K)	153
Crystal system	orthorhombic
Space group	P*nma*
***a* (Å)**	16.9127(5)
***b* (Å)**	25.0146(9)
***c* (Å)**	3.90987(16)
α (°)	90
β (°)	90
γ (°)	90
Volume (Å^3)	1654.1(1)
Z	4
***D*$_{ber}$ (g·cm^{-3})**	1.936
μ (mm)	-1 6.274
F(000)	944.0
Crystal size (mm)	0.316 × 0.06 × 0.033
Radiation	CuK_α (λ = 1.54184 Å)
2Θ (°)	$5.5 \leq 2\Theta \leq 61.5$
Index ranges	$-18 \leq h \leq 18$, $-26 \leq k \leq 27$, $-4 \leq l \leq 3$
Reflections collected	3178
Independent reflections	1297
Data/restraints/parameters	1297/0/127
Goodness-of-fit on F^2	1.044
Final R indexes	R_1 = 0.0445, wR_2 = 0.1163
Largest peak/hole (e Å^{-3})	0.76/-0.52
Measurement:	SuperNova, Dual, Atlas
Data reduction	
Absorption correction:	SADABS 2014
Structure solution:	SHELXS-2014
Refinement	SHELXS-2014

3,9-Diphenyldiindeno[4,3,2,1-cdef:4',3',2',1'-lmno]chrysene (52)

Empirical formula	$C_{38}H_{20}$
Formula weight	476.54
Temperature (K)	100
Crystal system	orthorhombic
Space group	$P2_12_12_1$
a (Å)	7.4347(4)
b (Å)	14.0208(7)
c (Å)	21.5954(10)
α (°)	90
β (°)	90
γ (°)	90
Volume (Å3)	2251.1(2)
Z	4
D_{ber} (g·cm^{-3})	1.406
μ (mm)	0.080
F(000)	992
Crystal size (mm)	0.41×0.21×0.07
Radiation	MoK_α (λ = 0.71073 Å)
2Θ (°)	3.4 ≤ 2Θ ≤ 57.4
Index ranges	-10 ≤ h ≤ 10, -18 ≤ k ≤ 18, -29 ≤ l ≤ 29
Reflections collected	100207
Independent reflections	5800
Data/restraints/parameters	5800/0/343
Goodness-of-fit on F^2	1.044
Final R indexes	R_1 = 0.0423, wR_2 = 0.1018
Largest peak/hole (e Å^{-3})	0.48/-0.23
Measurement:	APEX 3 (Bruker AXS, 2016)
Data reduction	SAINT (Bruker AXS, 2009)
Absorption correction:	SADABS 2014/5 (Bruker AXS, 2014)
Structure solution:	SHELXTL NT 6.12 (Bruker AXS, 2002)
Refinement	SHELXTL 2014/6 (Sheldrick, 2008)

Diindeno[1,2,3-cd:1',2',3'-jk]pyrene (60)

Empirical formula	$C_{28}H_{14}$
Formula weight	350.42
Temperature (K)	153.05(10)
Crystal system	monoclinic
Space group	C2/c
a (Å)	19.4832(12)
b (Å)	3.89259(16)
c (Å)	21.7491(11)
α (°)	90
β (°)	103.415(5)
γ (°)	90
Volume (Å^3)	1604.45(14)
Z	8
D_{ber} (g·cm^{-3})	1.451
μ (mm)	0.630
F(000)	728.0
Crystal size (mm)	0.785 × 0.075 × 0.045
Radiation	Cu*Kα* (*λ* = 1.54184)
2Θ (°)	8.358 ≤ *2Θ* ≤ 145.098
Index ranges	23 ≤ *h* ≤ 16, -4 ≤ *k* ≤ 3, -20 ≤ *l* ≤ 26
Reflections collected	2196
Independent reflections	1526
Data/restraints/parameters	1526/0/127
Goodness-of-fit on F^2	1.082
Final R indexes	R_1 = 0.0510, wR_2 = 0.1353
Largest peak/hole (e Å^{-3})	0.26/-0.23
Measurement:	SuperNova, Dual, Atlas
Data reduction	
Absorption correction:	SADABS 2014
Structure solution:	SHELXS-2014
Refinement	SHELXL-2014

10 Appendix D – References

[1] L. T. Scott, H. E. Bronstein, D. V. Preda, R. B. M. Ansems, Bratcher, M. S, Hagen, Stefan, *Pure Appl. Chem.* **1999**, *71*(2), 209–219.

[2] X. Li, F. Kang, M. Inagaki, *Small* **2016**, *12*(24), 3206–3223.

[3] H. Sakurai, T. Daiko, T. Hirao, *Science* **2003**, *301*(5641), 1878.

[4] M. Rickhaus, M. Mayor, M. Juríček, *Chem. Soc. Rev.* **2017**, *46*(6), 1643–1660.

[5] W. E. Barth, R. G. Lawton, *J. Am. Chem. Soc.* **1966**, *88*(2), 380–381.

[6] R. G. Lawton, W. E. Barth, *J. Am. Chem. Soc.* **1971**, *93*(7), 1730–1745.

[7] L. T. Scott, M. M. Hashemi, D. T. Meyer, H. B. Warren, *J. Am. Chem. Soc.* **1991**, *113*(18), 7082–7084.

[8] L. T. Scott, P.-C. Cheng, M. M. Hashemi, M. S. Bratcher, D. T. Meyer, H. B. Warren, *J. Am. Chem. Soc.* **1997**, *119*(45), 10963–10968.

[9] A. Borchard, K. Hardcastle, P. Gantzel, J. S. Siegella, *Tetrahedron Lett.* **1993**, *34*(2), 273–276.

[10] T. J. Seiders, K. K. Baldridge, J. S. Siegel, *J. Am. Chem. Soc.* **1996**, *118*(11), 2754–2755.

[11] A. Sygula, P. W. Rabideau, *J. Am. Chem. Soc.* **2000**, *122*(26), 6323–6324.

[12] A. Sygula, G. Xu, Z. Marcinow, P. W. Rabideau, *Tetrahedron* **2001**, *57*(17), 3637–3644.

[13] G. Xu, A. Sygula, Z. Marcinow, P. W. Rabideau, *Tetrahedron Lett.* **2000**, *41*(51), 9931–9934.

[14] A. M. Butterfield, B. Gilomen, J. S. Siegel, *Org. Process Res. Dev.* **2012**, *16*(4), 664–676.

[15] A. Sygula, P. W. Rabideau, *J. Am. Chem. Soc.* **1998**, *120*(48), 12666–12667.

[16] A. Sygula, P. W. Rabideau, *J. Am. Chem. Soc.* **1999**, *121*(34), 7800–7803.

[17] A. Sygula, S. D. Karlen, R. Sygula, P. W. Rabideau, *Org. Lett.* **2002**, *4*(18), 3135–3137.

[18] G. Mehta, G. Panda, S. R. Shah, A. C. Kunwar, *J. Chem. Soc, Perkin Trans. 1* **1997**(16), 2269–2272.

[19] H. K. Gupta, P. E. Lock, M. J. McGlinchey, *Organometallics* **1997**, *16*(16), 3628–3634.

[20] U.D. Priyakumar, G.N. Sastry, *Tetrahedron Lett.* **2001**, *42*(7), 1379–1381.

[21] T. Amaya, T. Hirao, *The Chemical Record* **2015**, *15*(1), 310–321.

[22] A. Sygula, P. W. Rabideau in *Carbon-rich compounds*. *From molecules to materials*; (Eds. M. M. Haley, R. R. Tykwinski), Wiley-VCH, Weinheim, **2006**, pp. 529–565.

[23] E. Clar, *Polycyclic Hydrocarbons*: Volume 1; Springer Berlin Heidelberg; Imprint: Springer, Berlin, Heidelberg, **1964**.

[24] E. Clar, *Polycyclic hydrocarbons*: Volume 2; Academic Press, London, New York, **1964-**.

[25] F. S. Ehrenhauser, *Polycyclic Aromatic Compounds* **2015**, *35*(2-4), 161–176.

[26] D. Lungerich, Dissertation, Friedrich-Alexander-Universität Erlangen-Nürnberg, **2017**.

[27] H. Ito, K. Ozaki, K. Itami, *Angew. Chem. Int. Ed.* **2017**, *56*(37), 11144–11164.

[28] F. B. Mallory, C. S. Wood, J. T. Gordon, L. C. Lindquist, M. L. Savitz, *J. Am. Chem. Soc.* **1962**, *84*(22), 4361–4362.

[29] R. J. Hayward, A. C. Hopkinson, C. C. Leznoff, *Tetrahedron* **1972**, *28*(3), 439–447.

[30] T. Sato, Y. Goto, K. Hata, *BCSJ* **1967**, *40*(8), 1994–1995.

[31] L. Liu, B. Yang, T. J. Katz, M. K. Poindexter, *J. Org. Chem.* **1991**, *56*(12), 3769–3775.

[32] K. B. Jørgensen, *Molecules* **2010**, *15*(6), 4334–4358.

[33] Z. Li, R. J. Twieg, *Chem. Eur. J.* **2015**, *21*(44), 15534–15539.

[34] C.-Y. Chiu, B. Kim, A. A. Gorodetsky, W. Sattler, S. Wei, A. Sattler, M. Steigerwald, C. Nuckolls, *Chem. Sci.* **2011**, *2*(8), 1480–1486.

[35] S. Xiao, S. J. Kang, Y. Wu, S. Ahn, J. B. Kim, Y.-L. Loo, T. Siegrist, M. L. Steigerwald, H. Li, C. Nuckolls, *Chem. Sci.* **2013**, *4*(5), 2018.

[36] P. U. Biedermann, T.-Y. Luh, D. T.-C. Wengc, C.-H. Kuo, J. J. Stezowski, I. Agranat, *Polycyclic Aromatic Compounds* **1996**, *8*(2-3), 167–175.

[37] R. Scholl, J. Mansfeld, *Ber. Dtsch. Chem. Ges.* **1910**, *43*(2), 1734–1746.

[38] M. Grzybowski, K. Skonieczny, H. Butenschön, D. T. Gryko, *Angew. Chem. Int. Ed.* **2013**, *52*(38), 9900–9930.

[39] C. D. Simpson, J. D. Brand, A. J. Berresheim, L. Przybilla, H. J. Räder, K. Müllen, *Chem. Eur. J.* **2002**, *8*(6), 1424–1429.

[40] M. Kawamura, E. Tsurumaki, S. Toyota, *Synthesis* **2018**, *50*(01), 134–138.

[41] J. Liu, A. Narita, S. Osella, W. Zhang, D. Schollmeyer, D. Beljonne, X. Feng, K.

Müllen, *J. Am. Chem. Soc.* **2016**, *138*(8), 2602–2608.

[42] S. Nobusue, K. Fujita, Y. Tobe, *Org. Lett.* **2017**, *19*(12), 3227–3230.

[43] K.Y. Amsharov, K. Simeonov, M. Jansen, *Carbon* **2007**, *45*(2), 337–343.

[44] K. Y. Amsharov, M. Jansen, *J. Org. Chem.* **2008**, *73*(7), 2931–2934.

[45] K. Amsharov, M. Jansen, *Chem. Commun.* **2009**(19), 2691–2693.

[46] L. T. Scott, *Angew. Chem. Int. Ed. Engl.* **2004**, *43*(38), 4994–5007.

[47] V. M. Tsefrikas, L. T. Scott, *Chem. Rev.* **2006**, *106*(12), 4868–4884.

[48] L. T. Scott, D. V. Preda in *Abstracts of papers, 219th ACS national meeting*. *San Francisco, CA, March 26 - 30, 2000*, Washington, DC, **2000**.

[49] L. T. Scott, *Pure Appl. Chem.* **1996**, *68*(2), 291–300.

[50] H. E. Bronstein, N. Choi, L. T. Scott, *J. Am. Chem. Soc.* **2002**, *124*(30), 8870–8875.

[51] S. Hagen, M. S. Bratcher, M. S. Erickson, G. Zimmermann, L. T. Scott, *Angew. Chem. Int. Ed. Engl.* **1997**, *36*(4), 406–408.

[52] A. H. Abdourazak, Z. Marcinow, A. Sygula, R. Sygula, P. W. Rabideau, *J. Am. Chem. Soc.* **1995**, *117*(23), 6410–6411.

[53] L. T. Scott, M. S. Bratcher, S. Hagen, *J. Am. Chem. Soc.* **1996**, *118*(36), 8743–8744.

[54] R. B. M. Ansems, L. T. Scott, *J. Am. Chem. Soc.* **2000**, *122*(12), 2719–2724.

[55] L. T. Scott, M. M. Boorum, B. J. McMahon, S. Hagen, J. Mack, J. Blank, H. Wegner, A. de Meijere, *Science* **2002**, *295*(5559), 1500–1503.

[56] S. Pascual, P. de Mendoza, A. M. Echavarren, *Org. Biomol. Chem.* **2007**, *5*(17), 2727–2734.

[57] Le Wang, P. B. Shevlin, *Tetrahedron Lett.* **2000**, *41*(3), 285–288.

[58] Le Wang, P. B. Shevlin, *Org. Lett.* **2000**, *2*(23), 3703–3705.

[59] H. A. Wegner, H. Reisch, K. Rauch, A. Demeter, K. A. Zachariasse, A. de Meijere, L. T. Scott, *J. Org. Chem.* **2006**, *71*(24), 9080–9087.

[60] E. A. Jackson, B. D. Steinberg, M. Bancu, A. Wakamiya, L. T. Scott, *J. Am. Chem. Soc.* **2007**, *129*(3), 484–485.

[61] G. Otero, G. Biddau, C. Sánchez-Sánchez, R. Caillard, M. F. López, C. Rogero, F. J. Palomares, N. Cabello, M. A. Basanta, J. Ortega, J. Méndez, A. M. Echavarren, R. Pérez, B. Gómez-Lor, J. A. Martín-Gago, *Nature* **2008**, *454*(7206), 865.

[62] J. R. Sanchez-Valencia, T. Dienel, O. Gröning, I. Shorubalko, A. Mueller, M.

Jansen, K. Amsharov, P. Ruffieux, R. Fasel, *Nature* **2014**, *512*(7512), 61.

[63] J. Cai, P. Ruffieux, R. Jaafar, M. Bieri, T. Braun, S. Blankenburg, M. Muoth, A. P. Seitsonen, M. Saleh, X. Feng, K. Müllen, R. Fasel, *Nature* **2010**, *466*(7305), 470.

[64] K. T. Rim, M. Siaj, S. Xiao, M. Myers, V. D. Carpentier, L. Liu, C. Su, M. L. Steigerwald, M. S. Hybertsen, P. H. McBreen, G. W. Flynn, C. Nuckolls, *Angew. Chem. Int. Ed.* **2007**, *46*(41), 7891–7895.

[65] K. Amsharov in *From polyphenylenes to nanographenes and graphene nanoribbons*, *Advances in Polymer Science*, *Vol. 278*; (Eds. K. Müllen, X. Feng), Springer, Cham, **2017**, pp. 127–145.

[66] K. Amsharov, M. Jansen, *Chem. Commun.* **2009**, *0*(19), 2691–2693.

[67] H. Amii, K. Uneyama, *Chem. Rev.* **2009**, *109*(5), 2119–2183.

[68] T. Hiyama, *Organofluorine Compounds*: Chemistry and Applications; Springer Berlin Heidelberg, Berlin, Heidelberg, s.l, **2000**.

[69] E. Clot, O. Eisenstein, N. Jasim, S. A. Macgregor, J. E. McGrady, R. N. Perutz, *Acc. Chem. Res.* **2011**, *44*(5), 333–348.

[70] J. Weaver, S. Senaweera, *Tetrahedron* **2014**, *70*(41), 7413–7428.

[71] T. A. Unzner, T. Magauer, *Tetrahedron Lett.* **2015**, *56*(7), 877–883.

[72] T. Stahl, H. F. T. Klare, M. Oestreich, *ACS Catal.* **2013**, *3*(7), 1578–1587.

[73] T. Ahrens, J. Kohlmann, M. Ahrens, T. Braun, *Chem. Rev.* **2015**, *115*(2), 931–972.

[74] K. Tamao, K. Sumitani, M. Kumada, *J. Am. Chem. Soc.* **1972**, *94*(12), 4374–4376.

[75] V. P. W. Böhm, C. W. K. Gstöttmayr, T. Weskamp, W. A. Herrmann, *Angew. Chem. Int. Ed.* **2001**, *40*(18), 3387–3389.

[76] T. Saeki, Y. Takashima, K. Tamao, *Synlett* **2005**(11), 1771–1774.

[77] T. Braun, R. N. Perutz, M. I. Sladek, *Chem. Commun.* **2001**(21), 2254–2255.

[78] A. Steffen, M. I. Sladek, T. Braun, B. Neumann, H.-G. Stammler, *Organometallics* **2005**, *24*(16), 4057–4064.

[79] N. Yoshikai, H. Mashima, E. Nakamura, *J. Am. Chem. Soc.* **2005**, *127*(51), 17978–17979.

[80] K. Manabe, S. Ishikawa, *Synthesis* **2008**, *2008*(16), 2645–2649.

[81] D. A. Widdowson, R. Wilhelm, *Chem. Commun.* **1999**(21), 2211–2212.

[82] K. Mikami, T. Miyamoto, M. Hatano, *Chem. Commun.* **2004**(18), 2082–2083.

[83] Y. M. Kim, S. Yu, *J. Am. Chem. Soc.* **2003**, *125*(7), 1696–1697.

[84] S. Bahmanyar, B. C. Borer, Y. M. Kim, D. M. Kurtz, S. Yu, *Org. Lett.* **2005**, *7*(6), 1011–1014.

[85] J. Ichikawa, H. Jyono, T. Kudo, M. Fujiwara, M. Yokota, *Synthesis* **2005**, *2005*(01), 39–46.

[86] J. Ichikawa, M. Yokota, T. Kudo, S. Umezaki, *Angew. Chem. Int. Ed.* **2008**, *47*(26), 4870–4873.

[87] N. Suzuki, T. Fujita, J. Ichikawa, *Org. Lett.* **2015**, *17*(20), 4984–4987.

[88] K. Fuchibe, H. Jyono, M. Fujiwara, T. Kudo, M. Yokota, J. Ichikawa, *Chem. Eur. J.* **2011**, *17*(43), 12175–12185.

[89] H. Isobe, S. Hitosugi, T. Matsuno, T. Iwamoto, J. Ichikawa, *Org. Lett.* **2009**, *11*(17), 4026–4028.

[90] K. Fuchibe, Y. Mayumi, N. Zhao, S. Watanabe, M. Yokota, J. Ichikawa, *Angewandte Chemie (International ed. in English)* **2013**, *52*(30), 7825–7828.

[91] K. Fuchibe, Y. Mayumi, N. Zhao, S. Watanabe, M. Yokota, J. Ichikawa, *Angew. Chem. Int. Ed.* **2013**, *125*(30), 7979–7982.

[92] O. Allemann, S. Duttwyler, P. Romanato, K. K. Baldridge, J. S. Siegel, *Science* **2011**, *332*(6029), 574–577.

[93] S. Duttwyler, C. Douvris, N. L. P. Fackler, F. S. Tham, C. A. Reed, K. K. Baldridge, J. S. Siegel, *Angew. Chem. Int. Ed.* **2010**, *49*(41), 7519–7522.

[94] X. Wu, X. C. Zeng, *Nano Lett.* **2009**, *9*(1), 250–256.

[95] A. K. Dutta, A. Linden, L. Zoppi, K. K. Baldridge, J. S. Siegel, *Angew. Chem. Int. Ed.* **2015**, *54*(37), 10792–10796.

[96] K. Y. Amsharov, M. A. Kabdulov, M. Jansen, *Chem. Eur. J.* **2010**, *16*(20), 5868–5871.

[97] K. Y. Amsharov, P. Merz, *J. Org. Chem.* **2012**, *77*(12), 5445–5448.

[98] O. Papaianina, V. A. Akhmetov, A. A. Goryunkov, F. Hampel, F. W. Heinemann, K. Y. Amsharov, *Angew. Chem. Int. Ed.* **2017**, *56*(17), 4834–4838.

[99] D. Sharapa, A.-K. Steiner, K. Amsharov, *physica status solidi (b)* **2018**, *255*(12).

[100] O. Papaianina, K. Y. Amsharov, *Chem. Commun.* **2016**, *52*(7), 1505–1508.

[101] K. Amsharov, *Phys. Status Solidi B* **2016**, *253*(12), 2473–2477.

[102] K. Y. Amsharov, M. A. Kabdulov, M. Jansen, *Angew. Chem.* **2012**, *124*(19), 4672–4675.

[103] K. Fuchibe, T. Akiyama, *J. Am. Chem. Soc.* **2006**, *128*(5), 1434–1435.

[104] K. Fuchibe, K. Mitomi, R. Suzuki, T. Akiyama, *Chem. Asian J.* **2008**, *3*(2), 261–271.

[105] T. L. Gianetti, R. G. Bergman, J. Arnold, *J. Am. Chem. Soc.* **2013**, *135*(22), 8145–8148.

[106] J. Terao, M. Nakamura, N. Kambe, *Chem. Commun.* **2009**(40), 6011–6013.

[107] W. Gu, M. R. Haneline, C. Douvris, O. V. Ozerov, *J. Am. Chem. Soc.* **2009**, *131*(31), 11203–11212.

[108] F. Wang, J. Hu, *Chin. J. Chem.* **2009**, *27*(1), 93–98.

[109] A. Kethe, A. F. Tracy, D. A. Klumpp, *Org. Biomol. Chem.* **2011**, *9*(12), 4545–4549.

[110] A. Okamoto, K. Kumeda, N. Yonezawa, *Chem. Lett.* **2010**, *39*(2), 124–125.

[111] C. Saboureau, M. Troupel, S. Sibille, J. Périchon, *J. Chem. Soc, Chem. Commun.* **1989**(16), 1138–1139.

[112] G. B. Deacon, P. C. Junk, D. Werner, *Eur. J. Inorg. Chem.* **2015**, *2015*(9), 1484–1489.

[113] S. Utsumi, T. Katagiri, K. Uneyama, *J. Fluor. Chem.* **2013**, *152*, 84–89.

[114] B. Leach, *Applied Industrial Catalysis;* Elsevier Science, Oxford, **1983**.

[115] L. D. Hart, E. Lense, Eds, *Alumina chemicals*: Science and technology handbook; American Ceramic Society, Westerville, Ohio, **1990**.

[116] M. Trueba, S. P. Trasatti, *Eur. J. Inorg. Chem.* **2005**, *2005*(17), 3393–3403.

[117] B. A. Latella, B. H. O'Connor, *J. Am. Ceram. Soc.* **1997**, *80*(11), 2941–2944.

[118] T. C. Chou, D. Adamson, J. Mardinly, T. G. Nieh, *Thin Solid Films* **1991**, *205*(2), 131–139.

[119] I. Levin, D. Brandon, *J. Am. Ceram. Soc.* **1998**, *81*(8), 1995–2012.

[120] K. Sohlberg, S. J. Pennycook, S. T. Pantelides, *J. Am. Chem. Soc.* **1999**, *121*(33), 7493–7499.

[121] A. A. Tsyganenko, P. P. Mardilovich, *J. Chem. Soc, Faraday Trans.* **1996**, *92*(23), 4843.

[122] G. Paglia, C. E. Buckley, T. J. Udovic, A. L. Rohl, F. Jones, C. F. Maitland, J. Connolly, *Chem. Mater.* **2004**, *16*(10), 1914–1923.

[123] T.-Z. Ren, Z.-Y. Yuan, B.-L. Su, *Langmuir* **2004**, *20*(4), 1531–1534.

[124] I. Levin, L. A. Bendersky, D. G. Brandon, M. Rühle, *Acta Mater.* **1997**, *45*(9), 3659–3669.

[125] R. McPherson, *J. Mater. Sci.* **1973**, *8*(6), 851–858.

[126] R. McPherson, *J. Mater. Sci.* **1980**, *15*(12), 3141–3149.

[127] M. Plummer, *J. Appl. Chem.* **1958**, *8*(1), 35–44.

[128] K. P. Sinha, A. P. B. Sinha, *J. Phys. Chem.* **1957**, *61*(6), 758–761.

[129] R.-S. Zhou, R. L. Snyder, *Acta Cryst. B.* **1991**, *47*(5), 617–630.

[130] Y. G. Wang, P. M. Bronsveld, J. T. M. DeHosson, B. Djuričić, D. McGarry, S. Pickering, *J. Am. Ceram. Soc.* **1998**, *81*(6), 1655–1660.

[131] S. J. Wilson, *J. Solid State Chem.* **1979**, *30*(2), 247–255.

[132] S. J. Wilson, J.D.C. Mc Connell, *J. Solid State Chem.* **1980**, *34*(3), 315–322.

[133] H. Knözinger, P. Ratnasamy, *Catalysis Reviews* **1978**, *17*(1), 31–70.

[134] M. Digne, P. Sautet, P. Raybaud, P. Euzen, H. Toulhoat, *J. Catal.* **2002**, *211*(1), 1–5.

[135] J. Hietala, A. Root, P. Knuuttila, *J. Catal.* **1994**, *150*(1), 46–55.

[136] R. Wischert, C. Copéret, F. Delbecq, P. Sautet, *Angew. Chem. Int. Ed.* **2011**, *50*(14), 3202–3205.

[137] M. Nguefack, A. F. Popa, S. Rossignol, C. Kappenstein, *Phys. Chem. Chem. Phys.* **2003**, *5*(19), 4279–4289.

[138] E. F. Sawilowsky, O. Meroueh, H. B. Schlegel, W. L. Hase, *J. Phys. Chem. A* **2000**, *104*(21), 4920–4927.

[139] W. Tochtermann, K. Oppenländer, U. Walter, *Chem. Ber.* **1964**, *97*(5), 1329–1336.

[140] C. G. Krespan, V. A. Petrov, *Chem. Rev.* **1996**, *96*(8), 3269–3302.

[141] Y.-T. Wu, J. S. Siegel, *Chem. Rev.* **2006**, *106*(12), 4843–4867.

[142] L. T. Scott, M. A. Petrukhina, *Fragments of fullerenes and carbon nanotubes*: Designed synthesis, unusual reactions, and coordination chemistry / by Lawrence T. Scott, Marina Petrukhina; Wiley, Oxford, **2012**.

[143] E.-C. Liu, M.-K. Chen, J.-Y. Li, Y.-T. Wu, *Chem. Eur. J.* **2015**, *21*(12), 4755–4761.

[144] C.-W. Lee, E.-C. Liu, Y.-T. Wu, *J. Org. Chem.* **2015**, *80*(21), 10446–10456.

[145] N. Abdurakhmanova, N. Amsharov, S. Stepanow, M. Jansen, K. Kern, K. Amsharov, *Carbon* **2014**, *77*, 1187–1190.

[146] S. Shkolnikov, Diplomarbeit, Friedrich-Alexander-Universität Erlangen-Nürnberg, **2016**.

[147] R. H. Mitchell, Y.-H. Lai, R. V. Williams, *J. Org. Chem.* **1979**, *44*(25), 4733–

4735.

[148] B. Kim, Y. Park, J. Lee, D. Yokoyama, J.-H. Lee, J. Kido, J. Park, *J. Mater. Chem. C* **2012**, *1*(3), 432–440.

[149] G.-Y. Xie, L. Jiang, T.-B. Lu, *Dalton Trans.* **2013**, *42*(39), 14092–14099.

[150] S. N. Spisak, J. Li, A. Y. Rogachev, Z. Wei, O. Papaianina, K. Amsharov, A. V. Rybalchenko, A. A. Goryunkov, M. A. Petrukhina, *Organometallics* **2016**, *35*(18), 3105–3111.

[151] A. Sygula, *Synlett* **2016**, *27*(14), 2070–2080.

[152] T. Kawase, H. Kurata, *Chem. Rev.* **2006**, *106*(12), 5250–5273.

[153] K. Tashiro, T. Aida, *Chem. Soc. Rev.* **2007**, *36*(2), 189–197.

[154] C. García-Simón, M. Costas, X. Ribas, *Chem. Soc. Rev.* **2016**, *45*(1), 40–62.

[155] S. Nakano, Y. Kage, H. Furuta, N. Kobayashi, S. Shimizu, *Chem. Eur. J.* **2016**, *22*(23), 7706–7710.

[156] K. Yoshida, A. Osuka, *Chem. Eur. J.* **2016**, *22*(27), 9396–9403.

[157] A. Sygula, *Eur. J. Org. Chem.* **2011**, *2011*(9), 1611–1625.

[158] A. Sygula, F. R. Fronczek, R. Sygula, P. W. Rabideau, M. M. Olmstead, *J. Am. Chem. Soc.* **2007**, *129*(13), 3842–3843.

[159] D.-C. Yang, M. Li, C.-F. Chen, *Chem. Commun.* **2017**, *53*(67), 9336–9339.

[160] H. A. Yemam, A. Mahl, U. Koldemir, T. Remedes, S. Parkin, U. Greife, A. Sellinger, *Sci. Rep, 5*, 13401.

[161] M. Takeda, S. Hiroto, H. Yokoi, S. Lee, D. Kim, H. Shinokubo, *J. Am. Chem. Soc.* **2018**, *140*(20), 6336–6342.

[162] F. Eisenhut, T. Lehmann, A. Viertel, D. Skidin, J. Krüger, S. Nikipar, D. A. Ryndyk, C. Joachim, S. Hecht, F. Moresco, G. Cuniberti, *ACS nano* **2017**, *11*(12), 12419–12425.

[163] K. Y. Amsharov, M. A. Kabdulov, M. Jansen, *Eur. J. Org. Chem.* **2009**, *2009*(36), 6328–6335.

[164] A. Mueller, K. Y. Amsharov, *Eur. J. Org. Chem.* **2015**, *2015*(14), 3053–3056.

[165] M. M. Boorum, Y. V. Vasil'ev, T. Drewello, L. T. Scott, *Science* **2001**, *294*(5543), 828–831.

[166] H. Y. Cho, R. B. M. Ansems, L. T. Scott, *Beilstein J. Org. Chem.* **2014**, *10*, 956–968.

[167] M. Treier, C. A. Pignedoli, T. Laino, R. Rieger, K. Müllen, D. Passerone, R. Fasel, *Nat. Chem.* **2011**, *3*(1), 61.

[168] K. Amsharov, N. Abdurakhmanova, S. Stepanow, S. Rauschenbach, M. Jansen, K. Kern, *Angew. Chem.* **2010**, *122*(49), 9582–9586.

[169] H. A. Wegner, L. T. Scott, A. de Meijere, *J. Org. Chem.* **2003**, *68*(3), 883–887.

[170] D. P. Sumy, N. J. Dodge, C. M. Harrison, A. D. Finke, A. C. Whalley, *Chem. Eur. J.* **2016**, *22*(14), 4709–4712.

[171] D. Lungerich, O. Papaianina, M. Feofanov, J. Liu, M. Devarajulu, S. I. Troyanov, S. Maier, K. Amsharov, *Nat. Commun, 9*(1), 4756.

[172] E. Clar, *Ber. dtsch. Chem. Ges. A/B* **1943**, *76*(4), 328–333.

[173] V. S. Thirunavukkarasu, K. Parthasarathy, C.-H. Cheng, *Angew. Chem. Int. Ed.* **2008**, *47*(49), 9462–9465.

[174] J. J. Mousseau, F. Vallée, M. M. Lorion, A. B. Charette, *J. Am. Chem. Soc.* **2010**, *132*(41), 14412–14414.

[175] J. Wang, G. Song, Y. Peng, *Tetrahedron Lett.* **2011**, *52*(13), 1477–1480.

[176] D. N. Korolev, N. A. Bumagin, *Tetrahedron Lett.* **2006**, *47*(25), 4225–4229.

[177] J. Barluenga, M. Trincado, E. Rubio, J. M. González, *Angew. Chem. Int. Ed.* **2006**, *45*(19), 3140–3143.

[178] S. Paul, S. Samanta, J. K. Ray, *Tetrahedron Lett.* **2010**, *51*(42), 5604–5608.

[179] C. Wang, S. Rakshit, F. Glorius, *J. Am. Chem. Soc.* **2010**, *132*(40), 14006–14008.

[180] S. Vuoti, J. Autio, M. Haukka, J. Pursiainen, *Inorganica Chim. Acta* **2009**, *362*(13), 4685–4691.

[181] J. Luo, K. Song, F. l. Gu, Q. Miao, *Chem. Sci.* **2011**, *2*(10), 2029.

[182] Y. Zhang, J. L. Petersen, K. K. Wang, *Tetrahedron* **2008**, *64*(7), 1285–1293.

[183] H. Lee, B. Kim, S. Kim, J. Kim, J. Lee, H. Shin, J.-H. Lee, J. Park, *J. Mater. Chem. C* **2014**, *2*(24), 4737–4747.

Scientific Contributions

Publications:

1. D. Lungerich, **O. Papaianina**, M. Feofanov, J. Liu, M. Devarajulu, S.I. Troyanov, S. Maier & K. Amsharov. Dehydrative π-extension to nanographenes with zig-zag edges. *Nature Communications* **2018**, *9*, Article number 4756.
2. **O. Papaianina**, V.A. Akhmetov, A.A. Goryunkov, F. Hampel, F.W. Heinemann, K.Y. Amsharov. Synthesis of Rationally Halogenated Buckybowls via Chemoselective Aromatic C-F Bond Activation. *Angewandte Chemie International Edition* **2017**, *56 (17)*, 4834-4838.
3. S.N. Spisak, J. Li, A.Y. Rogachev, Z. Wei, **O. Papaianina**, K.Y. Amsharov, A.V. Rybalchenko, A.A. Goryunkov, M.A. Petrukhina. From Corannulene to Indacenopicene: Effect of Carbon Framework Topology on Aromaticity and Reduction Limits. *Organometallics* **2016**, *35 (18)*, 3105-3111.
4. **Papaianina, O.**, Amsharov, K Y. Aluminum oxide mediated C-F bond activation in trifluoromethylated arenes. *Chemical Communications* **2016**, *52 (7)*, 1505-1508.

Conference proceedings:

1. **Papaianina, O.**, Amsharov, K.: *Facile synthesis of functional buckybowls via C-F bond activation*. 4th Erlangen Symposium on Synthetic Carbon Allotropes. Erlangen (Germany), **2017**. (Poster presentation)
2. **Papaianina, O.**, Amsharov, K.Y.: GDCh-JungChemikerForum. *Facile Synthesis of Fullerene Fragments via Selective C-F Bond Activation*. Mainz, (Germany), **2017**. (Poster talk, poster presentation)
3. **Papaianina, O.**, Amsharov, K.Y.: *Facile synthesis of functional buckybowls via C-F bond activation*. Graduate School Molecular Science. Kirchberg (Austria), **2017**. (Oral presentation)
4. **Papaianina, O.**, Amsharov, K. Yu.: *Facile Synthesis of Halogenated Buckybowls via C-F bond activation*. 18th European Symposium on Fluorine Chemistry. Kyiv (Ukraine), **2016**. (Poster presentation)

Acknowledgements

In the beginning, I would like to thank my supervisor *Dr. habil. Konstantin Amsharov* for giving me an opportunity of working in his group and supporting me throughout my time at the Friedrich-Alexander-Universität Erlangen-Nürnberg.
I really appreciate the assistance I received from the members of NMR department *apl. Prof. Dr. Walter Bauer*, *Dr. Harald Maid* and *Christian Placht*; MS department *Wolfgang Donaubauer* and *Margarete Dzialach*; X-ray department *Dr. Frank Hampel* and *Wolfgang Donaubauer*; the „Magazin“ staff *Hannelore Oschmann*, *Robert Panzer* and *Detlef Schagen*, glassblowers *Dominik Roth* and *Bahram Saberi*, electrician *Holger Wohlfahrt*.
Many thanks also to the secretary *Heike Fischer*, academic staff of the Chair of Organic Chemistry II *Dr. Marcus Speck* und *Dr. Michael Brettreich*.
I am profoundly grateful to *Dr. Frank Heinemann* and *Prof. Dr. S.I. Troyanov* for conducting of X-ray measurements.
A special mention of thanks to *Prof. Dr. Andrey Rogachev* and *Dr. Alexey Goryunkov* for conducting of DFT calculations.
I am deeply grateful to *Prof. Dr. Sabine Maier* and *Prof. Dr. Roman Fasel* who carried out the STM measurements.
I would like to express my gratitude to collaboration partners and co-authors *Prof. Dr. Marina A. Petrukhina, Dr. Sarah N. Spisak, Jingbai Li, Dr. Zheng Wei, Alexey V. Rybalchenko, Dr. Jia Liu* and *Mirunalini Devarajulu* for the interesting results in the field of organometallics and scanning tunneling microscopy.
I am also pleased to say thank you to *Dr. Edurne Nuin, Dr. Gonzalo Abellán, Katerina Maxouti* and *Dr. Maria Eugenia Pérez-Ojeda Rodriguez* for sharing their experience in organic and material chemistry.
My further regards go to the *groups* of Prof. Dr. Hirsch, Apl. Prof. Dr. Jux, Prof. Dr. Mokhir and Prof. Dr. von Delius.
I would also like to thank my reading and oral defense committee members *Prof. Dr. Andriy Mokhir*, *Prof. Dr. Andres Hirsch* and *Prof. Dr. Thomas Drewello.*
My warmest thanks and acknowledgement to my fellow labmates *Jörg Tomada*, *Arber Uka* and *Ann-Kristin Steiner (aka Anni)* for a great deal of advice in organic chemistry they gave me and for helping me to improve my German, *Dr. Kateryna Roshchina (aka Katia)* for being extremely helpful with answering some questions regarding optical spectroscopy as well as *Stanislav Shkolnikov*, *Dr. Dominik Lungerich*, *Dr.*

Dmitry Sharapa, Tobias Härtl, *Vladimir Akhmetov*, *Mikhail Feofanov*, *Dr. Naoto Suzuki* and *Julian Mitrovic* for the fun-time we spent together (both at work and BBQ evenings). I will never forget our stay in Mainz during the conference!..

I also thank my friends for encouraging and supporting me from start to finish of this work (too numerous to mention here, but you know who you are).

Lastly, my deepest thanks go to my parents, *Larisa* and *Stepan*, and my husband *Dimitri* for their unconditional love, continuous inspiration, enormous patience, backing me up in every stage of my life.